BioMed Research International

Stress Signaling Responses in Plants

Guest Editors: Marta Wilton Pereira Leite de Vasconcelos de Vasconcelos, Paloma Koprovski Menguer, Yanbo Hu, Luis Fernando Revers, and Raul Antonio Sperotto

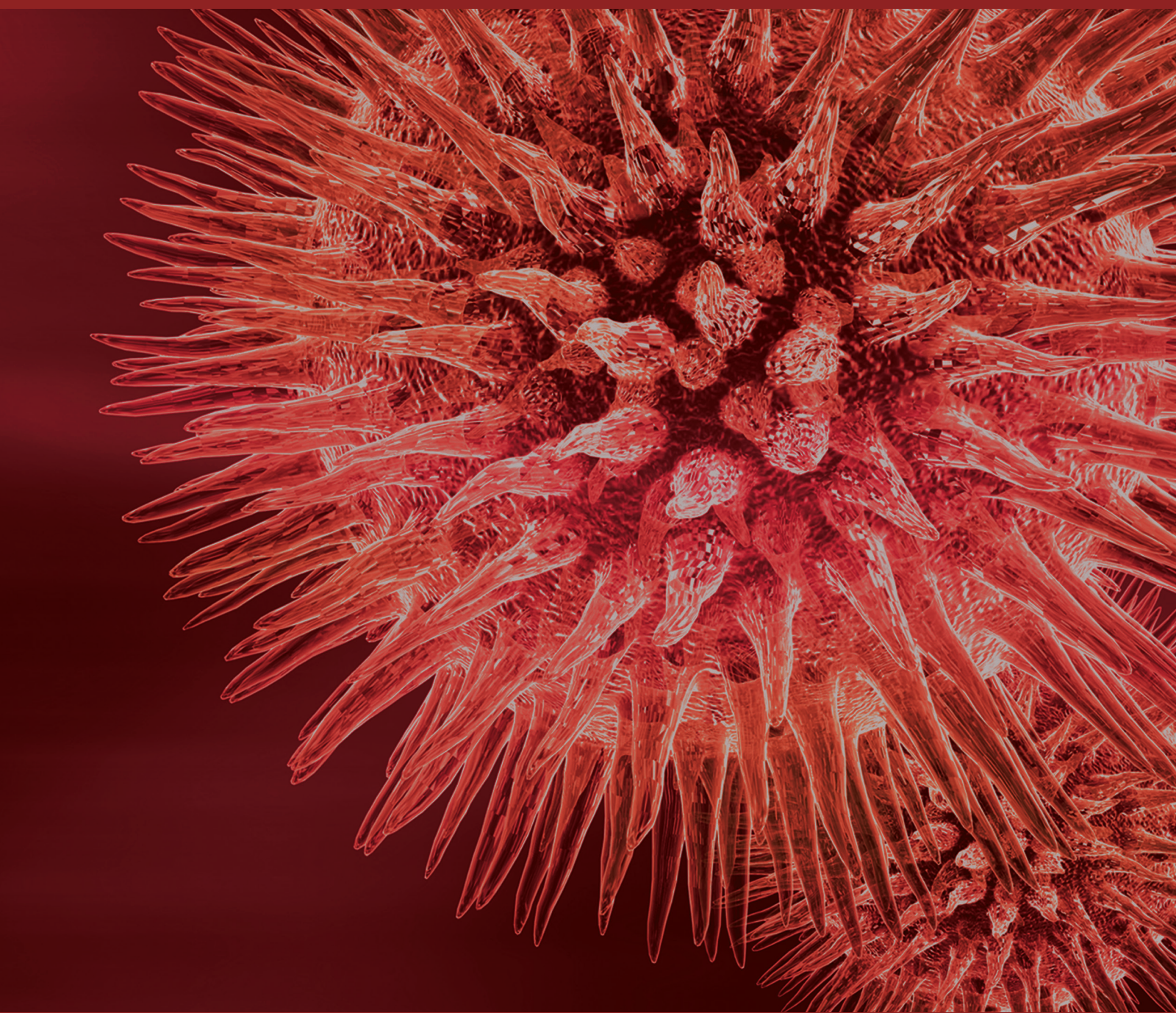

Stress Signaling Responses in Plants

BioMed Research International

Stress Signaling Responses in Plants

Guest Editors: Marta Wilton Pereira Leite de Vasconcelos de Vasconcelos, Paloma Koprovski Menguer, Yanbo Hu, Luis Fernando Revers, and Raul Antonio Sperotto

Contents

Hindawi Publishing Corporation
BioMed Research International
Volume 2016, Article ID 4720280, 2 pages
http://dx.doi.org/10.1155/2016/4720280

Editorial

Stress Signaling Responses in Plants

Marta Wilton Pereira Leite de Vasconcelos,[1] Paloma Koprovski Menguer,[2] Yanbo Hu,[3] Luis Fernando Revers,[4] and Raul Antonio Sperotto[5]

[1] *Universidade Católica Portuguesa, Centro de Biotecnologia e Química Fina (CBQF), Laboratório Associado, Escola Superior de Biotecnologia, Rua Arquiteto Lobão Vital, Apartado 2511, 4202-401 Porto, Portugal*
[2] *Universidade Federal do Rio Grande do Sul, 91501-970 Porto Alegre, RS, Brazil*
[3] *College of Life Science, Northeast Forestry University, No. 26 Hexing Road, Xiangfang District, Harbin 150040, China*
[4] *EMBRAPA Uva e Vinho, Rua Livramento 515, 95701-008 Bento Gonçalves, RS, Brazil*
[5] *Centro de Ciências Biológicas e da Saúde (CCBS), Programa de Pós-Graduação em Biotecnologia (PPGBiotec), Centro Universitário UNIVATES, Rua Avelino Tallini 171, 95900-000 Lajeado, RS, Brazil*

Correspondence should be addressed to Raul Antonio Sperotto; rasperotto@univates.br

Received 26 June 2016; Accepted 26 June 2016

Plants undergo continuous exposure to various biotic and abiotic stresses in their natural environment. To survive under such conditions, plants exhibit stress tolerance or stress avoidance through acclimation and adaptation mechanisms that ultimately reestablish cellular and organismal homeostasis or reduce episodic shock effects. These abilities involve intricate and complex mechanisms of perception, transduction, and transmission of stress stimuli, allowing optimal response to environmental conditions. The perception of stimuli and their expansion in cells involves signaling molecules such as intracellular calcium and reactive oxygen species, which intensify the action of particular signaling pathways. To date, the molecular mechanisms that are involved in each stress have been revealed comparatively independently, and so our understanding of convergence points between biotic and abiotic stress signaling pathways remains rudimentary. However, recent studies have revealed several molecules as promising candidates for common players that are involved in crosstalk between stress signaling pathways.

This special issue aimed to join original research and review articles related to understanding of plant responses to abiotic and biotic stress conditions, identifying novel players involved in plant responses to stress conditions, biotechnological strategies to increase plant tolerance to abiotic and biotic stresses, and understanding molecular interactions and crosstalks among different stress conditions.

M. Nourbakhsh-Rey and M. Libault in "Decipher the Molecular Response of Plant Single Cell Types to Environmental Stresses" explore *omic* studies to understand the response of single cell types to environmental stresses in order to clearly depict the contribution of each cell type composing the sample in response to stress. Cellular complexity of entire organs masks cell-specific responses to environmental stresses and logically leads to the dilution of the molecular changes occurring in each cell type composing the tissue/organ/plant in response to the stress. Specifically, the authors highlight that combining one or two *omic* analyses to look at single cell system biology can provide more precise molecular characterization and more dynamic models of the interactions between the plant and its environment.

J. Ren et al. in "Drought Tolerance Is Correlated with the Activity of Antioxidant Enzymes in *Cerasus humilis* Seedlings" describe the correlation between the activities of antioxidant enzymes and drought tolerance. By exploring drought-resistant and drought-susceptible *C. humilis* accessions, they compare the abilities of the contrasting genotypes to induce antioxidant defense under drought conditions. Their manuscript presents original data indicating that plants exhibiting a more efficient reactive oxygen species scavenging

system in response to drought conditions have enhanced membrane protection, an ability that could be directly linked to their higher adaptation to drought.

X. Tang et al. in "Reference Gene Selection for qPCR Normalization of *Kosteletzkya virginica* under Salt Stress" employed RT-qPCR to select the most stable reference gene of the perennial halophytic plant *K. virginica* under salinity stresses. The stable reference gene selected in this study will be very helpful for revealing the gene expression profiles of *K. virginica* under salt stress, allowing a better understanding of the salt-resistant mechanisms in halophyte plants.

Y. Oono et al. in "Genome-Wide Transcriptome Analysis of Cadmium Stress in Rice" used RNAseq strategy to elucidate the molecular basis of the rice response to cadmium (Cd) stress, a widespread heavy metal pollutant that is highly toxic to living cells, negatively affecting nutrient uptake and homeostasis in plants. In this work, rice plants were hydroponically treated with low Cd concentrations, revealing novel Cd-responsive transporters by analyzing gene expression under different Cd concentrations. This study could help to develop novel strategies for improving tolerance to Cd exposure in rice and other cereal crops.

J. S. Rohila et al. in "Leaf Proteome Analysis Reveals Prospective Drought and Heat Stress Response Mechanisms in Soybean" investigate the effect of drought, heat, and cooccurring drought and heat stresses in the leaf proteome of two contrasting soybean genotypes. The authors identified genes involved in photosynthesis that were differentially expressed during drought and heat stress conditions, suggesting that photosynthesis-related proteins could be affecting RuBisCO regulation, electron transport, and Calvin cycle during abiotic stress, which ultimately alter the carbon fixation in leaves. The authors discuss the role of heat shock-related proteins and ROS detoxification capacity via carbonic anhydrase as heat and drought tolerance mechanisms, respectively.

J. M. Garcia-Mina et al. in "Involvement of Hormone- and ROS-Signaling Pathways in the Beneficial Action of Humic Substances on Plants Growing under Normal and Stressing Conditions" review our current knowledge about the mechanisms by which soil humus affects soil fertility. In particular, they discuss the relationships between two main signaling pathway families that are affected by humic substances within the plant: hormone- and ROS-mediated signaling pathways. The authors aim to integrate these events in a more comprehensive model and point out future research directions to unveil the complete mechanisms of regulation.

W. Fang et al. in "Cloning and Expression Analysis of One Gamma-Glutamylcysteine Synthetase Gene (Hbγ-ECS1) in Latex Production in *Hevea brasiliensis*" isolated a γ-ECS gene from the rubber tree and investigated its function linked to thiol content in latex. To understand the relation between γ-ECS and thiols and to correlate these findings to latex flow, the authors conducted RT-qPCR analysis and found that the expression levels of Hbγ-ECS1 were induced by tapping and ethrel stimulation, and the expression was related to thiols content in the latex. When looking at long-term flowing latex, the gene was related to the duration of latex flow. This work may have important biotechnological applications, since rubber tree is a major commercial source of latex, which is used for rubber production.

A. Vian et al. in "Plant Responses to High Frequency Electromagnetic Fields" conducted an original review, looking at the possible effects of HF-EMFs, which are increasingly present in the environment (due to, e.g., cell phones, Wi-Fi, and different types of connected devices) on different essential plant metabolic activities, such as reactive oxygen species metabolism, Krebs cycle, pentose phosphate pathway, chlorophyll content, and terpene emission. They found that not only are most of these pathways indeed modified by HF-EMF exposure, but also radiation brings about alterations in gene expression and plant growth. The authors propose to consider nonionizing HF-EMF radiation as a noninjurious, albeit influential environmental factor that induces significant changes in plant metabolism.

Acknowledgments

We sincerely thank the editorial board for their approval of this concept and continuous help in the successful publication of this special issue. We would also like to thank contributors to this special issue for their scientifically sound papers. We extend our thanks to the reviewers for critical assessment of each paper, their constructive criticisms, and timely responses that made this special issue possible. We hope that this special issue will contribute to a more thorough understanding of the diverse aspects of plant stress signaling and response.

Marta Wilton Pereira Leite de Vasconcelos
Paloma Koprovski Menguer
Yanbo Hu
Luis Fernando Revers
Raul Antonio Sperotto

Hindawi Publishing Corporation
BioMed Research International
Volume 2016, Article ID 5657491, 8 pages
http://dx.doi.org/10.1155/2016/5657491

Research Article

Cloning and Expression Analysis of One Gamma-Glutamylcysteine Synthetase Gene (*Hbγ-ECS1*) in Latex Production in *Hevea brasiliensis*

Wei Fang, Luo Shi Qiao, Wu Ming, Qiu Jian, Yang Wen Feng, Gao Hong Hua, and Xiao Xian Zhou

Key Laboratory of Biology and Genetic Resources of Rubber Tree, Ministry of Agriculture, Rubber Research Institute, Chinese Academy of Tropical Agricultural Sciences, Danzhou, Hainan 571737, China

Correspondence should be addressed to Xiao Xian Zhou; xiaoxianzhou80@163.com

Received 8 December 2015; Revised 8 March 2016; Accepted 16 May 2016

Academic Editor: Marta W. P. L. de Vasconcelos

Rubber tree is a major commercial source of natural rubber. Latex coagulation is delayed by thiols, which belong to the important type of antioxidants in laticifer submembrane, and is composed of glutathione (GSH), cysteine, and methionine. The rate-limiting enzyme, γ-ECS, plays an important role in regulating the biosynthesis of glutathione under any environment conditions. To understand the relation between γ-ECS and thiols and to correlate latex flow with one-time tapping and continuous tapping, we cloned and derived the full length of one γ-ECS from rubber tree latex (*Hbγ-ECS1*). According to qPCR analysis, the expression levels of *Hbγ-ECS1* were induced by tapping and Ethrel stimulation, and the expression was related to thiols content in the latex. Continuous tapping induced injury, and the expression of *HbγECS1* increased with routine tapping and Ethrel-stimulation tapping (more intensive tapping). According to expression in long-term flowing latex, the gene was related to the duration of latex flow. *HbγECS1* was expressed in *E. coli* Rosetta using pET-sumo as an expression vector and the recombinant enzyme was purified; then we achieved 0.827 U/mg specific activity and about 66 kDa molecular weight. The present study can help us understand the complex role of *Hbγ-ECS* in thiols biosynthesis, which is influenced by tapping.

1. Introduction

Rubber tree (*Hevea brasiliensis*) is a major commercial source of natural rubber [1]. Expelled from rubber tree's laticifer, latex contains laticifer cytoplasm, usual kinds of plastids, characteristic organelles (lutoids and special plastids, such as Frey-Wyssling particles), and rubber particles. In laticifers, the thiols content is nearly 1 mM/L [2], and it is one of the main physiological indices related to the field [3, 4]. To meet the growing demand for high quality rubber, it is important to increase the yield of rubber trees. Therefore, the duration of the latex flow must be restricted to control the latex yield. Thiols, which can delay coagulation of latex, belong to the important type of antioxidants which act in the laticifer submembrane; thiols are closely related to the duration of latex flow. Glutathione (GSH), cysteine, and methionine form thiols in the latex of *Hevea brasiliensis* [4]. In the latex, the concentration of glutathione and cysteine is about 0.72 and 0.44 mM, respectively [5]. The total thiol groups expressed in cytosol amounted to 2.2 ± 0.5 mM [6]; in the latex, the concentration of thiol-related cytosol is about 0.5–0.9 mM [4]. Thiols are primarily associated with the redox potential of latex; moreover, GSH accounts for a major proportion of thiols in latex of rubber tree.

In previous studies, it has been reported that GSH is involved in various processes, including storage and transport of reduced sulphur. Furthermore, GSH serves as an electron donor in biochemical reactions; it is released as a stress response to reactive oxygen and heavy metals; it is also involved in the detoxification of xenobiotics [7–12]. In addition, GSH influences the tolerance of abiotic stresses, such as frost, salt, and chill [13–15]. Recent studies have also elucidated how GSH becomes one of the important players in biotic stress management as it interacts with various established messengers [16]. Interestingly, GSH is synthesized by

two ATP-dependent steps, which are catalyzed by the consecutive action of gamma-glutamylcysteine synthetase (γ-ECS); this enzyme forms gamma-glutamylcysteine (γ-EC) from cysteine and glutamate, and glutathione synthetase (GSHS) adds glycine to the γ-EC. Therefore, γ-ECS is regarded as a key enzyme in the biosynthesis of GSH [17–19].

In plants, gene of *γ-ECS* was first isolated from *Arabidopsis thaliana* [20]. The expression analysis showed that the transcripts of *γ-ECS* genes accumulate when plants encounter adverse environments, such as abnormal temperatures, salinity, osmotic stress, and heavy metals [21–23]. To confirm the functions of *γ-ECS*, it was isolated from *Brassica juncea* in previous study. According to this study, transgenic rice plants with the overexpression of *BrECS* can tolerate high salinity. In other words, an overexpression of *BrECS* enhances the growth, development, and yield of rice [24]. An overexpression of bacterial *γ-ECS* in the cytosol of *Populus tremula* and *Populus alba* leads to elevated levels of GSH [17]. This indicates that transgenic plants exhibit higher Cd^{2+} uptaken in their roots. In conclusion, transgenic poplars show higher tolerance to Cd [25]. In the latex of rubber trees, thiols content is one of the important physiological parameters, while γ-ECS is the rate-limiting enzyme for GSH synthesis [26]. However, we hardly know the underlying molecular mechanisms for the thiols content in latex. Furthermore, we still need to decipher the rubber tree's response to stimulations with different intensities. Thus, it is necessary to isolate new genes involved in the latex of rubber trees. The objective of this study is to isolate *γ-ECS* genes from rubber tree and to investigate its possible physiological functions against the thiols in the latex.

2. Materials and Methods

2.1. Materials. Latex is expelled and collected by successive tapping. Rubber tree clones Reyan8-79, Reyan7-33-97, PR107, and RRIM600 were grown in the Experimental Farm of the Chinese Academy of Tropical Agricultural Sciences, Hainan Province, China. Clones of Reyan8-79 latex samples were collected from ten-year-old virgin trees without treatment. Reyan7-33-97 was a young tapped rubber tree; for the first year, it was subjected to 2% Ethrel stimulation. It was used for collecting latex after being stimulated at different time periods (four different treatments were applied during 0, 12, 24, and 48 h). For different tapping intensity (including no tapping, routine tapping, and Ethrel stimulation), we used the clone PR107 in a thirty-year-old tree. We collected latex samples at different time periods (morning latex, afternoon latex, and next-day latex) from old rubber tree RRIM600. The samples of leaves, root, xylem, bark, and latex were collected from virgin Reyan7-33-97 trees without treatments.

2.2. Cloning of Two γ-ECS Genes. The extraction of total RNA was performed from 1 mL of fresh latex from rubber tree Reyan8-79 by the Plant RNA Mini Kit (Bioteke, China). Then, 1 μg of total RNA was annealed to an oligo (dT)18 primer and reverse-transcribed at 42°C for 1 h. Thus, we obtained the first strand of complementary DNA (cDNA) using RevertAid First Strand cDNA Synthesis Kit (Fermentas, USA) according to the manual. The homologously expressed sequence tags (EST) of *Hbγ-ECS1* were selected from the latex transcriptome database, and their full length was determined by rapid amplification of cDNA ends (RACE). Four primers (3′RACE-GSP: 5′-AAACAGGGAAAGCAGAGCA-3′, 3′RACE-NUP: 5′-ACATGCACTGTCCAGGTTAA-3′/5′RACE-GSP: 5′-TCTGCTTTCCCTGTTTGAGTCCTAT-3′, and 5′RACE-NSP: 5′-CCTCTTTGGTTAGCGGTTCT-3′) were used for 3′-terminus RACE and 5′-terminus RACE, respectively. Furthermore, PCR products were purified using the Agarose Gel DNA Purification Kit Ver. 2.0 (TaKaRa, Japan) and then they were sequenced. The open reading frame (ORF) region was identified using http://www.ncbi.nlm.nih.gov/gorf/gorf.html. Thereafter, the ORF region was verified by high fidelity PCR amplification (PrimeSTAR® HS DNA Polymerase, TaKaRa, Japan).

2.3. Bioinformatic Analysis. From the NCBI databases, we performed homology searches with BLAST (http://www.ncbi.nlm.nih.gov/BLAST) as the default parameter. Furthermore, the full length of amino acid sequences from γ-ECS of six organisms was aligned by ClustalW and imported into the Molecular Evolutionary Genetics Analysis (MEGA) package version 5 [27]. Then, the neighbor-joining method was used for performing phylogenetic analysis in MEGA. Bootstrap tests were conducted by 1000 replicates; the branch lengths were proportional to phylogenetic distances.

2.4. Analysis of Thiols Content. The thiols content in latex was measured by dithionitrobenzoic acid (DTNB) in a colorimetric method according to the protocol described in a previous study [2].

2.5. Gene Expression Analysis. Gene expression levels were detected by quantitative real-time PCR (qPCR) using 18S rRNA (GenBank Accession Number: AB268099) as an internal control (18s rRNA primers: 5′-GGTCGCAAGGCTGAAACT-3′/5′-ACGGGCGGTGTGTACAAA-3′). Total RNA (1 μg) was isolated from Reyan8-79, Reyan7-33-97, PR107, and RRIM600 latex. Single-stranded cDNA was prepared by 1.0 μg of total RNA which was reverse-transcribed from each sample using a one-step RT-PCR kit (Fermentas, USA). The primers' sequences were as follows: 5′-GAAAGCTGTTGCAGAGGAAATG-3′/5′-TCATATCTTCCCTTGGGCATAAC-3′. The SYBR Green real-time PCR assay was carried out in a total volume of 20 μL, containing 10 μL of 2x SYBR Green Master Mix (Applied Biosystems), 0.2 μM (each) of specific primers, and 100 ng of template cDNA. The amplification was achieved by the following PCR protocol: denaturation was carried out at 95°C for 30 s; then we performed 40 cycles of denaturation at 95°C for 5 s, annealing at 60°C for 20 s, and extension at 72°C for 20 s. During each analysis, a negative control without a cDNA template and a reference gene 18SrRNA were run to normalize the data and to evaluate the overall specificity. All the reactions were carried out in triplicate in 96-well plates of a CFX96 Real-Time PCR System (Bio-rad). The PCR products were analyzed using 2.0% agarose gels, which were stained with ethidium bromide to ensure that their sizes were within acceptable limits. The expression

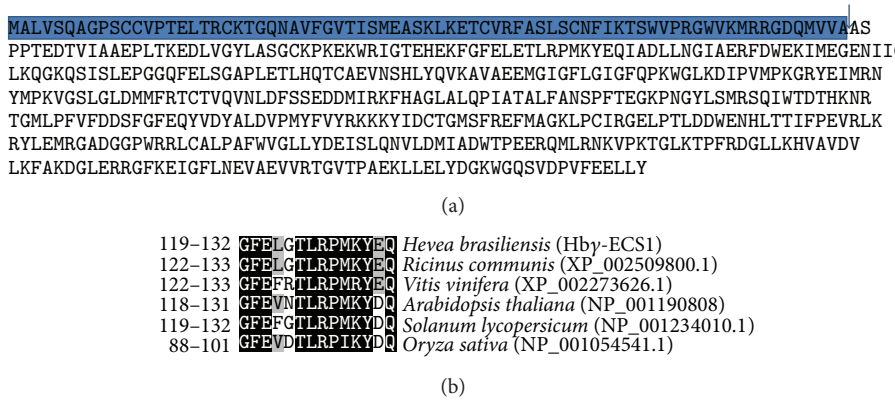

(a)

119–132	GFELGTLRPMKYEQ	*Hevea brasiliensis* (Hbγ-ECS1)
122–133	GFELGTLRPMKYEQ	*Ricinus communis* (XP_002509800.1)
122–133	GFEFRTLRPMRYEQ	*Vitis vinifera* (XP_002273626.1)
118–131	GFEVNTLRPMKYDQ	*Arabidopsis thaliana* (NP_001190808)
119–132	GFEFGTLRPMKYDQ	*Solanum lycopersicum* (NP_001234010.1)
88–101	GFEVDTLRPIKYDQ	*Oryza sativa* (NP_001054541.1)

(b)

Figure 1: Analysis of deduced amino acid sequence: (a) the deduced amino acid sequence of Hbγ-ECS1, showing the 74 amino acids in a long transit peptide of chloroplast, and its putative cleavage site (VAA). (b) Comparison of the deduced amino acid sequence of *Hevea brasiliensis* and other plant sources with a putatively oxidized GSH binding site.

levels are presented as a ratio relative to the control sample, which was set as 1.

2.6. Statistical Analysis. All the experiments were repeated at least three times using three biological replicates and every replicate contained at least five trees. The significant differences between data sets were evaluated by Student's t-test (5% significance, $P < 0.05$). The calculations were carried out by Microsoft Excel software.

2.7. Expression of Recombinant Hbγ-ECS1 in E. coli Rosetta. The purified double-restricted PCR product (primer: 5′-gactATGGCGCTTGTTTCTCAGGCAGGC-3′; 5′-ggcctTTAGTACAGTAGTTCCTCAAAAAC-3′) of *Hbγ-ECS1* was ligated within pET-sumo using T4 DNA ligase in its specific buffer. Ligation mixture transfected with competent cells *E. coli* DH5α and positive clones were confirmed by PCR and gene sequencing. The recombinant plasmid DNA was extracted and transformed *E. coli* Rosetta. The transformed *Rosetta* cells were grown in a 100 mL LB medium to an optical density of 0.5–0.7 at 37°C. The cells were induced by 0.5 mM Isopropyl β-D-1-thiogalactopyranoside (IPTG) and were harvested by centrifugation (8000 ×g 180 s). Pellet obtained was resuspended in NTA-0 buffer and disrupted by ultrasonic wave. Expression of *Hbγ-ECS1* was determined in both intracellular and extracellular fractions by 12% SDS-PAGE and was visualized after staining with a Coomassie Brilliant dye.

2.8. Fermentation, Purification of Inclusion Body, and Renaturation of Protein. 100 mL bacterium suspension was cultivated and centrifuged. Pellet was resuspended and disrupted by ultrasonic wave. The inclusion body was vibrated and resuspended until dissolved. Dissolved body was centrifuged and the supernatant was denatured protein. Purified protein was added in renaturation buffer (0.2% PEG 4000, 1 mM GSSG, and 2 mMh GSSH) for 12 h at 4°C and dialyzed in TE buffer for 3 days. The renaturation protein estimation was performed by the method of Bradford.

2.9. Enzyme Activity. The purified renaturation protein was assayed according to Rüegsegger and Brunold [28, 29]. For γ-ECS activity, the reaction was started by addition of the enzyme extract (140 μL) to give 500 μL assay mix containing 100 mM Hepes (pH 8.0), 50 mM $MgCl_2$, 20 mM glutamate, 1 mM cysteine, 5 mM ATP, 5 mM phosphoenolpyruvate, 5 mM DTT, and 10 U mL pyruvate kinase. The reaction mixture was incubated at 37°C for 45 min, and the reaction was stopped by addition of 100 μL of 50% TCA. The mixture was centrifuged, and the supernatant was used for estimation of phosphate content by the phosphomolybdate method.

3. Results

3.1. Bioinformatic Analysis. A new cDNA of γ-ECS homologous gene, *Hbγ-ECS1*, was isolated from *Hevea brasiliensis*. The obtained sequence included the translation start site (ATG) along with 223 bp of 5′UTR region and 168 bp of 3′UTR region, which were downstream to the stop codon (TAA). The complete ORF was composed of 1572 bp, encoding a polypeptide of 523 amino acids. The TargetP and the ChloroP software predicted the presence of a putative transit peptide of 74 amino acids in the *Hbγ-ECS1* putative protein sequence of chloroplast. It also detected the presence of conserved cleavage site Val AlaAla (VAA) (Figure 1(a)). The putative Hbγ-ECS1 protein displayed 90%, 82%, 78%, 81%, and 71% sequence similarity with γ-ECS protein sequence, which was isolated from *Ricinus communis*, *Vitis vinifera*, *Arabidopsis thaliana*, *Solanumly copersicum*, and *Oryza sativa*, respectively (Figure 2).

Upon multiple alignment of all the above six sequences, we observed that, barring the exception of transit peptide sequence, the remaining showed high similarity in their sequences. Notably, the transit peptide cleavage site in the plastids also had similar sequences. As shown in Figure 1(b), the putatively oxidized GSH binding site was also conserved [29].

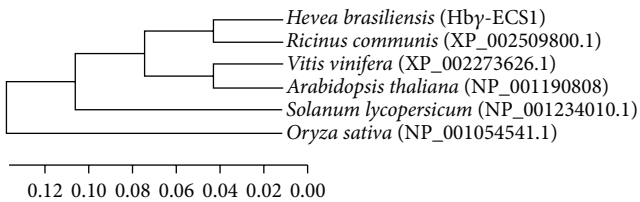

Figure 2: Phylogenetic analysis of Hbγ-ECS1, Hbγ-ECS2, and five other plants. The Latin name of the species and NCBI accession number are provided. The phylogenetic tree is based on the genetic distances of protein sequences, and it was generated by MEGA5.01 software using ClustalW for the alignment. We used a neighbor-joining algorithm with a total of 1000 bootstrap replicates.

3.2. Gene Expression

3.2.1. Tissue-Specific Expression. Real-time PCR reactions were carried out to determine the expression of *Hbγ-ECS1* in the five tissues (latex, xylem, bark, leaf, and root). The results showed that *Hbγ-ECS1* had a low expression level in the latex and leaf tissues, but it was highly expressed in the xylem and bark tissues (Figure 3(a)).

3.2.2. Expression Level Stimulated by Ethrel and Relation between Gene and Thiols Content in the Latex. Ethrel (2-chloroethylphosphonic acid) was used as a stimulation to increase latex production and reduce labor productivity. The expression level of *Hbγ-ECS1* was promoted 4 times after stimulation for 12 h and increased 8 times for 48 h. Ethrel stimulation significantly regulated the expression of *Hbγ-ECS1* (Figure 3(b)).

Thiol is one of the main physiological indices which are related to latex field. The physiological parameters (sugar content, inorganic phosphorus, etc.) of latex were comprehensively analyzed to find out why thiols content decreases within 24 h Ethrel stimulation after the metabolism of laticifers system was subjected to vigorous stimulation. We proposed that the consumption of thiols was more active than synthesis [27]. However, the thiols content increased due to the addition of thiols in 48 h Ethrel stimulation. It can be speculated that, at the initial stages, the high level of expression of *Hbγ-ECS1* complements the thiols content that was consumed previously by vigorous metabolism. This indicates that the gene regulated by Ethrel is related to the thiols content in the latex of rubber trees.

3.2.3. Gene Expression Level in Long-Term Flow Latex. The long-term flow of latex was the result of intensive tapping [30]. Based on ethylene gas-stimulation, long-term flowing latex in old-age RRIM600 rubber tree began from the first day of morning tapping until the morning of the next day, so the time periods of latex flow were divided into morning latex, afternoon latex, and next-day latex. The expression level of *Hbγ-ECS1* was higher in the afternoon latex than at the other times (Figure 3(c)). It can be speculated that thiols were consumed during the course of latex expulsion and the increasing expression of related genes complemented the reductive thiols.

3.2.4. Expression Level at Different Tapping Intensity. The degrees of three tapping intensities varied from weak to strong as follows: no tapping, routine tapping, and Ethrel-stimulation tapping. The degree of tapping intensity represents the level of rubber tree injury that was subjected to continuous tapping. Compared with the control (no tapping), the expression of *Hbγ-ECS1* increased significantly in the case of routine tapping and Ethrel-stimulation tapping for three months (Figure 3(d)).

3.3. Purification of Recombinant Enzyme. The purified fraction of *Hbγ-ECS1* was examined by running SDS-PAGE. Distinct protein band of 66 kDa was perceived as purified *Hbγ-ECS1*. No band at this position was observed in the controls (noninduced strain Rosetta/pET-sumo-*Hbγ-ECS1*, induced empty vector strain Rosetta/pET-sumo, wild *E. coli* Rosetta, and cell supernatant of induced strain Rosetta/pET-sumo-*Hbγ-ECS1*) (Figure 4).

3.4. Enzyme Activity. It was observed that the concentration of renaturation protein was 0.3 mg/mL. One enzyme activity unit was defined as 1 μmol inorganic phosphorus produced by ATPase decomposing ATP per hour per mg tissue protein. The enzyme activity calculation formula is as follows:

$$\begin{aligned}\gamma\text{-ECS enzyme activity } (\mathrm{U/mg}) &= \frac{\text{measured OD} - \text{control OD}}{\text{Standard OD} - \text{blank OD}} \\ &\times \text{Concentration of standard sample} \times \frac{60\,\text{min}}{6\,\text{min}} \\ &\div \text{Concentration of sample protein.}\end{aligned} \quad (1)$$

According to the measured OD, the mean result of enzyme activity was 0.827 U/mg.

4. Discussion

More reactive oxygen species (ROS) were generated by tapping [31], Ethrel stimulation [32], and latex flowing. The release of reactive oxygen is claimed to be responsible for the peroxidative degradation of the lutoid membrane. Lutoid is a special organelle in latex, in which hevein proteins rich in cysteine occupied 70% in lutoid whole proteins and hydrophobic groups with reduction activity exposed to protein surface. Hydrophobic groups linked N-acetyl glucose on rubber particles membrane under oxidation, which caused gathering of rubber particle and stopping of latex flowing [33]. Thiols, eliminating ROS through redox reaction, are important antioxidants to laticifer submembrane and beneficial to latex stability, prolonging flowing time and increasing production. GSH accounts for a major proportion of thiols in latex of rubber tree.

In higher plants, GSH is associated with protective mechanisms because it has multifaceted functions inside plant cells [14, 34–36]. Our results focused on the cloning and sequence analysis of *γ-ECS*, a rate-limiting enzyme that is associated

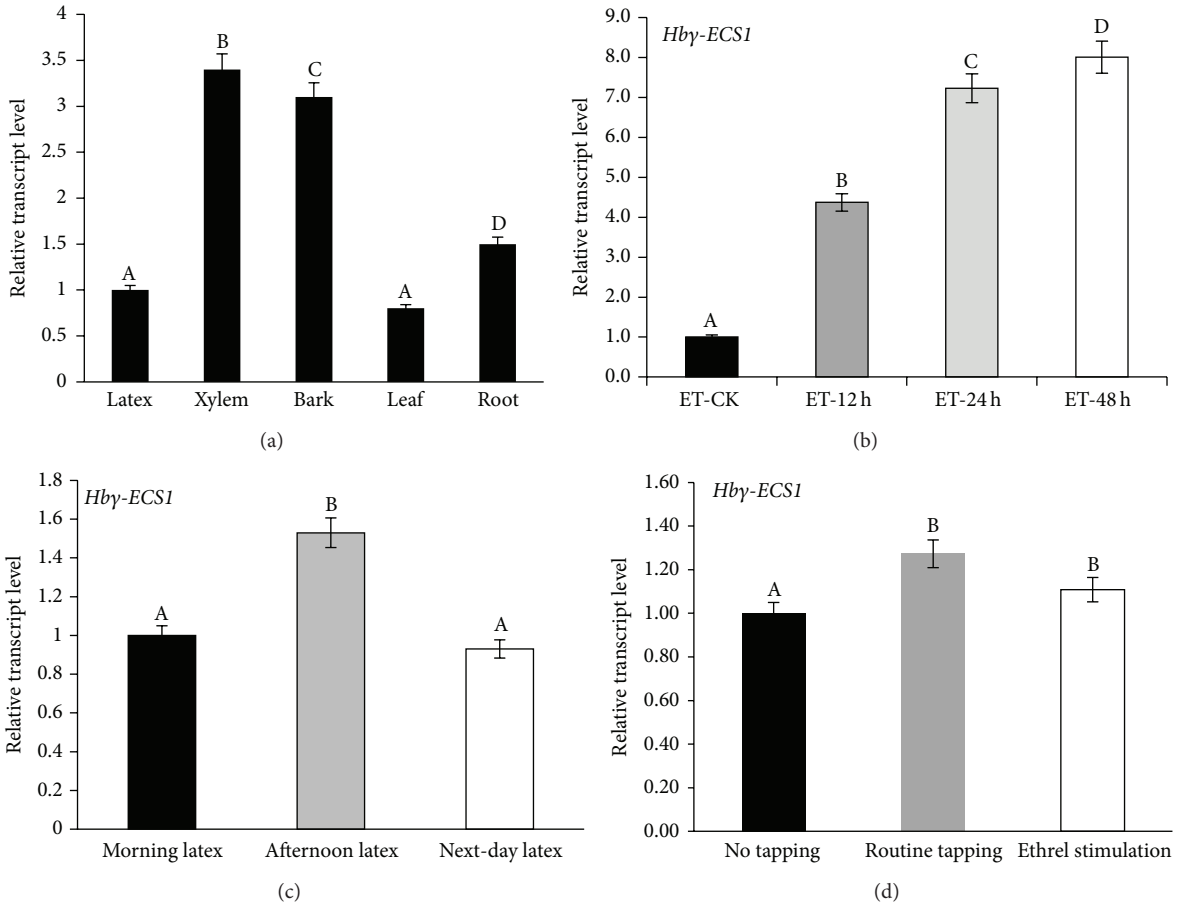

Figure 3: Expression analysis of two genes. (a) Expression profile of Hbγ-ECS1 in different tissues. (b) Expression patterns and relative mRNA levels of *Hbγ-ECS1* at different tapping times after Ethrel stimulation. (c) Expression patterns and relative mRNA levels of *Hbγ-ECS1* and *Hbγ-ECS2* in long-term flowing latex of RRIM600. The long-term flowing latex was divided into the following flow times: morning latex, afternoon latex, and next-day latex. (d) Expression patterns and relative mRNA levels of *Hbγ-ECS1* and *Hbγ-ECS2* after being subjected to three months of every tapping intensity in PR107 (this figure expressed the difference in three months). Tapping system: half spiral tapping every 3 days along with Ethrel stimulation (15 d). Quantitative RT-PCR analysis was carried out to determine the expression levels. The 18SrRNA (GenBank Accession Number: AB268099) was used as the control. Data are expressed as mean ± SD for three individual experiments ($n = 3$).

with GSH biosynthesis. Thus, we comprehensively investigated the regulation of mRNA expression levels in different clones of rubber trees that were subjected to Ethrel stress. We also determined the long-term flow of latex that is induced by continuous tapping. In *Arabidopsis thaliana*, a single copy of *γ-ECS* gene is present; in the *Oryza sativa* genome, two *γ-ECS* genes are present. In this case, we isolated one *γ-ECS* from latex of rubber tree and denoted it as *Hbγ-ECS1*. An identity analysis showed that Hbγ-ECS1 is identical to γ-ECSs found in other plants. Hbγ-ECS1 showed a similarity of 78% and 71% with γ-ECS of *Arabidopsis* and rice, respectively. The putative target peptide cleavage sequences are highly conserved, but the target itself is not conserved. As Hbγ-ECS1 has sequences that are highly similar to those of other plants, we conclude that the γ-ECS genes are highly conserved and their functions were important for the protein. This finding was in full agreement with the results of earlier studies [29].

When plants were challenged by heavy metals, salt, herbicides, hormones, extreme temperatures, and osmotic stresses, the expression levels of *γ-ECS* genes were stimulated [22, 37]. Owing to Ethrel stimulation, the latex yield increases up to 1.5–2.0-fold in rubber tree. Ethrel can improve latex yield, mainly by prolonging latex flow [4]. "Long-term flow" is a distinct feature of rubber tree long-term flowing latex (LFL); it has a longer flowing time than the normal flowing latex (NFL), whose flowing time is less than 6 h. On the one hand, the long duration of flowing time increases latex yield per tapping; on the other hand, rubber tree expends a lot of metabolic energy in case of long-term flow, so rubber plants take longer time for their renewal under such circumstances [30]. Our result indicated that Ethrel and long-term flow could enhance the mRNA transcription of *HbγECS1* in the latex. Consequently, as more thiols were synthesized in the latex under the stimulating conditions, the GSH-synthesizing capacity was also enhanced; thereby GSH levels were elevated [23]. Indeed, more GSH was detected in the latex when rubber tree was subjected to Ethrel stimulation. These results indicated that the regulatory mechanisms of *Hbγ-ECS1* in

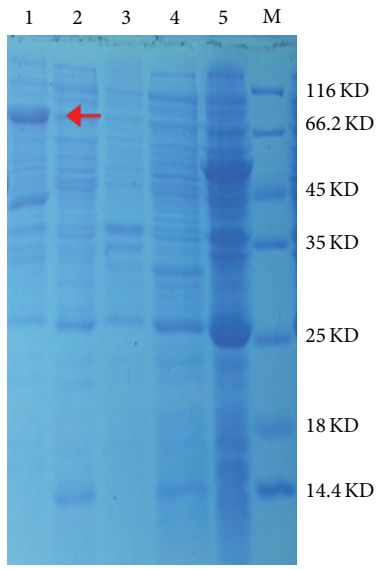

Figure 4: SDS-PAGE analysis of cloned *Hbγ-ECS1* expression. Partially purified recombinant *Hbγ-ECS1*, noninduced strain Rosetta/pET-sumo-*Hbγ-ECS1*, induced empty vector strain Rosetta/pET-sumo, wild *E. coli* Rosetta, cell supernatant of induced strain Rosetta/pET-sumo-*Hbγ-ECS1*, and protein ladder are present in lanes 1, 2, 3, 4, 5, and M, respectively.

Hevea brasiliensis are similar to those encountered in other plants. *HbγECS1* was more sensitive to Ethrel and increased significantly according to extending of Ethrel stimulation. However, owing to Ethrel and LFL, the latex production was higher than that witnessed in NFL. Hence, the expression of this gene is related to latex production.

Owing to Ethrel stimulation and long-term flow, the ephemeral stress response of *HbγECS1* was elicited in one tapping. Tapping means a kind of continuous injury to rubber tree. The expression level of *HbγECS1* varied with different tapping intensities, showing a durable reaction to tapping. Obviously, the expression levels of short-term and long-term tapping were not similar. There was an increase in the transcriptional levels of *HbγECS1* after the rubber tree was subjected to three-month routine tapping, but not significantly in Ethrel-stimulation tapping. This indicates that there was a feedback regulation mechanism according to the more tapping intensity; however, researchers had elucidated the role of feedback inhibition by GSH in *γECS* by a series of experiments. The injury induced by tapping and Ethrel stimulation could induce the generation of reactive oxygen in rubber tree latex [38–40]. The release of reactive oxygen leads to the peroxidative degradation of lutoid membrane. Moreover, thiol was one of the substances scavenging reactive oxygen, so it was closely related to the duration of latex flow. The expression of *Hbγ-ECS1* was regulated by the tapping intensity on rubber tree. *HbγECS1* was expressed in *E. coli* Rosetta using pET-sumo as an expression vector and the recombinant enzyme was tested for its ability catalyzing γ-EC biosynthesis from cysteine and glutamate. The molecular weight was about 66 kDa and frees up 7 KD comparing to anticipation because of his-tags.

On the basis of the information gathered in the present study, it was suggested that *Hbγ-ECS1* was a potential candidate that may be utilized in rubber tree genetic breeding for prolonging latex flowing time and increasing resistance.

Abbreviations

γ-ECS: Gamma-glutamylcysteine synthetase
GSH: Glutathione
GSHS: Glutathione synthetase
γ-EC: Gamma-glutamylcysteine
EST: Expressed sequence tags
RACE: Rapid amplification of cDNA ends
ORF: Open reading frame
qPCR: Quantitative real-time PCR
DTNB: Dithionitrobenzoic acid
MEGA: Molecular Evolutionary Genetics Analysis
TPD: Tapping panel dryness.

Competing Interests

The authors declare that they have no competing interests.

Acknowledgments

This work was supported by the National Natural Science Foundation of China (31200467) and China Agriculture Research System (CARS-34-GW7).

References

[1] A. Dusotoit-Coucaud, P. Kongsawadworakul, L. Maurousset et al., "Ethylene stimulation of latex yield depends on the expression of a sucrose transporter (*HbSUT1B*) in rubber tree (*Hevea brasiliensis*)," *Tree Physiology*, vol. 30, no. 12, pp. 1586–1598, 2010.

[2] F. Wei and X. Xiao, "Comparison on the physiological characters of three clones reyan7-33-97, PR107, RRIM600 of hevea brasiliensis," *Journal of Anhui Agrculture Science*, vol. 36, no. 18, pp. 7561–7563, 2008.

[3] F. Wei, S. Luo, J. Qiu et al., "Function of thiols in rubber tree latex and recent researches on thiols anabolism pathway in model plant," *Tropical Agrculture Science and Technology*, vol. 32, no. 8, pp. 12–17, 2012.

[4] J. D'auzac, J.-L. Jacob, and H. Chrestin, "Physiology of rubber tree latex," in *The Laticiferous Cell and Latex-A Model of Cytoplasm*, CRC Press, New York, NY, USA, 1989.

[5] A. I. McMullen, "Thiols of low molecular weight in Hevea brasiliensis latex," *Biochimica et Biophysica Acta*, vol. 41, no. 1, pp. 152–154, 1960.

[6] H. Chrestin, "Le compartiment vacuo-lysosomal (les lutoïdes) du latex d'Hevea Brasiliensis: son rôle dans le maintien de l'homéostasie et des les processus de sénescence des cellules laticifères," 1984.

[7] C. H. Foyer, H. Lopez-Delgado, J. F. Dat, and I. M. Scott, "Hydrogen peroxide- and glutathione-associated mechanisms of acclimatory stress tolerance and signalling," *Physiologia Plantarum*, vol. 100, no. 2, pp. 241–254, 1997.

[8] K. Ishikawa, K. Yoshimura, K. Harada et al., "AtNUDX6, an ADP-ribose/NADH pyrophosphohydrolase in Arabidopsis,

positively regulates NPR1-dependent salicylic acid signaling," *Plant Physiology*, vol. 152, no. 4, pp. 2000–2012, 2010.

[9] A. Mhamdi, J. Hager, S. Chaouch et al., "Arabidopsis GLUTATHIONE REDUCTASE1 plays a crucial role in leaf responses to intracellular hydrogen peroxide and in ensuring appropriate gene expression through both salicylic acid and jasmonic acid signaling pathways," *Plant Physiology*, vol. 153, no. 3, pp. 1144–1160, 2010.

[10] C. H. Foyer and G. Noctor, "Oxidant and antioxidant signalling in plants: a re-evaluation of the concept of oxidative stress in a physiological context," *Plant, Cell and Environment*, vol. 28, no. 8, pp. 1056–1071, 2005.

[11] A. D. Peuke and H. Rennenberg, "Phytoremediation," *EMBO Reports*, vol. 6, no. 6, pp. 497–501, 2005.

[12] R. B. Pereira, C. Sousa, A. Costa, P. B. Andrade, and P. Valentão, "Glutathione and the antioxidant potential of binary mixtures with flavonoids: synergisms and antagonisms," *Molecules*, vol. 18, no. 8, pp. 8858–8872, 2013.

[13] G. Kocsy, G. Szalai, A. Vágújfalvi, L. Stéhli, G. Orosz, and G. Galiba, "Genetic study of glutathione accumulation during cold hardening in wheat," *Planta*, vol. 210, no. 2, pp. 295–301, 2000.

[14] J. M. Ruiz and E. Blumwald, "Salinity-induced glutathione synthesis in Brassica napus," *Planta*, vol. 214, no. 6, pp. 965–969, 2002.

[15] L. D. Gomez, G. Noctor, M. R. Knight, and C. H. Foyer, "Regulation of calcium signalling and gene expression by glutathione," *Journal of Experimental Botany*, vol. 55, no. 404, pp. 1851–1859, 2004.

[16] S. Ghanta, D. Bhattacharyya, R. Sinha, A. Banerjee, and S. Chattopadhyay, "Nicotiana tabacum overexpressing γ-ECS exhibits biotic stress tolerance likely through NPR1-dependent salicylic acid-mediated pathway," *Planta*, vol. 233, no. 5, pp. 895–910, 2011.

[17] G. Noctor, A.-C. M. Arisi, L. Jouanin, K. J. Kunert, H. Rennenberg, and C. H. Foyer, "Glutathione: biosynthesis, metabolism and relationship to stress tolerance explored in transformed plants," *Journal of Experimental Botany*, vol. 49, no. 321, pp. 623–647, 1998.

[18] A. Galant, M. L. Preuss, J. C. Cameron, and J. M. Jez, "Plant glutathione biosynthesis: diversity in biochemical regulation and reaction products," *Frontiers in Plant Science*, vol. 2, article 45, 2011.

[19] G. Noctor, A. Mhamdi, S. Chaouch et al., "Glutathione in plants: an integrated overview," *Plant, Cell and Environment*, vol. 35, no. 2, pp. 454–484, 2012.

[20] M. J. May and C. J. Leaver, "Arabidopsis thaliana γ-glutamylcysteine synthetase is structurally unrelated to mammalian, yeast, and Escherichia coli homologs," *Proceedings of the National Academy of Sciences of the United States of America*, vol. 91, no. 21, pp. 10059–10063, 1994.

[21] H. J. Schäfer, S. Greiner, T. Rausch, and A. Haag-Kerwer, "In seedlings of the heavy metal accumulator *Brassica juncea* Cu^{2+} differentially affects transcript amounts for γ-glutamylcysteine synthetase (γ-ECS) and metallothionein (MT2)," *FEBS Letters*, vol. 404, no. 2-3, pp. 216–220, 1997.

[22] J. Wu, T. Qu, S. Chen, Z. Zhao, and L. An, "Molecular cloning and characterization of a γ-glutamylcysteine synthetase gene from *Chorispora bungeana*," *Protoplasma*, vol. 235, no. 1–4, pp. 27–36, 2009.

[23] C. Xiang and D. J. Oliver, "Glutathione metabolic genes coordinately respond to heavy metals and jasmonic acid in *Arabidopsis*," *Plant Cell*, vol. 10, no. 9, pp. 1539–1550, 1998.

[24] M.-J. Bae, Y.-S. Kim, I.-S. Kim et al., "Transgenic rice overexpressing the Brassica juncea gamma-glutamylcysteine synthetase gene enhances tolerance to abiotic stress and improves grain yield under paddy field conditions," *Molecular Breeding*, vol. 31, no. 4, pp. 931–945, 2013.

[25] L. A. Ivanova, D. A. Ronzhina, L. A. Ivanov, L. V. Stroukova, A. D. Peuke, and H. Rennenberg, "Over-expression of gsh1 in the cytosol affects the photosynthetic apparatus and improves the performance of transgenic poplars on heavy metal-contaminated soil," *Plant Biology*, vol. 13, no. 4, pp. 649–659, 2011.

[26] C.-R. Wu, C.-W. Tsai, S.-W. Chang, C.-Y. Lin, L.-C. Huang, and C.-W. Tsai, "Carnosic acid protects against 6-hydroxydopamine-induced neurotoxicity in in vivo and in vitro model of Parkinson's disease: involvement of antioxidative enzymes induction," *Chemico-Biological Interactions*, vol. 225, pp. 40–46, 2015.

[27] H. Li, J.-L. Han, J. Lin, Q.-S. Yang, and Y.-H. Chang, "A γ-glutamylcysteine synthetase gene from *Pyrus calleryana* is responsive to ions and osmotic stresses," *Plant Molecular Biology Reporter*, vol. 33, no. 4, pp. 1088–1097, 2014.

[28] A. Rüegsegger and C. Brunold, "Effect of cadmium on γ-glutamylcysteine synthesis in maize seedlings," *Plant Physiology*, vol. 99, no. 2, pp. 428–433, 1992.

[29] D. Sengupta, G. Ramesh, S. Mudalkar, K. R. R. Kumar, P. B. Kirti, and A. R. Reddy, "Molecular Cloning and Characterization of γ-Glutamyl Cysteine Synthetase (VrγECS) from roots of vigna radiata (L.) wilczek under progressive drought stress and recovery," *Plant Molecular Biology Reporter*, vol. 30, no. 4, pp. 894–903, 2012.

[30] F. Wei, S. Luo, Q. Zheng et al., "Transcriptome sequencing and comparative analysis reveal long-term flowing mechanisms in *Hevea brasiliensis* latex," *Gene*, vol. 556, no. 2, pp. 153–162, 2015.

[31] L. B. Poole, "The basics of thiols and cysteines in redox biology and chemistry," *Free Radical Biology & Medicine*, vol. 80, pp. 148–157, 2015.

[32] M. Zermiani, E. Zonin, A. Nonis et al., "Ethylene negatively regulates transcript abundance of ROP-GAP rheostat-encoding genes and affects apoplastic reactive oxygen species homeostasis in epicarps of cold stored apple fruits," *Journal of Experimental Botany*, vol. 66, no. 22, pp. 7255–7270, 2015.

[33] X. Gidrol, H. Chrestin, H.-L. Tan, and A. Kush, "Hevein, a lectin-like protein from Hevea brasiliensis (rubber tree) is involved in the coagulation of latex," *The Journal of Biological Chemistry*, vol. 269, no. 12, pp. 9278–9283, 1994.

[34] K. Ogawa, "Glutathione-associated regulation of plant growth and stress responses," *Antioxidants and Redox Signaling*, vol. 7, no. 7-8, pp. 973–981, 2005.

[35] R. Sánchez-Fernández, M. Fricker, L. B. Corben et al., "Cell proliferation and hair tip growth in the Arabidopsis root are under mechanistically different forms of redox control," *Proceedings of the National Academy of Sciences of the United States of America*, vol. 94, no. 6, pp. 2745–2750, 1997.

[36] C. Xiang, B. L. Werner, E. M. Christensen, and D. J. Oliver, "The biological functions of glutathione revisited in Arabidopsis transgenic plants with altered glutathione levels," *Plant Physiology*, vol. 126, no. 2, pp. 564–574, 2001.

[37] G. Innocenti, C. Pucciariello, M. Le Gleuher et al., "Glutathione synthesis is regulated by nitric oxide in Medicago truncatula roots," *Planta*, vol. 225, no. 6, pp. 1597–1602, 2007.

[38] D. Ke and A. Wang, "The effect of activated oxygen during the production of engenous ethylene induced by exogenous ethylene," *Plant Physiology Journal*, vol. 23, no. 1, pp. 67–72, 1997.

[39] X. Xiao, "Discussion of ethrel hurt and production mechanism in rubber tree," *Tropical Agrculture Science*, no. 4, pp. 7–11, 2000.

[40] L. Cai and X. Xiao, "Production and eliminating of active oxygen in rubber tree laticifers," *Journal of South China University of Tropical Agriculture*, vol. 6, no. 1, pp. 31–34, 2000.

Hindawi Publishing Corporation
BioMed Research International
Volume 2016, Article ID 3747501, 13 pages
http://dx.doi.org/10.1155/2016/3747501

Review Article

Involvement of Hormone- and ROS-Signaling Pathways in the Beneficial Action of Humic Substances on Plants Growing under Normal and Stressing Conditions

Andrés Calderín García,[1] Maite Olaetxea,[2] Leandro Azevedo Santos,[1] Verónica Mora,[2] Roberto Baigorri,[2] Marta Fuentes,[2] Angel Maria Zamarreño,[2] Ricardo Luis Louro Berbara,[1] and José María Garcia-Mina[2]

[1]*Soil Biology Laboratory, Department of Soil, Federal Rural University of Rio de Janeiro (UFRRJ), Rodovia BR 465 km 7, 23890-000 Seropédica, RJ, Brazil*
[2]*Department of Environmental Biology, Agricultural Chemistry and Biology Group-CMI Roullier, Faculty of Sciences, University of Navarra, C/Irunlarrea 1, 31008 Pamplona, Spain*

Correspondence should be addressed to Ricardo Luis Louro Berbara; rberbara@hotmail.com and José María Garcia-Mina; jgmina@unav.es

Received 31 December 2015; Revised 10 April 2016; Accepted 3 May 2016

Academic Editor: Yan-Bo Hu

The importance of soil humus in soil fertility has been well established many years ago. However, the knowledge about the whole mechanisms by which humic molecules in the rhizosphere improve plant growth remains partial and rather fragmentary. In this review we discuss the relationships between two main signaling pathway families that are affected by humic substances within the plant: one directly related to hormonal action and the other related to reactive oxygen species (ROS). In this sense, our aims are to try the integration of all these events in a more comprehensive model and underline some points in the model that remain unclear and deserve further research.

1. Humic Substances and Plant Development

Numerous studies have reported the beneficial effects of dissolved organic matter (DOM) in both mineral nutrition and development of plants cultivated in many different soil types [1–3]. These effects of DOM are normally related to the presence of a specific fraction of organic molecules known as humic substances (HS). The presence of HS in DOM results from the solubilization and/or runoff of a pool of soil organic matter produced by the transformation of vegetal and animal residues by the action of soil microorganisms and chemical reactions (redox reactions, hydrolysis, and polymerization), both influenced by the environmental conditions (temperature, humidity, soil texture, and pH) [4]. Depending on soil chemical composition and physical features, in soil matrix transformed organic matter is normally associated with minerals, mainly clays and silicates, forming organomineral complexes [4]. These organomineral complexes play a key role in the formation of soil microaggregates, which in turn improve soil porosity, water permeation, and oxygen exchange, thus enhancing soil fertility [2, 4]. In water solution, HS tends to aggregate forming new stable multimolecular systems with specific chemical and biological activities [5, 6]. In this sense, these molecular aggregates can be considered as a family of natural supramolecules or supermolecules [5, 6].

In terms of soil organic matter and more generally due to the complexity and heterogeneity of the humic supramolecules, their definition and classification are rather operational and are based on the different water solubility of HS components as a function of pH and ionic strength [4]: humic acids (HA) (soluble at basic pH but insoluble at acid pH), fulvic acids (FA) (soluble at acid and basic pH), and Humin (insoluble at all pH). Taking into account that HS classification is merely operational, we proposed the introduction in this classification the origin and/or chemical nature of the organic material employed to obtain HA, FA,

and Humin [7]. Thus, in this modified classification we have the following.

(i) Artificial HS (AHS). This indicates organic substances extracted by IHSS-method (IHSS, International Humic Substances Society) from organic materials modified or transformed by using diverse alternative or complementary process different from composting, such as controlled pyrolysis (biochar), chemical oxidation, and anaerobic digestion (digestates). These HS may be named Artificial HS (AHS), and their fractions are as follows: artificial humic acids (AHA) and artificial fulvic acids (AFA).

(ii) Fresh HS (FHS). This indicates organic substances extracted by IHSS-method from intact, non-biologically or chemically modified, fresh (living) organic materials, such as plant or animal fresh residues (leaves, whole shoot, root, animal or fish flour, wood, and seaweed). These HS may be named Fresh HS (FHS) and their fractions are as follows: fresh humic acids (FHA) and fresh fulvic acids (FFA).

(iii) Compost HS (CHS). This indicates organic substances extracted by IHSS-method from composted organic materials. These HS may be named Compost HS (CHS) and their fractions are as follows: compost humic acids (CHA) and compost fulvic acids (CFA).

(iv) Sedimentary HS (SHS). This indicates organic substances extracted by IHSS-method from naturally humified organic matter with sedimentary origin present in terrestrial (soils, coal, leonardite, and peats) and aquatic (lakes, rivers, and sea) environments. These HS may be named Sedimentary HS (SHS), and their fractions are as follows: sedimentary humic acids (SHA) and sedimentary fulvic acids (SFA).

In principle, only SHS and, by analogy, CHS should properly be considered as HS since they are produced from fresh organic materials and processes both present in natural environments.

A number of studies have reported that HS in solution, mainly SHS and CHS, can affect plant development [1–3, 7]. These effects of HS have normally been differentiated in indirect effects and direct effects [7, 8]. The indirect effects are linked to the action of HS on plant growth by modifying soil or substrate features in the rhizospheric area, principally the pool of potentially bioavailable nutrients and physical texture [7, 8]. The direct effects result from the direct interaction of HS with plant roots or leaves [7, 8]. These effects are reflected in significant changes in metabolic and developmental processes within the plant at transcriptional and posttranscriptional levels [7]. On the other hand, the whole action of HS on plant growth is also influenced by factors that are intrinsic and/or extrinsic to HS in itself. The former is related to HS functional and structural composition and spatial conformation, while the latter is associated with environmental conditions (abiotic and biotic stresses, soil fertility, and crop type), as well as agronomic practices and management (moment of application, doses, and type of application) [7].

In general, the HS concentrations in the rhizosphere that is necessary to affect plant development and mineral nutrition through indirect effects and/or direct effects mediated mechanisms are different to each other [8]. Thus, HS indirect effects can be observed for very low HS concentrations in soil solution (HS $< 5\ mg\ L^{-1}$) since their effects on plant growth are normally linked to their ability to provide complexed micronutrients to plants grown in soils prone to micronutrient deficiency [8–10]. However, consistent HS direct effects are associated with relatively high concentrations of HS in soil solution in the rhizospheric area (HS concentration range: 50–300 $mg\ L^{-1}$) [8]. Consequently, HS indirect effects mediated actions are probably the main general mechanism involved in the beneficial action of HS in nonirrigated crops growing in dry land types of soils (e.g., Mediterranean climate), while HS direct effects are probably present, along with HS indirect effects, in irrigated crops (pivot, drip, or sprinkle irrigation), where HS are applied through the irrigation system and therefore localized to the root area (greenhouses and open field irrigated crops).

It is well known that HS have beneficial effects on plant development when applied to both the rhizosphere and leaves (foliar sprays) [3, 8]. In this review we deal with the signaling pathways involved in the direct effects on plant development of HS present in the rhizosphere. Taking into account the relevance and novelty of recent results stressing the important role of reactive oxygen species- (ROS-) related signals in HS action on plant roots and plant development under abiotic stresses [11], we also focus our discussion on the crosstalk between the hormonal signaling pathways and ROS-related pathways related to the action of rhizospheric HS.

2. Main Signaling Pathways Involved in HS Action in Plants

Although the mechanism of action of HS has extensively been studied for many years, the knowledge about them is rather fragmentary and it has not been integrated in a comprehensive model yet [7]. In general, all findings reported so far clearly show that HS direct effects mediated action involves several different, but probably interconnected, mechanisms integrated into a complex network of events occurring at both transcriptional and posttranscriptional levels [7].

2.1. HS-Mediated Enhancement of Shoot Growth. In the case of rhizospheric HS, direct effects mediated actions have to derive from the interaction of HS with plant roots. Although the possible penetration of some HS fraction into root apoplast and epidermal cell areas has been proposed, results are not very conclusive yet [7]. However, the physical accumulation of HS on root surface has been proved and, therefore, some biological effects on plant development, either on root or on shoot, resulting from it cannot be ruled out [7, 11, 12].

Regarding shoot growth promotion, studies carried out in cucumber with a sedimentary humic acid (SHA) obtained from leonardite reported the important roles of cytokinins (CKs) and mineral nutrient root to shoot translocation in the

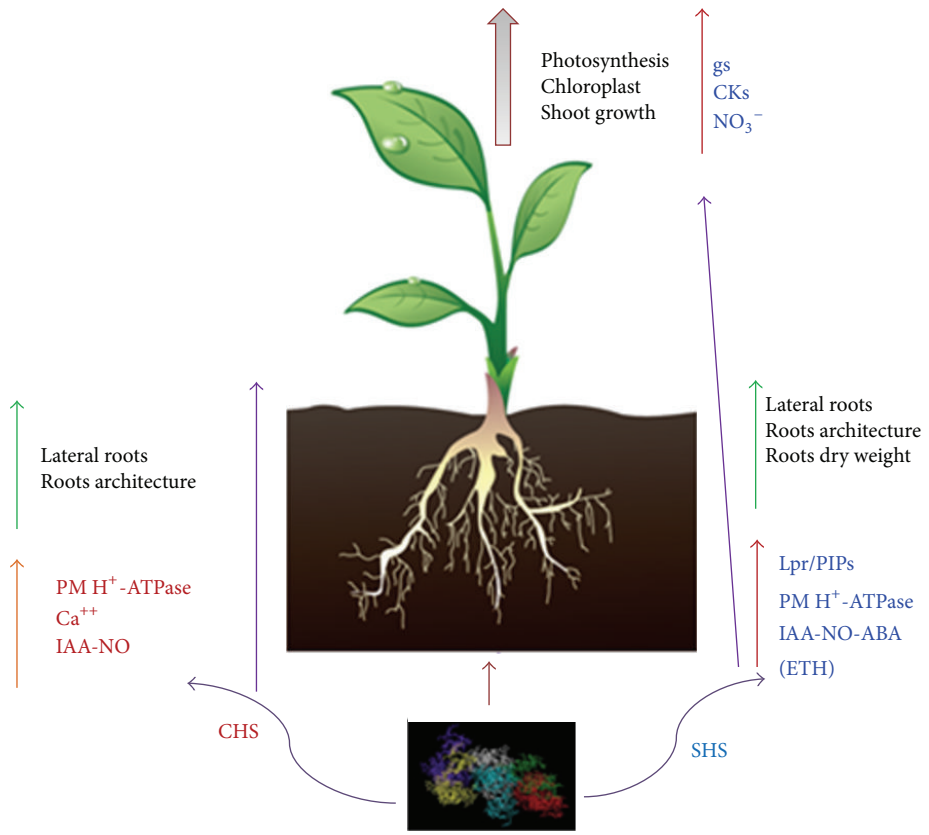

Figure 1: Main hormonal-related signaling pathways affected by humic substances obtained from compost (CHS) or natural sediments (SHS) and some of their biochemical and physiological effects at whole plant level. The metabolic effects of CHS (in red) are associated with stimulation of metabolic pathways belonging to the stimulation of H^+-ATPase (PM H^+-ATPase), Ca^{++} transport, and signaling pathways of auxin-nitric oxide (AUX-NO). Therefore, the morphological effects are related to stimulation of lateral roots and improved root architecture. The metabolic effects of SHS (in blue) in plants occur by stimulating the metabolic pathways belonging to the stimulation of H^+-ATPase enzymes, signaling through pathways of auxin-nitric oxide abscisic acid (Aux-NO-ABA), expression of responsive genes for membrane aquoporins (PIPs) and hydraulic conductivity (Lpr). Therefore, the morphological effects are related to stimulation of lateral root, root architecture improvements, and increased root biomass. These root physiological effects are associated with events in leaf related to stomatal conductance (gs), cytokinins (CKs), and nitrate (NO_3^-), finally setting off on effects on leaf growth, photosynthesis, and chloroplasts.

shoot growth promoting effect of SHA [13]. This effect was, in turn, linked to an increase in plasma membrane (PM) H^+-ATPase activity and nitrate root to shoot translocation [13, 14]. In line with this potential role of CKs in HS action on plants, further studies on rapeseed showed significant improvements in chloroplast functionality and photosynthesis upon the root application of a SHA obtained from black peat [15]. These physiological effects of SHA were consistent with the upregulation of gene-clusters directly linked to all abovementioned developmental functions such as photosynthesis, CKs signaling perception, and N, S, and C metabolisms [15].

On the other hand, the shoot growth promoting action of SHA in cucumber was dependent on the increase in indoleacetic acid (IAA) and nitric oxide (NO) concentrations in roots caused by SHA root application [14]. Recently, further studies also stressed the crucial role played by an abscisic acid- (ABA-) mediated increase in root hydraulic conductance and aquaporin gene expression in the shoot growth enhancement caused by SHA root application [12]. We have not found any information about the role of a HS-mediated increase in ROS, whether in the root or in the shoot, in the beneficial action of HS on shoot growth. Ongoing studies might throw light on this issue.

Overall, these results indicate that several interconnected hormone-dependent signaling pathways as well as physiological events are involved in the shoot promotion caused by HA with sedimentary origin (Figure 1).

2.2. HS-Mediated Enhancement of Root Growth. Regarding HS direct effects on root development, two main types of phenotypic effects might be distinguished: micromorphological effects (an increase in both absorbent hairs and lateral roots proliferation) and macromorphological effects (an increase in root dry weight, secondary roots number, and primary and secondary roots thickness) [20–23].

Several research groups working with HA obtained from vermicomposts of various vegetal residues (CHA) have reported their ability to promote lateral root proliferation and modify root architecture [21–23]. These studies showed that this effect was associated with an activation of root PM - H^+-ATPase activity and expressed through auxin (indoleacetic acid, IAA) and probably NO dependent pathways [21–25].

Further studies also suggested that these signaling pathways activated by CHA are expressed at posttranscriptional level through calcium-dependent protein phosphorylation [26]. These effects mediated by hormonal signaling pathways have been shown to be dominated by an upregulation of genes responsive to the synthesis of auxin in both roots (corn and tomato) as whole plant (*Arabidopsis*), as well as other genes encoding metabolic pathways belonging to the taking of nutrients [21–25] (Figure 1).

The effect of CHA has been explained in view of their suprastructural organization. Studies show that the HS may be present and may be released structural fragments and/or molecules to the rhizosphere, with auxin activity and/or structural arrangements similar to auxins [21]. In fact, it is not surprising that composted or vermicomposted fresh vegetal materials have low concentrations of several plant hormones in their molecular systems [21].

The results obtained in studies with HA from sedimentary origin (SHA) also showed the involvement of relevant phytoregulators in SHA-mediated effects on root development [7, 12–15]. The application of SHA to roots of cucumber plants was associated with significant phenotypic effects in roots both at micro- and at macromorphologic scales; these effects were associated with an increase in IAA, ethylene (ETH), NO, and abscisic acid (ABA) concentration in roots. However, further studies showed that the macromorphological effects of SHA could not be explained as a result of its action increasing IAA, ETH, or NO in roots. In consequence, other factors different from IAA, NO, or ETH have to be involved in SHA-mediated increases of root dry weight, secondary roots proliferation, and root thickness [20]. These results are consistent with other results showing that some effects on root architecture of a water soluble fraction of HS obtained from peat were not explained by auxin and/or ETH-dependent pathways in *Arabidopsis* [27] (Figure 1).

Regarding the physical and/or chemical events occurring at root surface as a result of the interaction of SHA with cell walls, the hypotheses proposed for CHA consisting of the presence of hormones and/or auxin-like structural domains in SHA superstructure are not suitable. This is because an extensive analysis of the main plant phytoregulators in SHA by using LC/MS/MS revealed that all these compounds were under detection limits [7, 12–15, 20]. Recent results suggest that the first events caused by SHA at root surface could result from a fouling-mediated transient blockage of cell wall pores, which in turn would be associated with a transient mild water stress, a beneficial stress, "eustress," that triggers downstream SHA-mediated effects on hormonal signaling pathways and plant development. This mechanism would be linked to the supramolecular conformation of SHA [12].

In this context, recent complementary studies suggest the potential role of a new family of molecules involved in signaling in plants [11, 16, 19, 28]. Several studies have shown the relevant role of ROS as an alternative signaling pathway for the regulation and expression of the effects of CHA on lateral root proliferation in rice [16, 19]. Although these results concerning ROS will be discussed below more in depth in connection with other hormonal regulated pathways affected by CHA, these studies clearly showed that CHA increased ROS production and accumulation in roots as well as the antioxidative enzyme network needed to modulate ROS final concentration [16, 28]. The CHA-mediated balance between ROS production and ROS scavenging seemed to be crucial for the signaling role of ROS in CHA direct effects on lateral root proliferation. Interestingly, the CHA-mediated effect on ROS homeostasis in rice roots was associated with a concomitant increase in root dry weight, an effect that was not explained by the increases of IAA, NO, or ETH mediated by SHA in cucumber [16, 19, 20]. This fact suggests that the whole effects caused by HS on root phenotype, both macro- and micromorphological, may involve two pathways, one hormonal-dependent (micromorphological effects) and the other ROS-dependent (macromorphological) (Figure 2).

The involvement of these two pathways is compatible with the role of Ca^{2+}-dependent protein kinase activity and protein phosphorylation as second messengers in the posttranscriptional expression of HS activity [26] (Figure 2).

3. Crosstalk between Hormone-Mediated Signaling and ROS-Mediated Signaling Pathways in HS Beneficial Effects on Plant Development

As commented above a number of studies have shown the ability of HS to promote plants shoot and root growths [3]. Studies carried out with HA obtained from vermicomposted materials and sediments reported that these HS's beneficial action in plants was functionally linked to an activation of several, interconnected, hormone-mediated signaling pathways; these effects of HS in roots involving some signaling pathways dependent on the hormonal network formed by IAA(ETH)-NO-ABA have been observed in several plant species and have been confirmed using the reporter gene *DR5:GUS* and the expression of auxin-responsive genes, including *IAA19* in *Arabidopsis* [7, 14, 22, 23, 29–32].

Root morphological auxin-like effects and their relationships with other mechanisms of action were investigated by Schmidt et al. [27], who demonstrated that no morphological changes in secondary roots or root hair defective (*rhd6*) mutant recovery occur in *Arabidopsis* with the application of low-molecular-weight HS. This study also showed that *Arabidopsis* strains transformed with the reporter gene *uidA* (GUS) fused to auxin-responsive promoters (*DR5:uidA* and *BA3:uidA*) showed no change or a low response to HS application, concluding that the effects of low-molecular-weight HS may alter root morphology, by increasing the root surface through auxin-independent signaling pathways. In this line, Mora et al. [20] demonstrated that increases in IAA and ETH levels as well as NO in cucumber plant roots had no decisive role in root macromorphological changes (root growth, secondary root proliferation, and root thickness) upon SHA application. The authors conclude that other effects different from those related to IAA, ETH, or NO could act coordinately or independently in stimulating root growth.

In parallel with these studies, other studies reported metabolic changes of reactive oxygen species (ROS) in

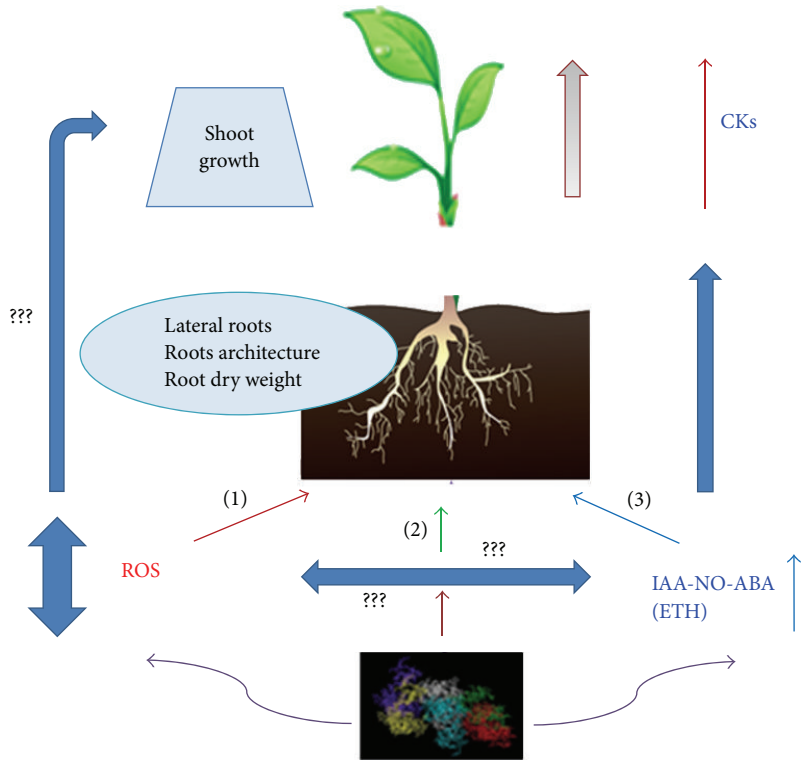

Figure 2: Hypothetical mechanism integrating hormonal-dependent and ROS-dependent signaling pathways in the whole action of humic substances on plant root and shoot. (1) ROS-dependent pathway, (2) hormonal ROS crosstalk pathway, and (3) hormonal-dependent pathway. ???: the causal relationships between IAA-NO-ABA and ROS are yet unknown.

rice plants upon vermicompost (VC) HA root application. Studies conducted by García et al. [11, 16, 19] demonstrated that the application of cattle manure VC-extracted HA (CHA) to rice plants stimulates certain oxidative metabolism components. CHA application regulates the activity of the enzymes peroxidase (POX), ascorbate peroxidase (APOX), catalase (CAT), and superoxide dismutase (SOD) differently depending on the concentration and exposure time, and this redox regulation simultaneously modulates leaf and root $O_2^{\bullet-}$ levels [16]. Regulation of oxidative metabolism in rice plants was demonstrated by the protective effects of CHA when applied to plants subjected to polyethylene glycol (PEG) induced water stress. The presence of CHA at concentrations of 40 mg (C) L^{-1} increased the levels of H_2O_2 and decreased lipid peroxidation, possibly via the transformation and control exercised by POX enzymes [19].

These studies also showed that CHA application promoted lateral root proliferation, in line with a large number of other studies [20, 22, 23, 29]. However, this study also observed an increase in root dry matter associated with no increase in endogenous root IAA levels in response to this application. This result is consistent with results reported by Mora et al. [20] showing that root growth SHA-mediated increase was independent of IAA, NO, and ETH. Conversely, significant increases in root H_2O_2 levels and POX enzymatic activity were found in young rice plants (Figure 3).

Taken together, these results show that CHA can, at least in part, regulate the oxidative metabolism associated with root growth. Accordingly, many studies have demonstrated the regulatory role of ROS in many signaling pathways, especially in plants growing under abiotic stresses [33].

The results discussed above on the regulation and control of ROS in roots by the action of HA indicate involvement of redox metabolism in the HS mode of action. These forms of action could occur in association (dependent or independent) with known hormonal signaling pathways. In this sense, studies have reported regulatory relationships between hormone and redox metabolism, specifically in signaling pathways related to both auxin metabolism and ROS [34, 35] (Figure 4).

Figure 4 shows three key points for understanding the auxin signaling pathways that may be affected by HS in their action on plant roots. Point 1 in Figure 4 identifies hormone recognition by the ABP1 receptor. Although recent studies showed that the role of this receptor in auxin-mediated recognition must be reevaluated [36], studies have also shown that the auxin signaling pathway is triggered by a perception complex composed of ABP1 and transmembrane kinases (TMK) [36]. However, there is no experimental evidence showing an activation of this ABP1 receptor or ABP1-TMK receptor complex by HS. The lack of evidence of HS binding to this receptor does not invalidate the fact that HS might act by increasing plant auxin synthesis or that auxin-like compounds present in HS, or even auxins themselves released by the structure of HS, might be recognized by these receptors.

Point 2 in Figure 4 shows auxin transport. Cellular influx (AUXIN1/LIKE-AUX1) and efflux (PIN-FORMED (PIN) and P-GLYCOPROTEIN (PGP)) auxin transporters have been

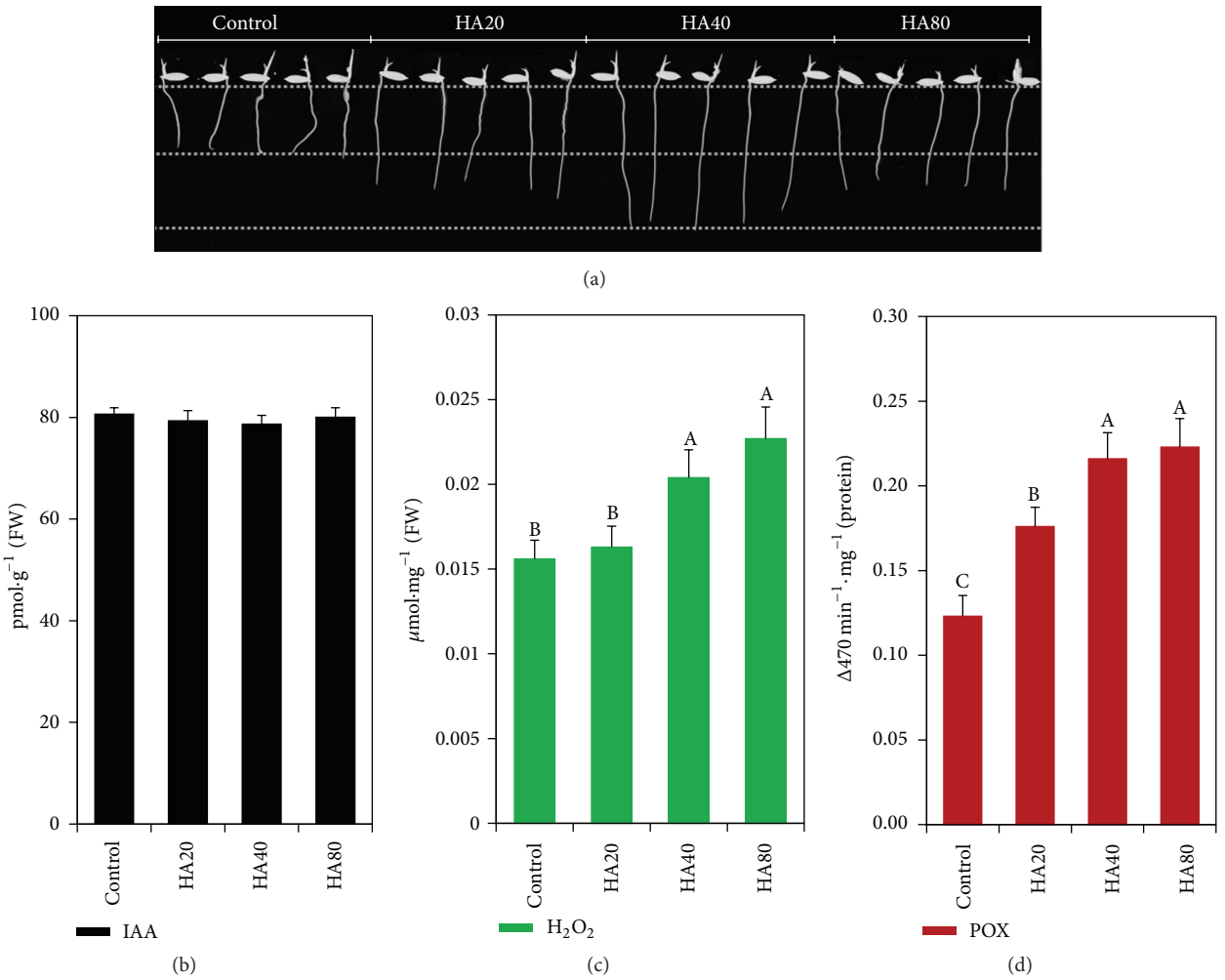

FIGURE 3: Relationship between rice plant root growth (root length) (a), indole-3-acetic acid (IAA) root levels (b), components of the root redox regulation system (H_2O_2 levels) (c), and the relative activity of peroxidases (POX) (d). The stimulation of root growth is dependent on the concentration of humic acid; in this case, 40 mg (C) L^{-1} stimulates the growth of the radicle (a) without the increase of indoleacetic acid concentrations in the roots (b); however, it is possible to observe increase in hydrogen peroxide concentrations (H_2O_2) and the peroxidases activity (POX). Different letters represent significant differences between the average values of treatments, as determined by Tukey's test; $p < 0.05$. The error bar represents the mean ± standard error (SE) of three replicates. (Figures were modified from the original papers published at García et al. [16] for better adapting to this review.)

identified in the literature, wherein AUX1 is involved in secondary root growth [37]. Although the action of HS on secondary root growth and emission as well as the root stimulation of H^+-ATPase enzymes has already been demonstrated, studies showing the involvement of auxin transporters in HS-mediated signaling pathways have not been published so far.

Point 3 in Figure 4 relates auxin signaling pathways to redox regulation. Plant oxidative system regulation by HS application was established decades ago by Vaughan et al. [38, 39], who showed that HA and fulvic acid (FA) inhibit the activity of POX in wheat plant roots and stimulate *in vitro* $O_2^{\bullet-}$ production [39]. In this line, HA application to maize plants also stimulated CAT activity and ROS production [28]. ROS production and stimulation of oxidative system enzymes have also been shown in rice plants [11]. In this context, few studies have investigated the gene expression codifying this enzymatic system. However, 9% of transcripts produced and stimulated by HA application in *Arabidopsis* have been shown to correspond to stress response metabolism using large-scale gene expression methods (microarray and cDNA-AFLP) [40]. The same response was observed in *Brassica napus*, wherein HA application stimulated 5.8% and 6.6% of stress response-related genes in shoots and roots, respectively [15].

3.1. Roles of ROS in Plant Root Growth and the Effects of HS on Plant Development. Most studies have shown a beneficial morphological effect on root system growth, albeit with different metabolic pathways involved in the HS mechanism of action in plants [20, 21]. The involvement of ROS in root cell elongation via Ca^{2+} channel activation is currently known [41]. ROS activation of Ca^{2+} channels is a key step in the regulation of other important processes, including antistress regulation and hormone signaling [42]. ROS produced by

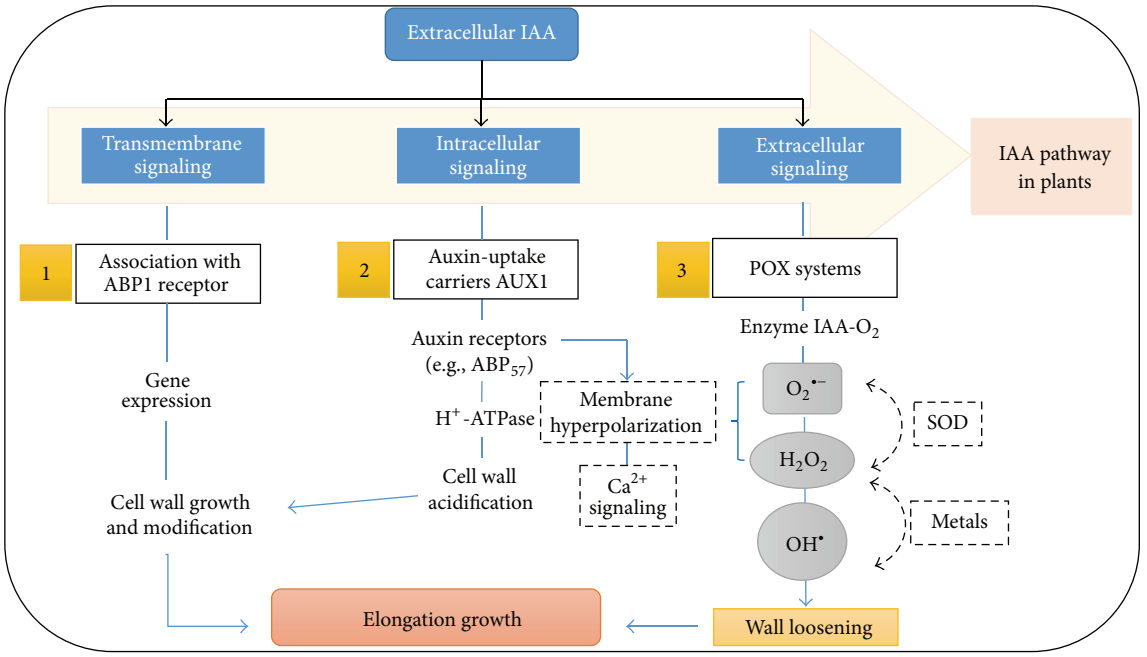

FIGURE 4: Mechanism of action via auxin signaling pathways compared to the redox mechanism in plant cell growth processes (adapted from [17]).

NADPH oxidase enzymes create a Ca^{2+}gradient in the apical root region, leading to secondary root growth [43]. Stimulation of calcium-dependent protein kinase (CPDK) activity in rice plant roots and increased *OsCPK7* and *OsCPK17* gene expression upon CHA application have been reported [26].

Although studies on the role of ROS as signaling molecules involved in root growth regulation remain ongoing, it has been reported that $OH^{\bullet}$ species resulting from an increase in apoplast H_2O_2may increase membrane permeability and therefore cellular Ca^{2+} influx [44]. $O_2^{\bullet-}$ and H_2O_2 are apparently directly related to secondary root growth and emission acting on different regions. Thus, $O_2^{\bullet-}$ predominantly accumulates in root elongation regions, whereas H_2O_2 accumulates in root differentiation regions [45].

Root CHA application has shown that several components of the redox regulation system are simultaneously stimulated during the root growth promoted by CHA. Root CHA application to rice plants generates increases of ROS located in different root regions depending on the species. The $O_2^{\bullet-}$ anions are detected at higher concentrations in the root elongation region of plants, whereas H_2O_2 is more concentrated in the root differentiation region (Figure 5(a)).

The CHA was also able to increase membrane permeability, as assessed by the release of electrolytes (Figure 5(b)). Simultaneously, the relative activities of SOD and CAT enzymes directly linked to the transformation and regulation of $O_2^{\bullet-}$ and H_2O_2 species, respectively, also responded to CHA application (Figures 5(c) and 5(d)).

The roles of ROS in metabolic processes related to plant cell differentiation, specifically those related to redox regulation and cell signaling pathways, are currently an open field of study. However, their involvement in secondary root growth and development is more evident today [46, 47]. Simultaneously, high ROS concentrations in plant tissues, primarily due to the presence of stresses, are known to have toxic effects and may trigger lipid peroxidation and protein denaturation reactions and occasionally lead to cell death [48, 49].

Therefore, the role of ROS as signaling molecules or intermediate species in the HS mode of action in plants seems to respond to a fine adjustment action of redox homeostasis, where the final result is in beneficial effects, including root growth. It is known that this mechanism may be highly dependent on the HS concentration applied to plants. Adverse effects on the root system have been observed in *Brachiaria* upon HA application at high concentrations, and a redox imbalance caused by the high concentrations applied may lead to impaired root growth (Figure 6).

3.2. ABA and Aquaporins as Important Factors Involved in the Effects of HS in Plants. ABA is a hormone that plays a key role in plant signaling pathways. ABA regulates and participates in H_2O_2 production and Ca^{2+} channel signaling for stomata opening and closing [46, 47]; at the same time, ABA regulates plasma membrane intrinsic protein (PIP) in rice plants under water stress conditions [50]. Others studies have shown that application to rice plants also stimulates the expression of genes of the tonoplast intrinsic aquaporin (TIP) subfamily [51], where the involvement of the TIP subfamily in osmoregulation and water flow through tonoplasts has been demonstrated [52].

Both ABA and TIP-PIP subfamilies are involved in the mechanisms of action of HS in plants. Thus, the root application of SHA to cucumber plants caused a differential increase in ABA levels in roots and shoots [12–14]. Conversely, the application of vermicompost CHA to rice

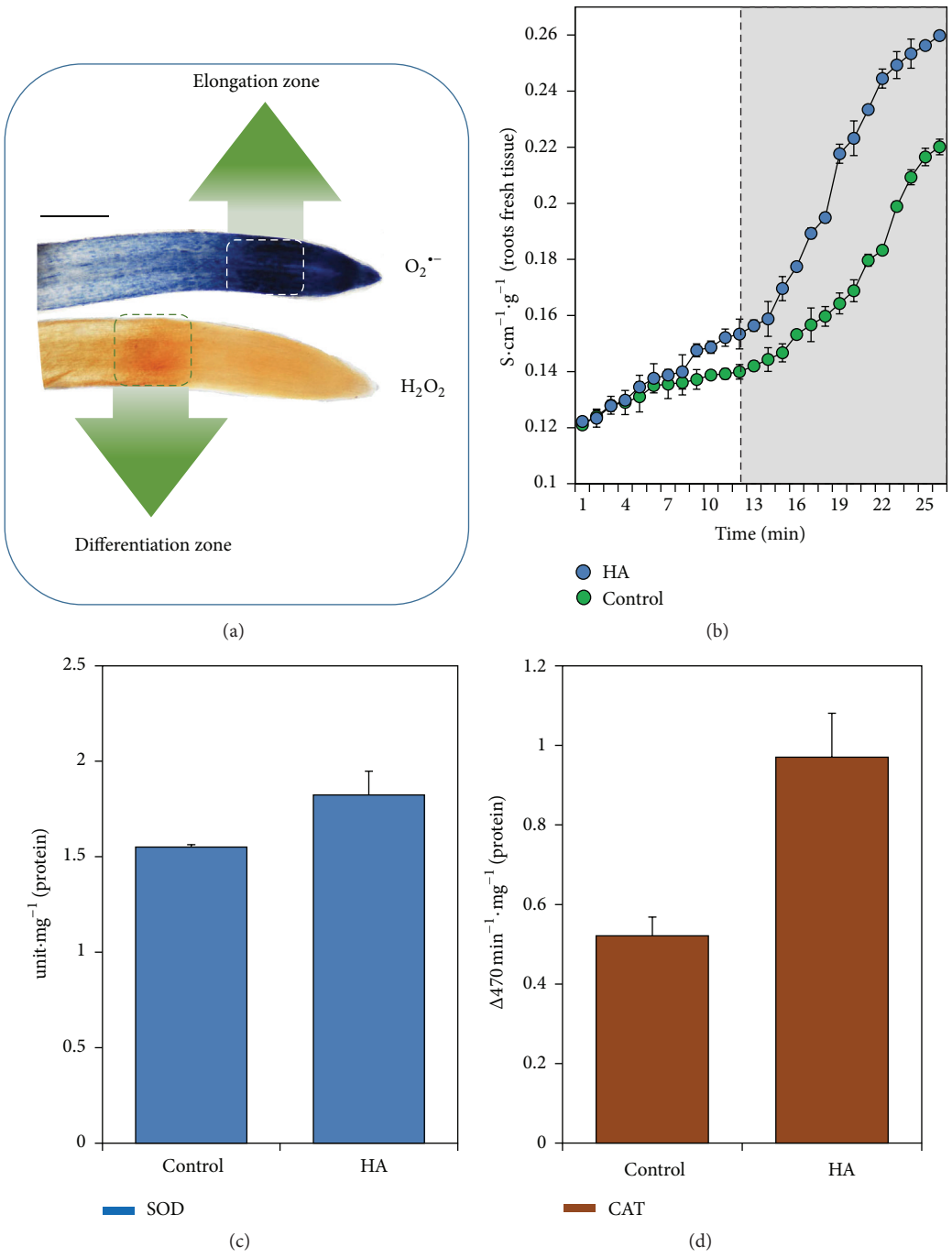

Figure 5: Effect of HA application in roots of rice plant. Histochemistry for determining the location of reactive oxygen species (ROS) ($O_2^{\bullet-}$ and H_2O_2) (a); membrane integrity (release of electrolytes) (b); superoxide dismutase (SOD) (c); and catalase (CAT) (d) enzymatic activity. The root application HA in plants modulates ROS content in the roots where superoxide anions ($O_2^{\bullet-}$) appear to be greater in cell elongation content region, while the H_2O_2 content seems to have greater differentiation in region (a). The presence of ROS seems to modify the permeability of the membrane (b) but under control exercised by the antioxidant metabolism (c and d). (These figures were modified from the original papers published at García et al. [18] for better adapting to this review.)

plants subjected to PEG-6000-induced water stress decreased the high levels of ABA in roots under stress [16]. This evidence indicates the involvement of ABA in the hormonal signaling pathways regulated by HA in plants growing under normal and stress environmental conditions. In this line, Olaetxea et al. [12] indicated the crucial role of root ABA and its regulation of root hydraulic conductivity in the shoot growth promoting action of a SHA in cucumber. On the other hand, the relationships between HA mediated effects in plants and root ABA signaling pathways also suggest a potential role of ABA-regulated aquaporins in HS action on plant development. In fact, Olaetxea et al.

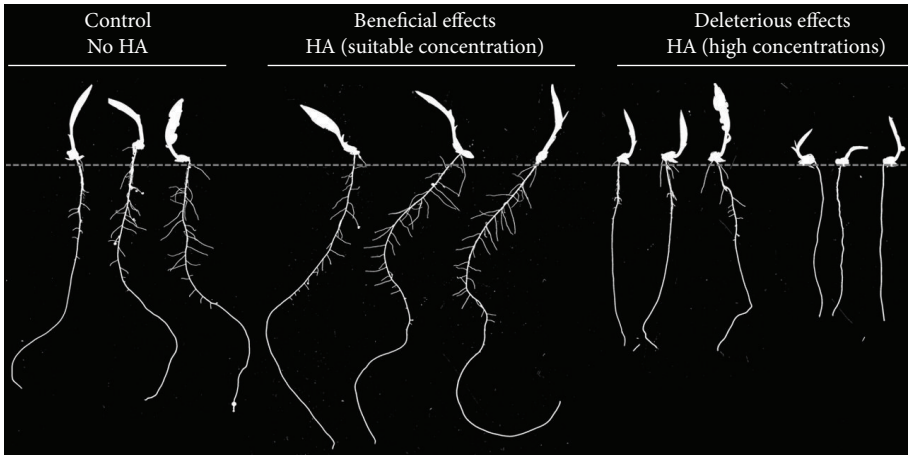

Figure 6: Root system growth and development in *Brachiaria* plants upon application of different concentrations of HA (unpublished data). HA were extracted from vermicompost of cattle manure. Images were recorded using the WinRHIZO software packet (Regent Instruments Inc., Quebec, Canada). Images are the representation of bioactivity experiments (nutrient solution) and reflect the first harvest (eight days after the transplant).

[12] reported that the ABA-mediated action of SHA was related to the regulation of ABA-dependent PIPs in cucumber roots.

In this sense, studies performed using CHA applied to roots of rice plants under normal and water stress growth conditions have shown that CHA regulates the gene expression of these isoforms both in leaves and in roots [16, 19] (Figure 7). García et al. [16] also observed that PEG-6000-induced water stress resulted in increased expression of *OsTIP1;2* isoform in rice roots (Figure 7(a)) in line with previous results showing the involvement of *OsTIP1;2* isoform in water flux through vacuoles [50].

Conversely, under normal growth conditions, high CHA concentrations caused increased expression of this isoform, suggesting that CHA application at high concentrations may induce physiological stress [16] (Figure 7(b)). This result confirms that, upon root application, HS concentrations unsuitable for plant growth may trigger physiological processes similar to those developed by plants under stress conditions [53] and can stimulate growth root under normal conditions [54] (Figure 7(b)).

4. Concluding Remarks

Overall, all results discussed above show that the whole mechanism responsible for the beneficial direct effects of HS on plant growth probably involves several complementary and interconnected signaling pathways related to both relevant hormonal networks and secondary messengers such as ROS and Ca^{2+} [7, 11, 21, 54]. In this sense, ROS probably play a pivotal role, either dependent on or independent of hormone signaling, which becomes much more relevant in plants subjected to abiotic stress.

Regarding the relevance of the origin of HS, it was noteworthy that both SHS and CHS presented many common hormone-mediated mechanisms regardless of their potential differences in structure [3, 4]. As for the signaling pathways involved in the mechanism of action of AHS or FHS on plant growth [3], we have not found consistent studies on this subject. However, even though these HS types may be used as biostimulants, their "humic nature" is very questionable. In this framework, studies oriented to better define what we can consider as "humic nature" become of great importance.

Thus, it becomes also clear that much further research is needed in order to integrate all signaling pathways affected by HS with different origins in a more comprehensive, holistic, model.

Abbreviations

ROS:	Reactive oxygen species
DOM:	Dissolved organic matter
HS:	Humic substances
HA:	Humic acids
FA:	Fulvic acids
AHS:	Artificial humic substances
AHA:	Artificial humic acids
AFA:	Artificial fulvic acids
FHS:	Fresh humic substances
FHA:	Fresh humic acids
FFA:	Fresh fulvic acids
CHS:	Compost humic substances
CHA:	Compost humic acids
CFA:	Compost fulvic acids
SHS:	Sedimentary humic substances
SHA:	Sedimentary humic acids
SFA:	Sedimentary fulvic acids
CKs:	Cytokinins
PM-H^+-ATPase:	Plasma membrane proton pumping
IAA:	Indoleacetic acid
NO:	Nitrogen oxide
ABA:	Abscisic acid
ETH:	Ethylene

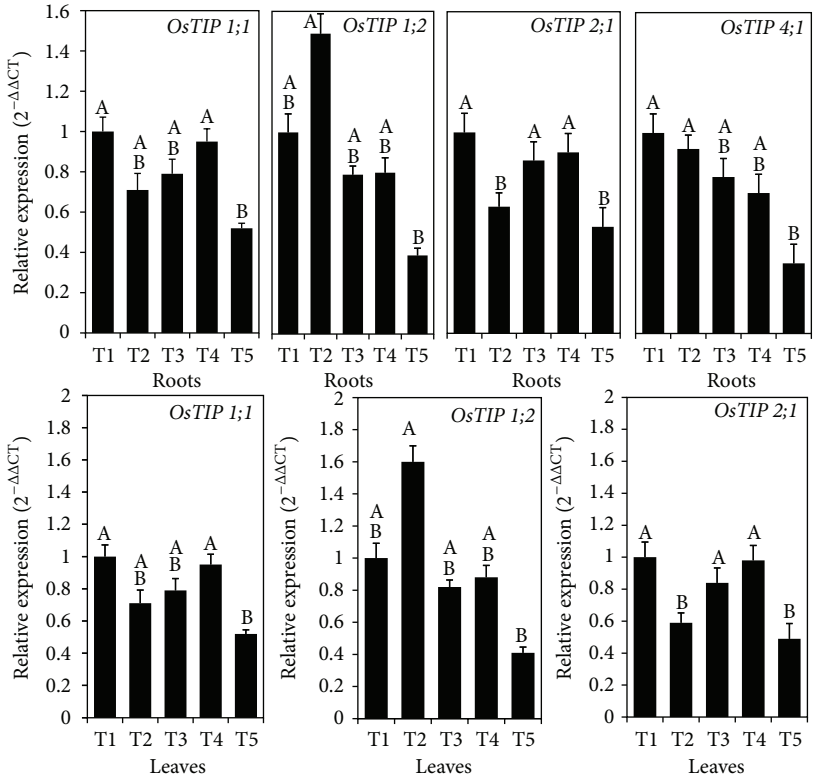

(a) HA application under stress conditions

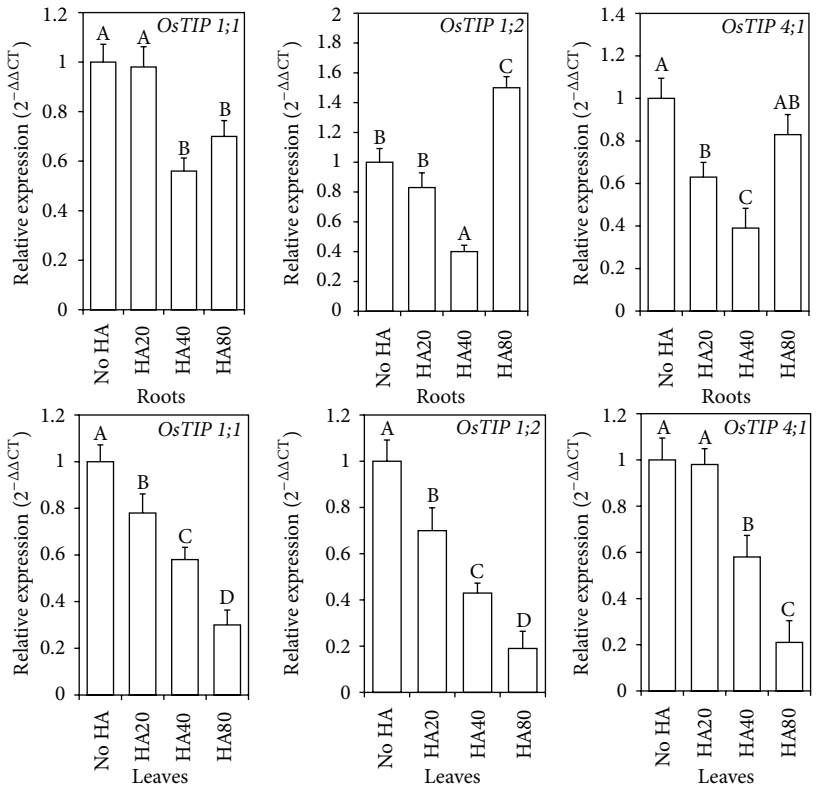

(b) HA application under normal conditions

Figure 7: Tonoplast aquaporin gene expression in rice plants subjected to treatments with HA under normal (b) and stress growth conditions (a). (a) (T1) – P–HA: no application of PEG-6000 or HA (control); (T2) + P–HA: PEG-6000 and no HA; (T3) + P + HA20: PEG-6000 and 20 mg (C) L^{-1} HA; (T4) + P + HA40: PEG-6000 and 40 mg (C) L^{-1} HA; (T5) + P + HA80: PEG-6000 and 80 mg (C) L^{-1} HA. (b) HA20 (20 mg (C) L^{-1}), HA40 (40 mg (C) L^{-1}), and HA80 (80 mg (C) L^{-1}) (adapted from [16, 19]). Different letters represent significant differences between the average values of treatments, as determined by Tukey's test; $p < 0.05$. The error bar represents the mean ± standard error (SE) of three replicates.

LC MS/MS:	Liquid chromatography-tandem mass spectrometry
DR5:GUS/uida and BA3:uida:	Auxin-responsive promoters fused with β-glucuronidase reporter gene
IAA19:	Indoleacetic acid-induced protein 19
rhd6:	Root hair defective 6 (*A. thaliana* mutant)
POX:	Peroxidases
APOX:	Ascorbate peroxidase
CAT:	Catalase
SOD:	Superoxide dismutase
ABP1:	Auxin binding protein 1
TMK:	Transmembrane kinase family
AUXIN1/LIKE-AUX1 (AUX/LAX):	Family of major auxin influx carriers
PIN-FORMED (PIN) and P-GLYCOPROTEIN (PGP):	Families of proteins are major auxin efflux carriers
cDNA-AFLP:	Complementary DNA-amplified fragment length polymorphism
NADPH:	Nicotinamide adenine dinucleotide phosphate, reduced form
CPDK:	Calcium-dependent protein kinases
PIP:	Plasma membrane intrinsic protein
TIP:	Tonoplast intrinsic protein.

Competing Interests

The authors declare that there is no conflict of interests regarding the publication of this paper.

Acknowledgments

Support for this work is provided by Science without Borders Program (Programa Ciência sem Fronteiras/PVE A060/2013) of National Counsel of Technological and Scientific Development of Brazil (CNPq), Roullier Group (France), and University of Navarra (Spain). Andrés Calderín García (sisFaperj: 2012028010) thanks Fundação de Amparo à Pesquisa do Estado do Rio de Janeiro (FAPERJ) for the grant.

References

[1] P. MacCarthy, C. E. Clapp, R. Malcom, and P. R. Bloom, *Humic Substances in Soil and Crop Sciences: Selected Readings*, American Society of Agronomy and Soil Science Society of America, Madison, Wis, USA, 1990.

[2] F. Magdoff and R. Weil, *Soil Organic Matter in Sustainable Agriculture*, CRC Press, New York, NY, USA, 2004.

[3] M. T. Rose, A. F. Patti, K. R. Little, A. L. Brown, W. R. Jackson, and T. R. Cavagnaro, "A meta-analysis and review of plant-growth response to humic substances: practical implications for agriculture," *Advances in Agronomy*, vol. 124, pp. 37–89, 2014.

[4] F. J. Stevenson, *Humus Chemistry: Genesis, Composition, Reactions*, John Wiley & Sons, New York, NY, USA, 1994.

[5] A. Piccolo, "The supramolecular structure of humic substances: a novel understanding of humus chemistry and implications in soil science," *Advances in Agronomy*, vol. 75, pp. 57–134, 2002.

[6] J. M. García-Mina, "Advantages and limitations of the use of an extended polyelectrolyte model to describe the proton-binding process in macromolecular systems. Application to a poly(acrylic acid) and a humic acid," *Journal of Physical Chemistry B*, vol. 111, no. 17, pp. 4488–4494, 2007.

[7] V. Mora, M. Olaetxea, E. Bacaicoa et al., "Abiotic stress tolerance in plants: exploring the role of nitric oxide and humic substances," in *Nitric Oxide in Plants: Metabolism and Role in Stress Physiology*, pp. 243–264, Springer, Amsterdam, The Netherlands, 2014.

[8] Y. Chen and T. Aviad, "Effects of humic substances on plant growth," in *Humic Substances in Soil and Crop Science: Selected Readings*, pp. 161–187, Americal Society of Agronomy and Soil Science Society of America, Madison, Wis, USA, 1990.

[9] Y. Chen, M. De Nobili, and T. Aviad, "Stimulatory effects of humic substances on plant growth," in *Soil Organic Matter in Sustainable Agriculture*, pp. 103–129, CRC Press, Boca Raton, Fla, USA, 2004.

[10] J. M. García-Mina, M. C. Antolín, and M. Sanchez-Diaz, "Metal-humic complexes and plant micronutrient uptake: a study based on different plant species cultivated in diverse soil types," *Plant and Soil*, vol. 258, no. 1-2, pp. 57–68, 2004.

[11] R. L. L. Berbara and A. C. García, "Humic substances and plant defense metabolism," in *Physiological Mechanisms and Adaptation Strategies in Plants Under Changing Environment*, P. Ahmad and M. R. Wani, Eds., pp. 297–319, Springer, New York, NY, USA, 2014.

[12] M. Olaetxea, V. Mora, E. Bacaicoa et al., "Abscisic acid regulation of root hydraulic conductivity and aquaporin gene expression is crucial to the plant shoot growth enhancement caused by rhizosphere humic acids," *Plant Physiology*, vol. 169, no. 4, pp. 2587–2596, 2015.

[13] V. Mora, E. Bacaicoa, A.-M. Zamarreño et al., "Action of humic acid on promotion of cucumber shoot growth involves nitrate-related changes associated with the root-to-shoot distribution of cytokinins, polyamines and mineral nutrients," *Journal of Plant Physiology*, vol. 167, no. 8, pp. 633–642, 2010.

[14] V. Mora, E. Bacaicoa, R. Baigorri, A. M. Zamarreño, and J. M. García-Mina, "NO and IAA key regulators in the shoot growth promoting action of humic acid in Cucumis sativus L.," *Journal of Plant Growth Regulation*, vol. 33, no. 2, pp. 430–439, 2014.

[15] L. Jannin, M. Arkoun, A. Ourry et al., "Microarray analysis of humic acid effects on Brassica napus growth: involvement of N, C and S metabolisms," *Plant and Soil*, vol. 359, no. 1-2, pp. 297–319, 2012.

[16] A. C. García, L. A. Santos, F. G. Izquierdo et al., "Potentialities of vermicompost humic acids to alleviate water stress in rice plants (Oryza sativa L.)," *Journal of Geochemical Exploration*, vol. 136, pp. 48–54, 2014.

[17] I. C. Mori, Y. Murata, and M. Uraji, "Integration of ROS and hormone signaling," in *Reactive Oxygen Species in Plant Signaling*, Signaling and Communication in Plants, pp. 25–42, Springer, Berlin, Germany, 2009.

[18] A. C. García, L. A. Santos, L. G. A. de Souza et al., "Vermicompost humic acids modulate the accumulation and metabolism of ROS in rice plants," *Journal of Plant Physiology*, vol. 192, pp. 56–63, 2016.

[19] A. C. García, L. A. Santos, F. G. Izquierdo, M. V. L. Sperandio, R. N. Castro, and R. L. L. Berbara, "Vermicompost humic acids

as an ecological pathway to protect rice plant against oxidative stress," *Ecological Engineering*, vol. 47, pp. 203–208, 2012.

[20] V. Mora, R. Baigorri, E. Bacaicoa, A. M. Zamarreño, and J. M. García-Mina, "The humic acid-induced changes in the root concentration of nitric oxide, IAA and ethylene do not explain the changes in root architecture caused by humic acid in cucumber," *Environmental and Experimental Botany*, vol. 76, pp. 24–32, 2012.

[21] S. Nardi, P. Carletti, D. Pizzeghello, and A. Muscolo, "Biological activities of humic substances," in *Biophysico-Chemical Processes Involving Natural Nonliving Organic Matter in Environmental Systems Vol 2, Part 1: Fundamentals and Impact of Mineral-Organic Biota Interactions on the Formation, Transformation, Turnover, and Storage of Natural Nonliving Organic Matter (NOM)*, pp. 309–335, Wiley, New York, NY, USA, 2009.

[22] L. P. Canellas and F. L. Olivares, "Physiological responses to humic substances as plant growth promoter," *Chemical and Biological Technologies in Agriculture*, vol. 1, no. 1, pp. 3–13, 2014.

[23] S. Trevisan, D. Pizzeghello, B. Ruperti et al., "Humic substances induce lateral root formation and expression of the early auxin-responsive IAA19 gene and DR5 synthetic element in *Arabidopsis*," *Plant Biology*, vol. 12, no. 4, pp. 604–614, 2010.

[24] L. P. Canellas, F. L. Olivares, A. L. Okorokova-Façanha, and A. R. Façanha, "Humic acids isolated from earthworm compost enhance root elongation, lateral root emergence, and plasma membrane H+-ATPase activity in maize roots," *Plant Physiology*, vol. 130, no. 4, pp. 1951–1957, 2002.

[25] D. B. Zandonadi, M. P. Santos, L. B. Dobbss et al., "Nitric oxide mediates humic acids-induced root development and plasma membrane H^+-ATPase activation," *Planta*, vol. 231, no. 5, pp. 1025–1036, 2010.

[26] A. C. Ramos, L. B. Dobbss, L. A. Santos et al., "Humic matter elicits proton and calcium fluxes and signaling dependent on Ca^{2+}-dependent protein kinase (CDPK) at early stages of lateral plant root development," *Chemical and Biological Technologies in Agriculture*, vol. 2, no. 1, pp. 1–12, 2015.

[27] W. Schmidt, S. Santi, R. Pinton, and Z. Varanini, "Water-extractable humic substances alter root development and epidermal cell pattern in *Arabidopsis*," *Plant and Soil*, vol. 300, no. 1-2, pp. 259–267, 2007.

[28] F. C. Cordeiro, C. Santa-Catarina, V. Silveira, and S. R. De Souza, "Humic acid effect on catalase activity and the generation of reactive oxygen species in corn (*Zea mays*)," *Bioscience, Biotechnology and Biochemistry*, vol. 75, no. 1, pp. 70–74, 2011.

[29] A. Muscolo, M. Sidari, and S. Nardi, "Humic substance: relationship between structure and activity. deeper information suggests univocal findings," *Journal of Geochemical Exploration*, vol. 129, pp. 57–63, 2013.

[30] L. P. Canellas, D. J. Dantas, N. O. Aguiar et al., "Probing the hormonal activity of fractionated molecular humic components in tomato auxin mutants," *Annals of Applied Biology*, vol. 159, no. 2, pp. 202–211, 2011.

[31] A. C. Silva, L. P. Canellas, F. L. Olivares et al., "Promoção do crescimento radicular de plântulas de tomateiro por substâncias húmicas isoladas de turfeiras," *Revista Brasileira de Ciência do Solo*, vol. 35, no. 5, pp. 1609–1617, 2011.

[32] L. B. Dobbss, L. P. Canellas, F. L. Olivares et al., "Bioactivity of chemically transformed humic matter from vermicompost on plant root growth," *Journal of Agricultural and Food Chemistry*, vol. 58, no. 6, pp. 3681–3688, 2010.

[33] R. Mittler, S. Vanderauwera, N. Suzuki et al., "ROS signaling: the new wave?" *Trends in Plant Science*, vol. 16, no. 6, pp. 300–309, 2011.

[34] H. Hirt, "Connecting oxidative stress, auxin, and cell cycle regulation through a plant mitogen-activated protein kinase pathway," *Proceedings of the National Academy of Sciences of the United States of America*, vol. 97, no. 6, pp. 2405–2407, 2000.

[35] H. Tsukagoshi, W. Busch, and P. N. Benfey, "Transcriptional regulation of ROS controls transition from proliferation to differentiation in the root," *Cell*, vol. 143, no. 4, pp. 606–616, 2010.

[36] Y. Gao, Y. Zhang, D. Zhang, X. Dai, M. Estelle, and Y. Zhao, "Auxin binding protein 1 (ABP1) is not required for either auxin signaling or *Arabidopsis* development," *Proceedings of the National Academy of Sciences of the United States of America*, vol. 112, no. 7, pp. 2275–2280, 2015.

[37] R. Swarup and B. Péret, "AUX/LAX family of auxin influx carriers—an overview," *Frontiers in Plant Science*, vol. 3, article 225, 2012.

[38] D. Vaughan, B. G. Ord, and R. E. Malcolm, "Effect of soil organic matter on some root surface enzymes of and uptakes into winter wheat," *Journal of Experimental Botany*, vol. 29, no. 6, pp. 1337–1344, 1978.

[39] D. Vaughan and R. E. Malcolm, "Effect of soil organic matter on peroxidase activity of wheat roots," *Soil Biology and Biochemistry*, vol. 11, no. 1, pp. 57–63, 1979.

[40] S. Trevisan, A. Botton, S. Vaccaro, A. Vezzaro, S. Quaggiotti, and S. Nardi, "Humic substances affect Arabidopsis physiology by altering the expression of genes involved in primary metabolism, growth and development," *Environmental and Experimental Botany*, vol. 74, no. 1, pp. 45–55, 2011.

[41] J. Foreman, V. Demidchik, J. H. F. Bothwell et al., "Reactive oxygen species produced by NADPH oxidase regulate plant cell growth," *Nature*, vol. 422, no. 6930, pp. 442–446, 2003.

[42] I. C. Mori and J. I. Schroeder, "Reactive oxygen species activation of plant Ca^{2+} channels. A signaling mechanism in polar growth, hormone transduction, stress signaling, and hypothetically mechanotransduction," *Plant Physiology*, vol. 135, no. 2, pp. 702–708, 2004.

[43] J. Šamaj, F. Baluška, and D. Menzel, "New signalling molecules regulating root hair tip growth," *Trends in Plant Science*, vol. 9, no. 5, pp. 217–220, 2004.

[44] V. Demidchik, S. N. Shabala, and J. M. Davies, "Spatial variation in H_2O_2 response of *Arabidopsis thaliana* root epidermal Ca^{2+} flux and plasma membrane Ca^{2+} channels," *The Plant Journal*, vol. 49, no. 3, pp. 377–386, 2007.

[45] C. Dunand, M. Crèvecoeur, and C. Penel, "Distribution of superoxide and hydrogen peroxide in *Arabidopsis* root and their influence on root development: Possible interaction with peroxidases," *New Phytologist*, vol. 174, no. 2, pp. 332–341, 2007.

[46] R. Schmidt, C. Caldana, B. Mueller-Roeber, and J. H. M. Schippers, "The contribution of SERF1 to root-to-shoot signaling during salinity stress in rice," *Plant Signaling and Behavior*, vol. 9, no. 1, Article ID e27540, 2014.

[47] N. Suzuki, R. M. Rivero, V. Shulaev, E. Blumwald, and R. Mittler, "Abiotic and biotic stress combinations," *New Phytologist*, vol. 203, no. 1, pp. 32–43, 2014.

[48] R. Mittler, "Abiotic stress, the field environment and stress combination," *Trends in Plant Science*, vol. 11, no. 1, pp. 15–19, 2006.

[49] Z.-M. Pei, Y. Murata, G. Benning et al., "Calcium channels activated by hydrogen peroxide mediate abscisic acid signalling in guard cells," *Nature*, vol. 406, no. 6797, pp. 731–734, 2000.

[50] H.-L. Lian, X. Yu, D. Lane, W.-N. Sun, Z.-C. Tang, and W.-A. Su, "Upland rice and lowland rice exhibited different PIP expression under water deficit and ABA treatment," *Cell Research*, vol. 16, no. 7, pp. 651–660, 2006.

[51] G.-W. Li, Y.-H. Peng, X. Yu et al., "Transport functions and expression analysis of vacuolar membrane aquaporins in response to various stresses in rice," *Journal of Plant Physiology*, vol. 165, no. 18, pp. 1879–1888, 2008.

[52] R. Kaldenhoff and M. Fischer, "Aquaporins in plants," *Acta Physiologica*, vol. 187, no. 1-2, pp. 169–176, 2006.

[53] S. Asli and P. M. Neumann, "Rhizosphere humic acid interacts with root cell walls to reduce hydraulic conductivity and plant development," *Plant and Soil*, vol. 336, no. 1, pp. 313–322, 2010.

[54] L. P. Canellas, F. L. Olivares, N. O. Aguiar et al., "Humic and fulvic acids as biostimulants in horticulture," *Scientia Horticulturae*, vol. 196, pp. 15–27, 2015.

Hindawi Publishing Corporation
BioMed Research International
Volume 2016, Article ID 4182071, 8 pages
http://dx.doi.org/10.1155/2016/4182071

Review Article

Decipher the Molecular Response of Plant Single Cell Types to Environmental Stresses

Mehrnoush Nourbakhsh-Rey and Marc Libault

Department of Microbiology and Plant Biology, University of Oklahoma, 770 Van Vleet Oval, Norman, OK 73019, USA

Correspondence should be addressed to Marc Libault; libaultm@ou.edu

Received 27 November 2015; Revised 18 February 2016; Accepted 28 February 2016

Academic Editor: Luis Fernando Revers

The analysis of the molecular response of entire plants or organs to environmental stresses suffers from the cellular complexity of the samples used. Specifically, this cellular complexity masks cell-specific responses to environmental stresses and logically leads to the dilution of the molecular changes occurring in each cell type composing the tissue/organ/plant in response to the stress. Therefore, to generate a more accurate picture of these responses, scientists are focusing on plant single cell type approaches. Several cell types are now considered as models such as the pollen, the trichomes, the cotton fiber, various root cell types including the root hair cell, and the guard cell of stomata. Among them, several have been used to characterize plant response to abiotic and biotic stresses. In this review, we are describing the various -omic studies performed on these different plant single cell type models to better understand plant cell response to biotic and abiotic stresses.

1. Use of Plant Single Cell Types to Study Plant Response to Environmental Stresses

The multicellular complexity of the samples collected to characterize plant response to environmental stress is a major limitation to clearly depict the contribution of each cell type composing the sample in response to the stress. In other words, -omic studies at the level of plant organs reflect the average response of the different cell types composing the organ (Figure 1). In order to fully understand the exact contribution of each plant cell type in regulating plant response to environmental stresses, the transcriptome, epigenome, proteome, metabolome, and interactomes (e.g., protein-protein and protein-DNA interactions) of each plant cell type composing the sample and their changes in response to environmental stresses should be independently characterized [1]. For instance, the characterization of the transcriptional response of the soybean root hair cell to rhizobial inoculation allowed the identification of almost two thousand differentially expressed genes [2]. This single plant cell type analysis represents a significant improvement compared to previous studies describing few hundred genes differentially expressed in root sections in response to rhizobial inoculation [3, 4]. Ultimately, the integration of these various datasets will lead to a global understanding of the molecular adaptation of plants to environment changes through the precise characterization of transcriptional regulatory networks [5]. Currently, the construction of these networks in response to environmental stresses is highly dependent on the nature of the samples used to collect biological information. For instance, working at the level of entire organs cannot depict the specific networks existing in each cell type composing the organ supporting the idea to study plant biological networks at the level of single cell types. Accordingly, this review highlights the recent progress in the field of plant adaptation in response to both biotic and abiotic stresses at the level of single cell types (Table 1).

2. Isolation of Plant Single Cell Types

The isolation of plant single cell types is limited by the cell wall, which provides both rigidity and structure to the plant and acts as a first barrier against pathogenic organisms. To

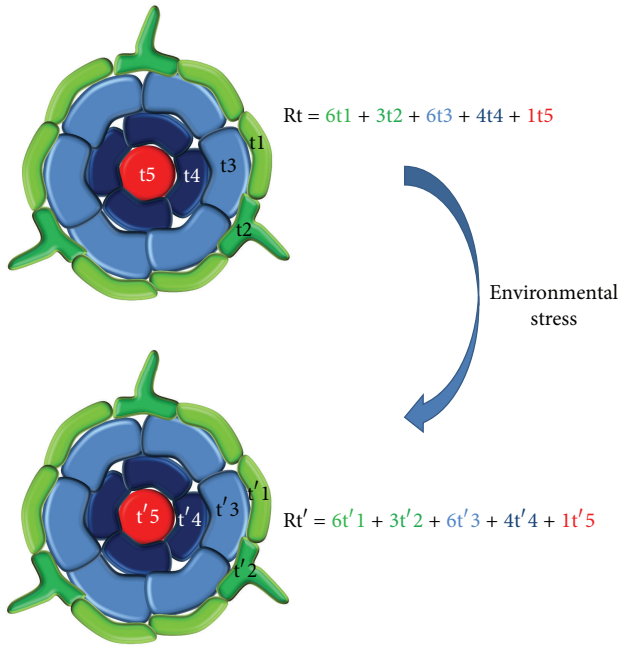

Figure 1: Root transcriptomic response to a stress (Rt and Rt′) is the sum of the individual responses of each cell type composing the root (t1 to t5; t′1 to t′5). Because plant cell transcriptomes are different between cell types, the cellular complexity of plant roots is not suitable to characterize gene networks. A single cell type model must be used to better characterize plant gene networks.

overcome this difficulty, different strategies were applied to isolate various cell types. These technologies include the use of cell sorting laser capture microdissection [6–9], sorting of single plant cell types upon cell type-specific GFP labeling and protoplastization [10, 11], and the application of the INTACT (Isolation of Nuclei TAgged in specific Cell Types) method which includes the labeling of single plant cell nuclei with a biotinylated nuclear envelope protein before their isolation using streptavidin-coated magnetic beads [12, 13]. Other methods have been applied to access in large quantities easily accessible single plant cell types such as cotton fiber and root hair cells [14–16]. More recently, an innovative methodology named Meselect which combined both a mechanical and an enzymatic treatment of the plant cells has been applied to isolate leaf epidermal, vascular, and mesophyll cells [17]. Lu et al. (2015) also developed another methodology allowing the isolation of generative cells (GCs), the sperm cells (SCs), and the vegetative nuclei (VN) from tomato pollens [18]. In this method GCs, SCs, and VN were isolated from germinated tomato pollen grains and growing pollen tubes and purified by Percoll density gradient centrifugation. Microscopic examination of fluorescein diacetate-stained samples confirmed the purity of GCs and SCs, respectively. Propidium iodide staining was used to confirm VN integrity.

Currently, only a limited number of single plant cell types have been isolated in quantities compatible with the application of -omic technologies. The most noticeable examples are the cotton fiber, pollen cells, and root hair cells [14, 16, 19–22]. Various root cell types from the model plant *Arabidopsis thaliana* have also been isolated preliminary to their molecular analyses including response to environmental stresses [23–26]. Our understanding of the biology of the plant female gametophyte which is composed of antipodal, central, egg, and synergid cells is also beneficiating from single cell type analyses [27].

3. Single Cell-Specific Transcriptomes in Response to Biotic and Abiotic Stress

Compared to other -omic datasets, plant single cell type transcriptomes and their changes in response to environmental stresses are currently the most complete. For instance, multiple studies have characterized the transcriptomic profile of *Arabidopsis thaliana* root cells and their response to abiotic stresses including nutrient deprivation (i.e., iron and sulfur), salinity, and low pH values as well as in response to stress-signaling plant hormones such as abscisic acid [24, 25].

Among root cells and across plant species, the root hair cell is likely the best transcriptionally characterized single cell type based on the ease to isolate them from the rest of the root. The root hair transcriptome has been characterized across different plant species including *A. thaliana* [13, 26, 28–31], *Glycine max* (i.e., 451 root hair specific transcripts characterized [2, 32]), and *Medicago truncatula* (i.e., 49 root hair specific transcripts characterized [33]). In legumes, this single plant cell type was also recently used as a model to study plant cell response to biotic stress because it is the first cell type infected by rhizobia, the nitrogen-fixing symbiotic bacteria [2, 33]. 219 and 79 soybean and *Medicago* genes were, repetitively, transcriptionally regulated in root hair cells in response to rhizobia including many genes functionally characterized for their role during nodulation [34]. Another plant single cell type model recently used to characterize the transcriptional changes occurring in response to pathogenic microorganisms was the *A. thaliana* mesophyll cell infected by the oomycete *Hyaloperonospora arabidopsidis* [35].

In addition to respond to various biotic stresses, plants are also constantly interacting, responding, and adapting to various abiotic stresses. Our understanding of those interactions is also benefiting from a single plant cell type transcriptomic approach. For instance, Sarah Assmann's group performed a transcriptomic analysis of *A. thaliana* guard cells in response to abscisic acid, a plant hormone acting on plant water conservation. 909 genes were specifically regulated in response to ABA in guard cells [36]. Plant resistance to heavy metal has also been investigated at the level of single plant cell types. For instance, trichomes are known to sequester heavy metals such as cadmium. Accordingly, a comparative transcriptomic analysis was conducted in *Nicotiana tabacum* trichomes in response to cadmium treatment [37]. Together, taking advantage of the specific biological function of single plant cell types, their transcriptomic analysis has the potential to reveal new plant regulatory genes in response to biotic and abiotic stresses due to the gain of sensitivity of the analysis. For instance, the barley β-extension *EXPB7* gene which was

Table 1: Various -omic analyses were conducted on different plant single cell types in response to both biotic and abiotic stresses.

Cell type	Omics		
	Transcriptome	Proteome	Metabolome
Trichome	*Nicotiana tabacum* L. cv. Xanthi (pathogenic stress; [37])	*Arabidopsis thaliana* (cold, hormone stimulus, and drought; [55]) *Artemisia annua* L. (dehydration stress, detoxification; [53]) *Nicotiana tabacum* (oxidative stress; [56, 57])	
Guard cell	*Arabidopsis thaliana* (dehydration stress; [36])	*Brassica napus* (ABA response; [59]) *Arabidopsis thaliana* (ABA response; [60])	*Vicia faba L.* (darkness and drought; [89]) *Arabidopsis thaliana* (nitric oxide response and ABA response, pathogenal infection, and UV radiation; [90–94])
Mesophyll cell	*Arabidopsis thaliana* (pathogenal infection; [35])		
Root hair	*Hordeum vulgare* L. ssp. *spontaneum* (drought stress; [38]) *Arabidopsis thaliana* (heat, cold, salt stress, oxidative stress, and abscisic acid stimulus; [28–31]) *Glycine max* (rhizobial infection; [2]) *Medicago truncatula* (rhizobial infection; [33])	*Glycine max* (rhizobial infection; [61–63])	*Glycine max* (rhizobial infection; [96–98])
Pollen, pollen tube	*Arabidopsis thaliana* (heat and osmotic stress; [19, 28])	*Arabidopsis thaliana* (pathogenic infection, oxidative stress; [42, 44–47]) *Zea maize* (oxidative stress; [48]) *Oryza sativa* (pathogen infection, oxidative stress; [43])	
Epidermal cell	*Mesembryanthemum crystallinum* (salinity stress; [88])		*Mesembryanthemum crystallinum* (salinity stress; [85])
Cotton fiber	*Gossypium arboreum* L. (drought stress; [14, 15])		

initially identified based on its differential expression in root hair cells in response to drought stress has been demonstrated to confer a better drought adaptation to the plant [38].

4. Characterization of the Proteomic Response of Single Plant Cell Type to Environmental Stresses

Proteins are the active molecules in the cells. The quantification of their relative abundance is critical to understand plant adaptation to environmental stresses. However, single cell type proteomes are challenging to establish because of the limited quantities of plant material available [39–41]. In addition, their posttranslational modifications are also affecting protein function and should logically be characterized at the level of single plant cell types.

A first effort in the establishment of single cell type proteome was the characterization of the pool of proteins in mature pollens. Pollen cell proteomics have been studied in different plant models such as *Arabidopsis thaliana* and *Oryza sativa* [42–45]. In *Arabidopsis thaliana* 130 differentially expressed proteins involved in pollen germination and pollen tube growth were identified via proteomic analyses [46]. Ultimately, proteomic analyses led to the establishment of the first protein reference map of mature pollen in *Arabidopsis* using two-dimensional gel electrophoresis (2DE), matrix-assisted laser desorption/ionization time of flight (MALDI-TOF), and electrospray quadrupole time of flight-mass spectrometry (EQ-TOF-MS) [47]. In maize, a comparative proteomic analysis allowed the characterization of differentially expressed proteins involved in pollen tube development and plant defense [48]. Among those proteins, several participate in pollen resistance to environmental stresses. For instance, proteomic analysis in *Arabidopsis* pollen helped to reveal the role of the ABI1 phosphatase 2C as a negative regulator of ABA signaling [49]. Similarly, in response to osmotic stress, glucose regulated (GRPs) and LEA-like *A. thaliana* proteins were strongly induced to protect the cells [47, 50, 51].

Trichome has also been subject to various proteomic analyses across different plant species such as *Artemisia annua*, *Arabidopsis*, and tobacco [52–54]. The establishment of the trichome proteome in *Arabidopsis thaliana* confirms the important role of this single cell type in sulfur metabolism and detoxification to enhance plant defense mechanisms [55]. Upon the identification in 1543 proteins in tobacco leaf trichomes [56], several enzymes also related to the detoxification including glutathione-S-transferase (GST), ascorbate-glutathione cycle enzymes, superoxide dismutases (SOD), cytosolic Cu/Zn SOD, and peroxidases were characterized in response to oxidative stress [56, 57]. The functional categorization of the *Arabidopsis* trichome proteome based on gene ontology (GO) terms also confirmed the role of trichomes in plant adaptation to abiotic (cold, temperature, drought, and heavy metal) and biotic stresses [54]. Similarly, in tobacco, proteins were also identified for their role in biotic stress responses such as chitinases and glucanases [56].

The guard cell proteome revealed the abundance of proteins involved in signaling, membrane transport, glycolysis, photosynthesis light reaction, and fatty acid biosynthesis [58]. Using isobaric tag for relative and absolute quantitation (iTRAQ) technology, several ABA-response proteins were identified in *Brassica napus* and *Arabidopsis* guard cells [59, 60]. In *B. napus*, 66 ABA-dependent and 38 ABA-decreased proteins were reported to have a special function in calcium oscillation, ROS reaction, photosynthesis, and signaling [59].

Comparative proteomic analyses in soybean also led to the identification of several root hair specific proteins differentially accumulated in response to *Bradyrhizobium japonicum* inoculation including more than 100 heat shock proteins involved in protein folding and stress responses [61, 62]. To provide a more complete view about the changes in the proteome of soybean root hair cells in response to rhizobium, Nguyen et al. (2012) also established its phosphoproteome and identified 273 root hair specific phosphopeptides regulated in response to *B. japonicum* infection [63].

5. Metabolomic Response of Single Plant Cell Types to Environmental Stresses

Similar to the other -omic approaches, the analysis of the cell type-specific metabolomes is affected by multicellular complexity of the tissues selected. In addition to their diversity, metabolomic analyses also suffer from the low concentration of many metabolites supporting the need for single plant cell type metabolomic approaches.

Microcapillary method is applied for sampling plant single cells content by using the oil-filled glass microcapillaries mounted on the micromanipulator [64–67]. This method benefits from cellular turgor pressure to study plant organ water relations at the single cell level, which allows investigating cellular macromolecules [68, 69]. The combination of the microcapillary method with other physical or chemical analytical methods (e.g., gas chromatography-time of flight-mass spectrometry (GC-TOF-MS) [70], laser capture microdissection (LCM), laser microdissection optionally coupled to laser pressure catapulting (LMPC) [71], and RT-PCR [67, 69]) helps researchers to characterize the metabolome of fully differentiated plant cell types [72]. Combined with the recent improvement of analytical technologies, the quantitative and qualitative analysis of plant single cell type metabolomes would provide new insights into the environmental stress responses of plant cells.

Various technologies are commonly used for metabolomic profiling including infrared spectroscopy [73], nuclear magnetic resonance (NMR) [74–76], mass spectrometry (MS) and gas chromatography-MS (GC-MS) [77, 78], matrix-assisted laser desorption/ionization (MALDI) [79], capillary electrophoresis coupled with laser induced fluorescence detection (CE/LIF) [80] or mass spectrometry (CE/MS) [81, 82], CE-negative electrospray ionization-MS, and electrospray ionization (ESI) [83]. These techniques vary in speed, selectivity, and sensitivity.

Several metabolomic studies at the level of single plant cell types have been described. For instance, focusing on the epidermal bladder cell (EBC), a specialized trichome cell from *Mesembryanthemum crystallinum* known to be morphologically altered under salt stress [84], Barkla and Vera-Estrella (2015) characterized their metabolomic response to salinity [85]. Comparing *M. crystallinum* EBC metabolomic salt-response with the metabolomes of other salt-tolerant plant species [86, 87], specific classes of metabolites enhancing plant adaptation to high salinity such as sugars and sugar alcohols have been identified. Similarly, having the goal to enhance plant resistance in response to salinity and heavy metals, metabolomic analyses revealed the accumulation of sulfur and glutathione in *Arabidopsis* and tobacco trichomes [88].

In the *Arabidopsis thaliana* and *Vicia faba* guard cells, several metabolomic studies revealed the relationships existing between the accumulation of flavonoids, reactive oxygen species, abscisic acid, nitric oxide, and auxin as important components of the signaling cascade controlling the stomatal movements in response to osmotic stresses and pathogenic organisms such as *Pseudomonas syringae* [89–94]. For instance, the increase in phenolic and flavonoid compounds in the *A. thaliana* guard cells provides an additional protection against pathogens, insects, and UV-B radiation [90]. Lipidomic analysis of *Commelina communis* and *A. thaliana* guard cells also revealed the role of fatty acids in the stomatal response of plants to both abiotic and biotic stresses [93, 95].

Plant single cell type metabolomic response to biotic stresses has also been established such as the soybean root hair metabolome and its regulation in response to *B. japonicum* inoculation. A total of 2610 root hair metabolites were identified using two biochemical methodologies: gas chromatography-mass spectrometry (GC-MS) and ultraperformance liquid chromatography-quadrupole time of flight-mass spectrometry (UPLC-QTOF-MS) [96]. Among them, 166 were highly regulated in response to *B. japonicum* inoculation including various flavonoids, amino acids, fatty acids, carboxylic acids compounds, and trehalose. The latter has been well described for its essential role during the nodulation process and, more specifically, its role on survival of the soybean symbiotic bacteria [97, 98].

New approaches are currently developed allowing the noninvasive analysis of single plant cell metabolome associated with a robust quantification and detection of plant single cell metabolites. Infrared-laser ablation electrospray ionization (LAESI) and UV-laser desorption/ionization (LDI) are two methods minimizing sample preparation and manipulation. The latter does not require an external matrix providing a larger spatial resolution of the single cell [99]. Complementary to LDI technology, LAESI highlights the colocalization of metabolites and metabolomic networks in plant samples such as *Spathiphyllum lynise* and *Aphelandra squarrosa* [100]. The LAESI was also successfully applied to analyze the metabolome of single epithelial cells in *Allium cepa*, the *Citrus aurantium* oil glands, and *Narcissus pseudonarcissus* bulbs [101, 102]. As a conclusion, LAESI and LDI are new noninvasive analytical methods compatible with the analysis of single plant cell metabolome. They represent attractive solutions to image known and unknown metabolomic networks in response to environmental stresses at the level of single plant cells.

6. Conclusion

Recent technological advances are now enabling the characterization of plant molecular responses to both biotic and abiotic stresses at the level of single plant cell types. -Omic studies on entire plant organs mask the cell-specific characteristics and lead to a dilution of the molecular changes. Accordingly, the scientific community highlighted the need for single plant cell type approaches to provide a more precise molecular characterization of plants response to the abiotic and biotic stresses. The combination of different molecular approaches and their integration will reveal at a systems level the complexity of plant cell adaptation to the stresses.

For instance, using tomato pollen cell as a model, Lopez-Casado et al. (2012) generated a proteomic analysis using RNA-seq database [103]. Single cell system biology by combination of one or two -omic analyses can also provide a more dynamic model of the interactions between the plant and its environment [104]. Therefore, integrating single cell type-specific proteomes, transcriptomes, and metabolomes would provide a better understanding of plant model regulatory networks in response to environmental stresses [22].

Competing Interests

The authors declare that they have no competing interests.

Acknowledgments

This work was supported by the National Science Foundation (Plant Genome Research Program, no. IOS-1339194, and CAREER Program, no. IOS-1453613) and by the US Department of Agriculture-Department of Energy Feedstock Program (no. DE-SC0012629).

References

[1] T. Nelson, N. Gandotra, and S. L. Tausta, "Plant cell types: reporting and sampling with new technologies," *Current Opinion in Plant Biology*, vol. 11, no. 5, pp. 567–573, 2008.

[2] M. Libault, A. Farmer, L. Brechenmacher et al., "Complete transcriptome of the soybean root hair cell, a single-cell model, and its alteration in response to *Bradyrhizobium japonicum* infection," *Plant Physiology*, vol. 152, no. 2, pp. 541–552, 2010.

[3] D. P. Lohar, N. Sharopova, G. Endre et al., "Transcript analysis of early nodulation events in *Medicago truncatula*," *Plant Physiology*, vol. 140, no. 1, pp. 221–234, 2006.

[4] N. Høgslund, S. Radutoiu, L. Krusell et al., "Dissection of symbiosis and organ development by integrated transcriptome analysis of *Lotus japonicus* mutant and wild-type plants," *PLoS ONE*, vol. 4, no. 8, Article ID e6556, 2009.

[5] L. Pu and S. Brady, "Systems biology update: cell type-specific transcriptional regulatory networks," *Plant Physiology*, vol. 152, no. 2, pp. 411–419, 2010.

[6] V. P. Klink, N. Alkharouf, M. MacDonald, and B. Matthews, "Laser Capture Microdissection (LCM) and expression analyses of *Glycine max* (soybean) syncytium containing root regions formed by the plant pathogen *Heterodera glycines* (soybean cyst nematode)," *Plant Molecular Biology*, vol. 59, no. 6, pp. 965–979, 2005.

[7] N. Ithal, J. Recknor, D. Nettleton, T. Maier, T. J. Baum, and M. G. Mitchum, "Developmental transcript profiling of cyst nematode feeding cells in soybean roots," *Molecular Plant-Microbe Interactions*, vol. 20, no. 5, pp. 510–525, 2007.

[8] S. Santi and W. Schmidt, "Laser microdissection-assisted analysis of the functional fate of iron deficiency-induced root hairs in cucumber," *Journal of Experimental Botany*, vol. 59, no. 3, pp. 697–704, 2008.

[9] H. Takehisa, Y. Sato, M. Igarashi et al., "Genome-wide transcriptome dissection of the rice root system: implications for developmental and physiological functions," *Plant Journal*, vol. 69, no. 1, pp. 126–140, 2012.

[10] C. Zhang, F. C. Gong, G. M. Lambert, and D. W. Galbraith, "Cell type-specific characterization of nuclear DNA contents within complex tissues and organs," *Plant Methods*, vol. 1, no. 1, article 7, 2005.

[11] S. V. Petersson, A. I. Johansson, M. Kowalczyk et al., "An auxin gradient and maximum in the arabidopsis root apex shown by high-resolution cell-specific analysis of IAA distribution and synthesis," *The Plant Cell*, vol. 21, no. 6, pp. 1659–1668, 2009.

[12] R. B. Deal and S. Henikoff, "The INTACT method for cell type-specific gene expression and chromatin profiling in *Arabidopsis thaliana*," *Nature Protocols*, vol. 6, no. 1, pp. 56–68, 2011.

[13] R. B. Deal and S. Henikoff, "A simple method for gene expression and chromatin profiling of individual cell types within a tissue," *Developmental Cell*, vol. 18, no. 6, pp. 1030–1040, 2010.

[14] A. B. Arpat, M. Waugh, J. P. Sullivan et al., "Functional genomics of cell elongation in developing cotton fibers," *Plant Molecular Biology*, vol. 54, no. 6, pp. 911–929, 2004.

[15] K. V. Padmalatha, G. Dhandapani, M. Kanakachari et al., "Genome-wide transcriptomic analysis of cotton under drought stress reveal significant down-regulation of genes and pathways involved in fibre elongation and up-regulation of defense responsive genes," *Plant Molecular Biology*, vol. 78, no. 3, pp. 223–246, 2012.

[16] M. Libault, L. Brechenmacher, J. Cheng, D. Xu, and G. Stacey, "Root hair systems biology," *Trends in Plant Science*, vol. 15, no. 11, pp. 641–650, 2010.

[17] J. Svozil, W. Gruissem, and K. Baerenfaller, "Proteasome targeting of proteins in Arabidopsis leaf mesophyll, epidermal and vascular tissues," *Frontiers in Plant Science*, vol. 6, article 376, 2015.

[18] Y. Lu, L. Wei, and T. Wang, "Methods to isolate a large amount of generative cells, sperm cells and vegetative nuclei from tomato pollen for "omics" analysis," *Frontiers in Plant Science*, vol. 6, article 391, 2015.

[19] J. D. Becker, L. C. Boavida, J. Carneiro, M. Haury, and J. A. Feijó, "Transcriptional profiling of arabidopsis tissues reveals the unique characteristics of the pollen transcriptome," *Plant Physiology*, vol. 133, no. 2, pp. 713–725, 2003.

[20] Q. Q. Wang, F. Liu, X. S. Chen, X. J. Ma, H. Q. Zeng, and Z. M. Yang, "Transcriptome profiling of early developing cotton fiber by deep-sequencing reveals significantly differential expression of genes in a fuzzless/lintless mutant," *Genomics*, vol. 96, no. 6, pp. 369–376, 2010.

[21] Z. Qiao and M. Libault, "Unleashing the potential of the root hair cell as a single plant cell type model in root systems biology," *Frontiers in Plant Science*, vol. 4, article 484, 2013.

[22] M. S. Hossain, T. Joshi, and G. Stacey, "System approaches to study root hairs as a single cell plant model: current status and future perspectives," *Frontiers in Plant Science*, vol. 6, article 363, 2015.

[23] K. Birnbaum, D. E. Shasha, J. Y. Wang et al., "A gene expression map of the arabidopsis root," *Science*, vol. 302, no. 5652, pp. 1956–1960, 2003.

[24] J. R. Dinneny, T. A. Long, J. Y. Wang et al., "Cell identity mediates the response of *Arabidopsis* roots to abiotic stress," *Science*, vol. 320, no. 5878, pp. 942–945, 2008.

[25] A. S. Iyer-Pascuzzi, T. Jackson, H. Cui et al., "Cell identity regulators link development and stress responses in the *Arabidopsis* root," *Developmental Cell*, vol. 21, no. 4, pp. 770–782, 2011.

[26] S. M. Brady, D. A. Orlando, J.-Y. Lee et al., "A high-resolution root spatiotemporal map reveals dominant expression patterns," *Science*, vol. 318, no. 5851, pp. 801–806, 2007.

[27] M. W. Schmid, A. Schmidt, and U. Grossniklaus, "The female gametophyte: an emerging model for cell type-specific systems biology in plant development," *Frontiers in Plant Science*, vol. 6, article 907, 2015.

[28] J. D. Becker, S. Takeda, F. Borges, L. Dolan, and J. A. Feijó, "Transcriptional profiling of Arabidopsis root hairs and pollen defines an apical cell growth signature," *BMC Plant Biology*, vol. 14, no. 1, article 197, 2014.

[29] P. Lan, W. Li, W.-D. Lin, S. Santi, and W. Schmidt, "Mapping gene activity of Arabidopsis root hairs," *Genome Biology*, vol. 14, no. 6, article R67, 2013.

[30] A. Bruex, R. M. Kainkaryam, Y. Wieckowski et al., "A gene regulatory network for root epidermis cell differentiation in Arabidopsis," *PLoS Genetics*, vol. 8, no. 1, Article ID e1002446, 2012.

[31] M. A. Jones, M. J. Raymond, and N. Smirnoff, "Analysis of the root-hair morphogenesis transcriptome reveals the molecular identity of six genes with roles in root-hair development in *Arabidopsis*," *The Plant Journal*, vol. 45, no. 1, pp. 83–100, 2006.

[32] M. Libault, A. Farmer, T. Joshi et al., "An integrated transcriptome atlas of the crop model *Glycine max*, and its use in comparative analyses in plants," *The Plant Journal*, vol. 63, no. 1, pp. 86–99, 2010.

[33] A. Breakspear, C. Liu, S. Roy et al., "The root hair 'infectome' of *Medicago truncatula* uncovers changes in cell cycle genes and reveals a requirement for Auxin signaling in rhizobial infection," *The Plant Cell*, vol. 26, no. 12, pp. 4680–4701, 2014.

[34] G. E. D. Oldroyd, "Speak, friend, and enter: signalling systems that promote beneficial symbiotic associations in plants," *Nature Reviews Microbiology*, vol. 11, no. 4, pp. 252–263, 2013.

[35] T. L. R. Coker, V. Cevik, J. L. Beynon, and M. L. Gifford, "Spatial dissection of the *Arabidopsis thaliana* transcriptional response to downy mildew using fluorescence activated cell sorting," *Frontiers in Plant Science*, vol. 6, article 527, 2015.

[36] R.-S. Wang, S. Pandey, S. Li et al., "Common and unique elements of the ABA-regulated transcriptome of Arabidopsis guard cells," *BMC Genomics*, vol. 12, article 216, 2011.

[37] E. Harada, J.-A. Kim, A. J. Meyer, R. Hell, S. Clemens, and Y.-E. Choi, "Expression profiling of tobacco leaf trichomes identifies genes for biotic and abiotic stresses," *Plant and Cell Physiology*, vol. 51, no. 10, pp. 1627–1637, 2010.

[38] X. He, J. Zeng, F. Cao et al., "*HvEXPB7*, a novel beta-expansin gene revealed by the root hair transcriptome of Tibetan wild barley, improves root hair growth under drought stress," *Journal of Experimental Botany*, vol. 66, no. 22, pp. 7405–7419, 2015.

[39] T. Okamoto, K. Higuchi, T. Shinkawa et al., "Identification of major proteins in maize egg cells," *Plant and Cell Physiology*, vol. 45, no. 10, pp. 1406–1412, 2004.

[40] M. Abiko, K. Furuta, Y. Yamauchi et al., "Identification of proteins enriched in rice egg or sperm cells by single-cell proteomics," *PLoS ONE*, vol. 8, no. 7, Article ID e69578, 2013.

[41] T. Uchiumi, T. Shinkawa, T. Isobe, and T. Okamoto, "Identification of the major protein components of rice egg cells," *Journal of Plant Research*, vol. 120, no. 4, pp. 575–579, 2007.

[42] I. S. Sheoran, K. A. Sproule, D. J. H. Olson, A. R. S. Ross, and V. K. Sawhney, "Proteome profile and functional classification of proteins in *Arabidopsis thaliana* (*Landsberg erecta*) mature pollen," *Sexual Plant Reproduction*, vol. 19, no. 4, pp. 185–196, 2006.

[43] S. Dai, L. Li, T. Chen, K. Chong, Y. Xue, and T. Wang, "Proteomic analyses of *Oryza sativa* mature pollen reveal novel proteins associated with pollen germination and tube growth," *Proteomics*, vol. 6, no. 8, pp. 2504–2529, 2006.

[44] J. Zou, L. Song, W. Zhang, Y. Wang, S. Ruan, and W.-H. Wu, "Comparative proteomic analysis of *Arabidopsis* mature pollen and germinated pollen," *Journal of Integrative Plant Biology*, vol. 51, no. 5, pp. 438–455, 2009.

[45] R. Holmes-Davis, C. K. Tanaka, W. H. Vensel, W. J. Hurkman, and S. McCormick, "Proteome mapping of mature pollen of *Arabidopsis thaliana*," *Proteomics*, vol. 5, no. 18, pp. 4864–4884, 2005.

[46] W. Ge, Y. Song, C. Zhang, Y. Zhang, A. L. Burlingame, and Y. Guo, "Proteomic analyses of apoplastic proteins from germinating *Arabidopsis thaliana* pollen," *Biochimica et Biophysica Acta (BBA)—Proteins and Proteomics*, vol. 1814, no. 12, pp. 1964–1973, 2011.

[47] S. Noir, A. Bräutigam, T. Colby, J. Schmidt, and R. Panstruga, "A reference map of the *Arabidopsis thaliana* mature pollen proteome," *Biochemical and Biophysical Research Communications*, vol. 337, no. 4, pp. 1257–1266, 2005.

[48] Y. Zhu, P. Zhao, X. Wu, W. Wang, M. Scali, and M. Cresti, "Proteomic identification of differentially expressed proteins in mature and germinated maize pollen," *Acta Physiologiae Plantarum*, vol. 33, no. 4, pp. 1467–1474, 2011.

[49] W. Zhang, C. Qin, J. Zhao, and X. Wang, "Phospholipase Dα1-derived phosphatidic acid interacts with ABI1 phosphatase 2C and regulates abscisic acid signaling," *Proceedings of the National Academy of Sciences of the United States of America*, vol. 101, no. 25, pp. 9508–9513, 2004.

[50] W. Wang, B. Vinocur, and A. Altman, "Plant responses to drought, salinity and extreme temperatures: towards genetic engineering for stress tolerance," *Planta*, vol. 218, no. 1, pp. 1–14, 2003.

[51] Y.-O. Kim, J. S. Kim, and H. Kang, "Cold-inducible zinc finger-containing glycine-rich RNA-binding protein contributes to the enhancement of freezing tolerance in *Arabidopsis thaliana*," *The Plant Journal*, vol. 42, no. 6, pp. 890–900, 2005.

[52] A. Sallets, M. Beyaert, M. Boutry, and A. Champagne, "Comparative proteomics of short and tall glandular trichomes of *Nicotiana tabacum* reveals differential metabolic activities," *Journal of Proteome Research*, vol. 13, no. 7, pp. 3386–3396, 2014.

[53] T. Wu, Y. Wang, and D. Guo, "Investigation of glandular trichome proteins in *Artemisia annua* L. using comparative proteomics," *PLoS ONE*, vol. 7, no. 8, Article ID e41822, 2012.

[54] S. Kryvych, S. Kleessen, B. Ebert, B. Kersten, and J. Fisahn, "Proteomics—the key to understanding systems biology of Arabidopsis trichomes," *Phytochemistry*, vol. 72, no. 10, pp. 1061–1070, 2011.

[55] S. Wienkoop, D. Zoeller, B. Ebert et al., "Cell-specific protein profiling in *Arabidopsis thaliana* trichomes: identification of trichome-located proteins involved in sulfur metabolism and detoxification," *Phytochemistry*, vol. 65, no. 11, pp. 1641–1649, 2004.

[56] E. Van Cutsem, G. Simonart, H. Degand, A.-M. Faber, P. Morsomme, and M. Boutry, "Gel-based and gel-free proteomic analysis of *Nicotiana tabacum* trichomes identifies proteins involved in secondary metabolism and in the (a)biotic stress response," *Proteomics*, vol. 11, no. 3, pp. 440–454, 2011.

[57] S. Amme, T. Rutten, M. Melzer et al., "A proteome approach defines protective functions of tobacco leaf trichomes," *Proteomics*, vol. 5, no. 10, pp. 2508–2518, 2005.

[58] S. Dai and S. Chen, "Single-cell-type proteomics: toward a holistic understanding of plant function," *Molecular and Cellular Proteomics*, vol. 11, no. 12, pp. 1622–1630, 2012.

[59] M. Zhu, B. Simons, N. Zhu, D. G. Oppenheimer, and S. Chen, "Analysis of abscisic acid responsive proteins in *Brassica napus* guard cells by multiplexed isobaric tagging," *Journal of Proteomics*, vol. 73, no. 4, pp. 790–805, 2010.

[60] Z. Zhao, B. A. Stanley, W. Zhang, and S. M. Assmann, "ABA-regulated G protein signaling in *Arabidopsis* guard cells: a proteomic perspective," *Journal of Proteome Research*, vol. 9, no. 4, pp. 1637–1647, 2010.

[61] J. Wan, M. Torres, A. Ganapathy et al., "Proteomic analysis of soybean root hairs after infection by *Bradyrhizobium japonicum*," *Molecular Plant-Microbe Interactions*, vol. 18, no. 5, pp. 458–467, 2005.

[62] L. Brechenmacher, T. H. N. Nguyen, K. Hixson et al., "Identification of soybean proteins from a single cell type: the root hair," *Proteomics*, vol. 12, no. 22, pp. 3365–3373, 2012.

[63] T. H. N. Nguyen, L. Brechenmacher, J. T. Aldrich et al., "Quantitative phosphoproteomic analysis of soybean root hairs inoculated with *Bradyrhizobium japonicum*," *Molecular & Cellular Proteomics*, vol. 11, no. 11, pp. 1140–1155, 2012.

[64] A. Tomos, P. Hinde, P. Richardson, J. Pritchard, and W. Fricke, "Microsampling and measurements of solutes in single cells," in *Plant Cell Biology: A Practical Approach*, N. Harris and K. J. Oparka, Eds., pp. 297–314, Oxford University Press, Oxford, UK, 1994.

[65] A. Tomos, A. Korolev, J. Farrar, K. Nicolay, R. Bowtell, and W. Koeckenberger, "Water and solute relations of the carrot cambium studied at single-cell resolution," in *Cell and Molecular Biology of Wood Formation*, pp. 101–112, Bios, Oxford, UK, 2000.

[66] S. Brandt, J. Kehr, C. Walz, A. Imlau, L. Willmitzer, and J. Fisahn, "A rapid method for detection of plant gene transcripts from single epidermal, mesophyll and companion cells of intact leaves," *The Plant Journal*, vol. 20, no. 2, pp. 245–250, 1999.

[67] S. P. Brandt, "Microgenomics: gene expression analysis at the tissue-specific and single-cell levels," *Journal of Experimental Botany*, vol. 56, no. 412, pp. 495–505, 2005.

[68] A. D. Tomos and R. A. Leigh, "The pressure probe: a versatile tool in plant cell physiology," *Annual Review of Plant Biology*, vol. 50, no. 1, pp. 447–472, 1999.

[69] J. Kehr, "High resolution spatial analysis of plant systems," *Current Opinion in Plant Biology*, vol. 4, no. 3, pp. 197–201, 2001.

[70] M. Schad, R. Mungur, O. Fiehn, and J. Kehr, "Metabolic profiling of laser microdissected vascular bundles of *Arabidopsis thaliana*," *Plant Methods*, vol. 1, no. 1, article 2, 2005.

[71] J. Kehr, "Single cell technology," *Current Opinion in Plant Biology*, vol. 6, no. 6, pp. 617–621, 2003.

[72] A. D. Tomos and R. A. Sharrock, "Cell sampling and analysis (SiCSA): metabolites measured at single cell resolution," *Journal of Experimental Botany*, vol. 52, no. 356, pp. 623–630, 2001.

[73] S. G. Oliver, M. K. Winson, D. B. Kell, and F. Baganz, "Systematic functional analysis of the yeast genome," *Trends in Biotechnology*, vol. 16, no. 9, pp. 373–378, 1998.

[74] R. G. Ratcliffe and Y. Shachar-Hill, "Probing plant metabolism with NMR," *Annual Review of Plant Biology*, vol. 52, no. 1, pp. 499–526, 2001.

[75] J. K. M. Roberts, "NMR adventures in the metabolic labyrinth within plants," *Trends in Plant Science*, vol. 5, no. 1, pp. 30–34, 2000.

[76] R. Bligny and R. Douce, "NMR and plant metabolism," *Current Opinion in Plant Biology*, vol. 4, no. 3, pp. 191–196, 2001.

[77] O. Fiehn, J. Kopka, P. Dörmann, T. Altmann, R. N. Trethewey, and L. Willmitzer, "Metabolite profiling for plant functional genomics," *Nature Biotechnology*, vol. 18, no. 11, pp. 1157–1161, 2000.

[78] U. Roessner, A. Luedemann, D. Brust et al., "Metabolic profiling allows comprehensive phenotyping of genetically or environmentally modified plant systems," *The Plant Cell*, vol. 13, no. 1, pp. 11–29, 2001.

[79] D. Sturtevant, Y.-J. Lee, and K. D. Chapman, "Matrix assisted laser desorption/ionization-mass spectrometry imaging (MALDI-MSI) for direct visualization of plant metabolites *in situ*," *Current Opinion in Biotechnology*, vol. 37, pp. 53–60, 2016.

[80] K. Arlt, S. Brandt, and J. Kehr, "Amino acid analysis in five pooled single plant cell samples using capillary electrophoresis coupled to laser-induced fluorescence detection," *Journal of Chromatography A*, vol. 926, no. 2, pp. 319–325, 2001.

[81] S. Sato, T. Soga, T. Nishioka, and M. Tomita, "Simultaneous determination of the main metabolites in rice leaves using capillary electrophoresis mass spectrometry and capillary electrophoresis diode array detection," *Plant Journal*, vol. 40, no. 1, pp. 151–163, 2004.

[82] T. Soga, Y. Ueno, H. Naraoka, Y. Ohashi, M. Tomita, and T. Nishioka, "Simultaneous determination of anionic intermediates for

Bacillus subtilis metabolic pathways by capillary electrophoresis electrospray ionization mass spectrometry," *Analytical Chemistry*, vol. 74, no. 10, pp. 2233–2239, 2002.

[83] R. D. Smith, J. A. Loo, C. G. Edmonds, C. J. Barinaga, and H. R. Udseth, "New developments in biochemical mass spectrometry: electrospray ionization," *Analytical Chemistry*, vol. 62, no. 9, pp. 882–899, 1990.

[84] D.-H. Oh, B. J. Barkla, R. Vera-Estrella et al., "Cell type-specific responses to salinity-the epidermal bladder cell transcriptome of *Mesembryanthemum crystallinum*," *New Phytologist*, vol. 207, no. 3, pp. 627–644, 2015.

[85] B. J. Barkla and R. Vera-Estrella, "Single cell-type comparative metabolomics of epidermal bladder cells from the halophyte *Mesembryanthemum crystallinum*," *Frontiers in Plant Science*, vol. 6, article 435, 2015.

[86] R. Lugan, M.-F. Niogret, L. Leport et al., "Metabolome and water homeostasis analysis of *Thellungiella salsuginea* suggests that dehydration tolerance is a key response to osmotic stress in this halophyte," *The Plant Journal*, vol. 64, no. 2, pp. 215–229, 2010.

[87] D. H. Sanchez, F. L. Pieckenstain, F. Escaray et al., "Comparative ionomics and metabolomics in extremophile and glycophytic *Lotus* species under salt stress challenge the metabolic preadaptation hypothesis," *Plant, Cell & Environment*, vol. 34, no. 4, pp. 605–617, 2011.

[88] G. Gutiérrez-Alcalá, C. Gotor, A. J. Meyer, M. Fricker, J. M. Vega, and L. C. Romero, "Glutathione biosynthesis in *Arabidopsis trichome* cells," *Proceedings of the National Academy of Sciences of the United States of America*, vol. 97, no. 20, pp. 11108–11113, 2000.

[89] X. Ou, Y. Gan, P. Chen, M. Qiu, K. Jiang, and G. Wang, "Stomata prioritize their responses to multiple biotic and abiotic signal inputs," *PLoS ONE*, vol. 9, no. 7, Article ID e101587, 2014.

[90] J.-M. He, X.-G. Ma, Y. Zhang et al., "Role and interrelationship of Gα protein, hydrogen peroxide, and nitric oxide in ultraviolet B-induced stomatal closure in *Arabidopsis* leaves," *Plant Physiology*, vol. 161, no. 3, pp. 1570–1583, 2013.

[91] T. Joudoi, Y. Shichiri, N. Kamizono et al., "Nitrated cyclic GMP modulates guard cell signaling in Arabidopsis," *Plant Cell*, vol. 25, no. 2, pp. 558–571, 2013.

[92] R. Desikan, M.-K. Cheung, J. Bright, D. Henson, J. T. Hancock, and S. J. Neill, "ABA, hydrogen peroxide and nitric oxide signalling in stomatal guard cells," *Journal of Experimental Botany*, vol. 55, no. 395, pp. 205–212, 2004.

[93] B. B. Misra, B. R. Acharya, D. Granot, S. M. Assmann, and S. Chen, "The guard cell metabolome: functions in stomatal movement and global food security," *Frontiers in Plant Science*, vol. 6, article 334, 2015.

[94] X. Jin, R.-S. Wang, M. Zhu et al., "Abscisic acid-responsive guard cell metabolomes of *Arabidopsis* wild-type and *gpa1* G-protein mutants," *The Plant Cell*, vol. 25, no. 12, pp. 4789–4811, 2013.

[95] Q. Sun, J. Liu, Q. Zhang et al., "Characterization of three novel desaturases involved in the delta-6 desaturation pathways for polyunsaturated fatty acid biosynthesis from *Phytophthora infestans*," *Applied Microbiology and Biotechnology*, vol. 97, no. 17, pp. 7689–7697, 2013.

[96] L. Brechenmacher, Z. Lei, M. Libault et al., "Soybean metabolites regulated in root hairs in response to the symbiotic bacterium *Bradyrhizobium japonicum*," *Plant Physiology*, vol. 153, no. 4, pp. 1808–1822, 2010.

[97] J. G. Streeter and M. L. Gomez, "Three enzymes for trehalose synthesis in *Bradyrhizobium* cultured bacteria and in bacteroids from soybean nodules," *Applied and Environmental Microbiology*, vol. 72, no. 6, pp. 4250–4255, 2006.

[98] J. G. Streeter, "Effect of trehalose on survival of *Bradyrhizobium japonicum* during desiccation," *Journal of Applied Microbiology*, vol. 95, no. 3, pp. 484–491, 2003.

[99] B. Bartels and A. Svatoš, "Spatially resolved in vivo plant metabolomics by laser ablation-based mass spectrometry imaging (MSI) techniques: LDI-MSI and LAESI," *Frontiers in Plant Science*, vol. 6, article 471, 2015.

[100] P. Nemes, A. A. Barton, and A. Vertes, "Three-dimensional imaging of metabolites in tissues under ambient conditions by laser ablation electrospray ionization mass spectrometry," *Analytical Chemistry*, vol. 81, no. 16, pp. 6668–6675, 2009.

[101] B. Shrestha and A. Vertes, "*In situ* metabolic profiling of single cells by laser ablation electrospray ionization mass spectrometry," *Analytical Chemistry*, vol. 81, no. 20, pp. 8265–8271, 2009.

[102] B. Shrestha, J. M. Patt, and A. Vertes, "*In situ* cell-by-cell imaging and analysis of small cell populations by mass spectrometry," *Analytical Chemistry*, vol. 83, no. 8, pp. 2947–2955, 2011.

[103] G. Lopez-Casado, P. A. Covey, P. A. Bedinger et al., "Enabling proteomic studies with RNA-Seq: the proteome of tomato pollen as a test case," *Proteomics*, vol. 12, no. 6, pp. 761–774, 2012.

[104] F. S. O. Fritzsch, C. Dusny, O. Frick, and A. Schmid, "Single-cell analysis in biotechnology, systems biology, and biocatalysis," *Annual Review of Chemical and Biomolecular Engineering*, vol. 3, pp. 129–155, 2012.

Hindawi Publishing Corporation
BioMed Research International
Volume 2016, Article ID 6021047, 23 pages
http://dx.doi.org/10.1155/2016/6021047

Research Article

Leaf Proteome Analysis Reveals Prospective Drought and Heat Stress Response Mechanisms in Soybean

Aayudh Das,[1,2] Moustafa Eldakak,[1] Bimal Paudel,[1] Dea-Wook Kim,[3] Homa Hemmati,[4] Chhandak Basu,[4] and Jai S. Rohila[1]

[1]*Department of Biology & Microbiology, South Dakota State University, Brookings, SD 57007, USA*
[2]*Department of Biochemistry and Biophysics, Texas A&M University, College Station, TX 77840, USA*
[3]*National Institute of Crop Science, Rural Development Administration (RDA), Wanju-gun, Jeollabuk-do 55365, Republic of Korea*
[4]*Department of Biology, California State University Northridge, Northridge, CA 91330, USA*

Correspondence should be addressed to Jai S. Rohila; jai.rohila@sdstate.edu

Received 10 November 2015; Accepted 1 February 2016

Academic Editor: Paloma K. Menguer

Drought and heat are among the major abiotic stresses that affect soybean crops worldwide. During the current investigation, the effect of drought, heat, and drought plus heat stresses was compared in the leaves of two soybean varieties, Surge and Davison, combining 2D-DIGE proteomic data with physiology and biochemical analyses. We demonstrated how 25 differentially expressed photosynthesis-related proteins affect RuBisCO regulation, electron transport, Calvin cycle, and carbon fixation during drought and heat stress. We also observed higher abundance of heat stress-induced EF-Tu protein in Surge. It is possible that EF-Tu might have activated heat tolerance mechanisms in the soybean. Higher level expressions of heat shock-related protein seem to be regulating the heat tolerance mechanisms. This study identifies the differential expression of various abiotic stress-responsive proteins that regulate various molecular processes and signaling cascades. One inevitable outcome from the biochemical and proteomics assays of this study is that increase of ROS levels during drought stress does not show significant changes at the phenotypic level in Davison and this seems to be due to a higher amount of carbonic anhydrase accumulation in the cell which aids the cell to become more resistant to cytotoxic concentrations of H_2O_2.

1. Introduction

Soybeans are one of the most important legume crops and have a major impact on the US and global economies. International markets use about half of the soybeans produced in the US, and its production is expected to alleviate the global demand for human consumption, biofuel production, and high-protein meal for animal feed [1]. In 2011, the total soybean production in the US was 83.29×10^{12} Kg with a total trade value of $40.2 billion [2, 3]. Heat and drought are the predominant abiotic stress factors that limit the growth and development of soybean plants by causing a reduction in carbon fixation by the photosynthetic apparatus of the plants, resulting in net yield losses [4]. At the cellular level, plants exhibit a variety of responses related to their physiology and biochemistry to overcome the stress. Drought stress causes reduced carbon assimilation due to stomatal closure, membrane damage, and distressed activity of various CO_2 fixation enzymes [5]. Heat stress increases membrane damage and impairs metabolic functions [6–8]. As a result, combination of drought and heat stress causes enormous economic losses for farmers [9].

Proteomic evaluation for the purpose of differentially regulated proteins identification in response to the drought, heat, and the combined stress has been monitored in various plants in context of the morphological and physiological changes [10–12]. Particularly, changes in proteomic expression during drought stress have been observed in major crops like rice and wheat which shows differential regulation of various proteins [13–15]. Earlier studies using proteomic and transcriptomic approaches also implicated the drought stress response mechanisms including alteration in the signal transduction pathway and plant's metabolism [16–19]. Moreover, in response to heat stress, many stress proteins

were originally identified as HSP which indicates plant's tolerance threshold [20]. To improve the understanding of the mechanisms underlying soybean responses to drought and heat stress, in the present investigation we have used a global proteomic approach combined with physiological and computational analysis [10, 21, 22]. The two major soybean varieties, Surge (yield 3,272 Kg/ha) and Davison (yield 4,074 Kg/ha), showing distinct physiological characteristics were used in this study. Proteomic analysis revealed differentially expressed proteins related to key biological processes (such as photosynthesis and respiration), various metabolic pathways (nitrogen metabolism and carbohydrate metabolism), and several other molecular processes (protein biosynthesis and ATP synthesis). Computational analysis predicted a protein network displaying the likely interactions between protein abundances and plant stress responses. These analyses will enable the development of plant molecular improvement programs to produce more effective strategies contributing to greater food security in the coming years. Since the proteins are the translated version of mRNA (proteomics approach may have advantage over transcriptomics approach [4]) several research groups have utilized the power of proteomic evaluations and combined it with physiological studies to create a link between plant physiology and the molecular signatory responses [10, 23]. The primary aim of this study was to investigate differential protein expression between two contrasting genotypes for drought and heat stress responses, and to reveal the drought and heat stress-responsive mechanisms in soybean at early stage of growth. Based on physiological analyses, we found that drought and heat stress decrease photosynthesis and reduce stomatal conductance and transpiration rates, which ultimately alter the net CO_2 concentrations in leaves. The proteomic analyses facilitated the characterization of a set of proteins whose expressions were altered under heat and drought stresses. We found that, in Surge, more proteins were downregulated during drought stress than during heat stress, but the combined stress conditions exerted a drastic effect at both the molecular and the phenotypic levels. In this study, we have identified genes involved in photosynthesis that were differentially expressed during drought and heat stress conditions. This differential expression is most likely the result of blocked interactions between RuBisCO, RuBisCO activase, electron transport chain, and downregulation of various Calvin cycle enzymes, which ultimately results in a net reduced level of photosynthesis [24]. This study identified greater accumulations of EF-Tu protein during heat stress in Surge. The results also indicated the accumulation of a 70 kDa stromal HSP, which we assume is crucial for plant survival during heat stress by activating heat tolerance responses [25]. Previously, it has been reported that drought and heat stresses may trigger the formation of reactive oxygen species (ROS) [26, 27]. Likewise, we also examined the drought and heat stress-induced changes in the production of ROS and found that, during drought stress, soybeans exhibited a significant increase in the level of hydrogen peroxide and an enhanced ROS detoxification capacity via carbonic anhydrase, which protects the plant against oxidative damage [28]. Plants use ABA as a signaling molecule while maintaining a positive water balance throughout the system, as physiological studies have shown [29–31]. Elevated ABA levels during heat stress are shown to protect the maize plant against heat-induced oxidative damage [32]. We quantified the ABA levels in soybean leaves during all the stress conditions and have discussed it in drought and heat stress contexts for soybean crop. At the level of computational analysis, we have constructed a protein-protein network to predict the interactions between the differentially expressed proteins [17].

2. Materials and Methods

2.1. Plant Growth Conditions. Soybean (*Glycine max* L. cultivars: Surge and Davison) seeds were planted in pots filled with Metromix 360 (Sun Gro Horticulture, Floodwood, Minnesota, USA). A total of eight, 6.0-liter size pots, each containing 4-5 individual soybean plants (biological replications), were placed in a growth chamber (Conviron, Canada) illuminated with white fluorescent light and incandescent bulbs (500 μmoles m^{-2} s^{-1}, 12 h photoperiod) at 25°C and 70% RH for 3 weeks. At this stage, 8 pots from each cultivar were separated into 4 groups (control, drought, heat, and drought plus heat; Figure S1 in Supplementary Material available online at http://dx.doi.org/10.1155/2016/6021047). Watering was done daily with 150 mL tap water per pot until the second trifoliate leaves emerged, after which various stress treatments were carried out. The first group was the control, and it was maintained under the conditions described above. For the second group, the plants were exposed to drought stress (no watering for 7 days). The third group contained plants that were exposed to heat stress (42°C daytime/35°C night time, 50% humidity) with normal watering schedules. The fourth group contained plants that were exposed to drought plus heat stress. Soil moisture sensors (SM 100, Spectrum Technologies) were inserted into all of the pots on the day the plants were exposed to abiotic stress to measure the % VWC for each treatment. The % VWC value was measured throughout the entire experimental period using a microstation data logger [33].

2.2. Measurement of Photosynthesis, Stomatal Conductance, Transpiration, and Leaf Water Potential. Photosynthesis, stomatal conductance, and the transpiration rate were measured, every day at noon, on the first and second trifoliate stage leaves for all the plants in each group and with three replications (following the rationale from previous published drought stress time point studies [34, 35]). We used CI-510 Photosynthesis System (CID Bio-Science) with the following parameters: leaf chamber area: 6.25 cm^2; flow rate: 0.3; time interval: 1 second; delay: 2 seconds; system: open; temperature: 25°C, as per the manufacturer's recommendations. Leaf water potential was measured using a pressure chamber (PMS Instrument) following the manufacturer's recommendations.

2.3. Sample Preparation for 2D-DIGE. Leaf samples collected from all treatments were snap-frozen under liquid nitrogen and stored in −80°C freezer until further use. Total protein was isolated according to the procedure of Hurkman

and Tanaka [36]. Ground soybean leaf tissue (500 mg) was homogenized in 5 mL of 2D cell lysis buffer (30 mM Tris-HCl, pH 8.8, 0.9 M sucrose, 10 mM EDTA, 0.4% 2-mercaptoethanol, 7 M urea, 2 M thiourea, and 4% CHAPS) and an equal volume of Tris-saturated phenol, vortexed for 30 seconds and incubated for 30 min at 4°C. Following homogenization and mixing, centrifugation was carried out for 15 min at 4°C at 6,000 rpm, and the phenol phase was collected in a fresh tube. Now, the proteins in the collected phase were precipitated overnight by adding 5 volumes of ice-cold 0.1 M ammonium acetate in 100% methanol at −20°C. Next day, after 20 min of centrifugation at 10,000 rpm, the protein pellet was washed in 5 mL of 0.1 M ammonium acetate in 100% methanol followed by a wash in 5 mL of ice-cold 80% acetone, and then a final wash in 4 mL of 70% ethanol. The protein pellet was air-dried and stored at −80°C until downstream experiments. Protein quantification assays were performed using the Bio-Rad reagent (catalog# 500-0006) on the Bio-Rad SmartSpec Plus spectrophotometer.

2.4. 2D-DIGE, Trypsin Digestion, and MALDI-TOF MS Analysis. 2D-DIGE analysis was performed by Applied Biomics (Hayward, CA, USA). For each sample set (either Surge or Davison with respective treatments, Figure S1), 30 μg of sample protein was mixed with 1.0 μL of diluted Cy3 or Cy5 dye (1 : 5 dilution in a 1 nmol μL^{-1} DMF stock) for labeling. A pooled protein sample containing equal amounts of all samples in the experiment was labeled with Cy2 using the same protocol. After vortexing, the tubes were incubated in the dark for 30 min on ice. Next, 1.0 μL of 10 mM lysine was added to each sample. After that, the samples were vortexed and incubated in the dark for 15 min on ice. Next, the Cy2, Cy3, and Cy5 labeled samples were mixed by adding 2X 2D sample buffer (Bio-Rad), followed by the addition of 100 μL of DeStreak solution and a rehydration buffer (Bio-Rad) up to 350 μL for the 13 cm gradient (pH 4–7) IPG strip. Upon completion of IEF, the IPG strips were incubated in freshly made equilibration buffers I and II (Bio-Rad) for 15 minutes with gentle shaking. The IPG strips were rinsed in Tris-glycine-SDS running buffer (Bio-Rad) and then transferred to 12% SDS-polyacrylamide gels, followed by sealing with 0.5% agarose solution for second-dimension electrophoresis. The SDS gels were electrophoresed at 175 volts at 15°C for 8 hrs. Gel images were scanned using Typhoon TRIO (GE Healthcare, PA, USA) and were analyzed using Image QuantTL software (version 6.0, GE Healthcare, USA) and then subjected to in-gel analysis and cross-gel analysis using DeCyder software, version 6.5 (GE Healthcare). The differential expression of the proteins was obtained from in-gel DeCyder software analysis [37]. This way, a total of 12 gels (Table S1) were run comprising protein samples from 8 different sets of treatments (Figure S1) and 3 replications each. The spots of interest were selected based on the in-gel analysis and statistical analyses (Table S2), p value of ≤0.1 and cut-off value of 1.5-fold, and were picked up using the Ettan Spot Picker (GE Healthcare). The picked gel spots were washed and digested in-gel using modified porcine trypsin protease (Trypsin Gold, Promega). The digested tryptic peptides were desalted using Zip-tip C18 (Millipore) and spotted on the MALDI plate. MALDI-TOF MS and TOF/TOF tandem MS were performed on a 5800 mass spectrometer (AB Sciex). The MALDI-TOF mass spectra were generated in the reflectron positive ion mode, and TOF/TOF tandem MS fragmentation spectra were acquired for each sample. On average, 4,000 laser shots per fragmentation spectrum were applied to each of the 5–10 most abundant ions present in each sample, excluding the trypsin autolytic peptides and other known background ions [38]. Both the resulting peptide mass and the associated fragmentation spectra were submitted to the MASCOT (version 2.4, Matrix Sciences, UK) in October 2014 to search the SwissProt database with 546,790 sequences. The searches were performed following the details of Poschmann et al. [39], for example, without constraining the protein MW or the pI value and with variable carbamidomethylation of cysteine and oxidation of methionine residues, a mass tolerance of 100 ppm, and allowing only one missed and/or nonspecific cleavage. Proteins with a protein score > 62 were considered to be assigned correctly. Candidates with either a protein score of CI % or an ion score of CI % greater than 95 were considered to be statistically significant. The protein peptide summary for all identified spots is listed in Supplementary Material Table S4.

2.5. ROS Measurement (Hydrogen Peroxide Quantification). The levels of H_2O_2 in leaves were measured using the Amplex® Red Hydrogen Peroxide/Peroxidase Assay Kit (Molecular Probes, catalog# A-22188) [40]. For this assay, manufacturer's protocol was followed. Briefly, 50 mg of the ground leaf powder was mixed with reaction buffer (pH 7.4), vortexed, and incubated on ice for 15 min. Then, the samples were centrifuged at 10,000 rpm for 10 min at 4°C, and the supernatant was collected. Next, 50 μL of the samples was loaded into a multiwell plate (clear bottom, black sides) followed by the addition of 50 μL of 100 μM Amplex® Red reagent and 0.2 U mL^{-1} HRP. The samples were incubated in the dark for 30 min at room temperature. Afterward, the fluorescence was measured at an emission wavelength of 620 nm using a Synergy 2 multimode microplate reader (BioTek); the blank value (buffer only) was subtracted from the sample's florescence values. Then, based on the standard curve, the H_2O_2 concentration was calculated in terms of nmol μL^{-1} sample [41].

2.6. Quantification of Abscisic Acid. ABA quantification was performed as outlined by Kim et al. [42]. Two hundred mg of ground leaf powder was suspended in 1 mL of sterile deionized water and incubated overnight at 4°C with constant shaking. The solution was centrifuged at 4,000 rpm for 20 min. Then, the supernatant was transferred to a clean microfuge tube ensuring that no leaf pieces were transferred. The solution then was dried completely using a vacuum concentrator. The dried precipitate was resuspended with 60 μL sterile deionized water and a 1 : 1000 dilution of the sample was made with TBS. ABA concentration was determined using a Phytodetek® ABA Test Kit (Agdia, USA) following the manufacturer's recommendations. A standard curve was generated using ABA standards (100, 20, 4, 0.8, 0.16, and 0.32 pmoles mL^{-1}). 100 μL of diluted sample per standard was

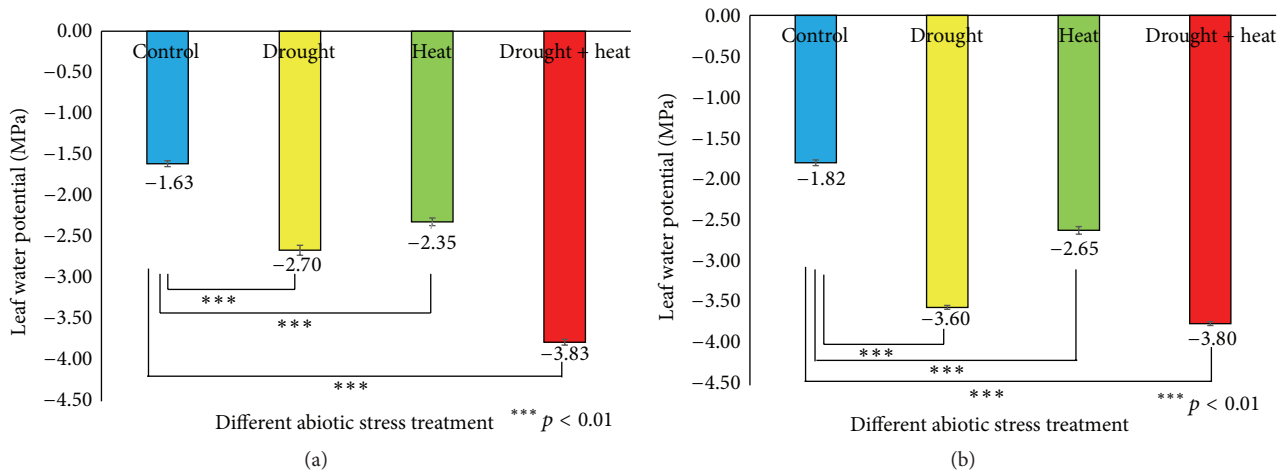

FIGURE 1: Bar diagrams showing the effect of various abiotic stresses on leaf water potential in two soybean cultivars Surge (a) and Davison (b). x-axis defines various abiotic stress treatments (drought, heat, and drought + heat) including control and y-axis defines leaf water potential in MPa (megapascal unit). Each value represents the mean ± SE of three replicates and the asterisks designate the significance of changes from their corresponding control (*** $p < 0.01$).

loaded onto an ABA-antibody coated multiwell plate, and the ABA concentration was determined according to manufacturer's guidelines. The absorbance values at 405 nm were read using Spectromax M3 (Molecular Devices). The ABA concentration was calculated using the slope of the standard curve based on the manufacturer's recommendations.

2.7. Computational Analysis and Protein-Protein Interaction Predictions. First, we mapped protein ID (using UniProt database) to the *Arabidopsis* accession numbers and performed a multiple sequence alignment of *Arabidopsis* homologs using CLUSTALO [43] to obtain the protein identities. To search the variety of functional connections between the 44 differentially expressed proteins, we used the online database resource STRING (http://string-db.org/) version 9.1 [44]. Then, after obtaining the primary interactions in STRING, we portrayed our different protein networks using Cytoscape software, version 3.0.1 [45].

2.8. Clustering and Statistical Analyses. For the clustering data, the $\log_2$-transformed expression values of the protein spots were used. Hierarchical clustering of the proteins was performed using Gene Cluster 3.0 [46] with Euclidean distance similarity metrics and the complete linkage method. The clusters were visualized using JAVA TREEVIEW [47]. The statistical significance of the results was evaluated using Student's t-test and a level of significance of $p \leq 0.05$ for the two group comparisons. Data analyses and graphical representations were performed using Microsoft Excel 2013.

3. Results

Understanding the mechanisms by which plants respond to drought, heat, and cooccurring drought and heat stresses plays a major role in optimizing crop performance under drought and high temperature conditions [16]. Figure S2 shows the phenotypic changes between soybean plants on the sixth day of the stress experiment.

3.1. Soil Moisture Content and Physiological Responses of Plants to Different Abiotic Stresses. To keep track of the soil moisture levels during the stress experiments, the soil water content was measured [48]. Figure S3 shows the soil moisture levels from Day 0 (prestress) to the sixth day of stress treatment. The leaf water potential is considered as a reliable parameter for quantifying the plant water stress response [49]. It was found (Figure 1) that, in Surge, stress reduced the leaf water potential from −1.63 MPa (control plants) to −2.70 MPa in drought-stressed plants, −2.35 MPa in heat-stressed plants, and −3.83 MPa in drought plus heat-stressed plants on the sixth day of stress. In Davison, we found that stress reduced the leaf water potential from −1.82 MPa (control plants) to −3.60 MPa in drought-stressed plants, −2.65 MPa in heat-stressed plants, and −3.80 MPa in drought plus heat-stressed plants, on the sixth day of stress.

Photosynthesis is among the primary processes affected by drought and heat stresses [50, 51]. In Surge control plants (Figure 2), it was found that there was no decrease in photosynthesis, whereas in drought-stressed plants a 19% decrease in photosynthesis was detected on the sixth day of stress. Interestingly, in heat-stressed plants, we found that the level of photosynthesis was identical to prestress condition; and in drought plus heat-stressed plants, we detected a 27.28% decrease in photosynthesis on the sixth day of stress compared to prestress (Day 0) conditions. In the Davison control plants, there was a 9% decrease in photosynthesis most likely due to a developmental effect and the water use efficiency of the plant on that particular day; in drought-stressed plants, there was a 34.36% decrease in photosynthesis; in heat-stressed plants, photosynthesis decreased to 6.55%; and in drought plus heat-stressed plants, we detected a huge decrease (28.13%) in photosynthesis on the sixth day of stress compared to prestress (Day 0) conditions.

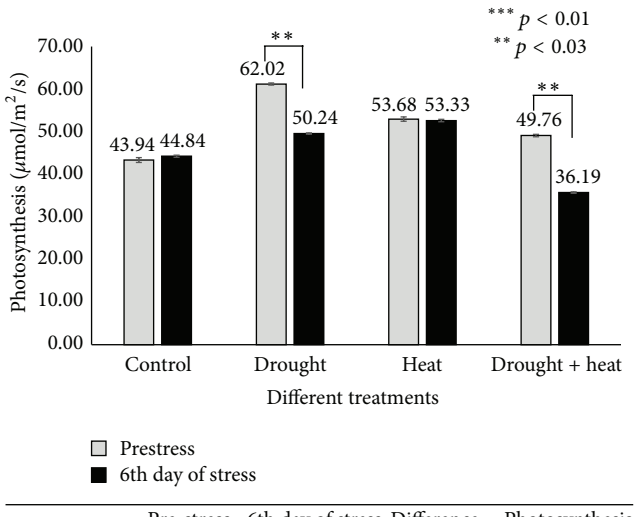

Surge	Pre-stress (μmol/m^2/s)	6th day of stress (μmol/m^2/s)	Difference (μmol/m^2/s)	Photosynthesis drop (%)
Control	43.94	44.84	−0.90	No drop
Drought	62.02	50.24	11.79	19.00
Heat	53.68	53.33	0.35	0.64
Drought + heat	49.76	36.19	13.57	27.28

(a)

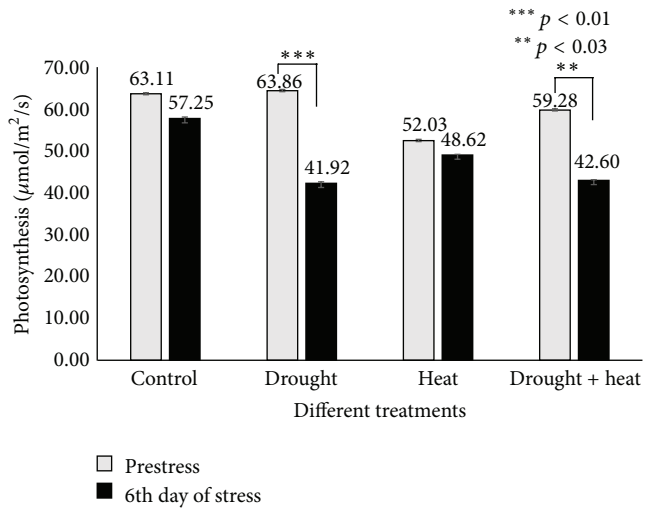

Davison	Prestress (μmol/m^2/s)	6th day of stress (μmol/m^2/s)	Difference (μmol/m^2/s)	Photosynthesis drop (%)
Control	63.11	57.25	5.86	9.28
Drought	63.86	41.92	21.94	34.36
Heat	52.03	48.62	3.41	6.55
Drought + heat	59.28	42.60	16.67	28.13

(b)

Figure 2: Bar diagram showing the effect of various abiotic stresses on photosynthesis in two soybean cultivars Surge (a) and Davison (b). x-axis defines various abiotic stress treatments (drought, heat, and drought + heat) including control and y-axis defines measurement of net photosynthesis (μmol/m^2/s). Each value represents the mean ± SE of three replicates and the asterisks designate the significance of changes from their resultant control ($^{***}p < 0.01$, $^{**}p < 0.03$).

Several studies have suggested changes in the transpiration rate or stomatal conductance in response to different stress conditions. Altering stomatal conductance causes a fluctuation in the leaf water potential by shifting the transpiration rate [52]. The results (Figure 3) revealed that, in Surge control plants, stomatal conductance was increased by 36.44% (at the same time, the transpiration rate increased by 59.84%), whereas in drought-stressed plants stomatal conductance was decreased by 21.18% (while the transpiration rate decreased by 73.02%) on the sixth day of stress compared to prestress (Day 0) conditions. In heat-stressed plants, stomatal conductance decreased by 15.94% (the transpiration rate decreased by 77.48%); and in drought plus heat-stressed plants, stomatal conductance decreased by 41.81% (the transpiration rate decreased by 130.35%) on the sixth day of stress compared to prestress (Day 0) conditions. In Davison control plants, we found that stomatal conductance decreased by 3.62% (the transpiration rate increased by 96.13%); in drought-stressed plants, stomatal conductance decreased by 13.05% (the transpiration rate decreased by 77.37%); in heat-stressed plants, stomatal conductance decreased by 1.53% (the transpiration rate decreased by 14.06%); and in cooccurring drought plus heat-stressed plants, stomatal conductance decreased by 15.45% (the transpiration rate decreased by 133.43%) on the sixth day of stress compared to prestress (Day 0) conditions.

Stomatal conductance also depends on the leaf temperature via the transpiration rates [52]. The analysis of present investigation indicated that leaf temperature increased in a nonproportional manner with stomatal conductance (Figure 4). We found that stomatal conductance reduced under all conditions in which the leaf temperature increased.

3.2. 2D-DIGE Analysis Followed by MALDI-TOF MS to Identify the Differentially Expressed Proteins in Response to Drought and Heat Stress. The comparison of the leaf proteins from the two soybean cultivars among the control, heat, drought, and drought plus heat stress conditions via 2D-DIGE analysis revealed a broad distribution in the pI range and in the molecular weight range. Figure 5 is a representative image of master gel, and supplemental Figures S4 and S5 show the Cy2/Cy3/Cy5 overlay images of all 12 gels run during the experiment. The protein spots were selected from the preparative gels for protein identification. Among the control and three treated groups, based on in-gel analysis, on average a total of 2600 spots were detected using DeCyder software. Of these, on average a total of 1,900–2,000 protein spots were matched among all other gels (Table SI); from here, a total of 108 spots were selected based on statistical analyses (p values; Table S2), and 92 differential spots were successfully identified using a threshold of significance of $p \leq 0.1$, and with a cut-off value of 1.5-fold increase/decrease in protein expressions. Of these identified spots, we determined the protein identity of 88 spots with high confidence (Tables S3 and S4), corresponding to 44 nonredundant differentially

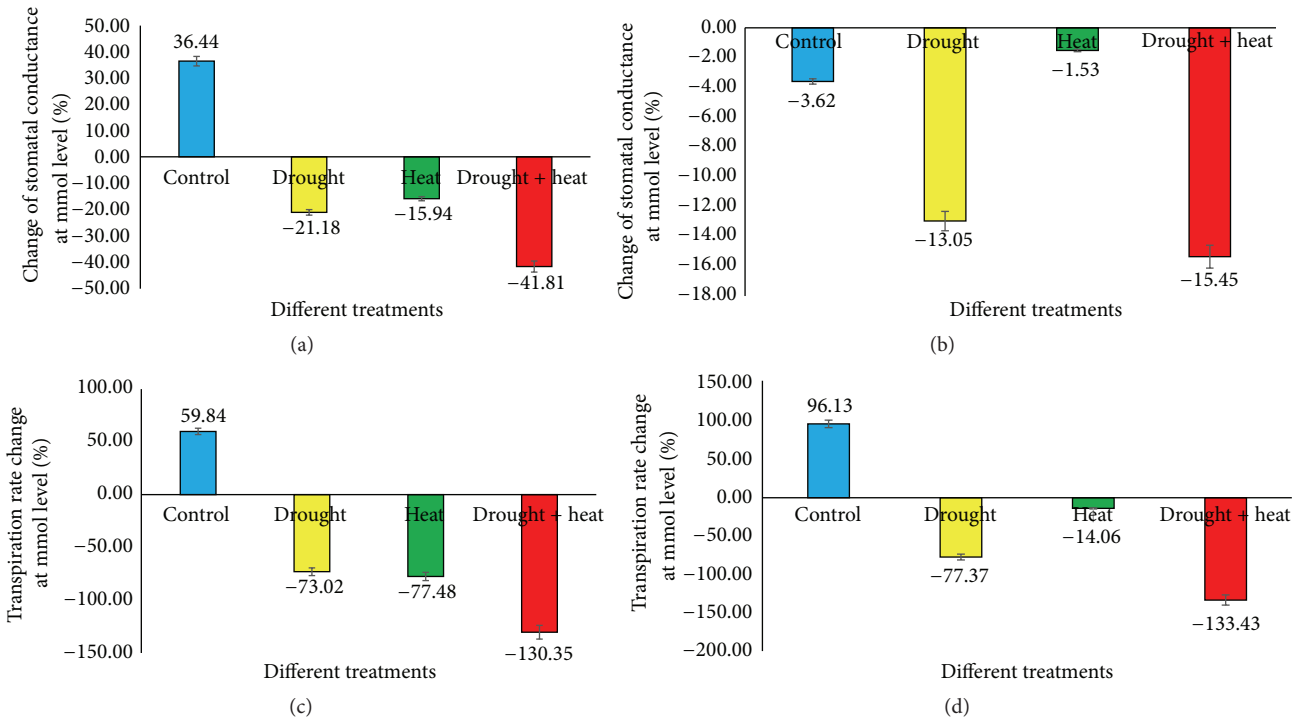

FIGURE 3: Bar diagram showing the comparison of stomatal conductance and transpiration rate profiles between Day 0 (prestress) and Day 6 under various stress conditions in two soybean cultivars Surge ((a), (c)) and Davison ((b), (d)). x-axis defines various abiotic stress treatments (drought, heat, and drought + heat) including control and y-axis defines percentage change of stomatal conductance at mmol level. Each value represents the mean ± SE of three replicates.

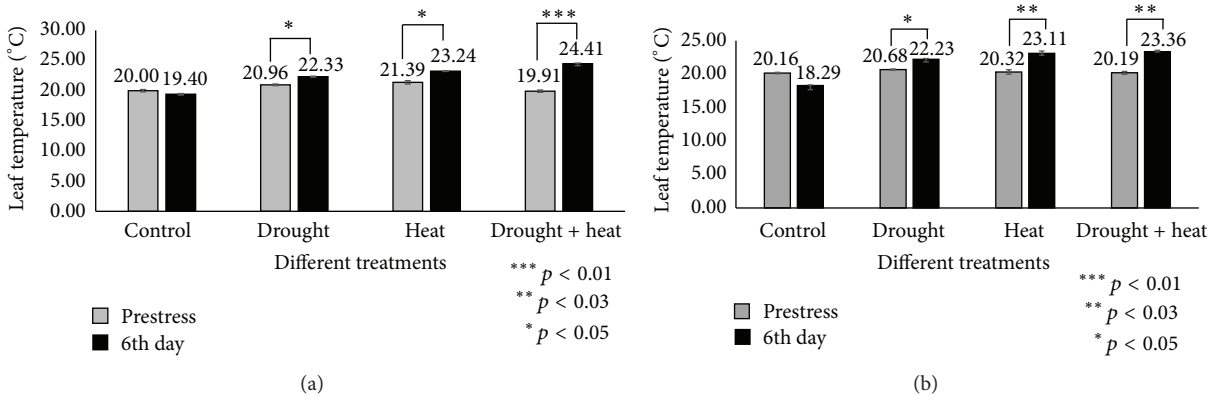

FIGURE 4: Bar diagrams showing temperature profiles of leaves between Day 0 (prestress) and Day 6 in two soybean cultivars Surge (a) and Davison (b). x-axis defines various abiotic stress treatments (drought, heat, and drought + heat) including control and y-axis defines measurement of leaf temperature OC. Each value represents the mean ± SE of three replicates and the asterisks designate the significance of changes from their subsequent control ($^{***}p < 0.01$, $^{**}p < 0.03$, and $^{*}p < 0.05$).

expressed proteins in both soybean varieties exposed to different stress conditions.

3.2.1. Genotypic Comparison at Molecular Levels for Different Stresses. For the genotypic comparisons between Surge and Davison soybean varieties, we examined three different stress conditions (heat, drought, and drought plus heat) and a control condition. Under drought stress conditions, out of the 44 differentially expressed proteins in Davison, 16 proteins were upregulated and 28 proteins were downregulated compared to Surge. Under heat stress conditions, 19 proteins were upregulated and 25 proteins were downregulated in Davison compared to Surge. Furthermore, when the soybean leaves were exposed to combined drought plus heat stress, 21 proteins were upregulated and 23 proteins were downregulated in Davison compared to Surge. To determine how these soybean leaf proteins vary under specific stress conditions, Venn diagram analysis of the number of differentially expressed leaf proteins was conducted (Figures 6(a) and 6(b)).

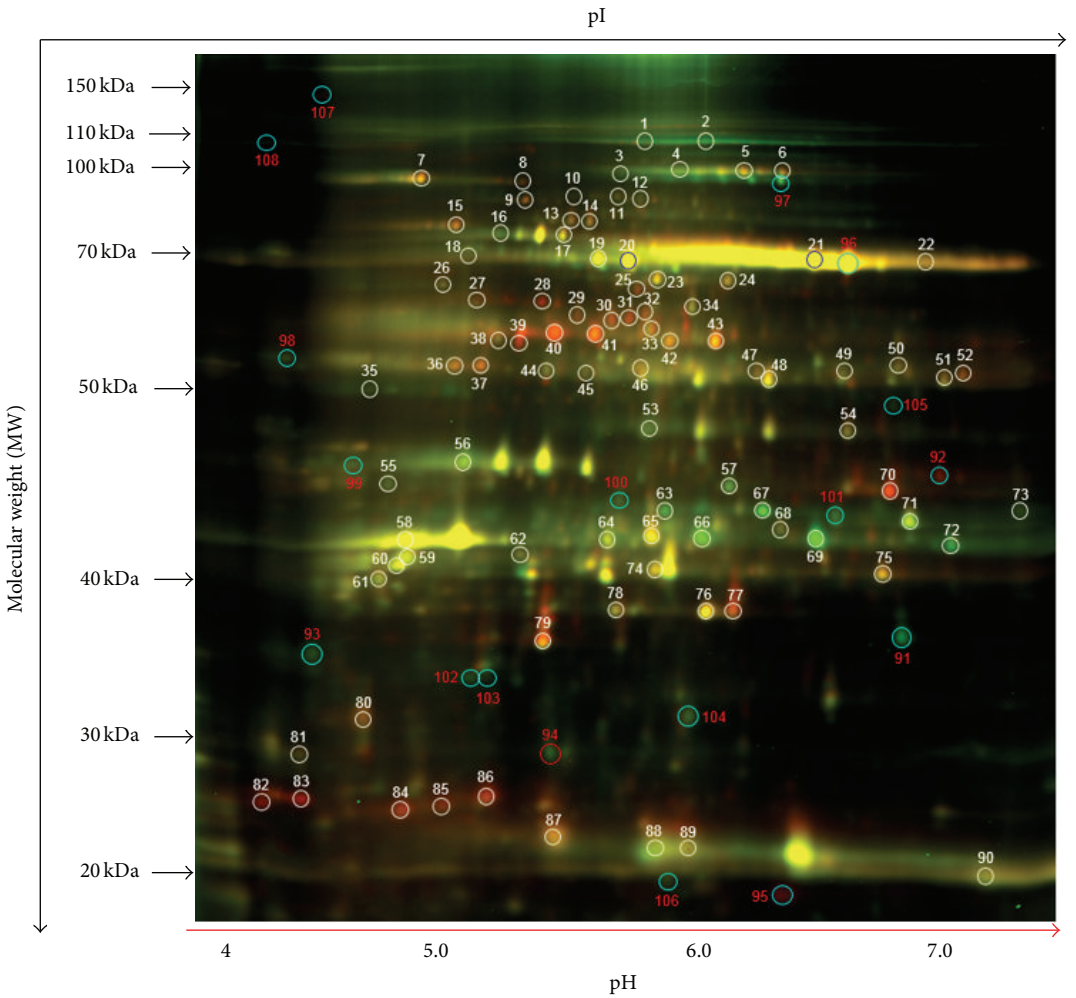

Figure 5: A representative figure showing 2D-DIGE analysis of differentially expressed soybean leaf proteins in response to heat, drought, and drought plus heat stresses. For each sample set, 30 μg of sample protein was mixed with 1.0 μL of diluted Cy3 or Cy5 dye for labeling. A pooled protein sample containing equal amounts of all samples was labeled with Cy2. Labeled samples were subjected to isoelectric focusing (pH 4–7) followed by 12% SDS-polyacrylamide gels. Gel images were scanned using Typhoon TRIO (GE Healthcare, PA, USA) and were analyzed using Image QuantTL software (version 6.0, GE Healthcare, USA) and then subjected to in-gel analysis and cross-gel analysis using DeCyder software, version 6.5 (GE Healthcare). The spot numbering on the merged 2D-DIGE image indicates the protein spots that were found statistically significant between various treatments for mass spectrometric identification.

Hierarchical clustering analysis was performed on the expression data for the 92 differentially expressed protein spots in Surge compared to Davison under control, heat stress, drought stress, and drought plus heat stress conditions to identify trends (Figure 7). Clustering analysis revealed the assignment of the 92 protein spots into 6 prominent clusters (I–VI). Cluster I contained two proteins that were downregulated in leaves when exposed to drought, and drought plus heat conditions, but were upregulated under heat stress conditions. Cluster II was comprised of leaf proteins that were downregulated under drought conditions but were not altered under the other conditions. Cluster III consisted of proteins that were upregulated in response to heat stress to a lesser extent than those in cluster I. Cluster IV included proteins that were not significantly altered in response to stress. The expression of protein spots in cluster V displayed remarkable variability; under heat stress conditions, these proteins were downregulated, but under combined drought and heat stress conditions, these proteins were upregulated. The proteins included in cluster VI displayed prominent downregulation under heat stress conditions but upregulation under combined drought and heat stress conditions.

3.2.2. Comparison of the Effects of Stress on Different Genotypes. To examine the molecular changes that occur under stress conditions, the leaf proteomes of both varieties were analyzed (Figure 6(c)). Under drought stress conditions, it was found that 11 proteins (stromal 70 kDa heat shock-related protein, ATP-dependent zinc metalloprotease, RuBisCO large subunit-binding protein subunit beta, elongation factor Tu, glutamine synthetase, photosystem II stability/assembly factor HCF136, malate dehydrogenase, fructose-bisphosphate aldolase, ferredoxin-NADP reductase,

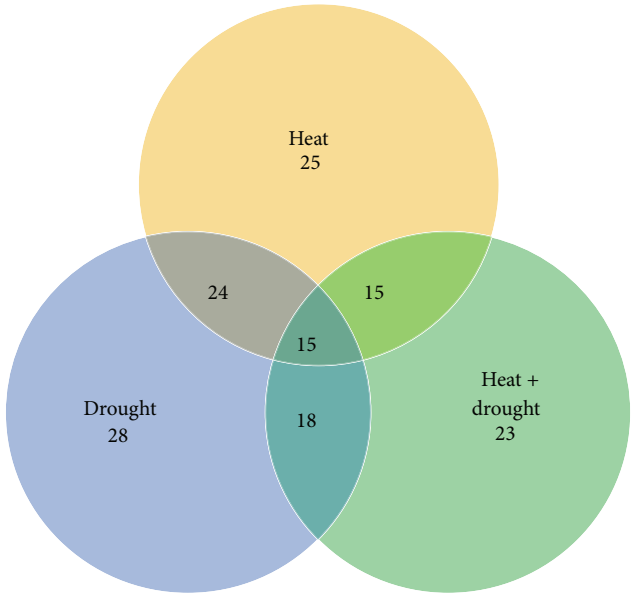

(a) Proteins *downregulated* in Davison compared to Surge in different stress conditions

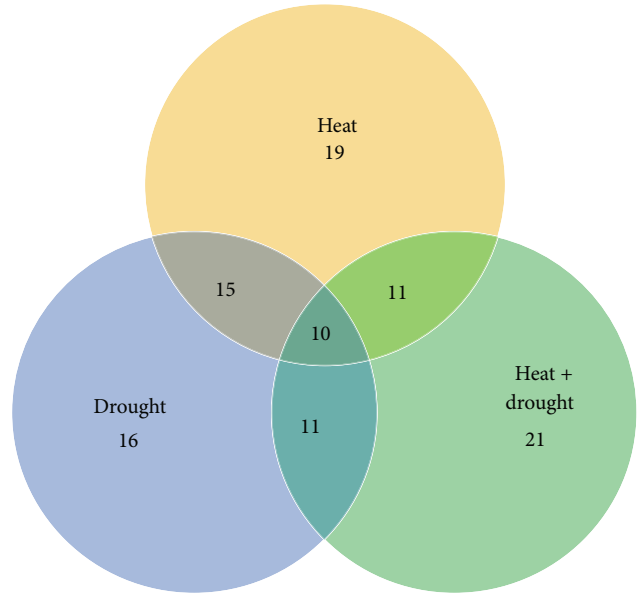

(b) Proteins *upregulated* in Davison compared to Surge in different stress conditions

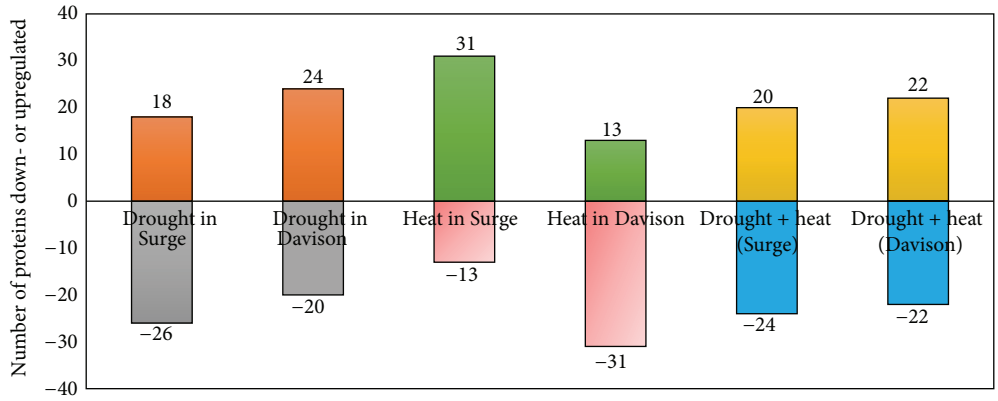

(c)

FIGURE 6: Venn diagram showing the proteins which are unique to respective genotype and stress. The number of downregulated (a) and upregulated (b) proteins and comparison of two genotypes in relation to number of proteins that get affected as a result of various stresses (c).

and chlorophyll a-b binding protein 6A) were upregulated in Davison but were downregulated in Surge.

Under heat stress conditions, 13 proteins were downregulated in Surge, whereas 31 proteins were downregulated in Davison compared to the control condition. The results revealed significant downregulation of 20 proteins in Davison. The most downregulated proteins include stromal 70 kDa heat shock-related protein, ATP-dependent zinc metalloprotease FTSH 8, elongation factor Tu, and ribulose bisphosphate carboxylase large chain, but all of these proteins were upregulated in Surge.

When the plants were exposed to drought plus heat stress, it was found that 22 proteins were downregulated and 22 proteins were upregulated in Davison, whereas 24 proteins were downregulated and 20 proteins were upregulated in Surge compared to plants under the control conditions. Under the drought plus heat stress conditions, 9 proteins were downregulated in Surge (the most downregulated proteins include stromal 70 kDa heat shock-related protein, ATP-dependent zinc metalloprotease FTSH 8, ribulose bisphosphate carboxylase small chain, and carbonic anhydrase 1). However, these proteins were upregulated in Davison.

3.3. Functional Correlation among the Identified Proteins under Drought and Heat Stress. To attain a better understanding of the early proteomic responses, a majority of the differentially expressed proteins identified were classified into various functional categories. This analysis (Figure 8(a)) indicated that the 92 significantly altered protein spots identified were found to be involved in different metabolic pathways and processes, including photosynthesis (65.56%), ATP synthesis (7.78%), protein biosynthesis (4.44%), superoxide dismutase activity (3.33%), protein folding (2.22%), lipid metabolism (2.22%), photorespiration/response to hypoxia

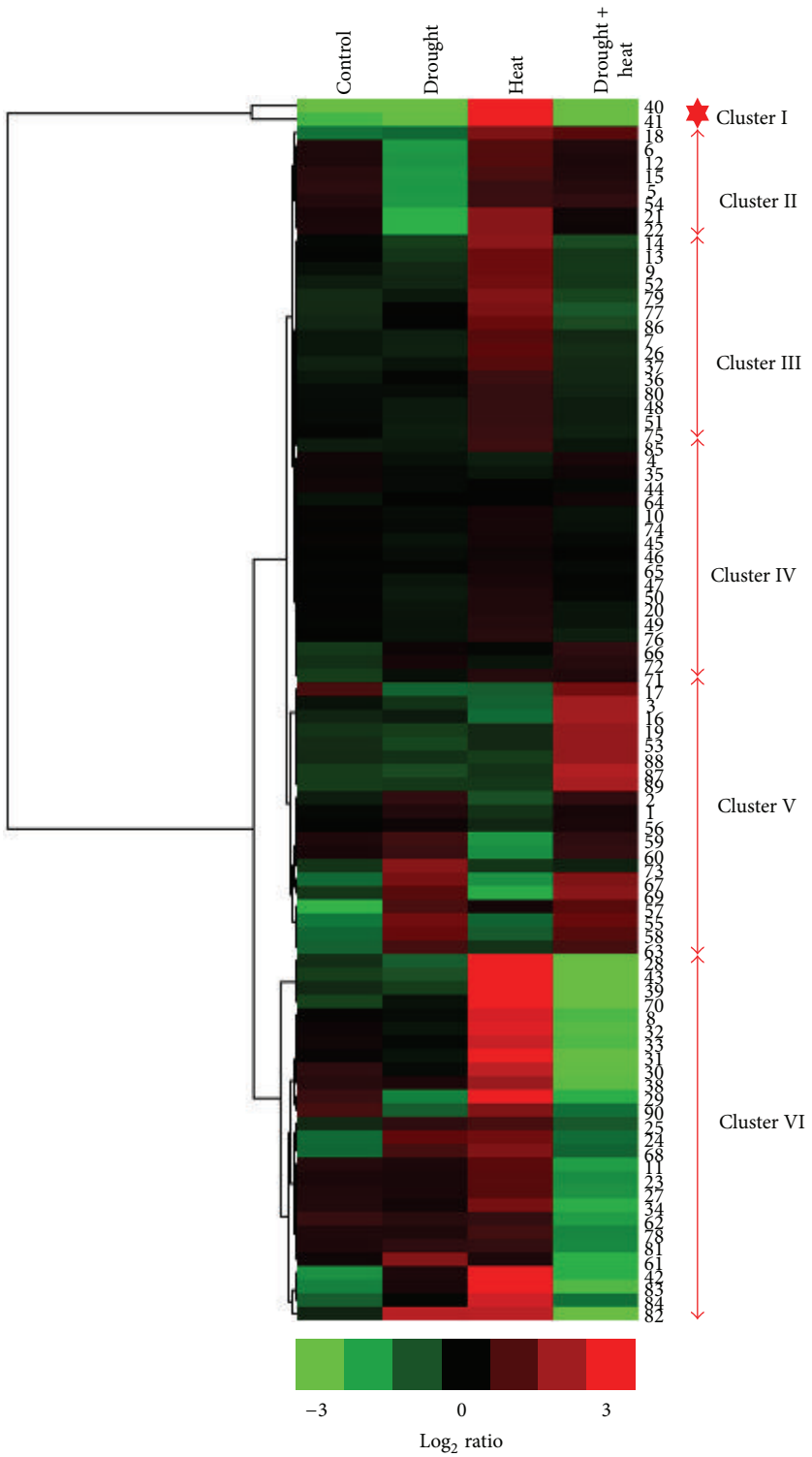

FIGURE 7: Heat map: Euclidean distance similarity metric and complete linkage method. Heat maps of proteins associated with soybean plants (pooled lines) exposed to different stress conditions. Hierarchical clustering was done based on the $\log_2$-transformed expression ratios of protein spots using Gene Cluster 3.0 software with the Euclidean distance similarity metric and complete linkage method. Clusters were visualized in JAVA TREEVIEW software.

(2.22%), respiration (2.22%), carbonate dehydratase activity (2.22%), acid phosphatase activity (2.22%), nitrogen fixation (1.11%), one-carbon metabolism (1.11%), calcium ion binding (1.11%), serine protease inhibitor (1.11%), and response to cold stress (1.11%).

An analysis was performed to elucidate the subcellular localization of the differentially expressed proteins (Figure 8(b)). A large portion of the differentially expressed proteins identified were predicted to be chloroplastic (86%), whereas most of the remaining proteins were predicted to be localized to the cytoplasm (5.55%), mitochondria (2.22%), vacuoles (2.22%), peroxisomes (1.11%), or ribosomes (1.11%).

3.4. Identified Proteins Affecting Photosynthesis under Drought and Heat Stress Conditions. In this study, 25 proteins that are directly or indirectly involved in photosynthesis were discovered as differentially expressed in soybeans in response to various stress conditions. Protein upregulation and downregulation in Davison compared to Surge are presented in Figure 9. The proteomic analysis revealed that, under drought stress, photosynthesis-related proteins, including ribulose bisphosphate carboxylase large chain (Spot 22), ribulose bisphosphate carboxylase/oxygenase activase (Spot 41), transketolase (Spot 40), sedoheptulose-1,7-bisphosphatase (Spot 37), fructose-bisphosphate aldolase 1 (Spot 48), phosphoglycerate kinase (Spot 43), oxygen-evolving enhancer protein 2-1 (Spot 74), chlorophyll a-b binding protein 3 (Spot 75), ATP-dependent zinc metalloprotease (Spot 9), ATP synthase subunit alpha (Spot 17), ATP synthase subunit beta (Spot 19), photosystem II stability/assembly factor HCF136 (Spot 45), and ferredoxin-NADP reductase (Spot 54), were downregulated in both soybean varieties (Figure 9). This indicates that drought stress favors a reduction in the activities of photosynthetic carbon reduction cycle enzymes, specifically ribulose-1,5-bisphosphate (RuBP) regeneration and inhibition of RuBisCO activity [53–55]. These findings also support the current physiological analysis of the photosynthesis.

The photosynthesis rate in higher plants depends on the activity of RuBisCO and the regeneration of RuBP. It has been reported that drought stress results in a rapid decrease in the abundance of RuBisCO small subunit (rbcS) in tomato [56]. Similarly, our analysis also revealed a decreased (2–4-fold) synthesis of RuBisCO large and small chain enzyme under drought stress which may have direct effect on photosynthesis. The literature suggests that this inhibition of RuBisCO activity was due to the binding of inhibitors such as 2-carboxyarabinitol 1 phosphate (CA1P) to RuBisCO [57]. However, the interactions between RuBisCO and inhibitors are known to be prevented by ATP hydrolysis and RuBisCO activase, which regulates the active site conformation of RuBisCO, removes the inhibitors and the bound inactive RuBP, and allows RuBisCO to undergo rapid carboxylation [58]. Furthermore, we found that, in response to drought stress, RuBisCO activase is also downregulated by 2-fold under stress conditions compared to the control conditions. This result suggests that, under drought stress, RuBisCO activase cannot prevent the interaction between RuBisCO and its inhibitors and cannot remove the bound RuBP to activate RuBisCO. Along with the downregulation of RuBisCO and RuBisCO activase, we found that, under drought stress, other key Calvin cycle enzymes that play a crucial role in carboxylation were downregulated, including transketolase (2-fold compared to the control condition), sedoheptulose-1,7-bisphosphatase (1–2.4-fold), fructose-bisphosphate aldolase 1 (1.5-fold), and phosphoglycerate kinase (4–17-fold). This result suggests that carboxylation is also reduced due to the inhibition of these enzymes, thereby decreasing the level of photosynthesis and ultimately affecting the growth and development of these soybean plants.

We found that, due to heat stress, crucial proteins that regulate electron transport activity were also downregulated including ATP synthase subunit alpha (2.18-fold in Surge compared to Davison), ATP synthase subunit beta (1.74-fold in Davison compared to Surge), photosystem II stability/assembly factor HCF136 (1.15-fold in in Davison compared to Surge), oxygen-evolving enhancer protein 2-1 (1.8-fold in Surge compared to Davison), and ferredoxin-NADP reductase (1.57-fold in Davison compared to Surge). These results suggest that, in both soybean cultivars, heat stress negatively affects electron transport activity, including PSII downregulation, thereby reducing the level of photosynthesis [59].

3.5. Upregulation of EF-Tu during Heat Stress in Surge and the Role of EF-Tu in Protecting the Photosynthesis Machinery. 2D-DIGE analysis revealed that the chloroplast protein synthesis elongation factor, EF-Tu protein (Spot 31), was upregulated by 4.6-fold in Surge compared to Davison under heat stress. Additionally, we found that, in Surge, under heat stress, fewer (13) proteins were downregulated than under drought stress, whereas 31 proteins were downregulated in Davison under heat stress. Chloroplast EF-Tu is a protein that is involved in the elongation of polypeptides during the translational process, and it belongs to a nuclear-encoded multigene family [60, 61]. The heat stress-induced accumulation of EF-Tu in mature plants is thought to protect the photosynthesis machinery [62]. It has been reported that maize EF-Tu plays a crucial role in heat tolerance by acting as a molecular chaperone, and it has been found to protect heat-labile citrate synthase, RuBisCO activase, and malate dehydrogenase from thermal accumulations [63, 64]. The results indicate that, upon heat stress, EF-Tu assembles in the cytosol in Surge (as seen by an increase in the protein levels of Spots 29–31). Therefore, based on these results, EF-Tu could serve as a biomarker of heat stress in soybeans.

Bioinformatics analysis of protein-protein interactions of this study revealed that the EF-Tu protein undergoes chaperone-mediated interaction with all photosynthesis-related enzymes, including RuBisCO activase, malate dehydrogenase, phosphoglycerate kinase, and sedoheptulose-1,7-bisphosphatase (Figure 12). An interaction between cpn60β and RuBisCO activase has been reported in *Arabidopsis* for acclimating photosynthesis to heat stress [65]. Consequently, it was found that, in Surge variety under heat stress, the expression of most proteins related to photosynthesis was conserved, that is, either upregulated or unchanged; in particular, RuBisCO activase (Spot 41) was upregulated 8.71-fold in Surge compared to Davison. We propose that

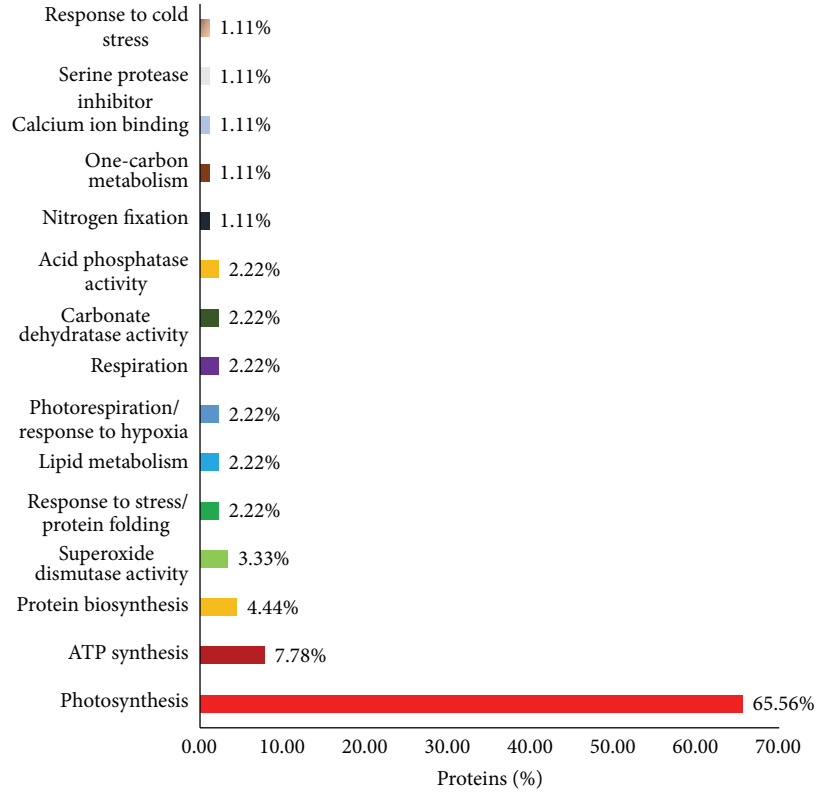

(a) Functional groups of differentially expressed proteins identified in the seedling

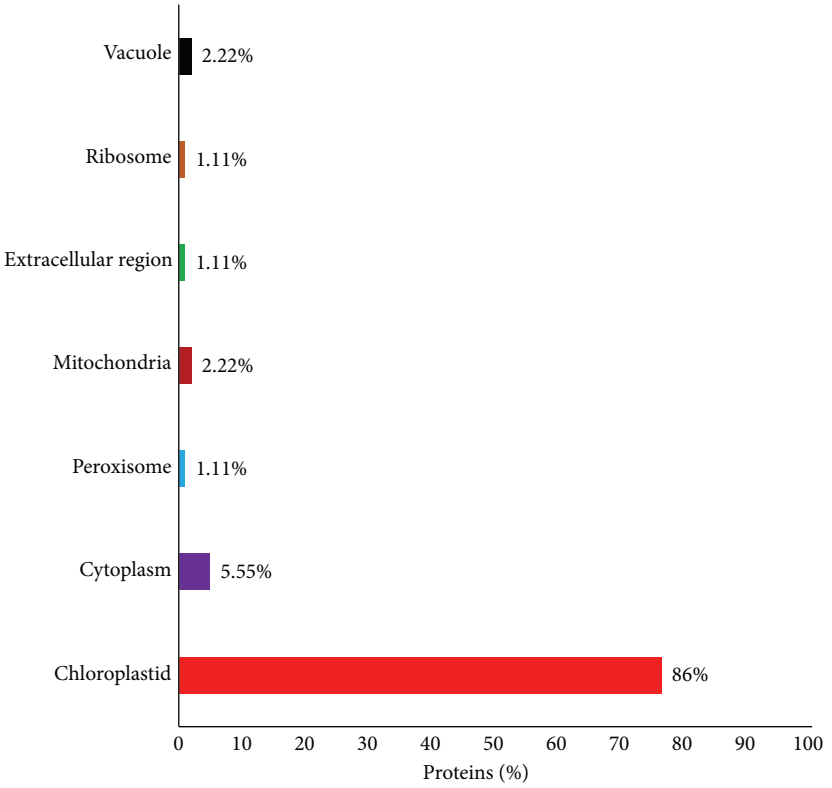

(b) The predicted subcellular localization of the identified proteins

FIGURE 8: Graphical representation of functional categories of identified proteins. x-axis defines various functional groups and y-axis indicates % of proteins. B-Mapping for the subcellular localization of the identified proteins. x-axis defines various subcellular organelles and y-axis indicates % of proteins. Numerical values symbolize the percentage of proteins in each functional class.

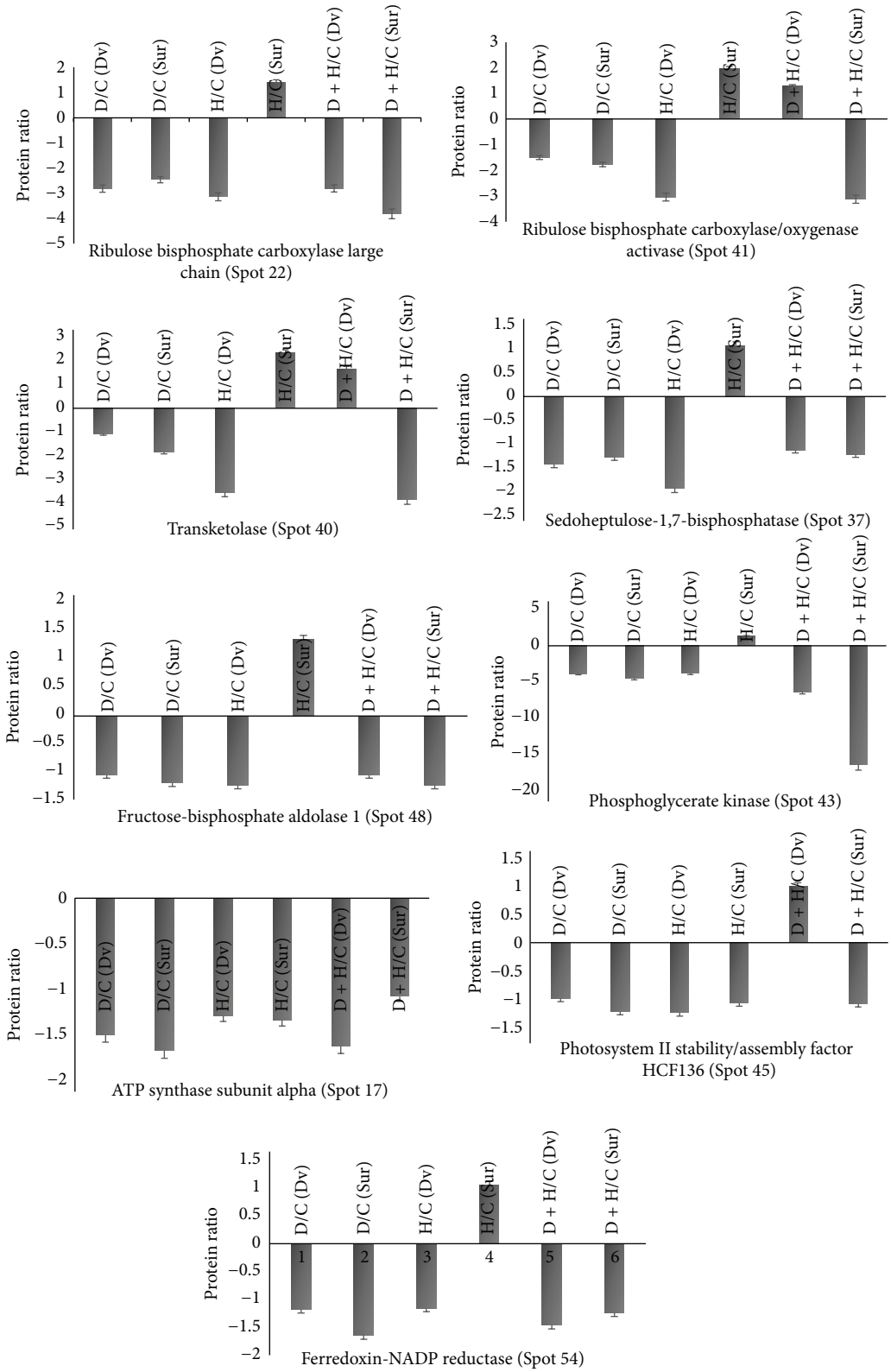

Figure 9: Bar diagrams showing differential regulation of photosynthesis-related proteins. This response is to various stress treatments in two soybean cultivars Surge and Davison. Dv = Davison; Sur = Surge; D = drought, H = heat, and D + H = drought plus heat stress. The protein abundance is presented as protein ratio (y-axis) compared to control in response to various abiotic stress treatments (drought, heat, and drought + heat) on x-axis.

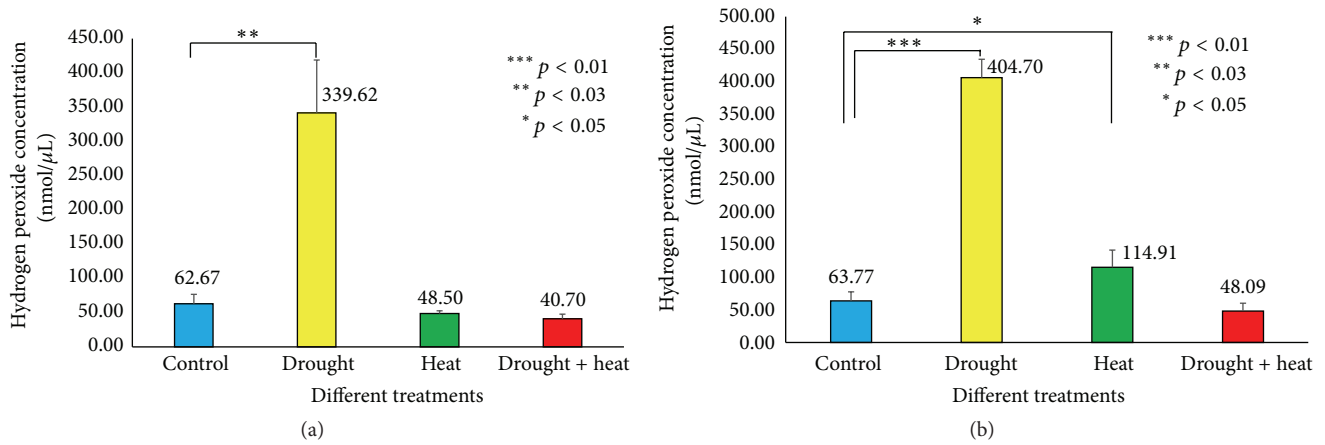

FIGURE 10: Bar diagram showing hydrogen peroxide levels under various stress treatments among Surge (a) and Davison (b). x-axis defines various abiotic stress treatments (drought, heat, and drought + heat) including control and the y-axis defines measurement of hydrogen peroxide concentration in nmol/μL. Each value represents the mean ± SE of five replicates and the asterisks designate the significance of changes from their subsequent control ($^{***}p < 0.01$, $^{**}p < 0.03$, and $^{*}p < 0.05$).

EF-Tu is synthesized upon heat stress and protects the heat-induced degradation of all photosynthesis-related proteins and enzymes, especially RuBisCO activase, maintaining the photosynthesis levels.

3.6. Role of Stromal Heat Shock-Related Protein during Severe Heat Stress. Based on 2D-DIGE analysis, we found that the stromal 70 kDa heat shock-related protein (Spot 8) was upregulated in Surge by 4.15-fold compared to Davison (Figure S6), and, compared to the control conditions, it was upregulated by 2.33-fold in Surge under heat stress conditions. This molecular chaperone maintains cellular homeostasis in cells under adverse abiotic stress conditions. It has been found that stromal 70 kDa heat shock-related protein of *Arabidopsis thaliana* is responsible for protein folding and can assist in protein refolding under heat stress conditions [66]. The results also indicate that, under heat stress, proteins related to the photosynthesis machinery are protected. Taken together, the analysis indicates that stromal 70 kDa heat shock-related protein plays a role in the maintenance or biogenesis of chloroplast proteins, thereby maintaining the level of photosynthesis [20, 67].

A further bioinformatics analysis of protein-protein interactions revealed that this HSP protein undergoes two-way interactions, one with a molecular chaperone (GrpE) and one directly with phosphoglycerate kinase. As discussed above, under heat stress, most proteins related to photosynthesis are more abundant in Surge than in Davison. Thus, we propose that stromal 70 kDa heat shock-related protein might activate a multiprotein interaction cascade that maintains the biogenesis of chloroplast proteins under heat stress and protects against the heat-induced degradation of all photosynthesis-related proteins and enzymes, preserving the photosynthesis levels.

3.7. Quantification of ROS and the Role of Carbonic Anhydrase in Plant Protection. Studies have shown that increasing levels of water stress in *Vigna* plants may increase ROS levels by means of hydrogen peroxide [28]. Results of present study (Figure 10) indicate a 5.4-fold elevation in the H_2O_2 level under drought stress compared to the control conditions in Surge (62.67 nmol μL^{-1} to 339.62 nmol μL^{-1}) and a nearly 6.3-fold elevation in Davison (63.77 nmol μL^{-1} to 404.70 nmol μL^{-1}) on the sixth day of stress. Under heat stress, we found no significant difference in the H_2O_2 level in Surge, but in Davison, the H_2O_2 level was increased by 1.8-fold.

The proteomic analysis shows that carbonic anhydrase 1 (Spot 72) is upregulated by 1.8-fold due to drought stress and by 1.6-fold due to combined drought plus heat stress in Davison (Figure S7). Carbonic anhydrase is a zinc-containing metalloenzyme, and the specific association between carbonic anhydrase and RuBisCO enables CO_2 to interact with RuBisCO and maintains the functional machinery of RuBisCO [68]. Under drought stress conditions, when plants detect a limitation of water availability, stomatal closure is triggered, which limits the entrance of CO_2, resulting in a net reduction of photosynthesis. This confers increased ROS accumulation with oxidative stress [69]. It has been reported that higher expression of carbonic anhydrase in the cell increases its resistance to cytotoxic concentrations of H_2O_2 [70]. Thus, it is possible that, under drought stress conditions, the upregulated expression of carbonic anhydrase in Davison principally makes the plant cells resistant to toxic H_2O_2 levels and protects the plant from oxidative stress. Although we detected a higher level of hydrogen peroxide in drought-stressed Davison plants, no significant phenotypic changes were detected on the sixth day of stress.

3.8. Quantification of ABA under Different Abiotic Stress Conditions. ABA is a phytohormone critical for plant growth and plays a key role in integrating various stress signals [71]. Several studies suggested that, in response to the water and high temperature stress, stomatal movement is controlled by ABA signaling [72]. In this study, we quantified the ABA concentration in the leaf under all the stress conditions

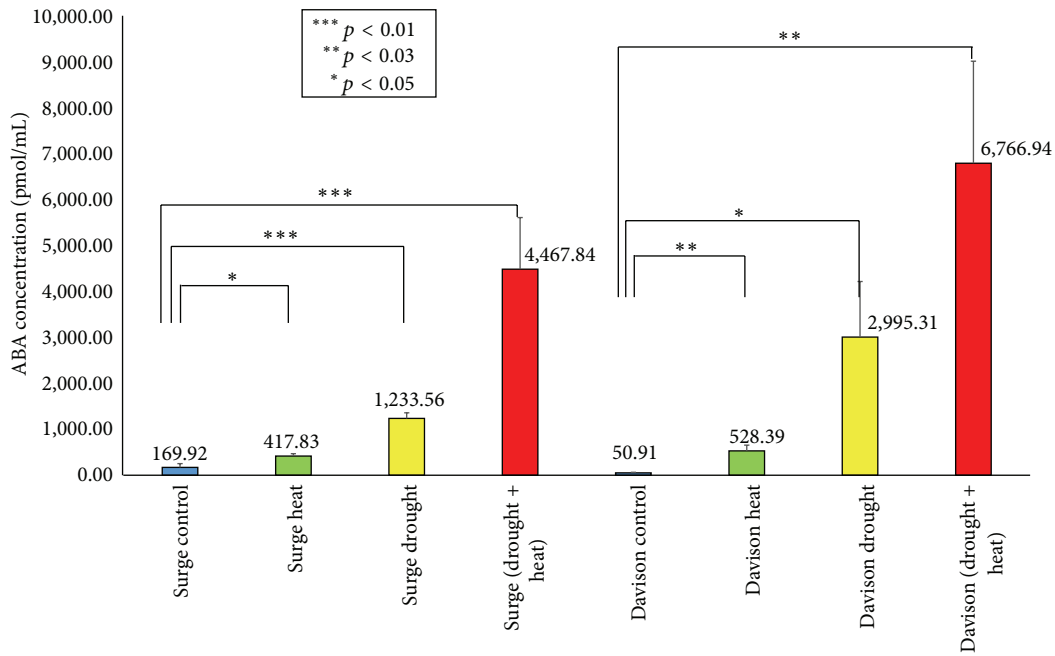

Figure 11: Bar diagram showing quantification of ABA in different abiotic stress conditions in Surge and Davison. x-axis defines various abiotic stress treatments (drought, heat, and drought + heat) including control and the y-axis defines measurement of ABA concentration (pmol/mL). Each value represents the mean ± SE of five replicates and the asterisks designate the significance of changes from their subsequent control ($^{***}p < 0.01$, $^{**}p < 0.03$, and $^{*}p < 0.05$).

(Figure 11). We found that, compared to the control plants, the highest level of accumulation of ABA occurred during the drought plus heat stress conditions. In Surge, it was 26-fold higher, and in Davison, it was 132-fold higher compared to the control conditions. In the drought-stressed leaves, we found ABA levels to be 7-fold higher in Surge and 58-fold higher in Davison compared to the control plants. Under heat stress, ABA is upregulated by 2-fold in Surge and 10-fold in Davison compared to the normal plants. Through investigating the change of abscisic acid (ABA) levels, we found that drought plus heat stress has the highest level of ABA accumulation, which also correlates with the stomatal conductance measurements.

3.9. The Identified Protein "Glutamine Synthetase" and Its Association with Nitrogen Metabolism. Based on the analysis of the soybean leaf proteome, we found that cytosolic glutamine synthetase leaf isozyme (Spot 33) was downregulated by 4-fold in Davison under drought stress conditions compared to Surge. This enzyme catalyzes a major reaction of nitrogen metabolism, that is, the assimilation of ammonium to glutamine using the substrate glutamic acid [73]. Reduction of glutamine synthetase expression under drought conditions has been reported as a protective mechanism for plants because the intermediate nitric oxide is an active radical. Thus, we predict that the same protective mechanism also occurs in soybean leaves [21, 74]. Additionally, it has been reported that the overexpression of cytosolic glutamine synthetase in poplar enhances the photorespiration under drought stress and that it also contributes to the protection of photosynthesis [75, 76].

3.10. Protein-Protein Interaction Analysis. For any systems-level understanding of cellular functions, it is crucial to appropriately elucidate all functional interactions between the proteins in the cell at a given time. We searched for a variety of functional protein-protein interactions between the differentially expressed proteins in soybeans in response to abiotic stress to obtain an improved understanding of these protein-protein interactions, including stable complexes, metabolic pathways, and a wide range of regulatory interactions [44] (Figure 12 and Table 1). From the network, we discovered 10 major proteins (most significantly, ribulose bisphosphate carboxylase, ribulose bisphosphate carboxylase/oxygenase activase, ATP synthase subunit alpha/beta, sedoheptulose-1,7-bisphosphatase, photosystem II stability/assembly factor HCF136, ferredoxin-NADP reductase, elongation factor Tu, and carbonic anhydrase 1) having more than 9 interactions that are considered to be at the central body of the network. Drought or heat stress mediated downregulation or upregulation of those central body proteins of the network may also affect their predicted partners, which ultimately could affect the molecular signaling by collapsing the whole cellular network.

4. Discussion

Drought and high temperature stress conditions cause extensive losses to crops', including soybean, production worldwide [77, 78]. Individually, the effect of drought or heat stress conditions on soybeans has been the subject of intense research [79, 80], but to the best of our knowledge, no such detailed proteomics-based study attempt has been made to

Table 1: Data used to predict protein-protein network. Protein spot numbers are corresponding to the 2D-DIGE gel and respective mass spectrometry based protein identifications are given as UniProt ID.

Spot number	Protein name	UniProt accession number
1	Acyl-[acyl-carrier-protein] desaturase 6	Q0J7E4
2	Lipoxygenase	Q43440
3	Ribulose bisphosphate carboxylase large chain	Q01873
4	Transketolase, chloroplastic	O20250
7	Stromal 70 kDa heat shock-related protein	Q02028
9	ATP-dependent zinc metalloprotease FTSH 8	Q8W585
13	RuBisCO large subunit-binding protein subunit beta	P08927
16	ATP synthase subunit alpha	Q2PMS8
19	ATP synthase subunit beta	Q2PMV0
28	Ribulose bisphosphate carboxylase/oxygenase activase	Q40281
29	Elongation factor Tu, chloroplastic	Q43467
33	Glutamine synthetase leaf isozyme	P15102
34	S-adenosylmethionine synthase 4	A7PRJ6
35	Probable calcium binding protein CML33	Q9SRP4
37	Sedoheptulose-1,7-bisphosphatase	O20252
42	Phosphoglycerate kinase	P12782
44	Photosystem II stability/assembly factor HCF136	O82660
46	Fructose-bisphosphate aldolase 1	Q01516
49	Malate dehydrogenase 1	Q9ZP06
50	Trypsin inhibitor 1	Q43667
52	Chloroplast stem-loop binding protein of 41 kDa b	Q9SA52
53	Ferredoxin-NADP reductase, leaf isozyme 1	Q9FKW6-1
56	Oxygen-evolving enhancer protein 1	P14226
58	Chlorophyll a-b binding protein of LHCII type I	P08221
59	Chlorophyll a-b binding protein	Q10HD0
60	Chlorophyll a-b binding protein 13	P27489
61	2-Cys peroxiredoxin BAS1-like	Q9C5R8
62	Ribulose bisphosphate carboxylase small chain PW9	P26667
63	Ribulose bisphosphate carboxylase small chain 2A	P26575
64	Superoxide dismutase [Fe]	P28759
66	Carbonic anhydrase 1	P46512
67	RuBisCO-associated protein	P39657
71	Stem 31 kDa glycoprotein	P10743
73	Stem 28 kDa glycoprotein	P15490
74	Oxygen-evolving enhancer protein 2-1	Q7DM39
76	Chlorophyll a-b binding protein 6A	P12360
77	Ribulose bisphosphate carboxylase large chain (fragment)	P28416
80	Ribosomal protein L7/L12	Q4BZ06
81	Glycine cleavage system H protein 1	P25855
87	Ribulose bisphosphate carboxylase small chain 1	P00865

date. The cooccurrence of drought plus heat stress is of special interest because they occur together in the field. Recent studies have revealed that the responses of plants to two different abiotic stresses that occur simultaneously are exclusive and cannot be directly inferred from the response of plants to each of the different stresses applied independently [81]. Thus, to emphasize the molecular, physiological, and proteomic aspects of stress combination and to unravel the underlying mechanisms of soybean responses to drought, heat stress, and cooccurring stresses, we performed a proteomic study combined with physiological and computational analysis to facilitate the discovery of genes that can enhance the tolerance capabilities of soybean crops to the stress conditions [82].

Reduced stomatal conductance is one of the most sensitive responses to drought stress, observed in kidney beans and various C3 plants [48, 83]. At the level of soybean physiology, we concluded that drought stress, heat stress, and drought plus heat stress reduce stomatal conductance, which is caused by decreasing the leaf water potential via transpiration rate alterations in both varieties. Stomatal conductance is also

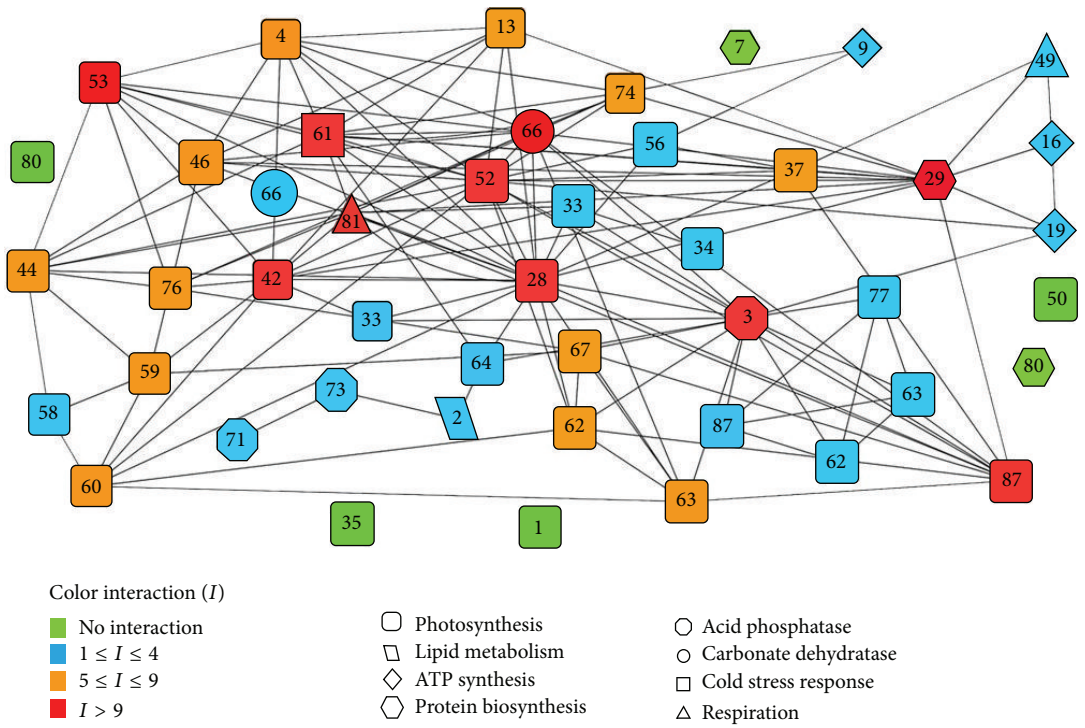

Figure 12: Protein-protein interaction network predictions made by bioinformatics analysis. The prediction is between differentially expressed proteins due to different stress conditions and identified by proteomic study. The network comprises 46 nodes and 139 edges. Symbol color corresponds to degree of interactions (color code on the left side). Symbol shapes indicate specific protein function. Node legends indicate the spot number corresponding to the particular protein spot from 2D-DIGE gel. Follow Table 1 for protein names for corresponding spot number [note: duplicate insertion of few spot numbers (Spot numbers 33, 62, 63, 66, and 87) is incorporated to avoid overcrowding of the network. Spot number 80 appears two times with two different shapes indicating that the same protein is counted for two different functions].

reliant on leaf temperature via transpiration rate, and we observed that the increase of leaf temperature is correlated to the stomatal conductance and transpiration rates. Photosynthesis is among the primary processes affected by the drought and heat stresses [16, 84, 85]. As soil moisture decreases during drought stress and cooccurring drought and heat stress, the water content of mesophyll tissue also reduces, ultimately affecting the photosynthetic physiology, principally carbon assimilation and energy use of the plant. Surprisingly, there was no such significant effect observed during heat stress alone, which actually establishes the fact that consequences of water deficiency have an enormous impact on altering the photosynthetic machinery [86].

Gel-based proteomic separation is widely used in various plants' studies to decipher abiotic stress-responsive mechanisms for its high precision exclusively for comparative proteomics [87]. Likewise, we used a gel-based proteomic approach to elucidate the mechanisms underlying the early responses of soybeans to various abiotic stresses. To propose a functional relationship among proteins in response to abiotic stress, we performed functional categorization and subcellular localization of various differentially expressed proteins [88, 89]. Our proteomic analysis revealed that a total of 44 proteins were significantly changed in soybean leaves after 6 days of different stress exposures (drought, heat, and drought plus heat), and their functional categorization showed that most of the differentially changed proteins were related to photosynthesis, ATP synthesis, and protein biosynthesis. The subcellular localization study reveals that most of the proteins are actively synthesized in chloroplast and cytoplasm. We found that 25 proteins related to photosynthesis were downregulated during stress conditions in both the soybean varieties. Most importantly, downregulation of RuBisCO and RuBisCO activase enzymes during drought stress reduces the carboxylation process because the limitation of the RuBisCO activase prevents the reactivation of RuBisCO molecules [53, 90]. Previous reports on *Phaseolus vulgaris* and drought stress showed that the Calvin cycle enzymes' activities are affected significantly [91]. Similarly, our study also indicates that, under drought stress, key enzymes of Calvin cycle—such as transketolase, sedoheptulose-1,7-bisphosphatase, fructose-bisphosphate aldolase 1, and phosphoglycerate kinase—that play major roles in carboxylation are also downregulated, resulting in reduced levels of photosynthesis, thus affecting the development and growth of the soybean plant. Figures 13 and 14 show models for how the photosynthesis level could be reduced after drought/heat stress via alternated protein expressions and protein-protein interactions. It was found that salt stress-induced effects in cowpea plants negatively affect nitrogen assimilation and overexpressed glutamine synthetase gene in rice modifies nitrogen metabolism during abiotic stress [92, 93]. Surprisingly, our soybean leaf proteome

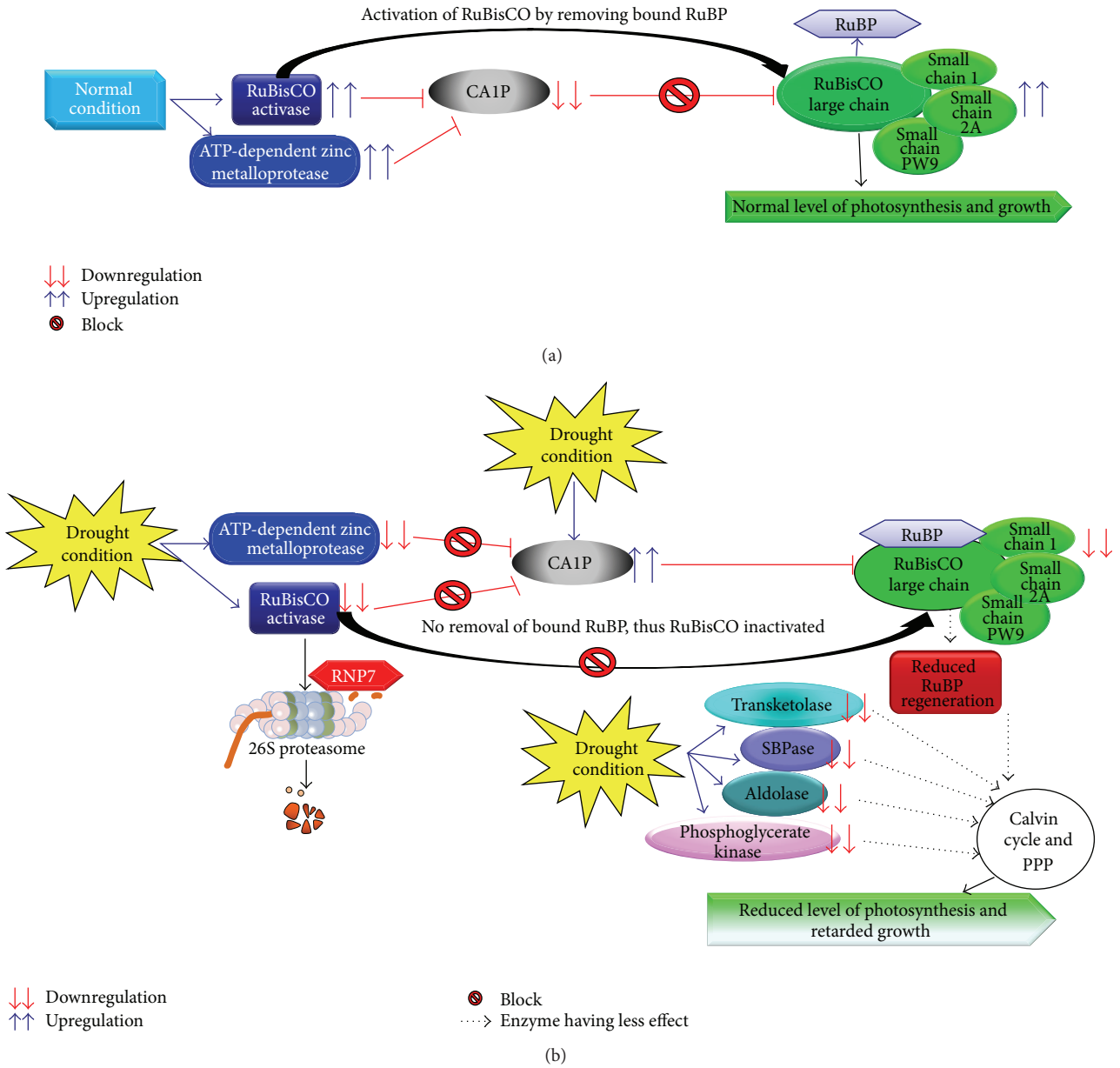

Figure 13: Predicted analysis of the mechanism by which the photosynthesis rate is reduced. (a) In normal condition, RuBisCO activase removes the RuBP from RuBisCO and photosynthesis is not affected. (b) During drought stress, RuBisCO activase and ATP-dependent zinc metalloprotease are downregulated and CA1P (2-carboxyarabinitol 1 phosphate, a potent inhibitor of RuBisCO) is upregulated; thus no removal of RuBP from RuBisCO occurs, and with that the Calvin cycle and pentose phosphate pathway (PPP) enzymes are downregulated which ultimately results in reduced level photosynthesis and retarded growth.

analysis revealed that cytosolic glutamine synthetase leaf isozyme, which is responsible for assimilation of ammonium to glutamine using substrate glutamic acid, was highly downregulated in Davison as compared to Surge during drought stress conditions, resulting in negatively affected nitrogen assimilation.

Studies have shown that heat stress reduces yields by limiting electron transport activity in cotton [94] and *Arabidopsis* [95]. The physiological and proteomic data of our study reveal that the PSII could be damaged during heat stress, and this damage reduces net photosynthesis levels in soybeans. Crucial proteins—for example, ATP synthase, HCF136, oxygen-evolving enhancer protein 2-1, and ferredoxin-NADP reductase that regulate the electron transport activity—were found to be downregulated during heat stress. Figure 14 shows the predicted analysis of irreversible inhibition of photosynthesis during heat stress and the protein-protein interplay that negatively affects the electron flow. During heat stress, we observed that the EF-Tu protein is highly upregulated in Surge, which is consistent with the earlier findings in heat tolerant maize [96]. So we predict that high levels of heat stress-induced expression of EF-Tu in Surge

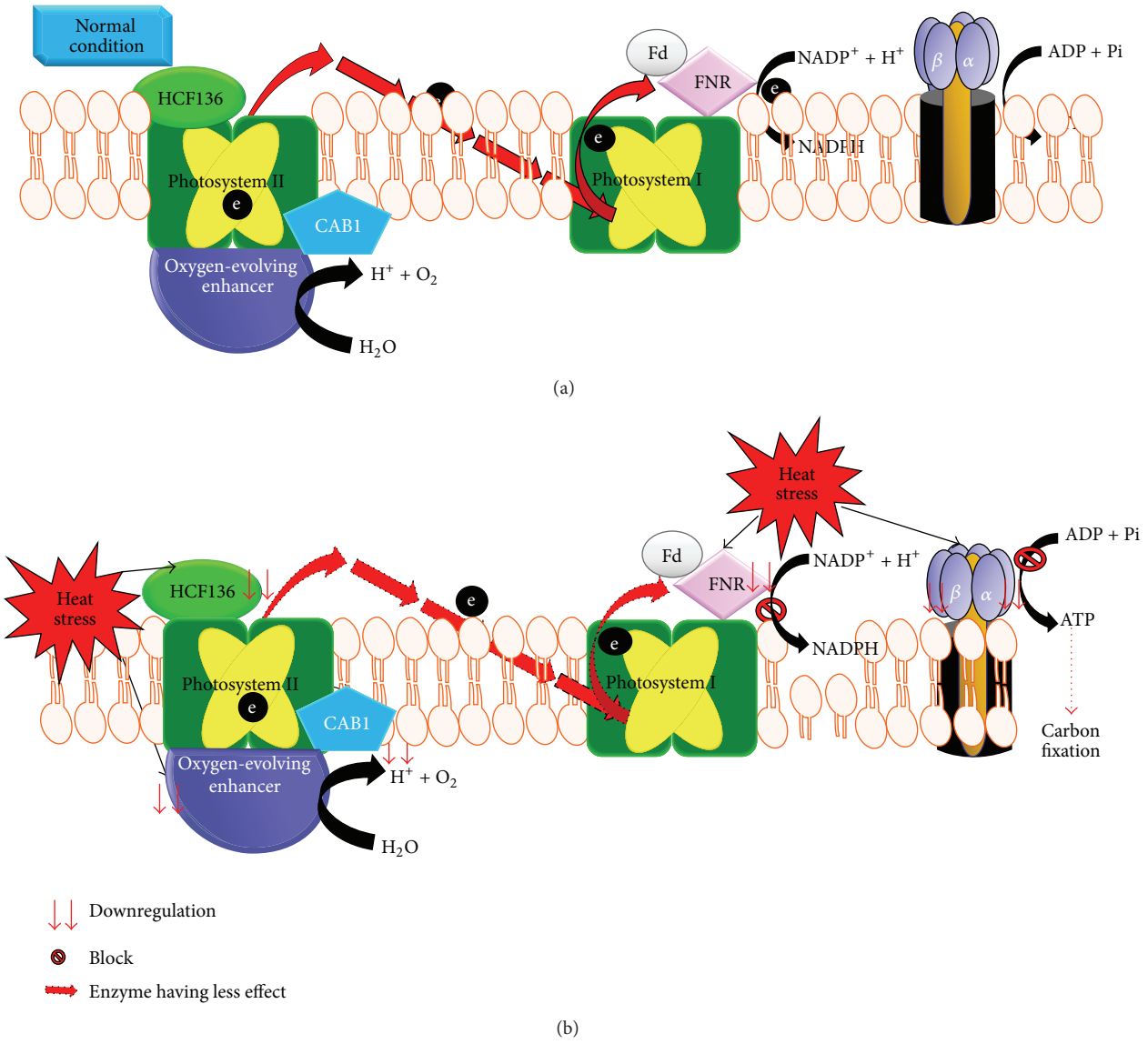

Figure 14: Predicted heat stress and electron transport block mechanism. Predicted analysis of irreversible inhibition of photosynthesis during heat stress and the protein-protein interplay that negatively affects the electron flow. (a) In normal condition, there is normal electron flow and no reduction in carbon fixation. (b) Due to heat stress effect, all key proteins that mediate electron flow are downregulated and block the electron flow, and as a result downregulation of ATP synthase reduces the production of ATP and as a result carbon fixation process slows down.

activate the heat stress tolerance mechanisms, which might actually be a safeguard for the heat-labile proteins such as citrate synthase, RuBisCO activase, and malate dehydrogenase from thermal degradation; and finally, this action at the cellular level enables the protection of photosynthetic machinery. In support of the heat tolerance mechanism in Surge, we found a higher accumulation of a stromal 70 kDa HSP, which we predict might regulate functionally vital processes crucial for the plant's survival. This finding is relevant to the earlier reports reporting that HSP family of chaperons can promote the protein refolding to maintain protein homeostasis under heat stress conditions [97]. The physiological study also indicates that, in Surge, there is no significant change of photosynthesis levels due to heat stress.

One of the inevitable outcomes from the biochemical assays is the increase of ROS level (hydrogen peroxide) during drought stress in both Surge and Davison. We also found higher amounts of carbonic anhydrase accumulation in the cell which probably aid the cell in becoming more resistant to cytotoxic concentrations of H_2O_2 in drought-stressed Davison plants; thus, significant changes at the phenotypic level were not noticed at the sixth day of the stress [70]. While investigating the changes in ABA levels during stress, we found that the cooccurrence of drought and heat stresses causes the highest accumulation of ABA in

soybeans compared to control plants, which is consistent with earlier findings in brassica and rice [98, 99]. This observation also correlates with the stomatal conductance measurements, statistical analysis by scatter plot of ABA concentration, and stomatal conductance measurement that shows a linear relationship with $R^2 > 0.95$, which indicates that an increase in ABA levels and a decrease in stomatal conductance have a kind of cause and effect relationship. While comparing the ABA measurement analysis and stomatal conductance measurement, we found that, in cooccurring drought and heat stress, stomatal conductance value is lowest while ABA levels are at the highest compared to drought-stressed and heat-stressed plants. After correlating the two observations, we concluded that the more severe the stress is, the more the ABA synthesis ultimately results in the stomatal closure, that is, lesser stomatal conductance. In response to the drought, heat, and cooccurring drought plus heat stresses, calcium levels elevate as probable calcium binding protein CML33 accumulates at higher levels [100]. These consequences activate the phosphoprotein cascade, which ultimately activates the transcription of ABA biosynthesis precursors and finally synthesizes ABA that aids in stomatal closure to reduce the transpiration levels, CO_2 assimilation, and photosynthesis for the sake of survival of the plant under adverse environmental conditions [71].

Finally, for the better understanding of the crosstalk between complex sets of abiotic stresses responsive proteins, we applied system biology approaches to determine the holistic outlook of the molecular responses [17, 101]. Our computational analysis of protein-protein interaction networks identifies 10 major proteinsthat havemore than 9 interactions considered to be at the central body of the network system. This protein network forecasts that drought or heat stress mediated downregulation or upregulation of those central body proteins of the network may also affect their predicted partners, which ultimately could affect the molecular signaling by collapsing the whole cellular network. This systems biology study will assist in the breeding of more abiotic stress tolerant soybean varieties having high nutritional value.

Proteomics study on rice by Kim et al. has shown that proteomic data can be used for crop improvement which eventually leads to food security [42]. A clearer understanding of differential expression of various stress-related proteins and inclusion of this knowledge to breed better varieties may trigger a speedy improvement of crop plants [26, 42]. The extensive application of such quantitative proteomic approaches together with mapping of posttranslational modifications will provide us with comprehensive insights of the regulation of various stress-responsive proteins in complex biological systems [102]. The agronomical perspective of the current study will support the soybean breeders to develop heat and drought tolerant soybean varieties.

Taken together, our study results identify the differential expression of a number of drought-, heat-, and cooccurring drought and heat-responsive proteins. The observed changes in leaf protein expressions suggest that the regulation of various molecular processes and signaling alters due to drought and heat stresses.

5. Conclusions

This study shows how drought, heat, and cooccurring drought and heat stresses alter the soybean leaf proteome. Differential expression of 44 abiotic stress-responsive proteins suggests that various signaling cascades and molecular processes are affected due to drought and heat stresses. Furthermore, the result suggests that many differentially expressed photosynthesis-related proteins perturb RuBisCO regulation, electron transport, and Calvin cycle during abiotic stress. These findings, as well as upregulation of EF-Tu and higher level expressions of HSP, will help in better understanding of the heat tolerance mechanisms in the soybean varieties. The biochemical and proteomic assays also explain how higher amount of carbonic anhydrase accumulation in the cell alleviates cytotoxic concentrations of H_2O_2 during drought stress. Moreover, we found that cooccurring drought and heat stresses have the highest level of ABA accumulations in Davison, which also correlates with our stomatal conductance measurements. Taken together, the results presented provide a proteomic level explanation for the abiotic stress effects on physiological processes of soybean plants during abiotic stress conditions.

Abbreviations

% VWC:	Percentage volume water content
2D-DIGE:	Two-dimensional differential in-gel electrophoresis
ABA:	Abscisic acid
CA1P:	2-Carboxyarabinitol 1 phosphate
CAB1:	Chlorophyll a-b binding protein 1
CML33:	Probable calcium binding protein
Cy2/Cy3/Cy5:	Cyanine dye 2, 3, or 5
DMF:	N, N-Dimethylformamide
EF-Tu:	Elongation factor Tu
Fd:	Ferredoxin
FNR:	Ferredoxin-$NADP^+$ oxidoreductase
HRP:	Horseradish peroxidase
HSP:	Heat shock-related proteins
PPP:	Pentose phosphate pathway
RH:	Relative humidity
RNP7:	Protein RNP-7
ROS:	Reactive oxygen species
RuBisCO:	Ribulose bisphosphate carboxylase oxygenase
STRING:	Search tool for the retrieval of interacting genes.

Conflict of Interests

The authors declare that they have no competing interests.

Authors' Contribution

The idea was conceived by Jai S. Rohila. Aayudh Das, Moustafa Eldakak, Bimal Paudel, Homa Hemmati, and Chhandak Basu did the experiments. Aayudh Das, Moustafa Eldakak, Bimal Paudel, Dea-Wook Kim, Homa Hemmati,

Chhandak Basu, and Jai S. Rohila did the data analyses. Aayudh Das, Chhandak Basu, and Jai S. Rohila wrote the paper.

Acknowledgments

The authors thank Dr. Senthil Subramanian for his assistance in seed procurement, Dr. Yajun Wu for his critical discussions and help with ROS measurements, and Mr. Nathan Serfling (Department of English, SDSU) for his help to improve the English of this paper. DWK acknowledges all support from Cooperative Research Program for Agriculture Science & Technology Development (Project no. PJ00953802) of Rural Development Administration, Republic of Korea. This work was supported by South Dakota Soybean Research & Promotion Council, South Dakota State University Agricultural Experiment Station, CRIS Project SD00H541-15, and the Department of Biology & Microbiology.

References

[1] P. H. Graham and C. P. Vance, "Legumes: importance and constraints to greater use," *Plant Physiology*, vol. 131, no. 3, pp. 872–877, 2003.

[2] South Dakota Soybean Research and Promotion Council, "Soybeans Make Big Economic Impact," 2014, http://sdsoybean.org/All_About_Soy/Economic_Impact.

[3] U.S.D.A, "Soybeans and Oil Crops," August 2014, http://www.ers.usda.gov/topics/crops/soybeans-oil-crops/related-data-statistics.aspx#.U9wFxfldU08.

[4] M. Eldakak, S. I. M. Milad, A. I. Nawar, and J. S. Rohila, "Proteomics: a biotechnology tool for crop improvement," *Frontiers in Plant Science*, vol. 4, no. 35, pp. 1–12, 2013.

[5] M. Farooq, A. Wahid, N. Kobayashi, D. Fujita, and S. M. A. Basra, "Plant drought stress: effects, mechanisms and management," *Agronomy for Sustainable Development*, vol. 29, no. 1, pp. 185–212, 2009.

[6] K. Kosová, P. Vítámvás, I. T. Prášil, and J. Renaut, "lant proteome changes under abiotic stress-contribution of proteomics studies to understanding plant stress response," *Journal of Proteomics*, vol. 74, no. 8, pp. 1301–1322, 2011.

[7] D. Jespersen and B. Huang, "Proteins associated with heat-induced leaf senescence in creeping bentgrass as affected by foliar application of nitrogen, cytokinins, and an ethylene inhibitor," *Proteomics*, vol. 15, no. 4, pp. 798–812, 2015.

[8] G.-T. Liu, L. Ma, W. Duan et al., "Differential proteomic analysis of grapevine leaves by iTRAQ reveals responses to heat stress and subsequent recovery," *BMC Plant Biology*, vol. 14, article 110, 2014.

[9] L. Rizhsky, H. Liang, and R. Mittler, "The combined effect of drought stress and heat shock on gene expression in tobacco," *Plant Physiology*, vol. 130, no. 3, pp. 1143–1151, 2002.

[10] J. A. Rollins, E. Habte, S. E. Templer, T. Colby, J. Schmidt, and M. Von Korff, "Leaf proteome alterations in the context of physiological and morphological responses to drought and heat stress in barley (*Hordeum vulgare* L.)," *Journal of Experimental Botany*, vol. 64, no. 11, pp. 3201–3212, 2013.

[11] P. P. Mohammadi, A. Moieni, S. Hiraga, and S. Komatsu, "Organ-specific proteomic analysis of drought-stressed soybean seedlings," *Journal of Proteomics*, vol. 75, no. 6, pp. 1906–1923, 2012.

[12] V. M. Rodríguez, P. Soengas, V. Alonso-Villaverde, T. Sotelo, M. E. Cartea, and P. Velasco, "Effect of temperature stress on the early vegetative development of *Brassica oleracea* L.," *BMC Plant Biology*, vol. 15, no. 145, pp. 1–9, 2015.

[13] G. M. Ali and S. Komatsu, "Proteomic analysis of rice leaf sheath during drought stress," *Journal of Proteome Research*, vol. 5, no. 2, pp. 396–403, 2006.

[14] Z. Peng, M. Wang, F. Li, H. Lv, C. Li, and G. Xia, "A proteomic study of the response to salinity and drought stress in an introgression strain of bread wheat," *Molecular and Cellular Proteomics*, vol. 8, no. 12, pp. 2676–2686, 2009.

[15] G. H. Salekdeh, J. Siopongco, L. J. Wade, B. Ghareyazie, and J. Bennett, "Proteomic analysis of rice leaves during drought stress and recovery," *Proteomics*, vol. 2, no. 9, pp. 1131–1145, 2002.

[16] M. M. Chaves, J. Flexas, and C. Pinheiro, "Photosynthesis under drought and salt stress: regulation mechanisms from whole plant to cell," *Annals of Botany*, vol. 103, no. 4, pp. 551–560, 2009.

[17] G. R. Cramer, K. Urano, S. Delrot, M. Pezzotti, and K. Shinozaki, "Effects of abiotic stress on plants: a systems biology perspective," *BMC Plant Biology*, vol. 11, article 163, 14 pages, 2011.

[18] J.-K. Zhu, "Salt and drought stress signal transduction in plants," *Annual Review of Plant Biology*, vol. 53, pp. 247–273, 2002.

[19] G. R. Cramer, S. C. Van Sluyter, D. W. Hopper, D. Pascovici, T. Keighley, and P. A. Haynes, "Proteomic analysis indicates massive changes in metabolism prior to the inhibition of growth and photosynthesis of grapevine (*Vitis vinifera* L.) in response to water deficit," *BMC Plant Biology*, vol. 13, no. 49, pp. 1–22, 2013.

[20] W. Wang, B. Vinocur, O. Shoseyov, and A. Altman, "Role of plant heat-shock proteins and molecular chaperones in the abiotic stress response," *Trends in Plant Science*, vol. 9, no. 5, pp. 244–252, 2004.

[21] C. Plomion, C. Lalanne, S. Claverol et al., "Mapping the proteome of poplar and application to the discovery of drought-stress responsive proteins," *Proteomics*, vol. 6, no. 24, pp. 6509–6527, 2006.

[22] W. Li, Z. Wei, Z. Qiao, Z. Wu, L. Cheng, and Y. Wang, "Proteomics analysis of alfalfa response to heat stress," *PLoS ONE*, vol. 8, no. 12, Article ID e82725, 2013.

[23] S. Muneer, Y. G. Park, A. Manivannan, P. Soundararajan, and B. R. Jeong, "Physiological and proteomic analysis in chloroplasts of *Solanum lycopersicum* L. under silicon efficiency and salinity stress," *International Journal of Molecular Sciences*, vol. 15, no. 12, pp. 21803–21824, 2014.

[24] G. Cornic and A. Massacci, "Leaf photosynthesis under drought stress," in *Photosynthesis and the Environment*, N. R. Baker, Ed., pp. 347–366, Springer, Amsterdam, The Netherlands, 1996.

[25] A. M. Timperio, M. G. Egidi, and L. Zolla, "Proteomics applied on plant abiotic stresses: role of heat shock proteins (HSP)," *Journal of Proteomics*, vol. 71, no. 4, pp. 391–411, 2008.

[26] G. K. Agrawal, R. Pedreschi, B. J. Barkla et al., "Translational plant proteomics: a perspective," *Journal of Proteomics*, vol. 75, no. 15, pp. 4588–4601, 2012.

[27] C. A. Jaleel, K. Riadh, R. Gopi et al., "Antioxidant defense responses: physiological plasticity in higher plants under abiotic constraints," *Acta Physiologiae Plantarum*, vol. 31, no. 3, pp. 427–436, 2009.

[28] S. P. Mukherjee and M. A. Choudhuri, "Implications of water stress-induced changes in the levels of endogenous ascorbic acid and hydrogen peroxide in Vigna seedlings," *Physiologia Plantarum*, vol. 58, no. 2, pp. 166–170, 1983.

[29] J. Mundy and N.-H. Chua, "Abscisic acid and water-stress induce the expression of a novel rice gene," *The EMBO Journal*, vol. 7, no. 8, pp. 2279–2286, 1988.

[30] I. E. Henson, "The heritability of abscisic acid accumulation in water-stressed leaves of pearl millet [*Pennisetum americanum* (L.) leeke]," *Annals of Botany*, vol. 53, no. 1, pp. 1–12, 1984.

[31] X. Wang, T. Kuang, and Y. He, "Conservation between higher plants and the moss *Physcomitrella patens* in response to the phytohormone abscisic acid: a proteomics analysis," *BMC Plant Biology*, vol. 10, article 192, 11 pages, 2010.

[32] M. Gong, Y.-J. Li, and S.-Z. Chen, "Abscisic acid-induced thermotolerance in maize seedlings is mediated by calcium and associated with antioxidant systems," *Journal of Plant Physiology*, vol. 153, no. 3-4, pp. 488–496, 1998.

[33] P. R. Houser, W. J. Shuttleworth, J. S. Famiglietti, H. V. Gupta, K. H. Syed, and D. C. Goodrich, "Integration of soil moisture remote sensing and hydrologic modeling using data assimilation," *Water Resources Research*, vol. 34, no. 12, pp. 3405–3420, 1998.

[34] X. Ma, N. L. Sukiran, H. Ma, and Z. Su, "Moderate drought causes dramatic floral transcriptomic reprogramming to ensure successful reproductive development in *Arabidopsis*," *BMC Plant Biology*, vol. 14, article 164, 2014.

[35] N. B. A. Thu, X. L. T. Hoang, H. Doan et al., "Differential expression analysis of a subset of GmNAC genes in shoots of two contrasting drought-responsive soybean cultivars DT51 and MTD720 under normal and drought conditions," *Molecular Biology Reports*, vol. 41, no. 9, pp. 5563–5569, 2014.

[36] W. J. Hurkman and C. K. Tanaka, "Solubilization of plant membrane proteins for analysis by two-dimensional gel electrophoresis," *Plant Physiology*, vol. 81, no. 3, pp. 802–806, 1986.

[37] M. L. Robbins, A. Roy, P.-H. Wang et al., "Comparative proteomics analysis by DIGE and iTRAQ provides insight into the regulation of phenylpropanoids in maize," *Journal of Proteomics*, vol. 93, pp. 254–275, 2013.

[38] D. Gupta, M. Eldakak, J. S. Rohila, and C. Basu, "Biochemical analysis of 'kerosene tree' Hymenaea courbaril L. Under heat stress," *Plant Signaling and Behavior*, vol. 9, no. 10, Article ID e972851, pp. 1–10, 2014.

[39] G. Poschmann, B. Sitek, B. Sipos et al., "Identification of proteomic differences between squamous cell carcinoma of the lung and bronchial epithelium," *Molecular & Cellular Proteomics*, vol. 8, no. 5, pp. 1105–1116, 2009.

[40] K. Aihara, K. J. Byer, and S. R. Khan, "Calcium phosphate–induced renal epithelial injury and stone formation: involvement of reactive oxygen species," *Kidney International*, vol. 64, no. 4, pp. 1283–1291, 2003.

[41] B. G. de los Reyes, S. J. Yun, V. Herath et al., "Phenotypic, physiological, and molecular evaluation of rice chilling stress response at the vegetative stage," in *Rice Protocols*, vol. 956 of *Methods in Molecular Biology*, pp. 227–241, Humana Press, New York, NY, USA, 2013.

[42] S. T. Kim, S. G. Kim, G. K. Agrawal, S. Kikuchi, and R. Rakwal, "Rice proteomics: a model system for crop improvement and food security," *Proteomics*, vol. 14, no. 4-5, pp. 593–610, 2014.

[43] F. Sievers and D. G. Higgins, "Clustal omega, accurate alignment of very large numbers of sequences," in *Multiple Sequence Alignment Methods*, pp. 105–116, Springer, 2014.

[44] D. Szklarczyk, A. Franceschini, M. Kuhn et al., "The STRING database in 2011: functional interaction networks of proteins, globally integrated and scored," *Nucleic Acids Research*, vol. 39, supplement 1, pp. D561–D568, 2011.

[45] P. Shannon, A. Markiel, O. Ozier et al., "Cytoscape: a software environment for integrated models of biomolecular interaction networks," *Genome Research*, vol. 13, no. 11, pp. 2498–2504, 2003.

[46] M. J. L. de Hoon, S. Imoto, J. Nolan, and S. Miyano, "Open source clustering software," *Bioinformatics*, vol. 20, no. 9, pp. 1453–1454, 2004.

[47] A. J. Saldanha, "Java Treeview-extensible visualization of microarray data," *Bioinformatics*, vol. 20, no. 17, pp. 3246–3248, 2004.

[48] K. Miyashita, S. Tanakamaru, T. Maitani, and K. Kimura, "Recovery responses of photosynthesis, transpiration, and stomatal conductance in kidney bean following drought stress," *Environmental and Experimental Botany*, vol. 53, no. 2, pp. 205–214, 2005.

[49] M. R. B. Siddique, A. Hamid, and M. S. Islam, "Drought stress effects on water relations of wheat," *Botanical Bulletin of Academia Sinica*, vol. 41, no. 1, pp. 35–39, 2000.

[50] D. R. Ort, "When there is too much light," *Plant Physiology*, vol. 125, no. 1, pp. 29–32, 2001.

[51] D. W. Lawlor and G. Cornic, "Photosynthetic carbon assimilation and associated metabolism in relation to water deficits in higher plants," *Plant, Cell & Environment*, vol. 25, no. 2, pp. 275–294, 2002.

[52] G. D. Farquhar and T. D. Sharkey, "Stomatal conductance and photosynthesis," *Annual Review of Plant Physiology*, vol. 33, no. 1, pp. 317–345, 1982.

[53] A. R. Reddy, K. V. Chaitanya, and M. Vivekanandan, "Drought-induced responses of photosynthesis and antioxidant metabolism in higher plants," *Journal of Plant Physiology*, vol. 161, no. 11, pp. 1189–1202, 2004.

[54] D. W. Lawlor, "Limitation to photosynthesis in water-stressed leaves: stomata vs. Metabolism and the role of ATP," *Annals of Botany*, vol. 89, pp. 871–885, 2002.

[55] H. Medrano, M. A. J. Parry, X. Socias, and D. W. Lawlor, "Long term water stress inactivates Rubisco in subterranean clover," *Annals of Applied Biology*, vol. 131, no. 3, pp. 491–501, 1997.

[56] J. C. V. Vu, R. W. Gesch, L. H. Allen Jr., K. J. Boote, and G. Bowes, "CO_2 enrichment delays a rapid, drought-induced decrease in rubisco small subunit transcript abundance," *Journal of Plant Physiology*, vol. 155, no. 1, pp. 139–142, 1999.

[57] B. Moore and J. R. Seeman, "Evidence that 2-carboxyarabinitol 1-phosphate binds to ribulose-1, 5-bisphosphate carboxylase in vivo," *Plant Physiology*, vol. 105, no. 2, pp. 731–737, 1994.

[58] M. M. Chaves, J. P. Maroco, and J. S. Pereira, "Understanding plant responses to drought—from genes to the whole plant," *Functional Plant Biology*, vol. 30, no. 3, pp. 239–264, 2003.

[59] M. Havaux and F. Tardy, "Temperature-dependent adjustment of the thermal stability of photosystem II in vivo: possible involvement of xanthophyll-cycle pigments," *Planta*, vol. 198, no. 3, pp. 324–333, 1996.

[60] J. H. Lee, I. H. Kang, K. L. Choi, W.-S. Sim, and J.-K. Kim, "Gene expression of chloroplast translation elongation factor Tu during maize chloroplast biogenesis," *Journal of Plant Biology*, vol. 40, no. 4, pp. 227–233, 1997.

[61] T. Moriarty, R. West, G. Small, D. Rao, and Z. Ristic, "Heterologous expression of maize chloroplast protein synthesis elongation factor (EF-Tu) enhances *Escherichia coli* viability under heat stress," *Plant Science*, vol. 163, no. 6, pp. 1075–1082, 2002.

[62] Z. Ristic, I. Momčilović, J. Fu, E. Callegari, and B. P. DeRidder, "Chloroplast protein synthesis elongation factor, EF-Tu, reduces thermal aggregation of rubisco activase," *Journal of Plant Physiology*, vol. 164, no. 12, pp. 1564–1571, 2007.

[63] I. Momcilovic and Z. Ristic, "Localization and abundance of chloroplast protein synthesis elongation factor (EF-Tu) and heat stability of chloroplast stromal proteins in maize," *Plant Science*, vol. 166, no. 1, pp. 81–88, 2004.

[64] D. Rao, I. Momcilovic, S. Kobayashi, E. Callegari, and Z. Ristic, "Chaperone activity of recombinant maize chloroplast protein synthesis elongation factor, EF-Tu," *European Journal of Biochemistry*, vol. 271, no. 18, pp. 3684–3692, 2004.

[65] M. E. Salvucci, "Association of Rubisco activase with chaperonin-60β: a possible mechanism for protecting photosynthesis during heat stress," *Journal of Experimental Botany*, vol. 59, no. 7, pp. 1923–1933, 2008.

[66] M. Latijnhouwers, X.-M. Xu, and S. G. Møller, "Arabidopsis stromal 70-kDa heat shock proteins are essential for chloroplast development," *Planta*, vol. 232, no. 3, pp. 567–578, 2010.

[67] P.-H. Su and H.-M. Li, "Arabidopsis stromal 70-kD heat shock proteins are essential for plant development and important for thermotolerance of germinating seeds," *Plant Physiology*, vol. 146, no. 3, pp. 1231–1241, 2008.

[68] M. R. Badger and G. D. Price, "The role of carbonic anhydrase in photosynthesis," *Annual Review of Plant Biology*, vol. 45, no. 1, pp. 369–392, 1994.

[69] M. H. C. de Carvalho, "Drought stress and reactive oxygen species," *Plant Signaling & Behavior*, vol. 3, no. 3, pp. 156–165, 2008.

[70] S. R. Räisänen, P. Lehenkari, M. Tasanen, P. Rahkila, P. L. Härkönen, and H. K. Väänänen, "Carbonic anhydrase III protects cells from hydrogen peroxide-induced apoptosis," *The FASEB Journal*, vol. 13, no. 3, pp. 513–522, 1999.

[71] N. Tuteja, "Abscisic acid and abiotic stress signaling," *Plant Signaling and Behavior*, vol. 2, no. 3, pp. 135–138, 2007.

[72] P. J. Kramer, "Changing concepts regarding plant water relations," *Plant, Cell & Environment*, vol. 11, no. 7, pp. 565–568, 1988.

[73] Q. Chen and C. D. Silflow, "Isolation and characterization of glutamine synthetase genes in *Chlamydomonas reinhardtii*," *Plant Physiology*, vol. 112, no. 3, pp. 987–996, 1996.

[74] S. Yan, Z. Tang, W. Su, and W. Sun, "Proteomic analysis of salt stress-responsive proteins in rice root," *Proteomics*, vol. 5, no. 1, pp. 235–244, 2005.

[75] R. T. El-Khatib, E. P. Hamerlynck, F. Gallardo, and E. G. Kirby, "Transgenic poplar characterized by ectopic expression of a pine cytosolic glutamine synthetase gene exhibits enhanced tolerance to water stress," *Tree Physiology*, vol. 24, no. 7, pp. 729–736, 2004.

[76] C. Xu and B. Huang, "Root proteomic responses to heat stress in two *Agrostis grass* species contrasting in heat tolerance," *Journal of Experimental Botany*, vol. 59, no. 15, pp. 4183–4194, 2008.

[77] S. S. Gill, N. A. Anjum, R. Gill, M. Mahajan, and N. Tuteja, "Abiotic stress tolerance and sustainable agriculture: a functional genomics perspective," in *Elucidation of Abiotic Stress Signaling in Plants*, G. K. Pandey, Ed., pp. 439–472, Springer, New York, NY, USA, 2015.

[78] L.-S. P. Tran and K. Mochida, "Identification and prediction of abiotic stress responsive transcription factors involved in abiotic stress signaling in soybean," *Plant Signaling & Behavior*, vol. 5, no. 3, pp. 255–257, 2010.

[79] I. Alam, S. A. Sharmin, K.-H. Kim, J. K. Yang, M. S. Choi, and B.-H. Lee, "Proteome analysis of soybean roots subjected to short-term drought stress," *Plant and Soil*, vol. 333, no. 1, pp. 491–505, 2010.

[80] P. R. Weisz, R. F. Denison, and T. R. Sinclair, "Response to drought stress of nitrogen fixation (acetylene reduction) rates by field-grown soybeans," *Plant Physiology*, vol. 78, no. 3, pp. 525–530, 1985.

[81] R. Mittler, "Abiotic stress, the field environment and stress combination," *Trends in Plant Science*, vol. 11, no. 1, pp. 15–19, 2006.

[82] H. Vanderschuren, E. Lentz, I. Zainuddin, and W. Gruissem, "Proteomics of model and crop plant species: status, current limitations and strategic advances for crop improvement," *Journal of Proteomics*, vol. 93, pp. 5–19, 2013.

[83] H. Medrano, J. M. Escalona, J. Bota, J. Gulías, and J. Flexas, "Regulation of photosynthesis of C_3 plants in response to progressive drought: stomatal conductance as a reference parameter," *Annals of Botany*, vol. 89, pp. 895–905, 2002.

[84] G. Cornic, "Drought stress inhibits photosynthesis by decreasing stomatal aperture—not by affecting ATP synthesis," *Trends in Plant Science*, vol. 5, no. 5, pp. 187–188, 2000.

[85] E. S. Tozzi, H. M. Easlon, and J. H. Richards, "Interactive effects of water, light and heat stress on photosynthesis in Fremont cottonwood," *Plant, Cell & Environment*, vol. 36, no. 8, pp. 1423–1434, 2013.

[86] W. Tezara, V. J. Mitchell, S. D. Driscoll, and D. W. Lawlor, "Water stress inhibits plant photosynthesis by decreasing coupling factor and ATP," *Nature*, vol. 401, no. 6756, pp. 914–917, 1999.

[87] D. Ghosh and J. Xu, "Abiotic stress responses in plant roots: a proteomics perspective," *Frontiers in Plant Science*, vol. 5, article 6, 13 pages, 2014.

[88] C. Brun, F. Chevenet, D. Martin, J. Wojcik, A. Guénoche, and B. Jacq, "Functional classification of proteins for the prediction of cellular function from a protein-protein interaction network," *Genome Biology*, vol. 5, no. 1, pp. R6.3–R6.13, 2003.

[89] A. Kumar, S. Agarwal, J. A. Heyman et al., "Subcellular localization of the yeast proteome," *Genes and Development*, vol. 16, no. 6, pp. 707–719, 2002.

[90] M. A. J. Parry, P. J. Andralojc, S. Khan, P. J. Lea, and A. J. Keys, "Rubisco activity: effects of drought stress," *Annals of Botany*, vol. 89, pp. 833–839, 2002.

[91] M. C. Dias and W. Brüggemann, "Limitations of photosynthesis in *Phaseolus vulgaris* under drought stress: gas exchange, chlorophyll fluorescence and Calvin cycle enzymes," *Photosynthetica*, vol. 48, no. 1, pp. 96–102, 2010.

[92] H. Cai, Y. Zhou, J. Xiao, X. Li, Q. Zhang, and X. Lian, "Overexpressed glutamine synthetase gene modifies nitrogen metabolism and abiotic stress responses in rice," *Plant Cell Reports*, vol. 28, no. 3, pp. 527–537, 2009.

[93] J. A. G. Silveira, A. R. B. Melo, R. A. Viégas, and J. T. A. Oliveira, "Salinity-induced effects on nitrogen assimilation related to growth in cowpea plants," *Environmental and Experimental Botany*, vol. 46, no. 2, pp. 171–179, 2001.

[94] R. R. Wise, A. J. Olson, S. M. Schrader, and T. D. Sharkey, "Electron transport is the functional limitation of photosynthesis in field-grown Pima cotton plants at high temperature," *Plant, Cell & Environment*, vol. 27, no. 6, pp. 717–724, 2004.

[95] R. Zhang and T. D. Sharkey, "Photosynthetic electron transport and proton flux under moderate heat stress," *Photosynthesis Research*, vol. 100, no. 1, pp. 29–43, 2009.

[96] S. K. Bhadula, T. E. Elthon, J. E. Habben, T. G. Helentjaris, S. Jiao, and Z. Ristic, "Heat-stress induced synthesis of chloroplast protein synthesis elongation factor (EF-Tu) in a heat-tolerant maize line," *Planta*, vol. 212, no. 3, pp. 359–366, 2001.

[97] M. Haslbeck, T. Franzmann, D. Weinfurtner, and J. Buchner, "Some like it hot: the structure and function of small heat-shock proteins," *Nature Structural and Molecular Biology*, vol. 12, no. 10, pp. 842–846, 2005.

[98] M. Dalal, D. Tayal, V. Chinnusamy, and K. C. Bansal, "Abiotic stress and ABA-inducible Group 4 *LEA* from *Brassica napus* plays a key role in salt and drought tolerance," *Journal of Biotechnology*, vol. 139, no. 2, pp. 137–145, 2009.

[99] M. A. Hossain, J.-I. Cho, M. Han et al., "The ABRE-binding bZIP transcription factor OsABF2 is a positive regulator of abiotic stress and ABA signaling in rice," *Journal of Plant Physiology*, vol. 167, no. 17, pp. 1512–1520, 2010.

[100] E. McCormack and J. Braam, "Calmodulins and related potential calcium sensors of Arabidopsis," *New Phytologist*, vol. 159, no. 3, pp. 585–598, 2003.

[101] M. Fujita, Y. Fujita, Y. Noutoshi et al., "Crosstalk between abiotic and biotic stress responses: a current view from the points of convergence in the stress signaling networks," *Current Opinion in Plant Biology*, vol. 9, no. 4, pp. 436–442, 2006.

[102] S. Komatsu, H.-P. Mock, P. Yang, and B. Svensson, "Application of proteomics for improving crop protection/artificial regulation," *Frontiers in Plant Science*, vol. 4, no. 522, pp. 1–3, 2013.

Hindawi Publishing Corporation
BioMed Research International
Volume 2016, Article ID 9851095, 9 pages
http://dx.doi.org/10.1155/2016/9851095

Research Article

Drought Tolerance Is Correlated with the Activity of Antioxidant Enzymes in *Cerasus humilis* Seedlings

Jing Ren,[1,2] Li Na Sun,[1] Qiu Yan Zhang,[1] and Xing Shun Song[1,3]

[1]*Department of Genetics, College of Life Science, Northeast Forestry University, Harbin 150040, China*
[2]*Key Laboratory of Dairy Science, Ministry of Education, College of Food Science, Northeast Agricultural University, Synergetic Innovation Center of Food Safety and Nutrition, Harbin, Heilongjiang 150030, China*
[3]*State Key Laboratory of Tree Genetics and Breeding, Northeast Forestry University, Harbin 150040, China*

Correspondence should be addressed to Xing Shun Song; sfandi@163.com

Received 26 November 2015; Revised 9 February 2016; Accepted 15 February 2016

Academic Editor: Luis Fernando Revers

Cerasus humilis, grown in the northern areas of China, may experience water deficit during their life cycle, which induces oxidative stress. Our present study was conducted to evaluate the role of oxidative stress management in the leaves of two *C. humilis* genotypes, HR (drought resistant) and ND4 (drought susceptible), when subjected to a long-term soil drought (WS). The HR plants maintained lower membrane injury due to low ROS and MDA accumulation compared to ND4 plants during a long-term WS. This is likely attributed to global increase in the activities of superoxide dismutase (SOD) isoenzymes and enzymes of the ascorbate-glutathione (AsA-GSH) cycle and maintenance of ascorbate (AsA) levels. Consistent closely with enzymes activities, the expression of cytosolic ascorbate peroxidase (cAPX) and dehydroascorbate reductase (DHAR) followed a significant upregulation, indicating that they were regulated at the transcriptional level for HR plants exposed to WS. In contrast, ND4 plants exhibited high ROS levels and poor antioxidant enzyme response, leading to enhanced membrane damage during WS conditions. The present study shows that genotypic differences in drought tolerance could be likely attributed to the ability of *C. humilis* plants to induce antioxidant defense under drought conditions.

1. Introduction

Drought is one of the most important manifestations of abiotic stress in plants. It is the major yield-limiting factor of crop plants and it actively and continuously determines the natural distribution of plant species [1]. To meet the needs of the growing world population, it is essential to effectively utilize dehydrated soil in drought-prone areas. However, the progress towards developing drought-tolerant crops is significantly hampered by the lack of highly tolerant genetic resources and the complexity in physiological and genetic traits. It is therefore important to identify the genetic resources and to understand the mechanisms of drought tolerance in plants that could result in high levels of tolerance to drought stress [2]. Plants evolve adaptations to different growth conditions and there exist great differences in their tolerance towards a variety of growth conditions. In fact, great differences are also observed within species, since different cultivars suited for different ecosystems or growing seasons have been developed by breeders [3].

Reactive oxygen species (ROS), also called active oxygen species (AOS) or reactive oxygen intermediates (ROI), are the result of the partial reduction of atmospheric O_2. Although the role of ROS production and control during drought stress is yet to be resolved, ROS seem to have a dual effect under abiotic stress conditions that depend on their overall cellular amount. If kept at relatively low levels they are likely to function as components of a stress-signaling pathway, triggering stress defense/acclimation responses. However, when reaching a certain level of phytotoxicity ROS become extremely deleterious, initiating uncontrolled oxidative cascades that damage cellular membranes and other cellular components resulting in oxidative stress and eventually cell death [4–6]. Plants have also developed strategies to minimize the deleterious effects of ROS which cause lipid peroxidation, protein denaturation, and DNA mutation [7].

Among them, the ROS-scavenging mechanism has received an increasing amount of attention. This mechanism consists of such enzymes as superoxide dismutase (SOD) and catalase (CAT) and the enzymes of the ascorbate-glutathione cycle (e.g., ascorbate peroxidase (APX), monodehydroascorbate reductase (MDAR), dehydroascorbate reductase (DHAR), and glutathione reductase (GR)) and nonenzymatic components such as ascorbate, glutathione, carotenoids, and tocopherol [8–10]. It is known that organelles with a highly oxidizing metabolic activity or an intense rate of electron flow, such as chloroplasts, mitochondria, and microbodies, are major sources of ROS. In accordance with this, different isoenzymes such as Cu/Zn-SOD, Fe-SOD, Mn-SOD, cytosol APX (cAPX), and microbody APX (mAPX) have been found in different organelles [11]. Although it has been generalized that the tolerance of a species to different stresses is closely correlated with its ROS-scavenging capacity [12], other tolerance (or avoidance) mechanisms have been suggested to modify genotype-dependent responses to stress, along with the different degrees of stress experienced, species, and plant ages [13–15].

Cerasus humilis (Bge.) Sok is a species of small, perennial, deciduous shrub belonging to Rosaceae family. It is distributed in the Inner Mongolia, Shanxi, and the northern areas of China. *C. humilis* fruits contain a variety of mineral elements beneficial to human health, especially a higher calcium content of fruit. In the early seedling periods, however, *C. humilis* not only grows slowly but is vulnerable to the environmental changes [16, 17]. Our previous studies found contrasting *C. humilis* genotypes Huai'rou (HR, drought-tolerant) and Nongda4 (ND4, drought-sensitive) in response to drought stress. However, the basic physiological, biochemical, and molecular mechanisms involved in stress tolerance are still unclear. The main objective of the present study was to compare the physiological effects of drought stress on the two *C. humilis* genotypes and to test the hypothesis that genotypic differences in growth response to drought are related to ROS-scavenging activity.

2. Material and Methods

2.1. Plant Material. Two *C. humilis* genotypes were used in this study. Huai'rou (HR) is a drought-tolerant genotype developed for arid areas while Nongda4 (ND4) is a drought-sensitive genotype developed for humid areas. All cuttings of 3-year-old plants were cut at the beginning of March in 2012, then transplanted into a container (35 × 35 × 25 cm) filled with organic soil, and irrigated regularly by half-strength Enshi nutrient solution under a 12 h photoperiod at temperatures ranging from about 17 to 25°C, photosynthetic photon flux density (PPFD) of 60 μmol (photon) m^{-2} s^{-1}, and the relative humidity of 70–75% in the greenhouse. At the end of May in 2015, plants at the 35–40-leaf stage were randomly allocated to one of two treatments: control plants (control) were watered daily to field capacity, while water was withheld from water-stressed plants (drought). The drought treatment lasted for 21 d; two mature leaves for each plant were removed and quickly frozen in liquid nitrogen, stored at −80°C for subsequent measurements of all physiological and biochemical parameters, with at least 30 plants per treatment.

Relative growth rate (RGR) was calculated by

$$\mathrm{RGR} = \frac{(\ln W_2 - \ln W_1)}{t_2 - t_1}, \quad (1)$$

where W_2 and W_1 were dry weight for seedlings at the beginning and at the end of the experiment, respectively, while $t_2 - t_1$ was the time duration for the treatment [18].

2.2. Determination of Reactive Oxygen Species and Lipid Peroxidation Level. $O_2^{\bullet-}$ was measured by monitoring nitrite formation from hydroxylamine in the presence of $O_2^{\bullet-}$, as described in [19] with slight modifications. Each 0.5 g of frozen leaf segment was homogenized in 3 mL of 65 mM potassium phosphate buffer (pH 7.8) and centrifuged at 5000 g for 10 min. The incubation mixture contained 0.9 mL of 65 mM phosphate buffer (pH 7.8), 0.1 mL 10 mM hydroxylamine hydrochloride, and 1 mL of the supernatant. Absorbance in the aqueous solution was measured at 530 nm. H_2O_2 content was measured by monitoring A_{410} of a titanium-peroxide complex, following the method described by [20]. As for the lipid peroxidation level, measured as the content of malondialdehyde (MDA), leaves were homogenized with 5 mL of 50 mM solution containing 0.07% $NaH_2PO_4 \cdot 2H_2O$ and 1.6% $Na_2HPO_4 \cdot 12H_2O$ and centrifuged at 20,000 ×g for 25 min in a refrigerated centrifuge. For measurement of MDA concentration, method of Heath and Packer was used [21].

2.3. Assay of SOD Isoenzymes Activities. To determine the activities of antioxidant enzymes, a crude enzyme extract was prepared by homogenizing 500 mg of leaf tissue in extraction buffer (0.5% Triton X-100 and 1% polyvinylpyrrolidone in 100 mM potassium phosphate buffer, pH 7.0) using a chilled mortar and pestle. The homogenate was then centrifuged at 15,000 ×g for 20 min at 4°C, and the supernatant was used for the enzymatic assays described below. SOD (EC 1.15.1.1) activity was assayed by monitoring the inhibition of photochemical reduction of nitro blue tetrazolium (NBT), according to [22]. Activities of different forms of SOD were identified by adding KCN and/or H_2O_2 in the reaction mixture [23]. KCN inhibits Cu/Zn-SOD but does not affect Mn-SOD nor Fe-SOD, whereas H_2O_2 inactivates Cu/Zn-SOD and Fe-SOD without affecting Mn-SOD. In addition, peroxidases might interfere with the SOD assay in the presence of exogenous H_2O_2 [24]. After extensive preliminary testing of a range of concentrations, KCN was added to the reaction mixture to a final concentration of 3 mM before the addition of H_2O_2 to a final concentration of 5 mM to eliminate interference from peroxidase and catalase enzymes [25].

2.4. Assay for APX-GSH Cycle Enzymes Activities and Contents of AsA and GSH. APX (EC1.11.1.11) activity was determined by monitoring the decrease in A_{290} according to [26]. MDAR (EC1.6.5.4) activity was measured by monitoring the decrease in A_{340} due to the NADH oxidation [27]. DHAR (EC1.8.5.1) was measured according to [28]. GR (EC1.6.4.2)

was determined following the procedure described by [29]. CAT (EC 1.11.1.6) activity was assayed in a reaction mixture containing 25 mM phosphate buffer (pH 7.0), 10 mM H_2O_2, and the enzyme. The decomposition of H_2O_2 was followed at 240 nm [30]. Ascorbate (AsA) and GSH content were determined according to [31, 32], respectively.

2.5. qRT-PCR Analysis. For qRT-PCR, duplicate samples were analysed in a Quantitative PCR instrument (Roche LightCycler 480 II, Switzerland). Total RNA was prepared using Trizol; then RNA was treated with RNase-free DNase I according to the manufacturer's instruction. One-microgram total RNA was performed in reverse transcription with RevertAid Reverse Transcriptase (Fermentas) and Oligo d(T)primers (TaKaRa). PCR amplification was performed with 40 cycles as follows: 94°C for 30 s, 58°C for 30 s, and 72°C for 30 s, followed by 72°C for 10 min. The relative expression levels of genes were presented by $2^{-\Delta\Delta CT}$. PCR reactions employed the following primers, actin-F (5′-GTGAAGGCTGGGTTTGCT-3′), actin-R (5′-CCCATCCCAACCATAACA-3′), DHAR-F (5′-CTCCTCCACCATCAAACA-3′), DHAR-R (5′-TTAGCCAAGTCCACCAAC-3′), cAPX-F (5′-AGCCCATCAAGCAACAGT-3′), and cAPX-R (5′-AGGGTCCTTCAAATCCAG-3′), respectively.

2.6. Statistic Analysis. Data are the average of at least three independent replicates. ANOVA, using *PC SAS* version *8.2* (*SAS Institute*, Cary, NC, USA), was conducted for all data and Duncan's Multiple-Range Test (DMRT) was used to evaluate treatment effects ($P < 0.05$) by using the data processing system statistical software package.

3. Results

3.1. Growth Response. First of all, we investigated changes in the relative growth rate (RGR) of two genotypes in response to WS (Figure 1). There was no significant difference between the two genotypes in RGR for *C. humilis* plants under control conditions. However, exposure to WS resulted in a significant reduction in RGR in ND4 from 0.9 to 0.6 g day^{-1}. In sharp contrast, no such decrease in RGR was observed for HR plants (Figure 1).

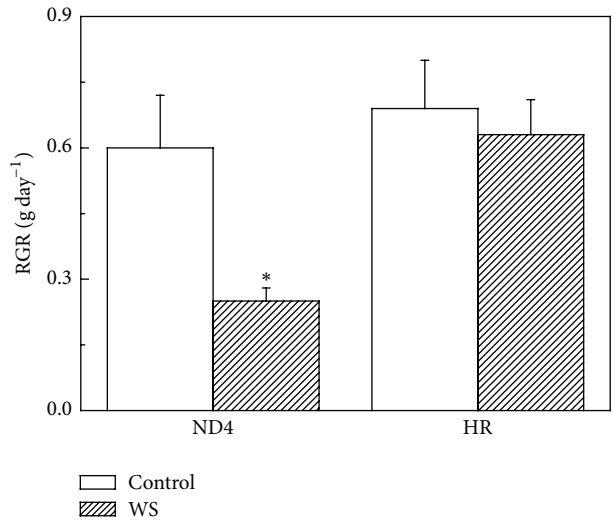

Figure 1: Effects of water stress (WS) on relative growth rate (RGR) as measured by dry matter production of *Cerasus humilis* leaves of Huai'rou (HR) and Nongda4 (ND4). Samples were collected after 21 d of treatment. The data are the mean of at least three replicates with standard errors shown by vertical bars. Asterisk (∗) indicates significant difference with control groups (well-watered) at the 0.05 level of probability by Duncan's Multiple-Range Test.

3.2. ROS Generation and Lipid Peroxidation. Exposure to WS resulted in $O_2^{\bullet-}$ production rate changes between the two *C. humilis* genotypes. The rate increased by 36% for ND4 while no significant change was observed for HR (Figure 2(a)). Meanwhile, HR plants showed a lower H_2O_2 content compared to ND4 when they were grown under WS. WS resulted in a 13% increase in H_2O_2 content in ND4 but not in HR (Figure 2(b)).

The lipid peroxidation level in the leaves grown under either WS or control conditions, measured as the content of malondialdehyde (MDA), is given (Figure 2(c)). Similar to the changes in H_2O_2 content, MDA content significantly increased in ND4 plants after exposure to a long-term WS while it was independent of the drought condition in HR seedlings.

3.3. SOD Activity. Total SOD activity remained almost unchanged for both genotypes throughout the experiment when the plants were grown at optimal growth conditions. However, a 67% increase in SOD activity was observed in HR plants under WS. In contrast, no significant increase was found in ND4 plants exposed to WS (Figure 3(a)).

A detailed examination was carried out to determine the response of three SOD isoenzymes to WS. There were no significant differences in the activity of Cu/Zn-SOD between the two genotypes (Figure 3(b)), while Fe-SOD and Mn-SOD were a little higher (but not significant) in HR than in ND4 for plants grown in optimal growth conditions (Figures 3(c) and 3(d)). A long-term WS resulted in a significant increase in Mn-SOD and Fe-SOD activity but not in Cu/Zn-SOD activity for HR plants. In contrast, there was a remarkable decrease in Cu/Zn-SOD activity for ND4 plants. WS had little effect on the activities of the Mn-SOD and Fe-SOD in ND4 plants (Figures 3(b), 3(c), and 3(d)).

3.4. CAT and AsA-GSH Cycle System Enzymes. Similar to the changes in total SOD activity, exposure to a long-term WS led to a significant increase in CAT activity in HR plants. However, for ND4 plants, there were no changes in CAT activity under either WS or control conditions (Figure 4(a)). APX activity showed changes very similar to CAT, increasing under WS in HR but not in ND4 plants (Figure 4(b)). For HR plants, WS resulted in a sharp increase by 79% in DHAR activity under WS. There was no significant difference in MDAR and GR activities under either WS or control conditions. For ND4 plants, however, a decrease by 63% in GR activities, with no changes in MDAR and DHAR activities, was observed under WS compared to the control plants (Figures 4(c), 4(d), and 4(e)).

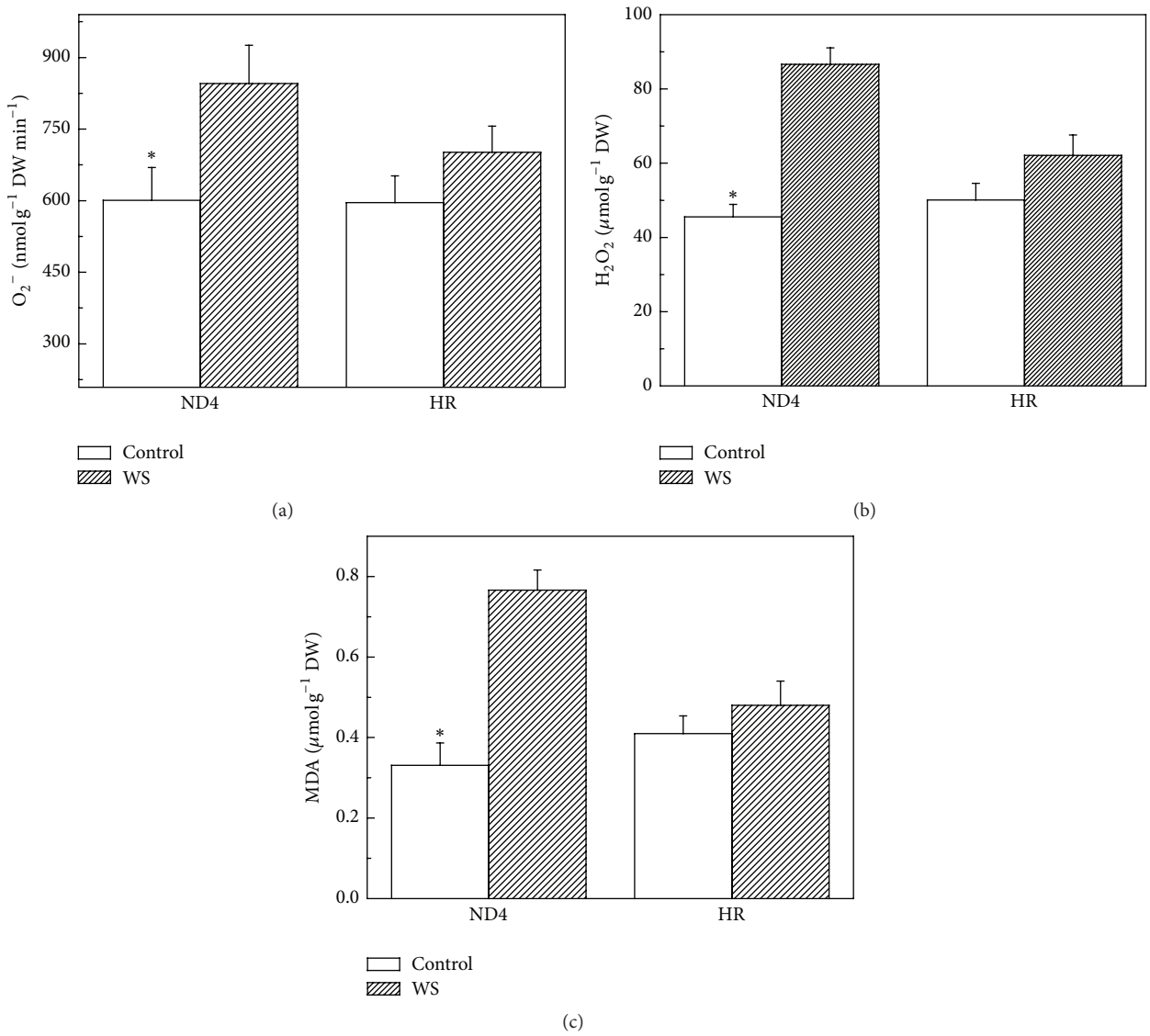

Figure 2: Effects of water stress (WS) on $O_2^{\bullet-}$ (a), H_2O_2 (b), and lipid peroxidation (expressed as malondialdehyde, MDA) (c) in *Cerasus humilis* leaves of Huai'rou (HR) and Nongda4 (ND4). Samples were collected after 21 d of treatment. The data shown are the mean of at least three replicates with standard errors shown by vertical bars. Asterisk (∗) indicates significant difference with control groups (well-watered) at the 0.05 level of probability by Duncan's Multiple-Range Test.

3.5. AsA and GSH Levels. As regards antioxidant contents, there were no significant differences in AsA contents between the two genotypes when grown under control conditions. However, WS induced higher AsA contents for HR (41%) than that for ND4 plants (12%). In comparison, WS had no measurable effect on GSH contents for both genotypes under either WS or control conditions (Figure 5).

3.6. cAPX and DHAR Transcript Levels. Furthermore, to examine the change in expression levels for some antioxidative enzymes in both *C. humilis* genotypes during WS, transcript levels of DHAR and cAPX genes were analysed by qRT-PCR in the same samples as used in the enzyme activity analysis. A sharp increase in transcript level of DHAR and cAPX was observed for HR plants under WS-period. However, for ND4, there were no changes in DHAR and cAPX expressions between treated and control seedlings (Figures 6(a) and 6(b)).

4. Discussion

Water stress is considered a detrimental factor for the production of crops worldwide. Thus, it is imperative to identify genetic resources tolerant to drought stress in an effort to stabilize agricultural production [2]. The present study was carried out to elucidate the physiological mechanism of two *C. humilis* genotypes by comparatively examining growth parameters, the $O_2^{\bullet-}$ and H_2O_2 concentrations, the level of lipid peroxidation, ROS metabolism, and gene expression responses.

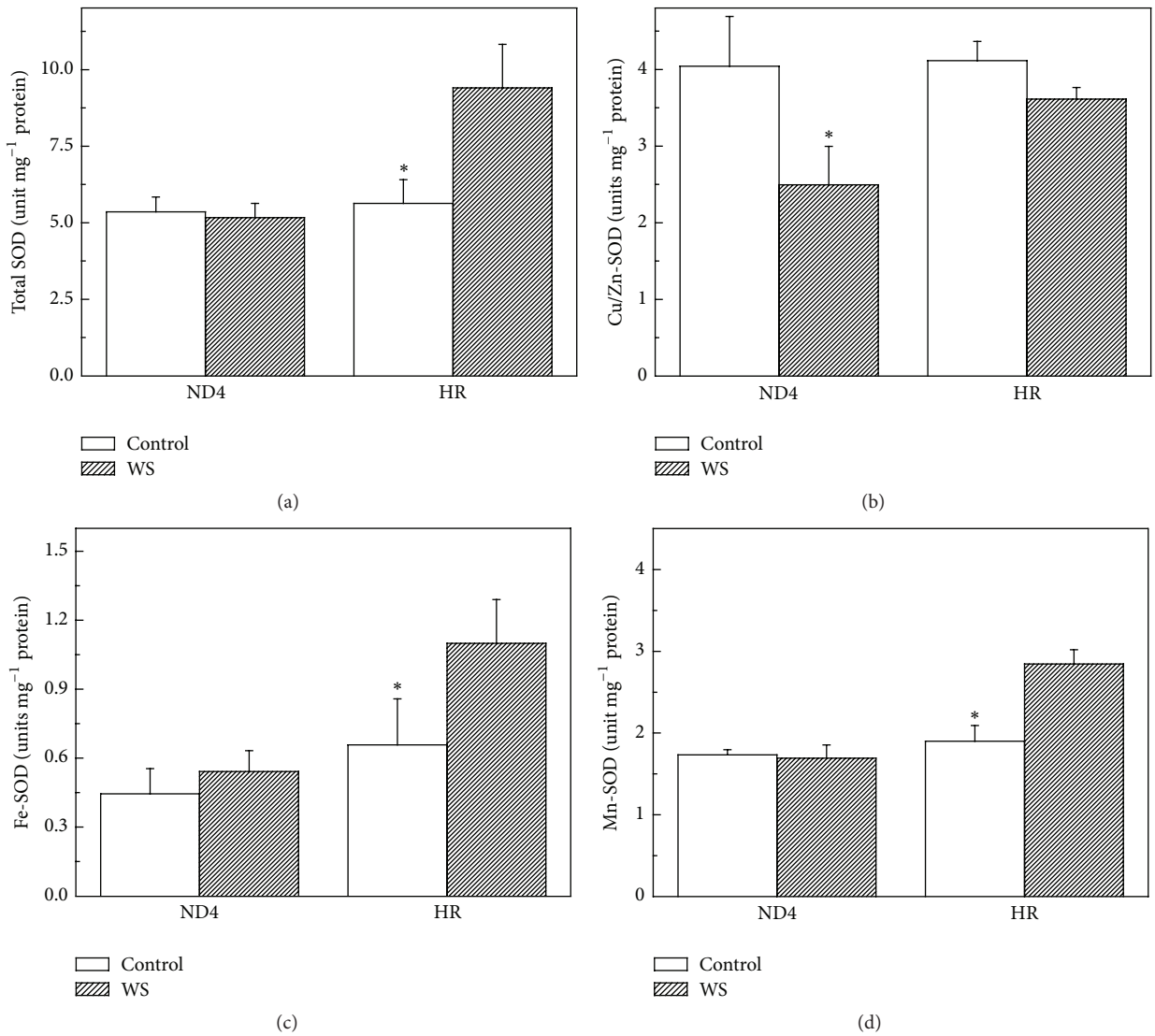

Figure 3: Effects of water stress (WS) on the activities of total SOD (a) and SOD isoenzymes including Cu/Zn-SOD (b), Fe-SOD (c), and Mn-SOD (d) in *Cerasus humilis* leaves of Huai'rou (HR) and Nongda4 (ND4). Samples were collected after 21 d of treatment. The data shown are the mean of at least three replicates with standard errors shown by vertical bars. Asterisk (∗) indicates significant difference with control groups (well-watered) at the 0.05 level of probability by Duncan's Multiple-Range Test.

In the present study, HR plants exhibited a higher relative growth rate than ND4 plants after exposure to WS (Figure 1), indicating that HR is more drought-tolerant than ND4. HR appears to have acquired greater adaptation to water shortage compared to ND4. ND4 plants show a more significant accumulation of ROS (Figures 2(a) and 2(b)), indicating that the oxidative stress occurred. A relatively less increase of ROS in HR implied that antioxidative system was likely, at least in part, involved in balancing the ROS levels. As an indicator of membrane lipid peroxidation, the MDA content of tolerant genotype HR showed less elevation under WS than in ND4 plants (Figure 2(c)), suggesting that the recovery ability of the tolerant genotype was higher than the sensitive genotype. Under stress conditions, the level of MDA accumulation is different in plant genotypes with contrasting tolerance. The formed MDA is capable of reacting with free amino groups of proteins and phospholipid components and initiating the appearance of ethylene in membranes. This may lead to alterations of the properties of whole membrane and also of the individual cell components under stress [33, 34].

SOD is one of the key components of the cell protection system against oxidative stress. It is known that SOD has three different isoenzymes distributed between different organelles. Cu/Zn-SOD is mostly located in chloroplasts, cytosol, and peroxisomes, while Fe-SOD and Mn-SOD are found mostly in chloroplasts and mitochondria, respectively [11]. As several isoforms of SOD differently contributing to the total activity of the enzyme are present in *C. humilis* leaves, it was important to assess the contribution of each isoform to the total activity of the enzyme under drought. Our

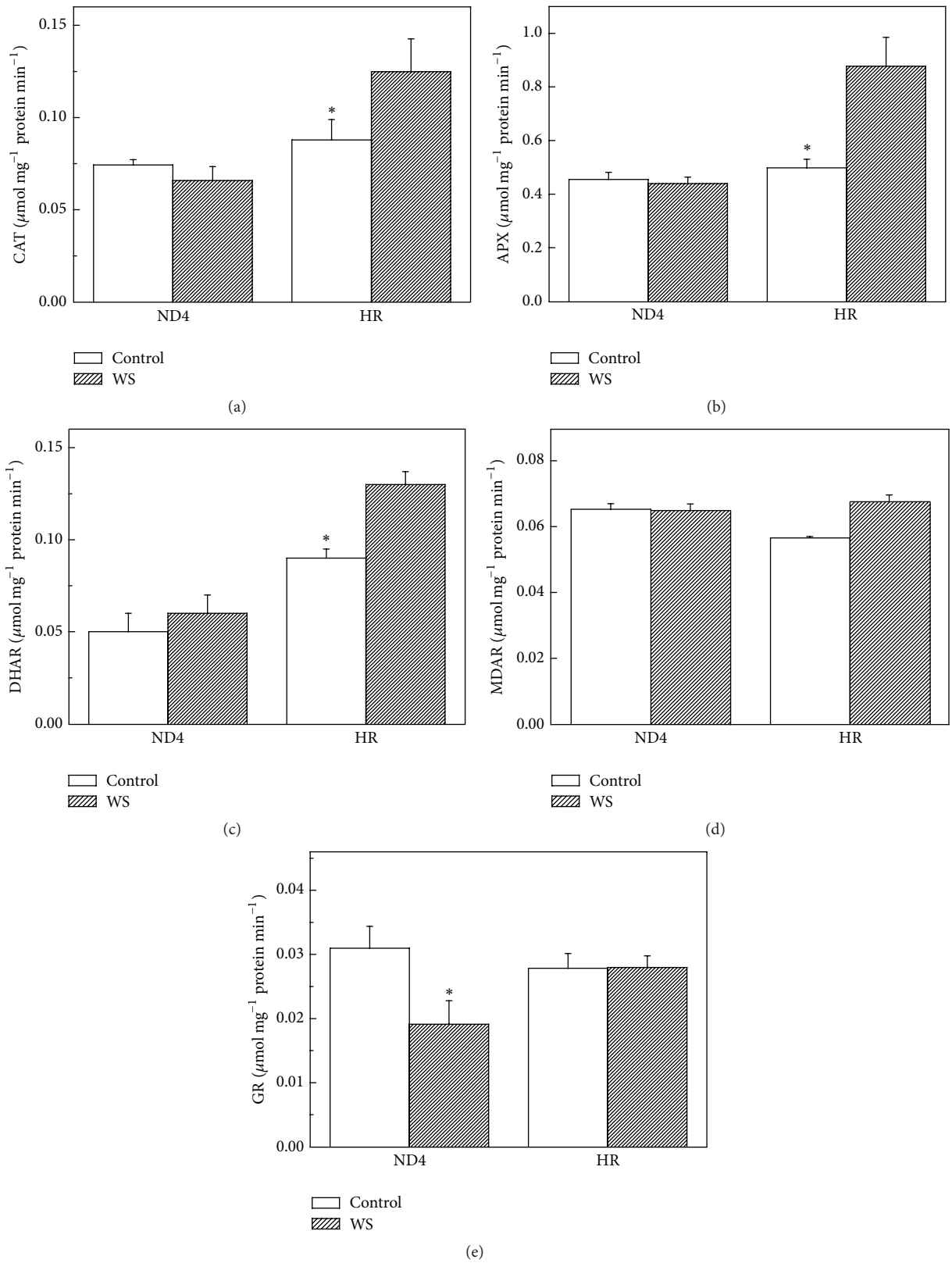

Figure 4: Effects of water stress (WS) on the activities of catalase (CAT) (a) and ascorbate-glutathione (AsA-GSH) cycle enzymes including ascorbate peroxidase (APX) (b), dehydroascorbate reductase (DHAR) (c), monodehydroascorbate reductase (MDAR) (d), and glutathione reductase (GR) (e) in *Cerasus humilis* leaves of Huai'rou (HR) and Nongda4 (ND4). Samples were collected after 21 d of treatment. The data are the mean of at least three replicates with standard errors shown by vertical bars. Asterisk (∗) indicates significant difference with control groups (well-watered) at the 0.05 level of probability by Duncan's Multiple-Range Test.

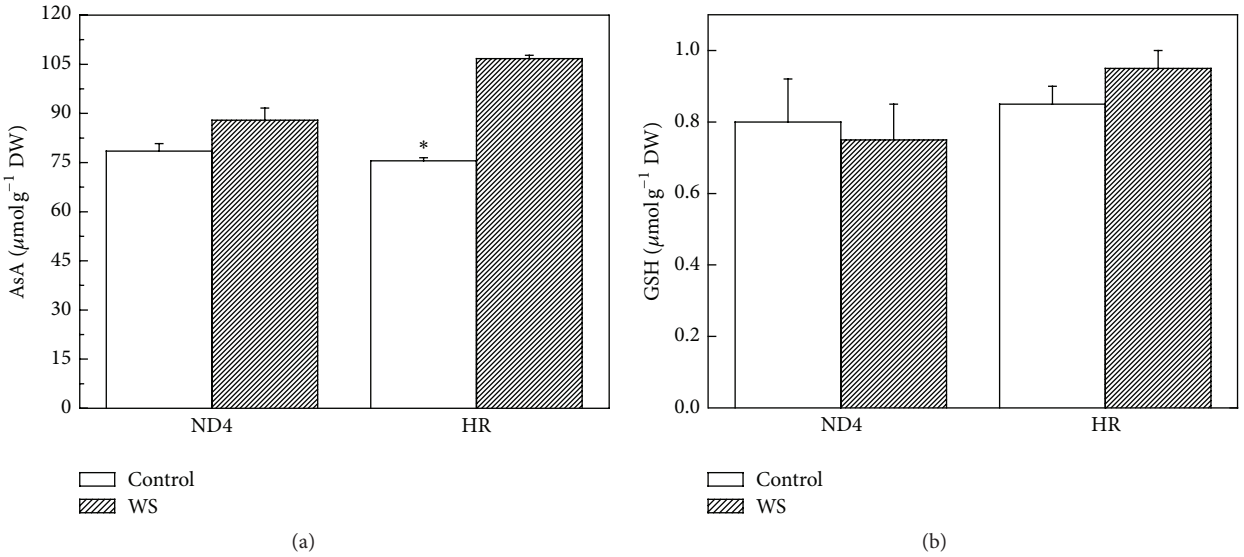

Figure 5: Effect of water stress (WS) on ascorbate (AsA) (a) and glutathione (GSH) (b) contents in *Cerasus humilis* leaves of Huai'rou (HR) and Nongda4 (ND4). Samples were collected after 21 d of treatment. The data are the mean of at least three replicates with standard errors shown by vertical bars. Asterisk (∗) indicates significant difference with control groups (well-watered) at the 0.05 level of probability by Duncan's Multiple-Range Test.

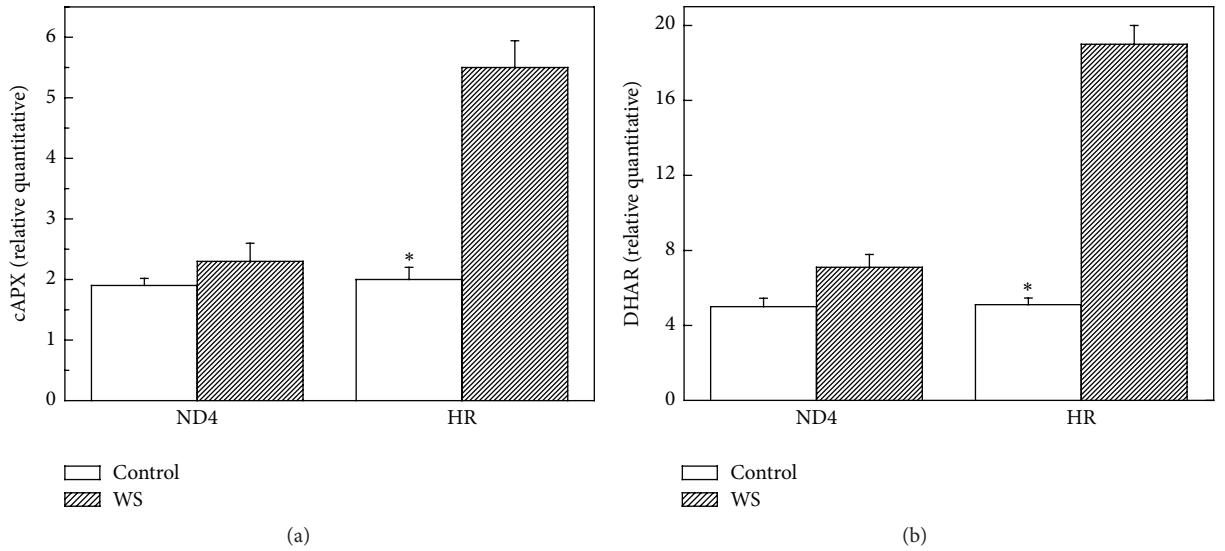

Figure 6: Effects of water stress (WS) on expression pattern of cytosol APX (cAPX) (a) and dehydroascorbate reductase (DHAR) (b) in *Cerasus humilis* leaves of Huai'rou (HR) and Nongda4 (ND4) by qRT-PCR. Data are the means of at least five replicates with standard errors shown by vertical bars. Asterisk (∗) indicates significant difference with control groups (well-watered) at the 0.05 level of probability by Duncan's Multiple-Range Test.

results on SOD isoenzyme activities (Figure 3) suggested that Fe-SOD and Mn-SOD could play the main role in detoxification of superoxide radicals in chloroplasts and mitochondria. Similar report has been shown in wheat varieties subjected to continuous soil drought [34]. Indirect evidence has been reported by Zhang et al. who found that overexpression of *Tamarix albiflonum TaMnSOD* increases drought tolerance in transgenic cotton [35]. The decrease of Cu/Zn-SOD activity for ND4 plants exposed to WS (Figure 3(b)) was likely attributed to the influence of H_2O_2. Similar results have been reported by Smirnoff [36].

CAT and APX in the AsA-GSH cycle enzymes are responsible for the decomposition of H_2O_2 generated by SOD in different cellular organelles. We found that the activity of CAT and APX showed similar patterns of change to that observed for SOD activity in HR plants (Figures 4(a) and 4(b)), suggesting that CAT and APX work in a coordinated manner to scavenge H_2O_2. The maintenance of CAT activity in leaves

of drought-stressed plants likely allowed the removal of photorespiratory H_2O_2 produced when plants are subjected to water deficit, especially under severe degrees of stress [37]. An analysis of the recent literature pointed out that an increase in CAT activity is generally positively related to the degree of drought experienced by plants [38–40] and that APX plays a positive key role in drought stress responses and following recovery from drought [38, 41, 42].

DHAR activity was increased significantly for HR plants exposed to WS (Figure 4(c)), indicating that DHAR is responsible for AsA regeneration in plant tissues. The results, along with the increased expressions of DHAR and cAPX (Figure 6), suggested that the two antioxidant enzymes were regulated in the transcript levels. In sharp contrast with the changes in SOD, APX, and DHAR activity, GR activity decreased in ND4 plants after the exposure to WS (Figure 4(e)). This decrease could be attributed to reduced NADPH availability since stress usually results in a decrease in the supply of reductants such as ATP and NADPH. It is also possible that ROS accumulation resulted in the inhibition of enzymes involved in the ROS-scavenging system [43]. Furthermore, our results also found that WS induced greater increases in AsA level in HR plants (Figure 5(a)), implying that it was likely involved in the operation of the ROS detoxification machinery assumed by APX/GSH cycle [44, 45].

In a brief conclusion, our findings demonstrate that the oxidative stress is differentially expressed in ND4 and HR in response to drought stress, with higher tolerance exhibited by the latter.

Conflict of Interests

The authors declare no conflict of interests regarding the publication of this paper.

Acknowledgments

This work was supported by Fundamental Research Funds for the Central Universities (2572015DA02, 2572014EA04), the National Natural Science Foundation of China (30800876, 31170569, and J1210053), and Scientific Research Foundation of Northeast Agricultural University.

References

[1] M. H. Cruz De Carvalho, "Drought stress and reactive oxygen species: production, scavenging and signaling," *Plant Signaling & Behavior*, vol. 3, no. 3, pp. 156–165, 2008.

[2] M. Zhang, Z.-Q. Jin, J. Zhao, G. Zhang, and F. Wu, "Physiological and biochemical responses to drought stress in cultivated and Tibetan wild barley," *Plant Growth Regulation*, vol. 75, pp. 567–574, 2015.

[3] R. W. Gesch, I.-H. Kang, M. Gallo-Meagher et al., "Rubisco expression in rice leaves is related to genotypic variation of photosynthesis under elevated growth CO_2 and temperature," *Plant, Cell and Environment*, vol. 26, no. 12, pp. 1941–1950, 2003.

[4] J. Dat, S. Vandenabeele, E. Vranová, M. Van Montagu, D. Inzé, and F. Van Breusegem, "Dual action of the active oxygen species during plant stress responses," *Cellular and Molecular Life Sciences*, vol. 57, no. 5, pp. 779–795, 2000.

[5] R. Mittler, "Oxidative stress, antioxidants and stress tolerance," *Trends in Plant Science*, vol. 7, no. 9, pp. 405–410, 2002.

[6] E. Vranová, D. Inzé, and F. Van Breusegem, "Signal transduction during oxidative stress," *Journal of Experimental Botany*, vol. 53, no. 372, pp. 1227–1236, 2002.

[7] A. Grover, M. Agarwal, S. K. Agarwal, C. Sahi, and S. Agarwal, "Production of high temperature tolerant transgenic plants through manipulation of membrane lipids," *Current Science*, vol. 79, pp. 557–559, 2000.

[8] K. Asada, "The water-water cycle in chloroplasts: scavenging of active oxygens and dissipation of excess photons," *Annual Review of Plant Biology*, vol. 50, pp. 601–639, 1999.

[9] K. Apel and H. Hirt, "Reactive oxygen species: metabolism, oxidative stress, and signal transduction," *Annual Review of Plant Biology*, vol. 55, pp. 373–399, 2004.

[10] K. Kaur, N. Kaur, A. K. Gupta, and I. Singh, "Exploration of the antioxidative defense system to characterize chickpea genotypes showing differential response towards water deficit conditions," *Plant Growth Regulation*, vol. 70, no. 1, pp. 49–60, 2013.

[11] R. G. Alscher, N. Erturk, and L. S. Heath, "Role of superoxide dismutases (SODs) in controlling oxidative stress in plants," *Journal of Experimental Botany*, vol. 53, no. 372, pp. 1331–1341, 2002.

[12] R. K. Sairam and G. C. Srivastava, "Changes in antioxidant activity in sub-cellular fractions of tolerant and susceptible wheat genotypes in response to long term salt stress," *Plant Science*, vol. 162, no. 6, pp. 897–904, 2002.

[13] M. Tausz, H. Šircelj, and D. Grill, "The glutathione system as a stress marker in plant ecophysiology: Is a stress-response concept valid?" *Journal of Experimental Botany*, vol. 55, no. 404, pp. 1955–1962, 2004.

[14] A. Sofo, N. Cicco, M. Paraggio, and A. Scopa, "Regulation of the ascorbate–glutathione cycle in plants under drought stress," in *Ascorbate–Glutathione Pathway and Stress Tolerance in Plants*, N. A. Anjum, M.-T. Chan, and S. Umar, Eds., pp. 137–189, Springer, Amsterdam, The Netherlands, 2010.

[15] A. Wujeska, G. Bossinger, and M. Tausz, "Responses of foliar antioxidative and photoprotective defence systems of trees to drought: a meta-analysis," *Tree Physiology*, vol. 33, no. 10, pp. 1018–1029, 2013.

[16] X. S. Song, Z. W. Shang, Z. P. Yin, J. Ren, M. C. Sun, and X. L. Ma, "Mechanism of xanthophyll-cycle-mediated photoprotection in *Cerasus humilis* seedlings under water stress and subsequent recovery," *Photosynthetica*, vol. 49, no. 4, pp. 523–530, 2011.

[17] Z. P. Yin, Z. W. Shang, C. Wei, J. Ren, and X. S. Song, "Foliar sprays of photosynthetic bacteria improve the growth and antioxidative capability on chinese dwarf cherry seedlings," *Journal of Plant Nutrition*, vol. 35, no. 6, pp. 840–853, 2012.

[18] R. Hunt, D. R. Causton, B. Shipley, and A. P. Askew, "A modern tool for classical plant growth analysis," *Annals of Botany*, vol. 90, no. 4, pp. 485–488, 2002.

[19] E. F. Elstner and A. Heupel, "Inhibition of nitrite formation from hydroxylammoniumchloride: a simple assay for superoxide dismutase," *Analytical Biochemistry*, vol. 70, no. 2, pp. 616–620, 1976.

[20] W. M. MacNevin and P. F. Urone, "Separation of hydrogen peroxide from organic hydroperoxides," *Analytical Chemistry*, vol. 25, no. 11, pp. 1760–1761, 1953.

[21] R. L. Heath and L. Packer, "Photoperoxidation in isolated chloroplasts: I. Kinetics and stoichiometry of fatty acid peroxidation," *Archives of Biochemistry and Biophysics*, vol. 125, no. 1, pp. 189–198, 1968.

[22] Q. Yu and Z. Rengel, "Micronutrient deficiency influences plant growth and activities of superoxide dismutases in narrow-leafed lupins," *Annals of Botany*, vol. 83, no. 2, pp. 175–182, 1999.

[23] C. N. Giannopolitis and S. K. Ries, "Superoxide dismutases-occurrence in higher plants," *Plant Physiology*, vol. 59, no. 2, pp. 309–314, 1977.

[24] Q. Yu, L. D. Osborne, and Z. Rengel, "Micronutrient deficiency changes activities of superoxide dismutase and ascorbate peroxidase in tobacco plants," *Journal of Plant Nutrition*, vol. 21, no. 7, pp. 1427–1437, 1998.

[25] G.-X. Chen and K. Asada, "Ascorbate peroxidase in tea leaves: occurrence of two isozymes and the differences in their enzymatic and molecular properties," *Plant and Cell Physiology*, vol. 30, no. 7, pp. 987–998, 1989.

[26] A. Jiménez, J. A. Hernández, L. A. del Río, and F. Sevilla, "Evidence for the presence of the ascorbate-glutathione cycle in mitochondria and peroxisomes of pea leaves," *Plant Physiology*, vol. 114, no. 1, pp. 275–284, 1997.

[27] O. Arrigoni, S. Dipierro, and G. Borraccino, "Ascorbate free radical reductase: a key enzyme of the ascorbic acid system," *FEBS Letters*, vol. 125, no. 2, pp. 242–244, 1981.

[28] D. A. Dalton, S. A. Russell, F. J. Hanus, G. A. Pascoe, and H. J. Evans, "Enzymatic reactions of ascorbate and glutathione that prevent peroxide damage in soybean root nodules," *Proceedings of the National Academy of Sciences of the United States of America*, vol. 83, no. 11, pp. 3811–3815, 1986.

[29] N. R. Madamanchi and R. G. Alscher, "Metabolic bases for differences in sensitivity of two pea cultivars to sulfur dioxide," *Plant Physiology*, vol. 97, no. 1, pp. 88–93, 1991.

[30] I. Cakmak and H. Marschner, "Magnesium deficiency and high light intensity enhance activities of superoxide dismutase, ascorbate peroxidase, and glutathione reductase in bean leaves," *Plant Physiology*, vol. 98, no. 4, pp. 1222–1227, 1992.

[31] C. L. M. Sgherri, M. Maffei, and F. Navari-Izzo, "Antioxidative enzymes in wheat subjected to increasing water deficit and rewatering," *Journal of Plant Physiology*, vol. 157, no. 3, pp. 273–279, 2000.

[32] C. L. M. Sgherri and F. Navari-Izzo, "Sunflower seedlings subjected to increasing water deficit stress: oxidative stress and defence mechanisms," *Physiologia Plantarum*, vol. 93, no. 1, pp. 25–30, 1995.

[33] R. K. Sairam and D. C. Saxena, "Oxidative stress and antioxidants in wheat genotypes: possible mechanism of water stress tolerance," *Journal of Agronomy and Crop Science*, vol. 184, no. 1, pp. 55–61, 2000.

[34] I. M. Huseynova, D. R. Aliyeva, and J. A. Aliyev, "Subcellular localization and responses of superoxide dismutase isoforms in local wheat varieties subjected to continuous soil drought," *Plant Physiology and Biochemistry*, vol. 81, pp. 54–60, 2014.

[35] D.-Y. Zhang, H.-L. Yang, X.-S. Li, H.-Y. Li, and Y.-C. Wang, "Overexpression of *Tamarix albiflonum TaMnSOD* increases drought tolerance in transgenic cotton," *Molecular Breeding*, vol. 34, no. 1, pp. 1–11, 2014.

[36] N. Smirnoff, "The role of active oxygen in the response of plants to water deficit and desiccation," *New Phytologist*, vol. 125, no. 1, pp. 27–58, 1993.

[37] A. Sofo, A. Scopa, M. Nuzzaci, and A. Vitti, "Ascorbate peroxidase and catalase activities and their genetic regulation in plants subjected to drought and salinity stresses," *International Journal of Molecular Sciences*, vol. 16, no. 6, pp. 13561–13578, 2015.

[38] M. Faize, L. Burgos, L. Faize et al., "Involvement of cytosolic ascorbate peroxidase and Cu/Zn-superoxide dismutase for improved tolerance against drought stress," *Journal of Experimental Botany*, vol. 62, no. 8, pp. 2599–2613, 2011.

[39] R. Mittler, S. Vanderauwera, N. Suzuki et al., "ROS signaling: the new wave?" *Trends in Plant Science*, vol. 16, no. 6, pp. 300–309, 2011.

[40] C. Pinheiro and M. M. Chaves, "Photosynthesis and drought: can we make metabolic connections from available data?" *Journal of Experimental Botany*, vol. 62, no. 3, pp. 869–882, 2011.

[41] R. Mittler and B. A. Zilinskas, "Regulation of pea cytosolic ascorbate peroxidase and other antioxidant enzymes during the progression of drought stress and following recovery from drought," *Plant Journal*, vol. 5, no. 3, pp. 397–405, 1994.

[42] A. Fini, L. Guidi, F. Ferrini et al., "Drought stress has contrasting effects on antioxidant enzymes activity and phenylpropanoid biosynthesis in *Fraxinus ornus* leaves: an excess light stress affair?" *Journal of Plant Physiology*, vol. 169, no. 10, pp. 929–939, 2012.

[43] S. M. Choi, S. W. Jeong, W. J. Jeong, S. Y. Kwon, W. S. Chow, and Y.-I. Park, "Chloroplast Cu/Zn-superoxide dismutase is a highly sensitive site in cucumber leaves chilled in the light," *Planta*, vol. 216, no. 2, pp. 315–324, 2002.

[44] S.-Y. Kwon, S.-M. Choi, Y.-O. Ahn et al., "Enhanced stress-tolerance of transgenic tobacco plants expressing a human dehydroascorbate reductase gene," *Journal of Plant Physiology*, vol. 160, no. 4, pp. 347–353, 2003.

[45] S.-H. Yang, L.-J. Wang, and S.-H. Li, "Ultraviolet-B irradiation-induced freezing tolerance in relation to antioxidant system in winter wheat (*Triticum aestivum* L.) leaves," *Environmental and Experimental Botany*, vol. 60, no. 3, pp. 300–307, 2007.

Hindawi Publishing Corporation
BioMed Research International
Volume 2016, Article ID 9739505, 9 pages
http://dx.doi.org/10.1155/2016/9739505

Research Article

Genome-Wide Transcriptome Analysis of Cadmium Stress in Rice

Youko Oono, Takayuki Yazawa, Hiroyuki Kanamori, Harumi Sasaki, Satomi Mori, Hirokazu Handa, and Takashi Matsumoto

Agrogenomics Research Center, National Institute of Agrobiological Sciences, Tsukuba, Ibaraki 305-8602, Japan

Correspondence should be addressed to Youko Oono; yoono@affrc.go.jp

Received 26 November 2015; Revised 26 January 2016; Accepted 28 January 2016

Academic Editor: Yan-Bo Hu

Rice growth is severely affected by toxic concentrations of the nonessential heavy metal cadmium (Cd). To elucidate the molecular basis of the response to Cd stress, we performed mRNA sequencing of rice following our previous study on exposure to high concentrations of Cd (Oono et al., 2014). In this study, rice plants were hydroponically treated with low concentrations of Cd and approximately 211 million sequence reads were mapped onto the IRGSP-1.0 reference rice genome sequence. Many genes, including some identified under high Cd concentration exposure in our previous study, were found to be responsive to low Cd exposure, with an average of about 11,000 transcripts from each condition. However, genes expressed constitutively across the developmental course responded only slightly to low Cd concentrations, in contrast to their clear response to high Cd concentration, which causes fatal damage to rice seedlings according to phenotypic changes. The expression of metal ion transporter genes tended to correlate with Cd concentration, suggesting the potential of the RNA-Seq strategy to reveal novel Cd-responsive transporters by analyzing gene expression under different Cd concentrations. This study could help to develop novel strategies for improving tolerance to Cd exposure in rice and other cereal crops.

1. Introduction

Cadmium (Cd) is a widespread heavy metal pollutant that is highly toxic to living cells. Accumulation of the nonessential metal Cd in plants is a major agricultural problem. Specifically, Cd is absorbed by the roots from the soil and transported to the shoot, negatively affecting nutrient uptake and homeostasis in plants, even in very small amounts. Many agricultural soils have become contaminated with Cd through the use of phosphate fertilizers, sludge, and irrigation water containing Cd. Cd exposure inhibits root and shoot growth and ultimately reduces yield. Furthermore, Cd accumulation in the edible parts of plants such as seed grains places humans at a risk because of its highly toxic effects on human health. Reducing the Cd concentration in plants below the maximum level indicated by the Codex Alimentarius Commission of FAO/WHO [1] is necessary to avoid negative impacts on human health. Thus, it is important to study the mechanisms of plant responses and defenses to Cd exposure to overcome this problem.

Cd causes oxidative stress and generates reactive oxygen species, which can cause damage in various ways such as reacting with DNA causing mutation, modifying protein side chains, and destroying phospholipids [2]. Various biochemical and physiological processes associated with defense systems are active in plants under Cd exposure. Many genes such as glutathione S-transferase (GST) for detoxification and cysteine-rich metallothioneins (MT) for defense against Cd toxicity respond to Cd stress in plants and might confer Cd tolerance in rice. Transporters with heavy metal binding domains are key factors for root uptake of Cd from soil and efflux pumping of Cd at the plasma membrane; however, the manner in which these genes respond to low Cd concentrations has not been well investigated in rice.

In a previous study, we investigated the gene expression of rice plants (*Oryza sativa* L. cv. Nipponbare) under a high Cd concentration using the RNA-Seq platform. A clear and detailed view of the transcriptomic changes triggered by Cd exposure is important to understand the gene expression network of the basal response to Cd stress. This could not be

obtained from past studies using the microarray platform, but RNA-Seq can accurately quantify gene expression levels over a broad dynamic range with high resolution and sensitivity [3]. We found that drought stress signaling pathways were activated under Cd exposure through the responses of many drought-related genes [4]. Thus, the recently elucidated scaffolding mechanisms for Cd signaling pathways are complex but of great importance. In this study, we performed rice transcriptome analysis under different low Cd concentrations using the RNA-Seq platform to deepen our understanding of Cd responses.

2. Materials and Methods

2.1. Sample Preparation. Rice (*Oryza sativa* ssp. *japonica* cv. Nipponbare) seeds were germinated and grown by hydroponic culture in Yoshida's solution [1.425 mM NH_4NO_3, 0.323 mM NaH_2PO_4, 0.513 mM K_2SO_4, 0.998 mM $CaCl_2$, 1.643 mM $MgSO_4$, 0.009 mM $MnCl_2$, 0.075 mM $(NH_4)_6Mo_7O_{24}$, 0.019 mM H_3BO_3, 0.155 mM $CuSO_4$, 0.036 mM $FeCl_3$, 0.070 mM citric acid, and 0.152 mM $ZnSO_4$] [5]. After 10 days, seedlings of uniform size and growth were subjected to Cd stress treatment by transferring them to a similar medium with 0.2, 1, or 50 μM Cd. These values were chosen based on a report that the total dissolved Cd in 64 fields with Cd-contaminated soils ranged from 0.03 to 182 μg/L [6] in previous experiences. The plants were maintained under Cd stress conditions for 14 d. Root and shoot samples were collected at approximately 9:00 AM, frozen in liquid nitrogen, and stored at −80°C until subsequent analyses. Total RNA was extracted from both root and shoot samples using an RNeasy Plant Kit (Qiagen, Hilden, Germany) according to the manufacturer's instructions. Construction of 34 cDNA libraries (2 tissues, 4 conditions, 2 treatments, and 2-3 replicates) from total RNA using a TruSeq RNA sample preparation kit and sequencing with the Illumina Genome Analyzer IIx (Illumina Inc., San Diego, CA, USA) was performed according to the manufacturer's protocols as a part of establishing TENOR (Transcriptome Encyclopedia of Rice, http://tenor.dna.affrc.go.jp/) [7]. The resulting RNA-Seq data were deposited in the DDBJ Sequence Read Archive (Accession number DRA000959).

2.2. Identification of Differentially Expressed Transcripts. The biological replicates (2-3) for each set of conditions were highly correlated (coefficient > 0.95), so reads from the same treatment were merged for subsequent analysis. Trimming of Illumina adaptor sequences and low-quality bases ($Q < 20$) by Cutadapt [8] and mapping of preprocessed reads to the IRGSP-1.0 genome assembly (http://rapdb.dna.affrc.go.jp/) were performed as described previously [9]. To estimate the expression levels of each transcript, all preprocessed reads were mapped to the IRGSP-1.0 genome assembly by Bowtie with default parameters [10]. The expression level for each transcript was calculated as the RPKM- (Reads per Kilobase Exon Model per million mapped reads-) derived read count [11] based on the number of uniquely mapped reads that overlapped with exonic regions. A G-test was performed to detect differentially expressed transcripts in the control and Cd treatments based on the statistical null hypothesis that the proportions of mapped reads to the transcripts were the same between the two conditions. A false discovery rate (FDR < 0.01) was used in multiple-hypothesis testing to correct for multiple comparisons. When calculating fold changes, 1 was added to avoid division by 0.

2.3. Hierarchical Clustering and Gene Ontology Enrichment Analysis. The Cd-responsive transcripts in root and shoot were used for hierarchical clustering analysis. We used the heatmap.2 in the R package gplots (version 2.11.0) to perform clustering analyses of transcripts. The Z scores were used to compare significant changes in gene expression. A Gene Ontology (GO) term was assigned to each transcript based on the GO annotations for biological process, molecular function, and cellular component in RAP-DB. GO enrichment was evaluated by Fisher's exact test with a FDR threshold of 5% for responsive transcripts in the biological process category of each cluster. The results were plotted as − log 10 of FDR values in a heatmap.

2.4. qRT-PCR Analysis. The expression of Cd upregulated genes in root sample was confirmed by qRT-PCR analysis. Rice seeds were germinated and grown in water in a growth chamber. After 10 days, the seedlings were subjected to different stress treatments by transferring them to water containing different reagents. RNA was extracted from them and the cDNA was synthesized according to the manufacturer's protocol and it is used for the further analysis as described previously [4]. The resulting cDNA was used for PCR amplification in the LightCycler 480 system (Roche, Basel, Switzerland) with each primer set (*Os04g0600300*: 5′-GGCGCTCTGAGAATCATCAC-3′, 5′-CATTCGGGAGCTCATCTCG-3′, *Os01g0692100*: 5′-ATTCACGAGTCCGCGATG-3′, 5′-CTCTCACCCGGATCACCC-3′, *Os12g0570700*: 5′-GCACTCATCTCAAGCTTTTC-3′, 5′-GCAAGACATCTTCTTGG-3′, *Os12g0571000*: 5′-ATTTCCTGAAGAGTTAAA-3′, 5′-TTCCGCAGCCGCAGCTTA-3′). The detection threshold cycle for each reaction was normalized using Ubiquitin1 primers (5′-CCAGGACAAGATGATCTGCC-3′, 5′-AAGAAGCTGAAGCATCCAGC-3′).

3. Results and Discussion

3.1. Low Cd Concentration Exposure of Rice Plants and Growth Retardation during the Treatment. We used rice plants grown in hydroponic culture, which enabled us to control the Cd exposure easily. High Cd concentration exposure has been previously shown to elicit robust physiological responses and gene expression as acute toxic responses in rice seedlings [12–14]. Growth retardation of the shoot was slightly visible after 1 d (data not shown), the leaves turned yellow and the leaf tips of the seedlings began to wilt after 4 d, and all leaf blades were curled completely and the seedlings were wilting after 10 d under high Cd concentration (50 μM) exposure (Figure 1). While no visible symptoms were observed in shoots under low Cd concentration exposure (0.2 and 1 μM Cd) after

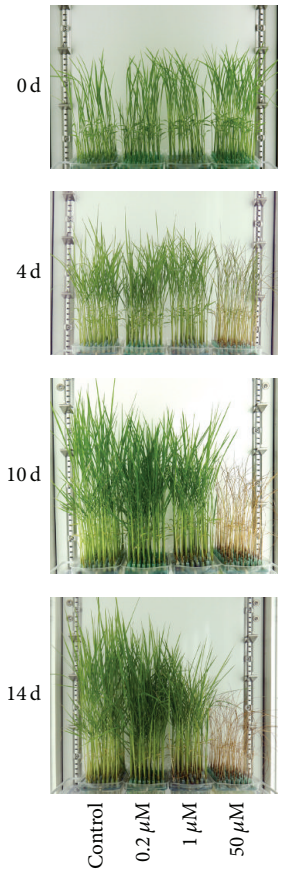

Figure 1: Phenotypic changes in rice plants grown in culture medium with low concentrations of Cd (0.2, 1 μM) and a high concentration of Cd (50 μM) from 0 to 14 d.

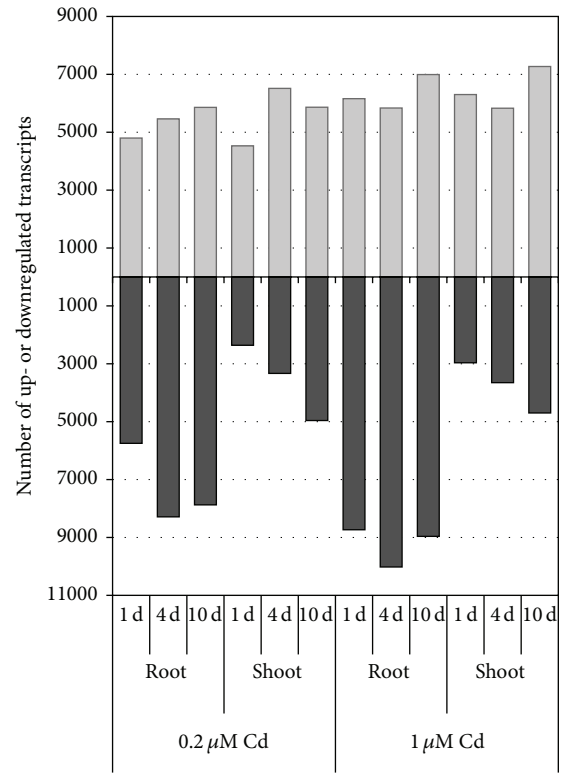

Figure 2: Distribution of upregulated and downregulated transcripts in roots and shoots in response to Cd exposure. RPKM fold changes at 1, 4, and 10 d were calculated for Cd-treated samples compared with nontreated samples (0 d). The total numbers of upregulated (upper) and downregulated (lower) transcripts in roots and shoots identified by RNA-Seq were determined by *G*-tests (FDR < 0.01) at each stress time point (1, 4, and 10 d) under 0.2 μM (left) and 1 μM (right) Cd exposure. The *x*-axis shows the time course and the *y*-axis shows the number of transcripts.

1 d, growth retardation occurred gradually compared with the control, with symptoms starting to appear after 7 d. Plants in the same growth chamber exposed to different Cd concentrations showed clear growth differences after 10 d (Figure 1). Even after 28 d, the seedlings under low Cd concentration exposure did not show yellow leaves or wilting (data not shown). These results suggested that high Cd concentration exposure causes fatal damage to plants while low Cd concentrations lead to growth retardation (Figure 1), which is supported by the fact that plant detoxification processes are insufficient to cope with this toxic metal beyond a 10 μM dose [15].

3.2. Gene Expression Profiles under Low Cd Concentration Exposure in Rice. We next analyzed the transcriptome profiles of the response to Cd exposure using RNA-Seq during plant growth, at 1, 4, and 10 d after Cd treatment, and before treatment (0 d). For each set of conditions, an average of approximately 15.1 million (92.2%) quality-evaluated reads (total 211 million) were mapped to the rice genome sequence and used for further analysis (Table S1 in Supplementary Material available online at http://dx.doi.org/10.1155/2016/9739505). The number of upregulated transcripts ranged from 4,529 to 6,515, whereas the number of downregulated transcripts ranged from 2,359 to 8,734 under 0.2 μM Cd (Figure 2). Twelve transcripts including GST, MT, and DREB (drought responsive element binding protein) 1E were upregulated more than 20-fold among the upregulated transcripts in roots at 0.2 μM Cd. The number of upregulated transcripts ranged from 5,830 to 7,271 whereas the number of downregulated transcripts ranged from 2,965 to 10,020 under 1 μM Cd (Figure 2). Fifty-one transcripts including GST, MT, Prx (peroxidase), and heat shock proteins were upregulated more than 20-fold among the upregulated transcripts in roots at 1 μM Cd (Table 1). Induction of detoxification enzymes against oxidation stress such as GST and Prx under Cd exposure might be associated with the defense system that confers Cd tolerance to plants [16–18] even at low Cd concentrations. The cysteine-rich MT might function as a ligand for chelation of metal ions to defend against Cd toxicity [19]. The DREB/C-repeat binding factor (CBF) specifically interacts with the DRE/CRT cis-acting element and controls the expression of many stress-inducible genes in plants [20]. The activation of gene expression in several drought stress signal pathways under Cd exposure has been reported [4]. Five *heat shock*

Table 1: Cadmium-upregulated transcripts identified in roots by RNA-Seq analysis.

Transcript	Description	Fold change					
		Root			Shoot		
		1 d	4 d	10 d	1 d	4 d	10 d
0.2 μM Cd							
Os10t0527400-01	Tau class GST protein 3	27.8	21.4	27.5	1.2	2.0	1.7
Os03t0283000-00	In2-1 protein	27.5	2.8	1.0	1.3	1.1	1.5
Os08t0156000-01	Conserved hypothetical protein	26.4	21.4	25.3	1.3	1.6	1.7
Os01t0627967-00	Hypothetical protein	26.1	16.5	24.1	1.5	1.9	1.4
Os04t0178300-02	Syn-copalyl diphosphate synthase	20.1	8.0	20.3	0.6	4.2	1.4
Os04t0301500-01	HLH (helix-loop-helix) DNA-binding domain containing protein	0.4	33.1	0.5	1.0	47.5	9.2
Os02t0676800-01	DREB1E (drought responsive element binding protein 1E)	0.9	28.7	0.9	1.2	10.9	2.0
Os02t0179200-01	Glutamine amidotransferase class-I domain containing protein	0.8	28.1	1.7	0.9	3.2	1.1
Os12t0154800-00	RmlC-like jelly roll fold domain containing protein	4.0	21.4	5.7	1.0	1.4	1.2
Os12t0570700-01	MT (metallothionein)-like protein type 1	18.6	20.3	15.8	0.9	1.0	0.9
Os03t0836800-01	IAA-amino acid hydrolase 1	4.3	6.5	33.6	1.0	1.0	1.0
Os10t0333700-00	Plant disease resistance response protein domain containing protein	9.7	6.0	21.6	1.0	1.0	1.0
1 μM Cd							
Os04t0178300-02	Syn-copalyl diphosphate synthase	122.0	32.1	25.5	0.5	1.0	3.6
Os04t0178300-01	Isoform 3 of Syn-copalyl diphosphate synthase	109.8	27.8	21.5	0.5	0.9	3.1
Os04t0178400-01	Cytochrome P450 CYP99A1	69.8	21.1	16.0	0.8	1.0	2.8
Os03t0267000-00	Heat shock protein 180	57.5	7.7	10.9	1.2	0.7	0.7
Os03t0266900-01	Heat shock protein 173	47.0	4.9	5.3	1.0	0.4	0.6
Os01t0136200-01	Heat shock protein 1	43.7	3.9	1.3	1.0	1.0	1.0
Os07t0190000-01	1-Deoxy-D-xylulose 5-phosphate synthase 2 precursor	42.4	11.5	8.6	0.7	1.1	3.9
Os07t0127500-01	PR-1a pathogenesis related protein precursor	40.0	5.6	5.0	0.8	0.8	2.1
Os07t0154100-01	Viviparous-14	38.8	5.2	1.5	1.1	1.4	2.3
Os07t0154201-00	Hypothetical gene	37.7	4.7	1.3	1.0	1.3	2.1
Os12t0555200-01	Probenazole-inducible protein PBZ1	37.7	13.5	10.9	0.3	0.5	2.2
Os06t0586000-01	Conserved hypothetical protein	37.6	9.3	6.5	0.6	0.9	1.4
Os10t0527400-01	Tau class GST protein 3	34.3	18.0	32.4	1.1	1.4	2.0
Os12t0555000-01	Probenazole-inducible protein PBZ1	33.2	13.5	11.0	0.6	0.7	2.5
Os03t0277700-01	Protein of unknown function DUF26 domain containing protein	32.8	7.6	3.4	1.0	0.6	1.0
Os11t0687100-01	von Willebrand factor (type A domain)	32.5	4.1	13.8	0.7	0.7	2.3
Os05t0211700-00	—	28.8	1.4	1.2	1.0	1.0	1.0
Os06t0662550-01	Conserved hypothetical protein	28.5	7.8	8.8	0.8	0.8	1.6
Os01t0944100-02	Conserved hypothetical protein	28.4	6.3	9.8	0.5	0.6	1.7
Os06t0568600-01	Ent-kaurene oxidase 1	27.1	28.1	11.0	0.6	1.4	4.7
Os12t0418600-01	Hypothetical conserved gene	26.7	2.0	1.3	1.0	1.0	1.0
Os12t0258700-01	Cupredoxin domain containing protein	26.2	14.7	10.6	0.7	1.1	7.1
Os01t0615100-01	Substilin/chymotrypsin-like inhibitor	25.6	9.5	7.9	0.7	1.0	1.8
Os04t0107900-02	Heat shock protein 81-1	25.6	2.5	1.6	1.0	1.0	0.9

Table 1: Continued.

Transcript	Description	Fold change					
		Root			Shoot		
		1 d	4 d	10 d	1 d	4 d	10 d
Os09t0493000-01	Conserved hypothetical protein	25.3	2.6	1.8	0.9	1.2	0.9
Os01t0627967-00	Hypothetical protein	25.3	19.5	21.6	1.3	1.8	1.4
Os01t0944100-03	Conserved hypothetical protein	25.2	4.6	6.3	0.6	0.6	1.8
Os04t0180400-01	Cytochrome P450 99A2	24.4	4.3	6.0	0.5	0.5	3.1
Os04t0108101-00	Hypothetical protein	24.4	2.3	1.4	1.0	1.0	1.0
Os02t0269600-00	Subtilase	22.6	7.8	4.1	0.3	1.2	6.0
Os01t0136000-00	Heat shock protein 175	22.5	3.1	1.2	1.0	1.4	1.2
Os04t0180500-00	Hypothetical protein	22.2	4.0	5.4	0.5	0.6	3.1
Os01t0946600-01	Conserved hypothetical protein	21.8	16.6	8.0	0.7	0.7	0.8
Os09t0255400-02	Indole-3-glycerol phosphate synthase	21.4	5.1	3.8	0.7	0.9	2.3
Os01t0348900-01	SalT gene product	21.2	6.5	8.9	0.1	0.1	0.2
Os12t0491800-01	Ent-kaurene synthase 1A	21.1	1.5	1.7	0.4	0.8	5.5
Os01t0132000-01	Wound-induced protease inhibitor	21.0	8.8	11.6	1.6	0.5	0.2
Os11t0592200-01	Chitin-binding allergen Bra r 2	20.7	3.4	2.8	0.7	0.5	1.6
Os01t0963000-01	Prx (Peroxidase) BP 1 precursor	20.6	3.8	4.4	0.7	1.1	1.3
Os08t0189600-01	Oryza sativa germin-like protein 8-7	20.6	11.5	6.7	2.1	1.5	0.8
Os07t0496250-01	Expansin-like B1	20.5	2.2	2.2	1.5	1.2	4.5
Os01t0963000-04	Prx (Peroxidase) BP 1 precursor	20.3	3.7	4.4	0.7	1.1	1.3
Os09t0255400-01	Indole-3-glycerol phosphate synthase	20.2	5.2	3.7	0.7	0.9	2.3
Os11t0601950-01	cDNA clone:002-114-B06	20.0	1.7	1.9	0.7	1.0	1.1
Os03t0129400-01	Hypothetical protein	10.3	27.1	17.6	1.0	1.9	3.6
Os01t0322700-01	Nonprotein coding transcript	12.2	25.5	15.7	0.9	1.3	2.5
Os03t0129400-02	EST AU078206 corresponds to a region of the predicted gene	9.4	24.3	16.3	1.1	1.4	2.8
Os12t0570700-01	MT (metallothionein)-like protein type 1	16.7	21.2	17.7	0.8	0.8	3.1
Os12t0571000-01	MT (metallothionein)-like protein type 1	13.9	20.0	13.0	0.9	1.0	3.6
Os08t0156000-01	Conserved hypothetical protein	15.4	17.9	26.0	1.1	1.5	1.6
Os03t0836800-01	IAA-amino acid hydrolase 1	0.7	4.0	23.7	1.0	1.0	1.0

Reads were mapped to the rice genome and responsive genes were identified by *G*-tests. Transcripts upregulated more than 20-fold in one or more treatments/time points in roots are shown. Transcripts in bold were upregulated under both 1 and 0.2 μM Cd exposure.

proteins (*Hsp*s) were strongly upregulated in roots under 1 μM Cd, with the greatest relative expression at 1 d (Table 1). These genes may contribute to cellular homeostasis by protecting macromolecules such as enzymes, protein complexes, and membranes under Cd exposure. This result suggested that the roots of hydroponically cultured rice might be affected more directly and earlier by Cd exposure. There was a difference between the low Cd concentrations in that no *Hsps* were strongly upregulated in roots at 0.2 μM Cd (Table 1), suggesting that the effect of this condition might be small or show time lag. In shoots, 15 and 11 transcripts were upregulated more than 20-fold among the upregulated transcripts under 0.2 and 1 μM Cd, respectively (Table S2). Nine transcripts including Nramp1 (natural resistance-associated macrophage protein) were upregulated under both 0.2 and 1 μM Cd (Table S2). In *Arabidopsis*, Nramp1 localizes to the plasma membrane and functions as a high-affinity transporter for manganese (Mn) uptake [21], while OsNramp5 uptakes Mn and Cd [22]. Transporters with heavy metal binding domains are often capable of transporting several metals, such as Fe, Zn, Mn, and Cd, because of their low substrate specificity [23–26]. We found that upregulation of a HLH DNA-binding domain containing transcription factor (*Os04g0301500*) in both roots and shoots peaked at 4 d under 0.2 μM Cd; this protein may function as a regulatory factor under Cd exposure (Table 1, Table S2). The number of downregulated transcripts in roots peaked at 4 d after Cd exposure, while the number in shoots gradually increased under low Cd concentration exposure (Figure 2). A few dozen transcripts were downregulated less than 0.05-fold among the downregulated transcripts in roots and shoots under Cd exposure (Table S2). Therefore, a small part of transcripts were strongly

up- or downregulated among several thousand responsive transcripts under low Cd concentration exposure. Large-scale changes in gene expression occurred in rice under Cd exposure, even at low concentrations, possibly because Cd is a nonessential metal for the plant.

To obtain a functional annotation of responsive transcripts under Cd exposure, we used GO biological process categories. The responsive transcripts in shoot and root were clustered into several groups based on their expression patterns. GO enrichment analysis was performed using clustered transcripts assigned by GO terms in RAP-DB (The Rice Annotation Project Database [http://rapdb.dna.affrc.go.jp/]) (Supplementary Figure S1). Enriched GO terms significantly in each cluster may represent the functional categories in rice under Cd exposure. Enriched GO terms of gradually upregulated transcripts under Cd exposure include metal ion transport (GO:0030001) (cluster 3 in root under 0.2 μM Cd, cluster 4 in root under 1 μM Cd), which may function in Cd transport. Response to oxidative stress (GO:0006979) and responsive to oxidative stress (GO:0006979) were also included in cluster 3 and cluster 4, respectively. This suggested that they might function in defense against Cd. Enriched GO terms of gradually downregulated transcripts under Cd exposure include translation (GO:0006412), translation elongation (GO:0006414), DNA replication (GO:0006260), and DNA repair (GO:0006281) (cluster 1 in root under 0.2 μM Cd, cluster 2 in root under 1 μM Cd). Photosynthesis, light harvesting (GO:0009765), and photosynthesis (GO:0015979) were also included in both clusters. These may function in plant growth. Thus, these correspond to the observed changes in phenotype (Figure 1), which clearly validated the RNA-Seq expression profiling data obtained from rice tissue under Cd stress condition. However, the pattern of gene expression is quite complex and would require more detailed analysis.

3.3. Constitutively Expressed Genes Responded Differently under Low Cd Concentration to High Cd Concentration. As many genes responded to both low and high Cd concentrations [4], we assessed the effect of the stress degree on rice seedlings through the expression of constitutively expressed genes. We investigated the expression of 18 genes annotated by the RAP that were expressed constitutively in 39 tissues collected throughout the life cycle of the rice plant from two varieties according to 190 Affymetrix GeneChip Rice Genome Arrays, in addition to four genes annotated by the RAP that have frequently been used as internal controls in expression analyses [27]. The results showed that the expression of more than half of them fluctuated drastically (>2 or <2) in roots or shoots after 1 d of high Cd concentration exposure (Figure 3). This drastic response may be partly because RNA-Seq can accurately quantify gene expression levels over a broad dynamic range with high resolution and sensitivity [10, 28, 29]. However, our results suggest that their expression is greatly affected by strong stress, even though they are expressed constitutively across the developmental course. Note that a high Cd concentration can cause fatal damage to rice seedlings, such as by affecting homeostasis, which corresponds to the observed changes in phenotype (Figures 1 and 3).

3.4. Comparative Gene Expression Analysis between Low and High Cd Concentrations Reveals Novel Cd-Responsive Transporters. We investigated the expression of metal transporter genes containing metal ion binding Pfam domains [PF01554 (MatE), PF08370 (PDR_assoc), PF01545 (Cation_efflux), PF02535 (Zip), PF00403 (HMA), and PF01566 (Nramp)] that may function in Cd transport under Cd exposure. The expression of 183 transport transcripts was compared between low and high Cd concentration treatments in roots and shoots at 1 d, because Cd uptake from the hydroponic culture and efflux pumping are initial responses to Cd exposure (Figure 4, Table S3). The transcripts tended to be more responsive in roots and shoots under higher Cd concentration exposure. This result indicated the potential of the RNA-Seq strategy to reveal novel Cd-responsive transporters by analyzing gene expression under exposure to different Cd concentrations. The responsive transcripts might function in roots at the early stage of Cd exposure. No transcripts were upregulated more than 3-fold in shoots under low Cd exposure (Figure 4, Table S3), suggesting that the effect takes more time to appear in shoots. *Os03g0667500* (Zip, root) encoding iron-regulated transporter 1 (IRT1) was upregulated more than 5-fold under low Cd concentrations but responded only slightly under the high Cd concentration. IRT1s often transport Cd because of their low substrate specificity [24–26, 30]. *Os02g0585200* (HMA, root), *Os03g0152000* (HMA, root), *Os0g0584800* (HMA, root), *Os01g0609900* (PDR_assoc, shoot), and *Os01g0609300* (PDR_assoc, shoot) showed the highest (32-fold) upregulation under high Cd concentration exposure and responded only slightly to low Cd concentrations (Table S3). The balance between Cd and various other metal ions in the hydroponic culture might affect the expression of these genes, because specific systems for transporting Cd may have not developed in rice as it is a nonessential metal. The effects of other ions on the expression of transporters [4] and responsive genes associated with defense systems against Cd (Supplementary Figure S2) have been indicated.

4. Conclusions

We generated gene expression profiles for rice seedlings grown under low Cd concentrations. Phenotypic observations and constitutive gene expression indicated that low Cd concentrations cause growth retardation but are far from being fatal in rice. Several genes associated with defense systems were strongly upregulated; the expression of metal ion transporter genes tended to correlate with Cd concentration and GO enrichment analysis of the clustered genes based on their expression patterns, suggesting that our transcriptome profiles reflect responses to Cd in rice. Our data also suggest that it could be dangerous to eat plants that do not show specific Cd pollution symptoms growing in soil contaminated by small amounts of Cd. Establishing the exact composition and organization of the transcriptional network underlying the response to Cd exposure will provide a robust tool for improving crops in the future, for example, by creating low Cd uptake plants.

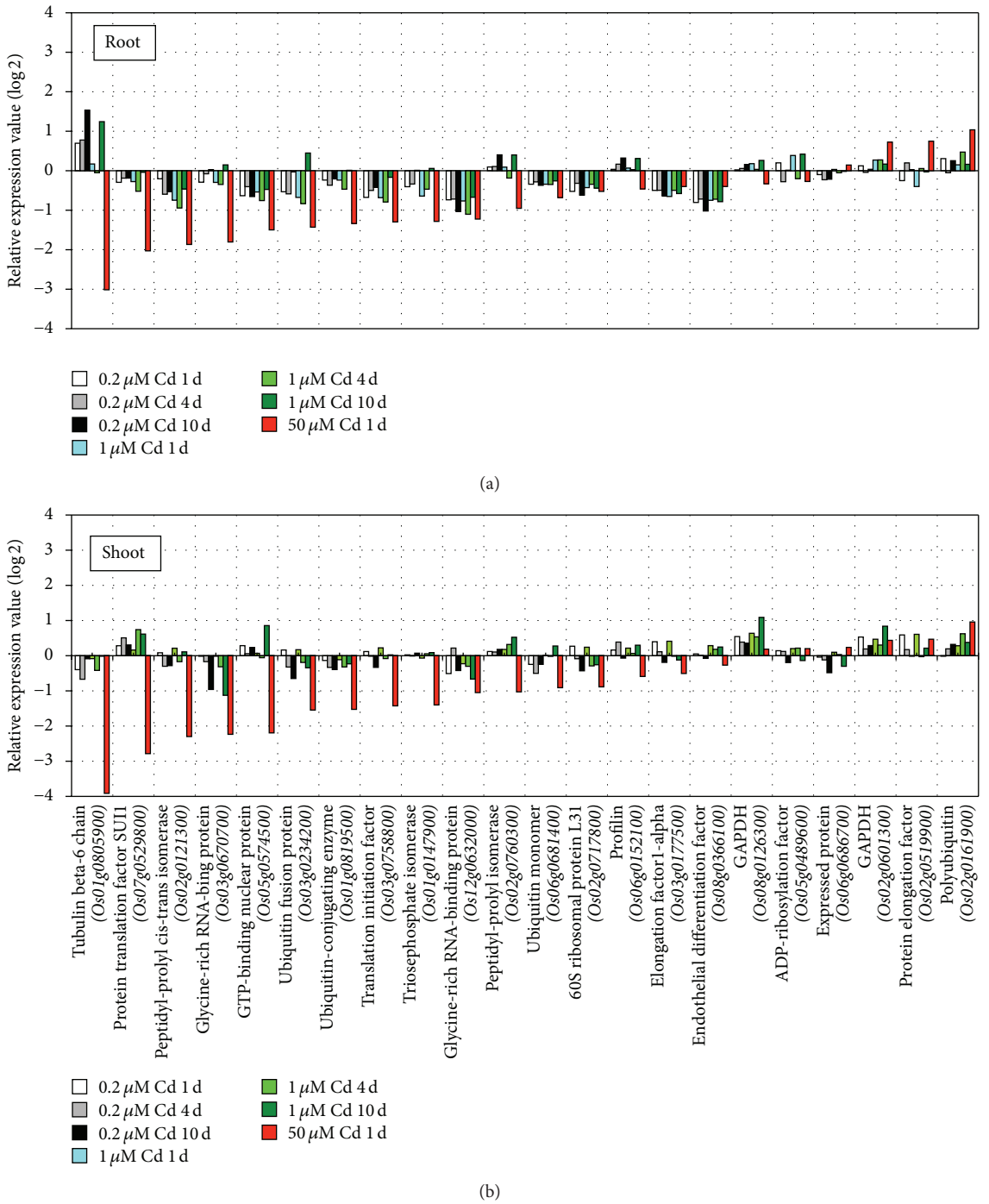

Figure 3: Response of constitutively expressed genes in roots and shoots to Cd exposure. The relative expression of constitutively expressed genes [27] in roots (a) and shoots (b) is shown under Cd exposure at each stress time point (1, 4, and 10 d) during 0.2 μM (white, grey, and black) and 1 μM (light blue, light green, and green) Cd exposure compared with nontreatment (0 d). The red bar shows the relative expression at 1 d under 50 μM Cd exposure. The x-axis shows the genes and the y-axis shows relative expression. Wang et al. [27] suggested the following genes as candidates for constitutive expression: glycine-rich RNA-binding protein (*Os12g0632000*), expressed protein (*Os06g0686700*), profilin (*Os06g0152100*), ADP-ribosylation factor (*Os05g0489600*), triosephosphate isomerase (*Os01g0147900*), glycine-rich RNA-binding protein (*Os03g0670700*), peptidyl-prolyl cis-trans isomerase (*Os02g0121300*), endothelial differentiation factor (*Os08g0366100*), ubiquitin monomer (*Os06g0681400*), protein translation factor SUI1 (*Os07g0529800*), GAPDH (*Os08g0126300*), polyubiquitin (*Os02g0161900*), protein elongation factor (*Os02g0519900*), translation initiation factor (*Os03g0758800*), ubiquitin-conjugating enzyme (*Os01g0819500*), GTP-binding nuclear protein (*Os05g0574500*), peptidyl-prolyl isomerase (*Os02g0760300*), and 60S ribosomal protein L31 (*Os02g0717800*). Their paper also introduced the following genes that have frequently been used as internal controls in expression analyses: elongation factor1-alpha (*Os03g0177500*), ubiquitin fusion protein (*Os03g0234200*), GAPDH (*Os02g0601300*), and tubulin beta-6 chain (*Os01g0805900*).

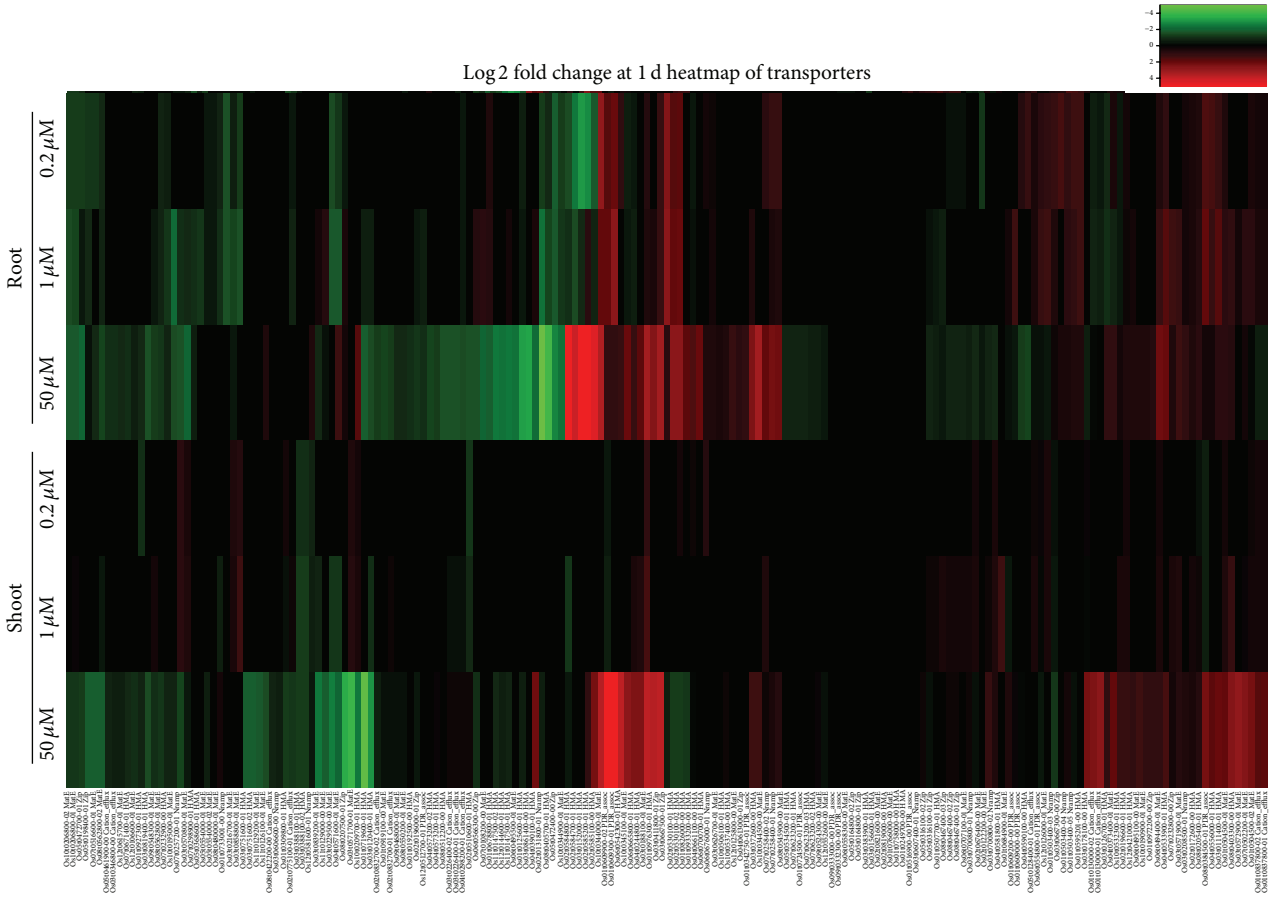

Figure 4: Expression profiling of metal ion transporter genes in roots and shoots under Cd exposure at 1 d demonstrates Cd concentration-dependent differences. Heatmap analysis of metal ion transporters containing Pfam domains [PF01554 (MatE), PF08370 (PDR_assoc), PF01545 (Cation_efflux), PF02535 (Zip), PF00403 (HMA), and PF01566 (Nramp)]. The relative expression values under 0.2, 1, and 50 μM Cd (data from [4]) are presented. The color scale shows log2-transformed transcript levels for each gene.

Conflict of Interests

The authors declare that there is no conflict of interests regarding the publication of this paper.

Authors' Contribution

Youko Oono and Takashi Matsumoto conceived and designed the experiments. Takashi Matsumoto performed sampling. Hiroyuki Kanamori, Harumi Sasaki, and Satomi Mori performed the experiments. Youko Oono, Takayuki Yazawa, and Hiroyuki Kanamori analyzed the data and contributed analysis tools. Youko Oono wrote the paper. Hirokazu Handa and Takashi Matsumoto contributed valuable insights into the discussion and revision of the paper. Youko Oono and Takayuki Yazawa contributed equally to this work.

Acknowledgments

The authors thank Ms. F. Aota, Ms. K. Ohtsu, and Ms. K. Yamada for technical assistance. This work was supported by a grant from the Ministry of Agriculture, Forestry and Fisheries of Japan (Genomics for Agricultural Innovation, RTR-0001).

References

[1] CODEX, "Report of the 38th session of the CODEX Committee on Food Additives and Contaminants," ALINORM 06/29/12, Codex Alimentarius Commission, 2006.

[2] B. Halliwell and J. M. C. Gutteridge, "Oxygen-toxicity, oxygen radicals, transition-metals and disease," *Biochemical Journal*, vol. 219, no. 1, pp. 1–14, 1984.

[3] Z. Wang, M. Gerstein, and M. Snyder, "RNA-Seq: a revolutionary tool for transcriptomics," *Nature Reviews Genetics*, vol. 10, no. 1, pp. 57–63, 2009.

[4] Y. Oono, T. Yazawa, Y. Kawahara et al., "Genome-wide transcriptome analysis reveals that cadmium stress signaling controls the expression of genes in drought stress signal pathways in rice," *PLoS ONE*, vol. 9, no. 5, Article ID e96946, 2014.

[5] S. Yoshida, D. A. Forno, J. H. Cock, and K. A. Gomez, *Laboratory Manual for Physiological Studies of Rice*, International Rice Research Institute, Manila, Philippines, 3rd edition, 1976.

[6] S. Sauve, W. A. Norvell, M. McBride, and W. Hendershot, "Speciation and complexation of cadmium in extracted soil solutions," *Environmental Science & Technology*, vol. 34, no. 2, pp. 291–296, 2000.

[7] Y. Kawahara, Y. Oono, H. Wakimoto et al., "TENOR: database for comprehensive mRNA-Seq experiments in rice," *Plant and Cell Physiology*, vol. 57, no. 1, article e7, 2016.

[8] M. Martin, "Cutadapt removes adapter sequences from high-throughput sequencing reads," *EMBnet Journal*, vol. 17, no. 1, pp. 10–12, 2011.

[9] Y. Oono, Y. Kawahara, H. Kanamori et al., "mRNA-seq reveals a comprehensive transcriptome profile of rice under phosphate stress," *Rice*, vol. 4, no. 2, pp. 50–65, 2011.

[10] H. Li and R. Durbin, "Fast and accurate short read alignment with Burrows-Wheeler transform," *Bioinformatics*, vol. 25, no. 14, pp. 1754–1760, 2009.

[11] A. Mortazavi, B. A. Williams, K. McCue, L. Schaeffer, and B. Wold, "Mapping and quantifying mammalian transcriptomes by RNA-Seq," *Nature Methods*, vol. 5, no. 7, pp. 621–628, 2008.

[12] M. Zhang, X. Liu, L. Yuan et al., "Transcriptional profiling in cadmium-treated rice seedling roots using suppressive subtractive hybridization," *Plant Physiology and Biochemistry*, vol. 50, no. 1, pp. 79–86, 2012.

[13] K. Lee, D. W. Bae, S. H. Kim et al., "Comparative proteomic analysis of the short-term responses of rice roots and leaves to cadmium," *The Journal of Plant Physiology*, vol. 167, no. 3, pp. 161–168, 2010.

[14] K. Shah, R. G. Kumar, S. Verma, and R. S. Dubey, "Effect of cadmium on lipid peroxidation, superoxide anion generation and activities of antioxidant enzymes in growing rice seedlings," *Plant Science*, vol. 161, no. 6, pp. 1135–1144, 2001.

[15] L. Perfus-Barbeoch, N. Leonhardt, A. Vavasseur, and C. Forestier, "Heavy metal toxicity: cadmium permeates through calcium channels and disturbs the plant water status," *Plant Journal*, vol. 32, no. 4, pp. 539–548, 2002.

[16] R. Mittler, S. Vanderauwera, N. Suzuki et al., "ROS signaling: the new wave?" *Trends in Plant Science*, vol. 16, no. 6, pp. 300–309, 2011.

[17] C. Frova, "The plant glutathione transferase gene family: genomic structure, functions, expression and evolution," *Physiologia Plantarum*, vol. 119, no. 4, pp. 469–479, 2003.

[18] C. Cosio and C. Dunand, "Specific functions of individual class III peroxidase genes," *Journal of Experimental Botany*, vol. 60, no. 2, pp. 391–408, 2009.

[19] C. Cobbett and P. Goldsbrough, "Phytochelatins and metallothioneins: roles in heavy metal detoxification and homeostasis," *Annual Review of Plant Biology*, vol. 53, pp. 159–182, 2002.

[20] K. Yamaguchi-Shinozaki and K. Shinozaki, "Transcriptional regulatory networks in cellular responses and tolerance to dehydration and cold stresses," *Annual Review of Plant Biology*, vol. 57, pp. 781–803, 2006.

[21] R. Cailliatte, A. Schikora, J.-F. Briat, S. Mari, and C. Curie, "High-affinity manganese uptake by the metal transporter NRAMP1 is essential for *Arabidopsis* growth in low manganese conditions," *Plant Cell*, vol. 22, no. 3, pp. 904–917, 2010.

[22] A. Sasaki, N. Yamaji, K. Yokosho, and J. F. Ma, "Nramp5 is a major transporter responsible for manganese and cadmium uptake in rice," *Plant Cell*, vol. 24, no. 5, pp. 2155–2167, 2012.

[23] N. Satoh-Nagasawa, M. Mori, N. Nakazawa et al., "Mutations in rice (*Oryza sativa*) heavy metal ATPase 2 (*OsHMA2*) restrict the translocation of zinc and cadmium," *Plant and Cell Physiology*, vol. 53, no. 1, pp. 213–224, 2012.

[24] Y. O. Korshunova, D. Eide, W. G. Clark, M. L. Guerinot, and H. B. Pakrasi, "The IRT1 protein from Arabidopsis thaliana is a metal transporter with a broad substrate range," *Plant Molecular Biology*, vol. 40, no. 1, pp. 37–44, 1999.

[25] N. E. Grossoehme, S. Akilesh, M. L. Guerinot, and D. E. Wilcox, "Metal-binding thermodynamics of the histidine-rich sequence from the metal-transport protein IRT1 of Arabidopsis thaliana," *Inorganic Chemistry*, vol. 45, no. 21, pp. 8500–8508, 2006.

[26] S. Lee and G. An, "Over-expression of OsIRT1 leads to increased iron and zinc accumulations in rice," *Plant, Cell and Environment*, vol. 32, no. 4, pp. 408–416, 2009.

[27] L. Wang, W. Xie, Y. Chen et al., "A dynamic gene expression atlas covering the entire life cycle of rice," *Plant Journal*, vol. 61, no. 5, pp. 752–766, 2010.

[28] G. M. He, X. P. Zhu, A. A. Elling et al., "Global epigenetic and transcriptional trends among two rice subspecies and their reciprocal hybrids," *Plant Cell*, vol. 22, no. 1, pp. 17–33, 2010.

[29] T. T. Lu, G. J. Lu, D. L. Fan et al., "Function annotation of the rice transcriptome at single-nucleotide resolution by RNA-seq," *Genome Research*, vol. 20, no. 9, pp. 1238–1249, 2010.

[30] P. Pedas, C. K. Ytting, A. T. Fuglsang, T. P. Jahn, J. K. Schjoerring, and S. Husted, "Manganese efficiency in Barley: identification and characterization of the metal ion transporter HvIRT1," *Plant Physiology*, vol. 148, no. 1, pp. 455–466, 2008.

Hindawi Publishing Corporation
BioMed Research International
Volume 2016, Article ID 1830262, 13 pages
http://dx.doi.org/10.1155/2016/1830262

Review Article

Plant Responses to High Frequency Electromagnetic Fields

Alain Vian,[1] Eric Davies,[2] Michel Gendraud,[3] and Pierre Bonnet[4,5]

[1] *Université d'Angers, Campus du Végétal, UMR 1345 IRHS, CS 60057, SFR 4207 QUASAV, 49071 Beaucouzé Cedex, France*
[2] *Department of Plant and Microbial Biology, North Carolina State University, P.O. Box 7612, Raleigh, NC 27695, USA*
[3] *Université Blaise Pascal, 24 avenue des Landais, 63177 Aubière Cedex, France*
[4] *Institut Pascal, Université Blaise Pascal, BP 10448, 63000 Clermont-Ferrand, France*
[5] *CNRS, UMR 6602, 63171 Aubière, France*

Correspondence should be addressed to Alain Vian; alain.vian@univ-angers.fr

Received 25 November 2015; Accepted 17 January 2016

Academic Editor: Yan-Bo Hu

High frequency nonionizing electromagnetic fields (HF-EMF) that are increasingly present in the environment constitute a genuine environmental stimulus able to evoke specific responses in plants that share many similarities with those observed after a stressful treatment. Plants constitute an outstanding model to study such interactions since their architecture (high surface area to volume ratio) optimizes their interaction with the environment. In the present review, after identifying the main exposure devices (transverse and gigahertz electromagnetic cells, wave guide, and mode stirred reverberating chamber) and general physics laws that govern EMF interactions with plants, we illustrate some of the observed responses after exposure to HF-EMF at the cellular, molecular, and whole plant scale. Indeed, numerous metabolic activities (reactive oxygen species metabolism, α- and β-amylase, Krebs cycle, pentose phosphate pathway, chlorophyll content, terpene emission, etc.) are modified, gene expression altered (calmodulin, calcium-dependent protein kinase, and proteinase inhibitor), and growth reduced (stem elongation and dry weight) after low power (i.e., nonthermal) HF-EMF exposure. These changes occur not only in the tissues directly exposed but also systemically in distant tissues. While the long-term impact of these metabolic changes remains largely unknown, we propose to consider nonionizing HF-EMF radiation as a noninjurious, genuine environmental factor that readily evokes changes in plant metabolism.

1. Introduction

High frequency electromagnetic fields (HF-EMF, i.e., frequencies from 300 MHz to 3 GHz, wavelengths from 1 m to 10 cm) are mainly human-produced, nonionizing electromagnetic radiations that do not naturally occur in the environment, excluding the low amplitude VHF (very high frequency) cosmic radiation. HF-EMF are increasingly present in the environment [1] because of the active development of wireless technology, including cell phones, Wi-Fi, and various kinds of connected devices. Since living material is not a perfect dielectric, it readily interferes with HF-EMF in a way that depends upon several parameters, including (but not restricted to) its general shape, the conductivity and density of the tissue, and the frequency and amplitude of the EMF. The interaction between the living material and the electromagnetic radiation may (or not) induce an elevation of the tissue temperature, thus defining the thermal (versus nonthermal) associated metabolic responses. In the case of a thermal response, the resulting heat dissipation is normalized with the specific absorption rate (SAR) index. This has led to considerable research efforts to study the possible biological effects due to exposure to HF-EMF. While the vast majority of these studies have focused on animals and humans because of health concerns, with contradictory or nonconclusive results [2], numerous experiments have also been performed on plants. Plants are outstanding models compared to animals to conduct such investigations: they are immobile and therefore keep a constant orientation in the EMF and their specific scheme of development (high surface area to volume ratio) makes them ideally suited to efficiently intercept EMF [3]. It is also quite easy in plants to

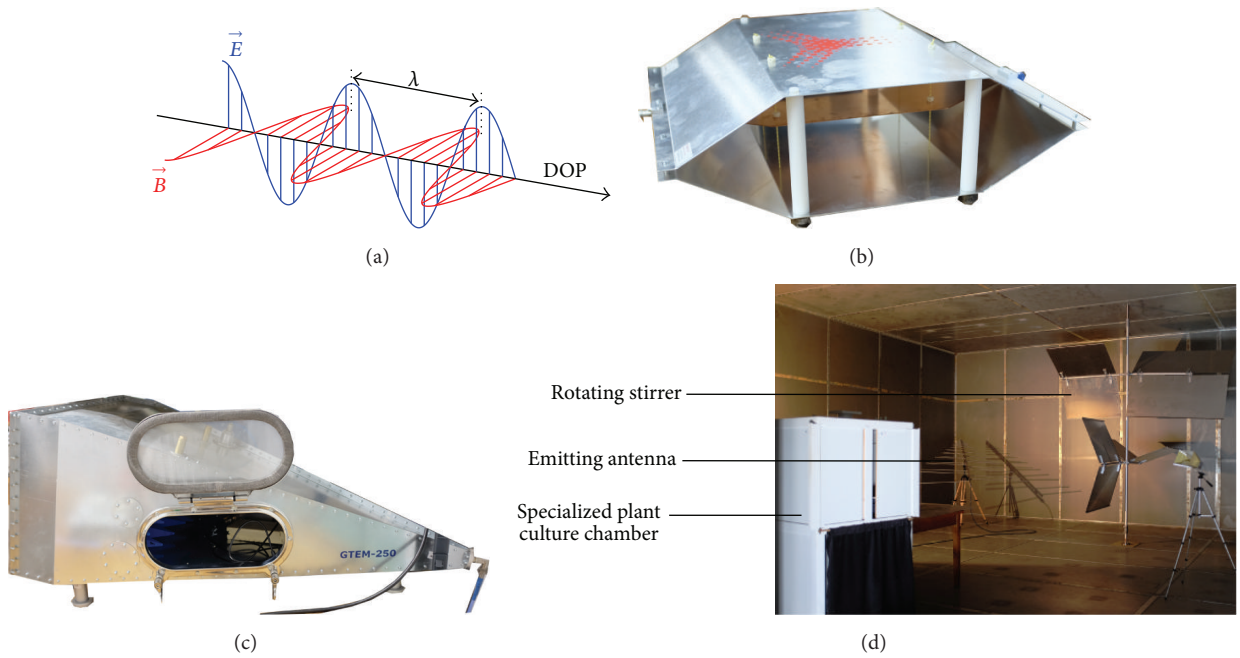

Figure 1: Electromagnetic wave and experimental set-up. (a) Schematic representation of an electromagnetic plane wave showing the transverse and space varying electric (E) and magnetic field (B). The wavelength (λ) is the distance between two crests. DOP: direction of propagation. (b) A TEM cell (transverse electromagnetic cell). (c) A GTEM cell (gigahertz transverse electromagnetic cell). (d) MSRC (mode stirred reverberation chamber). Note the double-sided metallic walls, the emitting antenna, the rotating stirrer, and the specialized culture chamber that stands in the "working volume" where the electromagnetic field characteristics have been extensively characterized.

achieve genetically stable plant lines through the selection of species that favor asexual reproduction [4] or self-pollination [5]. Furthermore, metabolic mutants are easily available for several species and constitute invaluable tools to understand the way the EMF signal is transduced [6]. Indeed, several reports have pointed out that plants actually perceive HF-EMF of even small amplitudes and transduce them into molecular responses and/or alterations of their developmental scheme [3–9]. The way that HF-EMF interact with plants remains essentially unanswered. However, since EMF evoke a multitude of responses in plants, they might be considered as a genuine environmental stimulus. Indeed, EMF exposure alters the activity of several enzymes, including those of reactive oxygen species (ROS) metabolism [7], a well-known marker of plant responses to various kinds of environmental factors. EMF exposure also evokes the expression of specific genes previously implicated in plant responses to wounding [5, 8] and modifies the development of plants [9]. Furthermore, these responses are systemic insofar as exposure of only a small region of a plant results in almost immediate molecular responses throughout the plant [6]. These responses were abolished in the presence of calcium chelators [6] or inhibitors of oxidative phosphorylation [10] which implies the involvement of ATP pools. In the present review, we describe exposure devices, SAR determination methods, and biological responses (at both the cellular/molecular and whole plant levels) observed after plant exposure to EMF. We focused this review on radiated (i.e., EMF that are emitted through an antenna) HF-EMF (mainly within the range of 300 MHz–3 GHz) and consequently will not address the biological effects of static magnetic fields (SMF), extremely low frequency electromagnetic fields (ELF), or HF current injection, since their inherent physical properties are dramatically different from those of high frequencies. Therefore, the HF-EMF we consider should be viewed through the prism of classical electromagnetism: macroscopic electrodynamics phenomena described in terms of vector and scalar fields.

2. Exposure Systems and Dosimetry

HF-EMF are a combination of an electric field and a magnetic field governed by Maxwell's equations. At high frequency, these vector quantities are coupled and obey wave equations whether for propagating waves or for standing waves. In vacuum, the former travel at the speed of light ($\approx 3 \cdot 10^8$ m s^{-1}) and have the structure of a plane wave (Figure 1(a)). In other media, the speed decreases and the spatial distribution for the electric and the magnetic fields are generally arbitrary (thus not being a plane wave). The latter, which do not propagate but vibrate up and down in place, appear in some particular conditions (e.g., bounded medium like metallic cavity) and play important roles in many physical applications (resonator, waveguide, etc.).

In both cases, HF-EMF are characterized by an amplitude of the electric (E) or magnetic (H) components (measured in volts or amperes per meter), a frequency f (number of

cycles per second of the wave quantity, measured in hertz), and a wavelength λ (distance between wave crests, measured in meters). These properties are related through the following equation:

$$\lambda = \frac{c}{f} = c \times T, \quad (1)$$

where c is the speed of the wave in the considered medium and T is the period of the wave (time between successive wave crests, measured in seconds). The wavelength λ is then the distance traveled by the wave during a period T.

The electromagnetic power density associated with an electromagnetic wave (measured in watts per square meter) is obtained by a vector product between the electric and magnetic field vectors (namely, the Poynting vector) for every point in space. The total HF-EMF power crossing any given surface is derived from Poynting's theorem [11]. For an incident plane wave in vacuum, the time-averaged electromagnetic power P_i (measured in watts) illuminating a surface of 1 m^2 orthogonal to the direction of propagation is given by the following equation:

$$P_i = \frac{E^2}{2 \times Z_0}, \quad (2)$$

where Z_0 is the characteristic impedance of free vacuum space (377 Ω).

The absorbed electromagnetic power (Pd), converted to heat by Joule effect in a volume (V) and averaged over a time period, is given by (3) for an electrically and magnetically linear material that obeys Ohm's law (conductivity σ in siemens per meter):

$$Pd = \iiint_v \frac{\sigma \times E^2}{2} dV. \quad (3)$$

2.1. Diversity of Exposure Devices. Due to the wide variety of electromagnetic waves, physicians developed a lot of electromagnetic exposure facilities, mainly for electromagnetic compatibility (EMC) test purposes. Some of these devices are used for plant exposure to HF-EMF.

HF-EMF exposure set-up is usually made up with the following two basic elements: (i) HF source (radio frequency generator, Gunn oscillator) associated with a radiating element (antenna, strip-line) and (ii) a structure that allows the propagation of EM waves and the exposure of the sample. The simplest exposure set-up relies on the use of standard cell phones as a source of HF-EMF [12, 13] radiating in an open-area test site. While this apparatus has the advantage of being simple and economical, it poses many limitations that may compromise the quality of the exposure. Indeed, these communication devices are operated with different protocols that may modify or even interrupt the emitted power. Also, the biological samples are placed in the immediate neighborhood of the antenna, which is a region where the electromagnetic field is not completely established (near-field conditions) and therefore is difficult to measure; this situation may constitute an issue for bioelectromagnetics studies. These apparatuses are nowadays used only in a small proportion of studies. Moreover, the use of open-area test sites exposes the biological samples to the uncontrolled electromagnetic ambient environment. The use of shielded rooms is a good solution to overcome this issue. Indeed, anechoic chambers provide shielded enclosures, which are designed to completely absorb reflected electromagnetic waves. However, these facilities are often large structures requiring specific equipment and costly absorbers to generate an incident plane wave (far-field illumination) and are consequently seldom used for plant exposure [14, 15].

In contrast, numerous studies are based upon dedicated apparatus of relatively small volume (Figure 1(b)), namely, the transverse electromagnetic (TEM) cell [16]. TEM cells are usually quite small (about 50 cm long × 20 cm wide) and therefore only allow the use of seeds or seedlings as plant models. Many TEM cells are based upon the classic "Crawford cell" [17]. They consist of a section of rectangular coaxial transmission line tapered at each end to adapt to standard coaxial connectors. A uniform plane wave of fixed polarization and direction is generated in the sample space for experiments between the inner conductor (septum) and the upper metallic wall. Because this cost-efficient device is enclosed, high amplitude EMF can be developed with relatively little injected power. Under some conditions, two parallel walls of the TEM cell can be removed (therefore constituting the so-called open TEM cell) without dramatically compromising the performances. This configuration is adequate to allow plant lighting. Special attention must still be paid to the relative position of the samples in the system since the disposition of the different organs within the EMF could severely affect the efficiency of the plant samples' coupling with the electromagnetic field. The main TEM cell limitation is that the upper useful frequency is bound by its physical dimensions limiting the practical size of samples at high frequency.

The gigahertz transverse electromagnetic (GTEM) cell has emerged as a more recent EMF emission test facility (Figure 1(c)) [18]. It is a hybrid between an anechoic chamber and a TEM cell and could therefore be considered as a high frequency version of the TEM cell. The GTEM cell comprises only a tapered section, with one port and a broadband termination. This termination consists of a 50 Ω resistor board for low frequencies and pyramidal absorbers for high frequencies. This exposure device removes the inherent upper frequency limit of TEM cell while retaining some of its advantages (mainly the fact that no antenna set-up is required and the fact that high field strength could be achieved with low injected power).

Waveguides are another kind of screened enclosures that are seldom used in plant exposure [19, 20]. These classical and easy to use exposure devices generate traveling waves along the transmission coordinate and standing waves along the transverse coordinates. In contrast to the TEM cell, waveguides do not generate uniform plane waves but rather allow the propagation of more complex EMF, namely, propagation modes. Each mode is characterized by a cutoff frequency below which the mode cannot propagate. When the ends of the waveguide are short-circuited, a so-called

resonant cavity is constituted, from which a recent large facility, originally designed for EMC studies, namely, the mode stirred reverberation chamber (MSRC, Figure 1(d)), is based. While this equipment is expensive and technically difficult to set up, it is the state of the art in terms of electromagnetic field characteristics, allowing the establishment of an isotropic and homogeneous field in a volume large enough to hold a dedicated plant culture chamber (either transparent or shielded toward EMF [6]). This latter characteristic permits experiments on large plants that are kept in an adequate controlled environment [6]. Our group pioneered the use of this facility, based on judicious combinations of standing waves patterns in a complex screened enclosure, in plant bioelectromagnetics studies [8] and extensively described the MSRC functionality [21]. Finally, each exposure set-up may differ in concept, polarization, frequency, or incident power but these setups always need to be optimally designed and based on well-understood physical concepts in order to assess well-controlled HF-EMF exposure conditions (homogeneity, repeatability, reproducibility, etc.).

2.2. Different Types of Exposure Signals. From each of the previous exposure devices, two very different types of EMF can be used to expose plants. The most commonly encountered mode is the continuous wave (CW) mode, in which the biological samples are continuously exposed for a specific duration to an EMF of given frequency and amplitude (rarely more than a few dozen V m^{-1}). The second mode is the pulsed electromagnetic field (PEMF) mode, in which the biological samples are subjected to several series of discontinuous pulses of ultrashort duration EMF (within the range of μs to ns) and usually of very high amplitude (up to several hundred kV m^{-1}). This last kind of exposure [22, 23] is seldom used because of the scarcity and great complexity of the equipment needed to generate the EMF and the difficulty to design the dedicated antennae able to deliver such ultrashort power surges [24].

The HF-EMF could also be modulated (i.e., varied in time at a given, usually much lower frequency). Only a few studies explicitly addressed modulation effect on biological responses. Răcuciu et al. [25] exposed maize caryopses to low levels (7 dBm), 900 MHz RF field, for 24 h in either continuous wave (CW), amplitude modulated (AM), or frequency modulated (FM) modes. They found that 12-day-old plant lengths were reduced by about 25% in modulated EMF (AM or FM type) compared to control (unexposed samples), while CW exposure had an opposite (growth stimulation) effect, suggesting that EMF modulation actually modifies biological responses.

2.3. Dosimetry. In order to compare the biological effects observed in different exposure conditions, the National Council on Radiation Protection and Measurements officially introduced in 1981 an EMF exposure metric, the specific absorption rate (SAR). The formal definition of this basic dosimetry (the amount of dose absorbed) is "the time derivative of the incremental energy absorbed (dW) by (dissipated in) an incremental mass contained in a volume (dV) of a given density ρ." From this definition and (3), the SAR (measured in W kg^{-1}) is given by the following equation:

$$\mathrm{SAR} = \frac{d}{dt}\left(\frac{dW}{\rho \times dV}\right) = \frac{\sigma \times E^2}{2 \times \rho}. \quad (4)$$

SAR is the power absorbed by living tissue during exposure to CW-EMF (this quantity does not apply to PEMF mode because of the very short duration of the pulses that do not cause temperature increase in the samples). SAR can be calculated from the dielectric characteristics of plant tissues at the working frequencies, using (4). While ρ could be easily determined, the value of σ is dependent upon the frequency and is difficult to assess in the range of GHz. It is usually evaluated from the literature [40], since the experimental set-up to measure this parameter at a given frequency (waveguide, open waveguide, and coaxial line technique, e.g., D-Line) is rarely used because of its complex set-up. From the biological heat-transfer equation, the SAR can also be determined using the temperature increase evoked in plant tissue after exposure to EMF, using the following equation:

$$\mathrm{SAR} = C \times \left(\frac{dT}{dt}\right)_{t \to 0}, \quad (5)$$

where C is the heat capacity (J K^{-1} kg^{-1}, which is available for some tissues in the literature) and dT (measured in Kelvin) is the sample temperature increase corresponding to the elapsed time dt (measured in second) since the beginning of HF-EMF exposure. Either for animals or plants, the SAR measurement is subject to uncertainty [46]. Since the specific heat is frequency independent and the temperature distribution is usually more uniform than the internal electric field, (5) provides, for detectable temperature increases, a better way for SAR estimation.

In animal and human tissue, SAR is determined using dedicated phantoms [47] filled with a special liquid that mimics the dielectric properties of biological fluids. While this approach is adequate in animals, in which the developmental scheme produced volumes, it could not be adapted to most plant organs (e.g., leaves) that have a high surface area to volume ratio [3] but could be used in fruits and tuberous structures. In contrast, surface temperature can be easily assessed with dedicated instruments (e.g., Luxtron® fiber optic temperature probe) and used to feed (5) [45]. The SAR can also be determined using the differential power method based on the measurement of power absorption (reviewed in [48]) that takes place in the absence or presence of biological samples [39]. The SAR is then calculated by dividing the absorbed power by the mass of the living material.

3. Biological Responses

Biological responses should be considered as reporters of, and evidence for, the plant's ability to perceive and interact with EMF. These responses can take place at the subcellular level, implying molecular events or modification of enzymatic activities, or at the level of the whole plant, taking the form of growth modification. Tables 1–3 summarize some work

Table 1: Metabolic pathways affected after plant exposure to HF-EMF radiations.

Enzymes or metabolites	Metabolic pathways	Organisms	Exposure conditions	Response to EMF
Phenylalanine ammonia-lyase	Phenylpropanoids	*Phaseolus vulgaris*	N/A (PEMF)	Synergistic action with growth regulators in cultured cells [26]
Polyphenol oxidase	Polyphenols	*Vigna radiata*	900 MHz, up to 4 h, 8.55 μW cm^{-2}	8.5-fold increase [27]
α- and β-amylases	Starch metabolism	*Vigna radiata*	900 MHz, up to 4 h, 8.55 μW cm^{-2}	2.5- and 15-fold increase for α- and β-amylases, respectively [27]
α- and β-amylases, starch phosphorylases	Starch metabolism	*Zea mays*	1800 MHz, up to 4 h, 332 mW m^{-2}	2-fold increase for amylases. −73% for starch phosphorylases [28]
Water soluble sugars	Sugar metabolism	*Phaseolus vulgaris*	900 MHz, 4 h	2-fold reduction in soluble sugars [12]
Acid and alkaline invertases	Sucrose metabolism	*Zea mays*	1800 MHz, up to 4 h, 332 mW m^{-2}	1.8- and 2.6-fold increase for acid and alkaline forms, respectively [28]
Malate and NADP isocitrate dehydrogenases, glucose-6P dehydrogenase	Krebs cycle, pentose phosphate pathway	*Plectranthus*	900 MHz, 1 h	Lower activity (−10 to −30%) at the end of the stimulus and then a 2-fold increase 24 h later [29]
ATP content and adenylate energy charge (AEC)	Energetic metabolism	*Solanum lycopersicon*	900 MHz, 10 min, 5 V m^{-1}	Drop of ATP content (30%) and AEC (0.8 to 0.6) 30 min after the stimulus [10]
MDA content, H_2O_2, superoxide dismutase, catalase, guaiacol peroxidase, glutathione reductase, ascorbate peroxidase	Lipid peroxidation-oxidative metabolism	*Vigna radiata*	900 MHz, 8.55 μW cm^{-2}	All oxidative metabolism markers increased (2-fold to 5-fold) [7]
MDA and H_2O_2 content, catalase, ascorbate peroxidase	Lipid peroxidation	*Lemna minor*	400 and 900 MHz, 2 to 4 h, 10 to 120 V m^{-1}	MDA and H_2O_2 content, catalase and ascorbate peroxidase activities increased (10–30%) [30]
Peroxidases	Oxidative metabolism	*Vigna radiata, Lemna minor*	900 MHz, 1 to 4 h, 8.55 μW cm^{-2} or 41 V m^{-1}	Peroxidase activities increased [18, 27]
MDA, oxidized and reduced glutathione, NO synthase	Oxidative metabolism-NO metabolism	*Triticum aestivum*	2.45 GHz, 5 to 25 s, 126 mW mm^{-2} concomitantly with NaCl treatment	Exposure to EMF reduced the oxidative response of plants to high salt treatment [31]
Protein metabolism-DNA damage	Oxidative protein and DNA damage (comet assay)	*Nicotiana tabacum*	900 MHz, 23 V m^{-1}	Carbonyl content and tail DNA value increased (1.8-fold and 30%, resp.) [30]
Protein metabolism	Protein content	*Phaseolus vulgaris, Vigna radiata, Triticum aestivum*	Cell phone, 4 h	Drop in protein content in *Phaseolus* (71%) and *Vigna* (57%) [27, 32] and *Triticum* [13]
Amino acid metabolism	Proline accumulation	*Zea mays, Vigna radiata*	940 MHz, 2 days Cell phone, 2 h, 8.55 μW cm^{-2}	1.8- and 5-fold increase in *Z. mays* [33] and *V. radiata* [7], respectively
Global terpene emission	Monoterpene metabolism	*Petroselinum crispum, Apium graveolens, Anethum graveolens*	900–2400 MHz, 70–100 mW m^{-2}	Enhanced emission of terpene compounds [34]

reporting HF-EMF effects observed at the scale of the whole plant, biochemical processes, or gene regulation, respectively.

3.1. Cellular and Molecular Level. Numerous reports [4, 7, 33] indicate an increase in the production of malondialdehyde (MDA, a well-known marker of membrane alteration) along with ROS metabolism activation after exposing plants to HF-EMF (Table 1). Membrane alteration and ROS metabolism activation are likely to establish transduction cascades that enable specific responses. Indeed, the critical role of calcium,

Table 2: Genes whose expression is altered after plant exposure to HF-EMF.

Gene	Organism	Function	Exposure conditions	Response to EMF exposure
lebZIP1	*Solanum lycopersicon, whole plant*	Transcription factor	900 MHz, 5 V m^{-1}, CW in a MSRC	Increase (3-fold to 4-fold) [6, 8]
lebZIP1	*Solanum lycopersicon, whole plant*	Transcription factor	Cell phone	Increase (3-4-fold) [35]
cam	*Solanum lycopersicon, whole plant*	Ca^{2+} signal transduction	900 MHz, 5 V m^{-1}, CW in a MSRC	Increase (5-fold) [5, 10]
cdpk	*Solanum lycopersicon, whole plant*	Ca^{2+} signal transduction	900 MHz, 5 V m^{-1}, CW in a MSRC	Increase (5-fold) [10]
cmbp	*Solanum lycopersicon, whole plant*	mRNA metabolism	900 MHz, 5 V m^{-1}, CW in a MSRC	Increase (6-fold) [5]
pin2	*Solanum lycopersicon, whole plant*	Proteinase inhibitor	900 MHz, 5 V m^{-1}, CW in a MSRC	Increase (4.5-fold [5] and 2.5-fold) [6]
pin2	*Solanum lycopersicon, whole plant*	Proteinase inhibitor	900 MHz, cell phone	Increase (2-fold) [35]
At4g26260	*Arabidopsis thaliana, cell suspension culture*	Similar to myo-inositol oxygenase	1.9 GHz, 8 mW cm^{-2}	Decrease (0.3-fold) [36]
At3g47340	*Arabidopsis thaliana, cell suspension culture*	Glutamine-dependent asparagine synthetase	1.9 GHz, 8 mW cm^{-2}	Decrease (0.4-fold) [36]
At3g15460	*Arabidopsis thaliana, cell suspension culture*	Brix domain protein	1.9 GHz, 8 mW cm^{-2}	Decrease (0.5-fold) [36]
At4g39675	*Arabidopsis thaliana, cell suspension culture*	Expressed protein	1.9 GHz, 8 mW cm^{-2}	Increase (1.5-fold) [36]
At5g10040	*Arabidopsis thaliana, cell suspension culture*	Expressed protein	1.9 GHz, 8 mW cm^{-2}	Increase (1.4-fold) [36]
AtCg00120	*Arabidopsis thaliana, cell suspension culture*	ATPase alpha subunit (chloroplast)	1.9 GHz, 8 mW cm^{-2}	Increase (1.4-fold) [36]

a crucial second messenger in plants, has long been pointed out [6, 10]: the responses (e.g., changes in calm-n6, lecdpk-1, and pin2 gene expression) to EMF exposure are severely reduced when plants are cultivated with excess of calcium or in the presence of calcium counteracting agents (Figure 2) such as chelators (EGTA and BAPTA) or a channel blocker ($LaCl_3$). The importance of calcium in the establishment of the plant response is also highlighted by the fact that early gene expression associated with EMF exposure involves at least 2 calcium-related products (calmodulin and calcium-dependent protein kinase) [5, 10]. This response is also energy-dependent: an important drop (30%, Figure 3) in ATP content and adenylate energy charge (AEC) occurs after HF-EMF exposure [10]. It is not clear for now if the AEC drop is the consequence of altered membranes allowing passive ATP exit or if higher consumption of ATP occurred because of increased metabolic activity. Indeed, it is well known that a drop in AEC stimulates the catabolic enzymatic pathways through allosteric modulations. Nevertheless, inhibiting ATP biosynthesis with the decoupling agent carbonyl cyanide *m*-chlorophenyl hydrazone (CCCP) abolished plant responses to EMF exposure [10]. Nitric oxide (NO) is another signaling molecule that is tightly related to environmental factors' impact on plants [49]. NO rapidly increases after various kinds of stimuli including drought stress or wounding. Chen et al. [50] recently demonstrated the increased activity of nitric oxide synthase and accumulation of NO after exposing caryopses of wheat for 10 s to high power 2.45 GHz EMF. Similarly, Qiu et al. [51] showed in wheat that the tolerance to cadmium evoked by microwave pretreatment was abolished by the addition of 2-(4-carboxyphenyl)-4,4,5,5-tetramethylimidazoline-1-oxyl-3-oxide (carboxy-PTIO), an NO scavenger, suggesting that microwave-induced NO production was involved in this mechanism. Taken together, these results advocate for the EMF induction of NO synthase. However, these studies used high power EMF (modified microwave oven) as stimulating tool and the fact that a temperature increase of the sample was the cause of NO increase is not excluded. To our knowledge, the involvement of NO has not yet been demonstrated after low power (i.e., non-thermal) EMF exposure. Furthermore, well-known actors of plant responses to environmental stimuli are also involved: the tomato mutants *sitiens* and *JL-5* for abscisic (ABA) or jasmonic (JA) acids biosynthesis, respectively, display normal responses (accumulation of stress-related transcripts) when whole plants are exposed to EMF [6]. In contrast, very rapid distant responses to local exposure that occur in the wild plants (Figure 4(a)) are impaired in *sitiens* ABA mutant (Figure 4(b)) and *JL-5* mutants, highlighting the existence of a transmitted signal (whose genesis and/or transmission is dependent on ABA and JA) in the whole plant after local exposure [6]. The nature of this signal is still unknown, but very recent work has demonstrated that membrane potential is affected after exposure to EMF [14]. It could therefore be

Table 3: Morphogenetic responses observed after plant exposure to HF-EMF.

Plant species	Exposure conditions	Responses to HF-EMF exposure and references
Raphanus sativus	Gunn generator 10.5 GHz, 14 mW, exposure of seeds and hypocotyls	Germination inhibition (45%), reduction of hypocotyl elongation (40%) [37]
Lens culinaris	Cell phone, 1800 MHz (1 mW), exposure of dormant seeds	Reduction of seedlings' root growth (60%) and mitotic index (12%). Abnormal mitosis increased (52%) [38]
Vigna radiata	Cell phone, 900 MHz, 8.55 μW cm^{-2}	Rhizogenesis (root number and length) severely affected [7]
Vigna radiata	Cell phone, 900 MHz, 8.55 μW cm^{-2}	Inhibition of germination (50%), hypocotyl (46%), and root growth (59%). Dry weight reduced by 43% [27]
Phaseolus aureus, Vigna radiata	Cell phone, 4 h exposure	Root and stem elongations severely affected (−44 and −39%, resp.) [12, 32]
Vigna radiata, Lablab purpureus	1.8 GHz, 0.48–1.45 mW cm^{-2}	Reduction of height and fresh weight [39]
Zea mays	1 GHz, 1 to 8 h, 0.47 W cm^{-2}	Reduced growth of 12-day-old plants (about 50% after 8 h of exposure) [40]
Zea mays	1800 MHz, 4 h, 332 mW m^{-2}	Reduced growth of roots and coleoptiles (16 and 22%, resp.) [28]
Vigna radiata, Triticum aestivum	Cell phone, 900 MHz, 4 h exposure	Growth reduction (21 and 50%) in *Vigna* and *Triticum*, respectively [13]
Triticum aestivum, Cicer arietinum, Vigna radiata, Vigna aconitifolia	Klystron-based EMF generator, 9.6 GHz, 1 dBm to 3.5 dBm	Growth and biomass reduction [41]
Vigna radiata, Ipomoea aquatica	425 MHz, 2 h, 1 mW	Growth stimulation of primary root [16]
Glycine max	900 MHz, 5.7 to 41 V m^{-1}	Inhibition of epicotyl and/or root growth, depending on exposure set-up [9]
Lemna minor	400–1900 MHz, 23 to 390 V m^{-1}, whole plant exposure	Growth slowed down, at least in the first days following exposure [18]
Trigonella foenum-graecum, Pisum sativum	900 MHz, 0.5–8 h	Increased root size, nodule number, and size [42]
Hibiscus sabdariffa	Resulting field from a GSM base antenna (not measured)	Reduction of flower bud abscission with increasing distances from the antenna [43]
Linum usitatissimum	Cell phone or Gunn generator (105 GHz), 2 h	Production of epidermic meristems under calcium deprivation condition [44]
Rosa hybrida	900 MHz, 5–200 V m^{-1}, whole plant exposure in MSRC	Delayed and reduced (45%) growth of secondary axes [45]

hypothesized that electrical signals (action potential and/or variation potential) could be the transmitted signal, strongly implying that HF-EMF is a genuine environmental factor.

3.1.1. Alterations of Enzymatic Activities. Table 1 summarizes some of the enzymatic activities that are modified after exposing plants to HF-EMF. As previously noted, ROS metabolism is very often activated after plant exposure to EMF. Enzymatic activities such as peroxidase, catalase, superoxide dismutase, and ascorbate peroxidase have twofold to fourfold increase [4, 7, 18, 27, 33]. The question remains open to determine if this could be the consequence of a direct action of EMF on living tissue. Indeed, the very low energy that is associated with the EMF at these frequencies makes them nonionizing radiations. Side effects of elevated ROS metabolism are also noted: H_2O_2 production [4, 7], MDA increases [4, 7, 33], and protein damage [30]. An increase in polyphenol oxidase [27] and phenylalanine ammonia-lyase [26] may indicate stress responses linked to an increased lignification, a common response of plants to environmental stress.

Protein content is reduced in *Vigna* and *Phaseolus* [27, 32] as well as in *Triticum* [13]. It is not yet known if the decrease in protein content results from an increase in protein degradation and/or a decrease in protein synthesis, but this may constitute a stimulating field of investigation, since evidence shows that mRNA selection from translation occurs after plant exposure to HF-EMF [10]. Hydrolytic enzymatic activities (α- and β-amylases and invertases) responsible for the production of soluble sugar increase in germinating seeds after exposure to HF-EMF [12, 28, 32], while the starch phosphorylase activity, phosphorolytic and potentially reversible, is diminished. In contrast, HF-EMF exposure causes a drop of soluble sugar that may be related to the inhibition of Krebs cycle and pentose phosphate pathway in *Plectranthus* (Lamiaceae) leaves after exposure to 900 MHz EMF [29], suggesting that seeds and adult leaves respond in

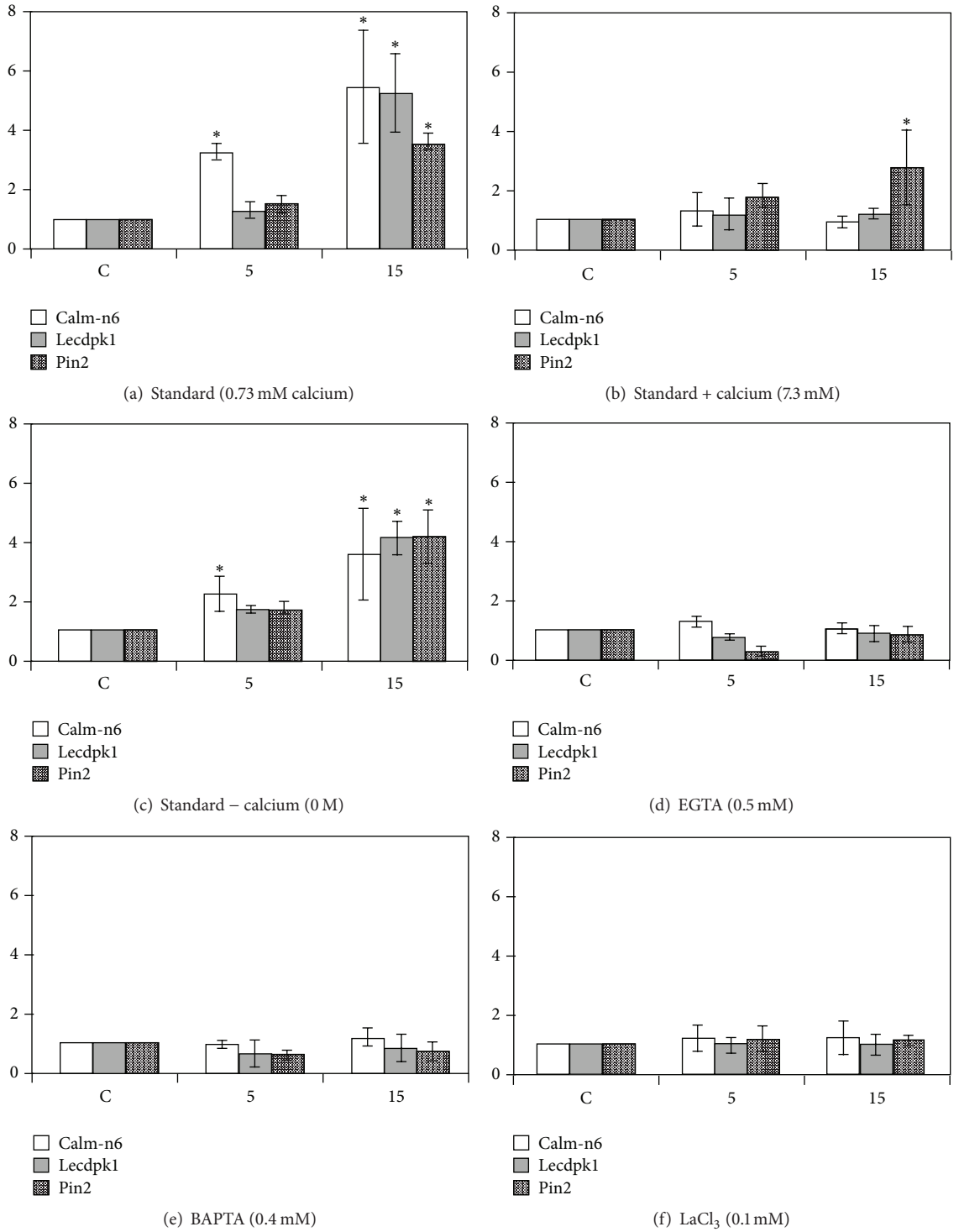

Figure 2: Effect of calcium concentration in culture medium on calm-n6 (calmodulin), pin2 (proteinase inhibitor), and lecdpk1 (calcium-dependent protein kinase) transcript accumulation in response to the HF-EMF exposure. (a) Standard medium (0.73 mM of calcium). (b) Tenfold extra calcium (7.3 mM). (c) No calcium (0 mM). (d) No calcium (0 mM) with 0.5 mM of EGTA. (e) No calcium (0 mM) with 0.4 mM of BAPTA (1,2-bis(o-aminophenoxy)ethane-N,N,N′,N′-tetraacetic acid), a specific Ca^{2+} chelator. (f) No calcium (0 mM) with 0.1 mM $LaCl_3$. Bars represent mean values ± SE from at least three independent experiments. An asterisk over the bars states the significant differences according to the one-sided Mann-Whitney U test. Reproduced from [10], with permission.

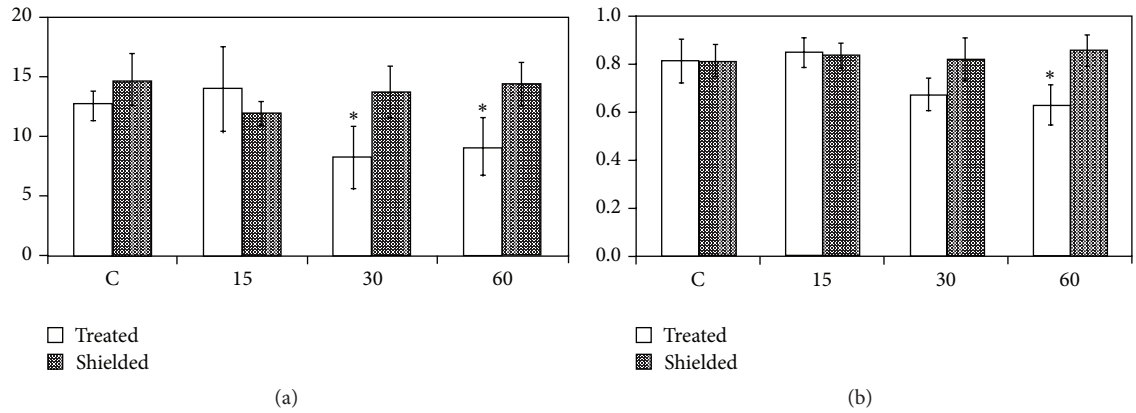

Figure 3: ATP concentration and adenylate energy charge (AEC) changes after HF-EMF exposure (5 V m^{-1}, 10 min) in a mode stirred reverberation chamber. C: control, unexposed plants. 15, 30, and 60: time (min) after the end of HF-EMF exposure. (a) ATP concentration (pmol mg^{-1} Prot.). (b) Adenylate energy charge (ratio). Bars represent mean values ± SE from at least three independent experiments. An asterisk over the bars states the significant differences according to the one-sided Mann-Whitney U test. Reproduced from [10], with permission.

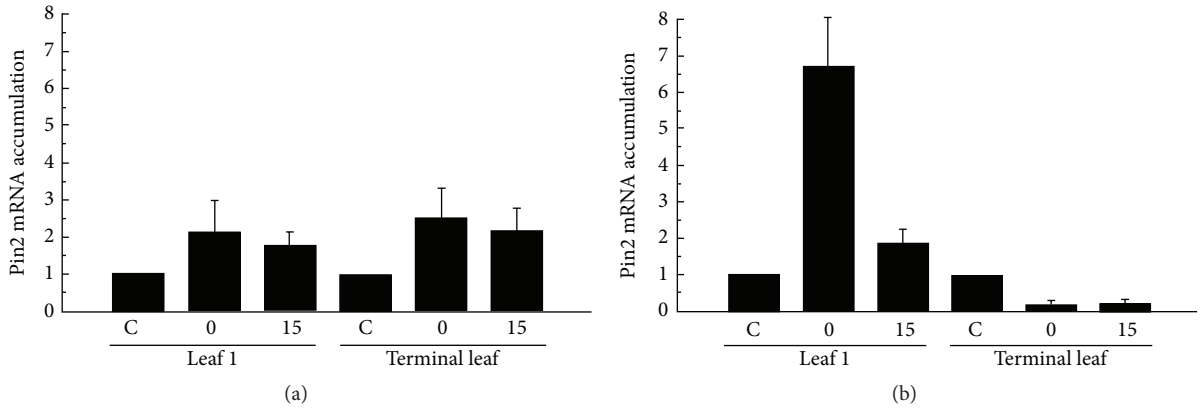

Figure 4: Local and systemic responses after HF-EMF exposure. (a) Systemic response after local exposure to HF-EMF in wild type. Local and distant responses after stimulation of leaf 1 (with the rest of the plant being protected from the EMF). The stimulated tissue (leaf 1) and distant one (terminal leaf) both displayed responses (accumulation of pin2 transcript). HF-EMF exposure: 5 V m^{-1}, 10 min. (b) Impairment of distant response after exposure to HF-EMF in *sitiens* (ABA deficient) mutant. The stimulated tissue (leaf 1) displays the response to EMF exposure (accumulation of pin2 transcript), while the response in the distant tissue (terminal leaf) is impaired. HF-EMF exposure: 5 V m^{-1}, 10 min. Reproduced from [6], with permission.

a different way to HF-EMF exposure. The accumulation of proline, reported by several authors [7, 33], and an increase in terpenoid emission and content in aromatic plants [34] are also classical responses of plants to environmental stresses.

3.1.2. Modification of Gene Expression. While numerous reports focused on enzymatic activities alterations after exposure to EMF, only a few studies concentrate on gene expression modifications (Table 2). Tafforeau et al. [44] demonstrated using Gunn generator (105 GHz) several reproducible variations in 2D gel electrophoresis profiles, showing that gene expression is likely to be altered by the exposure treatment. Jangid et al. [52] provided indirect proof (RAPD profiles) suggesting that high power microwave irradiation (2450 MHz, 800 W cm^{-2}) modifies gene expression in *Vigna aconitifolia*, while these results do not exclude a possible thermal effect of microwave treatment. *Arabidopsis thaliana* suspension-cultured cells exposed to HF-EMF (1.9 GHz, 8 mW cm^{-2}) showed differential expression of several genes (p values < 0.05) compared to the control (unexposed) condition in microarray analysis [36]. Most of them are downregulated (while At4g39675, At5g10040, and AtCg00120 displayed a slight increase; see Table 2). However, the RT-PCR p value lowers the significance of these variations and these authors consequently concluded the absence of HF-EMF effect on plant gene expression. In contrast, short duration, high frequency, low amplitude EMF exposure (10 min, 900 MHz, 5 V m^{-1}) performed on whole 3-week-old tomatoes in MSRC [5, 6, 8, 10] demonstrated altered expressions of at least 5 stress-related genes (Table 2), suggesting that

whole plants are more sensitive to HF-EMF than cultured cells. These experiments have been independently replicated by Rammal et al. [35], using a longer exposure period and a far less sophisticated exposure set-up (cell phone). Stress responses of plants quite often display a biphasic pattern [53]: a very rapid increase in transcript accumulation that lasts 15–30 min, followed by a brief return to basal level, and then a second increase (after 60 min). This pattern was observed after tomato exposure to EMF so we questioned the meaning of the early and late population of transcripts in terms of physiological significance by measuring their association to polysomes (which reflects their putative translation to proteins). We found that the early (0–15 min) mRNA population was only faintly associated with polysomes, yet being poorly translated, while the late mRNA population (60 min) is highly associated with polysomes [10]. This result strongly suggests that only the late mRNA population may have a physiological importance since it is the only one to be efficiently translated into proteins.

3.2. Whole Plant Level. The biochemical and molecular modifications observed after plant exposure to EMF and described in the previous paragraphs might induce morphogenetic alterations of plant development. Indeed, an increasing number of studies report modifications of plant growth after exposure to HF-EMF (Table 3). These treatments are effective at different stages of plant development (seeds, seedlings, or whole plants) and may affect different organs or developmental processes including seeds germination and stem and root growth, indicating that biological samples of even small sizes (a few mm) are able to perceive HF-EMF. Seed exposure to EMF generally results in a reduced germination rate [27, 37, 39], while in other cases germination is unaffected [42] or even stimulated [16]. The seedlings issued from EMF-exposed seeds displayed reduced growth of roots and/or stem [13, 28, 32, 37–39, 41] but rarely a stimulatory effect [16]. This point strongly differs from exposure to static magnetic fields or extremely low frequency EMF, in which the stimulatory effects on growth are largely predominant [54]. Ultrashort pulsed high power EMF (PEMF, 4 μs, 9.3 GHz, 320 kV m^{-1}) also tends to stimulate germination of seeds of radish, carrot, and tomato and increase plant height and photosynthetic surface area in radish and tomato [20] and roots of tobacco seedlings [22]. These different effects of PEMF compared to HF-EMF on plants may be related to their fundamental difference in terms of physical properties. Exposure to HF-EMF of seedlings or plants (rather than seeds) also generally resulted in growth inhibition [9, 18, 27, 28, 39]. Singh et al. [7] showed that rhizogenesis (root number and length) is severely affected in mung bean after exposure to cell phone radiation, possibly through the activation of several stress-related enzymes (peroxidases and polyphenol oxidases). Akbal et al. [38] showed that root growth was reduced by almost 60% in *Lens culinaris* seeds exposed in the dormant state to 1800 MHz EMF radiation. Concomitantly, these authors reported an increase in ROS-related enzymes, lipid peroxidation, and proline accumulation, with all of these responses being characteristic of plant responses to stressful conditions. Afzal and Mansoor [13] investigated the effect of a 72 h cell phone exposure (900 MHz) on both monocotyledonous (wheat) and dicotyledonous (mung bean) plants seeds: germination was not affected, while the seedlings of both species displayed growth inhibition, protein content reduction, and strong increase in the enzymatic activities of ROS metabolism. It is however worth noting that growth of mung bean and water convolvulus seedlings exposed at a lower frequency (425 MHz, 2 h, 1 mW) is stimulated because of higher elongation of primary root [11], while duckweed (*Lemna minor*, Araceae) growth was significantly slowed down not only by exposure at a similar frequency (400 MHz, 4 h, 23 V m^{-1}) but also after exposure at 900 and 1900 MHz for different field amplitudes (23, 41, and 390 V m^{-1}) at least in the first days following the exposure [18]. Surducan et al. [15] also found stimulation of seedling growth in bean and maize after exposure to EMF (2.452 GHz, 0.005 mW cm^{-2}). Senavirathna et al. [55] studied real-time impact of EMF radiation (2 GHz, 1.42 W m^{-2}) on instantaneous growth in the aquatic plant, parrot's feather (*Myriophyllum aquaticum*, Haloragaceae), using nanometer scale elongation rate fluctuations. These authors demonstrated that EMF-exposed plants displayed reduced fluctuation rates that lasted for several hours after the exposure, strongly suggesting that plants' metabolism experienced a stressful situation. It is worth noting that the exposure did not cause any plant heating (as measured using sensitive thermal imaging). Some other kind of morphological changes also occurred after plant exposure to HF-EMF: induction of epidermal meristems in flax [44], flower bud abscission [43], nitrogen-fixation nodule number increase in leguminous [42], or delayed reduced growth of secondary axis in *Rosa* [45].

These growth reductions may be related to a lower photosynthetic potential since Răcuciu et al. [40] showed that exposing 12-day-old maize seedlings to 0.47 W kg^{-1} 1 GHz EMF induces a drop in photosynthetic pigment content: the diminution was especially important in chlorophyll a, which was reduced by 80% after 7 h of exposure. Ursache et al. [56] showed that exposure of maize seedlings to microwave (1 mW cm^{-2}, 10.75 GHz) also caused a drop in chlorophyll a and b content. Similarly, Hamada [57] found a decrease in chlorophyll content in 14-day-old seedlings after exposing the caryopses for 75 min at 10.5 GHz. Kumar et al. showed a 13% decrease in total chlorophyll after 4 h exposure of maize seedlings to 1800 MHz (332 mW m^{-2}). These modifications may be related to abnormal photosynthetic activity, which relies on many parameters, including chlorophyll and carotenoid content. Senavirathna et al. [58] showed that exposing duckweeds to 2–8 GHz, 45–50 V m^{-1} EMF induced changes in the nonphotosynthetic quenching, indicating a potential stressful condition. Three aromatic species belonging to Apiaceae family (*Petroselinum crispum*, *Apium graveolens*, *and Anethum graveolens*) strongly respond to global system for mobile communications radiation (GSM, 0.9 GHz, 100 mW cm^{-2}) or wireless local area network (WLAN, 2.45 GHz, 70 mW cm^{-2}) exposure by decreasing the net assimilation rate (over 50%) and the stomatal conductance (20–30%) [34].

4. Conclusion and Future Prospects

An increasing number of reports highlight biological responses of plants after exposure to HF-EMF at the molecular and the whole plant level. The exposure conditions are, however, far from being standardized and illustrate the diversity of exposure conditions employed. However, future work should avoid exposure in near-field conditions (i.e., in immediate vicinity of the emission antenna) where the field is instable and difficult to characterize. Similarly, the use of communication devices (i.e., cell phones) should be avoided as emission sources since it may be difficult to readily control the exposure conditions because of built-in automation that may overcome the experimental set-up. The use of specialized devices (TEM cells, GTEM cell, waveguides, MSRC, etc.) in which a precise control of exposure condition can be achieved is highly preferable.

Shckorbatov [59] recently reviewed the possible interactions mechanisms of EMF with living organisms. While the classical targets (interaction with membranes, free radicals, and intracellular regulatory systems) have all been observed in plants, a convincing interpretation of the precise mechanism of HF-EMF interaction with living material is still needed. Alternative explanation (i.e., electromagnetic resonance achieved after extremely high frequency stimulation which matches some kind of organ architecture) has also been proposed for very high frequency EMF (several dozen GHz) [60]. However, the reality of this phenomenon *in vivo* (studied for now only through numerical simulations) and its formal contribution to the regulation of plant development have not yet been experimentally established. Amat et al. [61] proposed that light effects on plants arose not only through chromophores, but also through alternating electric fields which are induced in the medium and able to interact with polar structures through dipole transitions. The possible associated targets (ATP/ADP ratio, ATP synthesis, and Ca^{2+} regulation) are also those affected by exposure to HF-EMF [10]. It could therefore be speculated that HF-EMF may use similar mechanisms. The targeted pathways, especially Ca^{2+} metabolism, are well known to modulate numerous responses of plants to environmental stress. While deeper understanding of plant responses to HF-EMF is still needed, these treatments may initiate a set of molecular responses that may affect plant resistance to environmental stresses, as already demonstrated in wheat for $CaCl_2$ [62] or UV [63] tolerances, and constitute a valuable strategy to increase plant resistance to environmental stressful conditions.

Conflict of Interests

The authors declare that there is no conflict of interests regarding the publication of this paper.

Acknowledgments

The authors would like to gratefully acknowledge the LRC BIOEM ("Laboratoire de Recherche Conventionné"—LRC no. 002-2011-CEA DAM/Institut Pascal) for its financial support.

References

[1] A. Balmori, "Electromagnetic pollution from phone masts. Effects on wildlife," *Pathophysiology*, vol. 16, no. 2-3, pp. 191–199, 2009.

[2] H. Kleinlogel, T. Dierks, T. Koenig, H. Lehmann, A. Minder, and R. Berz, "Effects of weak mobile phone—electromagnetic fields (GSM, UMTS) on well-being and resting EEG," *Bioelectromagnetics*, vol. 29, no. 6, pp. 479–487, 2008.

[3] A. Vian, C. Faure, S. Girard et al., "Plants respond to GSM-like radiations," *Plant Signaling & Behavior*, vol. 2, no. 6, pp. 522–524, 2007.

[4] M. Tkalec, K. Malarić, and B. Pevalek-Kozlina, "Exposure to radiofrequency radiation induces oxidative stress in duckweed *Lemna minor* L.," *Science of the Total Environment*, vol. 388, no. 1–3, pp. 78–89, 2007.

[5] D. Roux, A. Vian, S. Girard et al., "Electromagnetic fields (900 MHz) evoke consistent molecular responses in tomato plants," *Physiologia Plantarum*, vol. 128, no. 2, pp. 283–288, 2006.

[6] É. Beaubois, S. Girard, S. Lallechere et al., "Intercellular communication in plants: evidence for two rapidly transmitted systemic signals generated in response to electromagnetic field stimulation in tomato," *Plant, Cell and Environment*, vol. 30, no. 7, pp. 834–844, 2007.

[7] H. P. Singh, V. P. Sharma, D. R. Batish, and R. K. Kohli, "Cell phone electromagnetic field radiations affect rhizogenesis through impairment of biochemical processes," *Environmental Monitoring and Assessment*, vol. 184, no. 4, pp. 1813–1821, 2012.

[8] A. Vian, D. Roux, S. Girard et al., "Microwave irradiation affects gene expression in plants," *Plant Signaling and Behavior*, vol. 1, no. 2, pp. 67–69, 2006.

[9] M. N. Halgamuge, S. K. Yak, and J. L. Eberhardt, "Reduced growth of soybean seedlings after exposure to weak microwave radiation from GSM 900 mobile phone and base station," *Bioelectromagnetics*, vol. 36, no. 2, pp. 87–95, 2015.

[10] D. Roux, A. Vian, S. Girard et al., "High frequency (900 MHz) low amplitude (5 V m^{-1}) electromagnetic field: a genuine environmental stimulus that affects transcription, translation, calcium and energy charge in tomato," *Planta*, vol. 227, no. 4, pp. 883–891, 2008.

[11] J. A. Stratton, *Electromagnetic Theory*, McGraw-Hill, New York, NY, USA, 1941.

[12] V. P. Sharma, H. P. Singh, R. K. Kohli, and D. R. Batish, "Mobile phone radiation inhibits *Vigna radiata* (mung bean) root growth by inducing oxidative stress," *Science of the Total Environment*, vol. 407, no. 21, pp. 5543–5547, 2009.

[13] M. Afzal and S. Mansoor, "Effect of mobile phone radiations on morphological and biochemical parameters of Mung bean (*Vigna radiata*) and wheat (*Triticum aestivum*) seedlings," *Asian Journal of Agricultural Sciences*, vol. 4, no. 2, pp. 149–152, 2012.

[14] M. D. H. J. Senavirathna and T. Asaeda, "Radio-frequency electromagnetic radiation alters the electric potential of *Myriophyllum aquaticum*," *Biologia Plantarum*, vol. 58, no. 2, pp. 355–362, 2014.

[15] E. Surducan, V. Surducan, A. Butiuc-Keul, and A. Halgamagy, "Microwaves irradiation experiments on biological samples," *Studia Univesitas Babes-Bolyai Biologia*, vol. 58, no. 1, pp. 83–98, 2013.

[16] P. Jinapang, P. Prakob, P. Wongwattananard, N. E. Islam, and P. Kirawanich, "Growth characteristics of mung beans and water

convolvuluses exposed to 425-MHz electromagnetic fields," *Bioelectromagnetics*, vol. 31, no. 7, pp. 519–527, 2010.

[17] M. L. Crawford, "Generation of standard EM fields using TEM transmission cells," *IEEE Transactions on Electromagnetic Compatibility*, vol. 16, no. 4, pp. 189–195, 1974.

[18] M. Tkalec, K. Malarić, and B. Pevalek-Kozlina, "Influence of 400, 900, and 1900 MHz electromagnetic fields on *Lemna minor* growth and peroxidase activity," *Bioelectromagnetics*, vol. 26, no. 3, pp. 185–193, 2005.

[19] L. M. Liu, F. Garber, and S. F. Cleary, "Investigation of the effects of continuous-wave, pulse- and amplitude-modulated microwaves on single excitable cells of chara corallina," *Bioelectromagnetics*, vol. 3, no. 2, pp. 203–212, 1982.

[20] A. Radzevičius, S. Sakalauskiene, M. Dagys et al., "The effect of strong microwave electric field radiation on: (1) vegetable seed germination and seedling growth rate," *Zemdirbyste*, vol. 100, no. 2, pp. 179–184, 2013.

[21] S. Lalléchère, S. Girard, D. Roux, P. Bonnet, F. Paladian, and A. Vian, "Mode Stirred Reverberation Chamber (MSRC): a large and efficient tool to lead high frequency bioelectromagnetic in vitro experimentation," *Progress in Electromagnetics Research B*, vol. 26, pp. 257–290, 2010.

[22] G. Cogalniceanu, M. Radu, D. Fologea, and A. Brezeanu, "Short high-voltage pulses promote adventitious shoot differentiation from intact tobacco seedlings," *Electro- and Magnetobiology*, vol. 19, no. 2, pp. 177–187, 2000.

[23] K. Dymek, P. Dejmek, V. Panarese et al., "Effect of pulsed electric field on the germination of barley seeds," *LWT—Food Science and Technology*, vol. 47, no. 1, pp. 161–166, 2012.

[24] B. Cadilhon, L. Pécastaing, S. Vauchamp, J. Andrieu, V. Bertrand, and M. Lalande, "Improvement of an ultra-wide-band antenna for high-power transient applications," *IET Microwaves, Antennas and Propagation*, vol. 3, no. 7, pp. 1102–1109, 2009.

[25] M. Răcuciu, S. Miclăuş, and D. E. Creangă, "Non-thermal, continuous and modulated rf field effects on vegetal tissue developed from exposed seeds," in *Electromagnetic Field, Health and Environment*, A. Krawczyk, R. Kubacki, S. Wiak, and C. Lemos Antunes, Eds., vol. 29 of *Studies in Applied Electromagnetics and Mechanics*, pp. 142–148, IOS Press, Amsterdam, The Netherlands, 2008.

[26] D. B. Jones, G. P. Bolwell, and G. J. Gilliatt, "Amplification, by pulsed electromagnetic fields, of plant growth regulator induced phenylalanine ammonia-lyase during differentiation in suspension cultured plant cells," *Electromagnetic Biology and Medicine*, vol. 5, no. 1, pp. 1–12, 1986.

[27] V. P. Sharma, H. P. Singh, D. R. Batish, and R. K. Kohli, "Cell phone radiations affect early growth of vigna radiate (Mung Bean) through biochemical alterations," *Zeitschrift für Naturforschung C*, vol. 65, no. 1-2, pp. 66–72, 2010.

[28] A. Kumar, H. P. Singh, D. R. Batish, S. Kaur, and R. K. Kohli, "EMF radiations (1800 MHz)-inhibited early seedling growth of maize (*Zea mays*) involves alterations in starch and sucrose metabolism," *Protoplasma*, pp. 1–7, 2015.

[29] M. Kouzmanova, M. Dimitrova, D. Dragolova, G. Atanasova, and N. Atanasov, "Alterations in enzyme activities in leaves after exposure of *Plectranthus Sp.* plants to 900 MHZ electromagnetic field," *Biotechnology & Biotechnological Equipment*, vol. 23, supplement 1, pp. 611–615, 2009.

[30] S. Radic, P. Cvjetko, K. Malaric, M. Tkalec, and B. Pevalek-Kozlina, "Radio frequency electromagnetic field (900 MHz) induces oxidative damage to DNA and biomembrane in tobacco shoot cells (Nicotiana tabacum)," in *Proceedings of the IEEE/MTT-S International Microwave*, pp. 2213–2216, IEEE, Honolulu, Hawaii, USA, June 2007.

[31] Y.-P. Chen, J.-F. Jia, and Y.-J. Wang, "Weak microwave can enhance tolerance of wheat seedlings to salt stress," *Journal of Plant Growth Regulation*, vol. 28, no. 4, pp. 381–385, 2009.

[32] V. P. Sharma, G. Singh, and R. K. Kohli, "Effect of mobile phone EMF on biochemical changes in emerging seedlings of *Phaseolus aureus* Roxb," *The Ecoscan*, vol. 3, no. 3-4, pp. 211–214, 2009.

[33] H. Zare, S. Mohsenzadeh, and A. Moradshahi, "Electromagnetic waves from GSM a mobile phone simulator and abiotic stress in *Zea mays* L," *Journal of Nutrition & Food Sciences*, vol. S11, p. 3, 2015.

[34] M.-L. Soran, M. Stan, Ü. Niinemets, and L. Copolovici, "Influence of microwave frequency electromagnetic radiation on terpene emission and content in aromatic plants," *Journal of Plant Physiology*, vol. 171, no. 15, pp. 1436–1443, 2014.

[35] M. Rammal, F. Jebai, H. Rammal, and W. H. Joumaa, "Effects of long term exposure to RF/MW radiations on the expression of mRNA of stress proteins in *Lycopersicon esculentum*," *WSEAS Transactions on Biology and Biomedicine*, vol. 11, pp. 10–14, 2014.

[36] J. C. Engelmann, R. Deeken, T. Müller, G. Nimtz, M. R. G. Roelfsema, and R. Hedrich, "Is gene activity in plant cells affected by UMTS-irradiation? A whole genome approach," *Advances and Applications in Bioinformatics and Chemistry*, vol. 1, pp. 71–83, 2008.

[37] A. Scialabba and C. Tamburello, "Microwave effects on germination and growth of radish (*Raphanus sativus* L.) seedlings," *Acta Botanica Gallica*, vol. 149, no. 2, pp. 113–123, 2002.

[38] A. Akbal, Y. Kiran, A. Sahin, D. Turgut-Balik, and H. H. Balik, "Effects of electromagnetic waves emitted by mobile phones on germination, root growth, and root tip cell mitotic division of *Lens culinaris* Medik," *Polish Journal of Environmental Studies*, vol. 21, no. 1, pp. 23–29, 2012.

[39] Y. C. Chen and C. Chen, "Effects of mobile phone radiation on germination and early growth of different bean species," *Polish Journal of Environmental Studies*, vol. 23, no. 6, pp. 1949–1958, 2014.

[40] M. Răcuciu, C. Iftode, and S. Miclaus, "Inhibitory effects of low thermal radiofrequency radiation on physiological parameters of Zea mays seedlings growth," *Romanian Journal of Physics*, vol. 60, no. 3-4, pp. 603–612, 2015.

[41] L. Ragha, S. Mishra, V. Ramachandran, and M. S. Bhatia, "Effects of low-power microwave fields on seed germination and growth rate," *Journal of Electromagnetic Analysis and Applications*, vol. 3, no. 5, pp. 165–171, 2011.

[42] S. Sharma and L. Parihar, "Effect of mobile phone radiation on nodule formation in the leguminous plants," *Current World Environment Journal*, vol. 9, no. 1, pp. 145–155, 2014.

[43] A. O. Oluwajobi, O. A. Falusi, and N. A. Zubbair, "Flower bud abscission reduced in hibiscus sabdariffa by radiation from GSM mast," *Environment and Pollution*, vol. 4, no. 1, 2014.

[44] M. Tafforeau, M.-C. Verdus, V. Norris et al., "Plant sensitivity to low intensity 105 GHz electromagnetic radiation," *Bioelectromagnetics*, vol. 25, no. 6, pp. 403–407, 2004.

[45] A. Grémiaux, S. Girard, V. Guérin et al., "Low-amplitude, high-frequency electromagnetic field exposure causes delayed and reduced growth in Rosa hybrida," *Journal of Plant Physiology*, vol. 190, pp. 44–53, 2016.

[46] V. J. Berdinas-Torres, *Exposure's systems and dosimetry of large-scale in vivo studies [Ph.D. thesis]*, Swiss Federal Institute of Technology, Zürich, Switzerland, 2007.

[47] M. J. Van Wyk, M. Bingle, and F. U. C. Meyer, "Antenna modeling considerations for accurate SAR calculations in human phantoms in close proximity to GSM cellular base station antennas," *Bioelectromagnetics*, vol. 26, no. 6, pp. 502–509, 2005.

[48] S. Miclăuş and M. Răcuciu, "A dosimetric study for experimental exposures of vegetal tissues to radiofrequency fields," in *Electromagnetic Field, Health and Environment*, A. Krawczyk, R. Kubacki, S. Wiak, and C. Lemos Antunes, Eds., vol. 29 of *Studies in Applied Electromagnetics and Mechanics*, pp. 133–141, IOS Press, Amsterdam, The Netherlands, 2008.

[49] J. León, M. C. Castillo, A. Coego, J. Lozano-Juste, and R. Mir, "Diverse functional interactions between nitric oxide and abscisic acid in plant development and responses to stress," *Journal of Experimental Botany*, vol. 65, no. 4, pp. 907–921, 2014.

[50] Y.-P. Chen, J.-F. Jia, and X.-L. Han, "Weak microwave can alleviate water deficit induced by osmotic stress in wheat seedlings," *Planta*, vol. 229, no. 2, pp. 291–298, 2009.

[51] Z.-B. Qiu, J.-L. Guo, M.-M. Zhang, M.-Y. Lei, and Z.-L. Li, "Nitric oxide acts as a signal molecule in microwave pretreatment induced cadmium tolerance in wheat seedlings," *Acta Physiologiae Plantarum*, vol. 35, no. 1, pp. 65–73, 2013.

[52] R. K. Jangid, R. Sharma, Y. Sudarsan, S. Eapen, G. Singh, and A. K. Purohit, "Microwave treatment induced mutations and altered gene expression in *Vigna aconitifolia*," *Biologia Plantarum*, vol. 54, no. 4, pp. 703–706, 2010.

[53] A. Vian, C. Henry-Vian, and E. Davies, "Rapid and systemic accumulation of chloroplast mRNA-binding protein transcripts after flame stimulus in tomato," *Plant Physiology*, vol. 121, no. 2, pp. 517–524, 1999.

[54] J. A. Teixeira da Silva and J. Dobránszki, "Magnetic fields: how is plant growth and development impacted?" *Protoplasma*, 2015.

[55] M. D. H. J. Senavirathna, T. Asaeda, B. L. S. Thilakarathne, and H. Kadono, "Nanometer-scale elongation rate fluctuations in the *Myriophyllum aquaticum* (Parrot feather) stem were altered by radio-frequency electromagnetic radiation," *Plant Signaling and Behavior*, vol. 9, no. 4, Article ID e28590, 2014.

[56] M. Ursache, G. Mindru, D. E. Creangă, F. M. Tufescu, and C. Goiceanu, "The effects of high frequency electromagnetic waves on the vegetal," *Romanian Journal of Physics*, vol. 5, no. 1-2, pp. 133–145, 2009.

[57] E. A. M. Hamada, "Effects of microwave treatment on growth, photosynthetic pigments and some metabolites of wheat," *Biologia Plantarum*, vol. 51, no. 2, pp. 343–345, 2007.

[58] M. D. H. J. Senavirathna, A. Takashi, and Y. Kimura, "Short-duration exposure to radiofrequency electromagnetic radiation alters the chlorophyll fluorescence of duckweeds (Lemna minor)," *Electromagnetic Biology and Medicine*, vol. 33, no. 4, pp. 327–334, 2014.

[59] Y. Shckorbatov, "The main approaches of studying the mechanisms of action of artificial electromagnetic fields on cell," *Journal of Electrical & Electronic Systems*, vol. 3, no. 2, 2014.

[60] A. M. Pietak, "Structural evidence for electromagnetic resonance in plant morphogenesis," *BioSystems*, vol. 109, no. 3, pp. 367–380, 2012.

[61] A. Amat, J. Rigau, R. W. Waynant, I. K. Ilev, and J. J. Anders, "The electric field induced by light can explain cellular responses to electromagnetic energy: a hypothesis of mechanism," *Journal of Photochemistry and Photobiology B: Biology*, vol. 82, no. 2, pp. 152–160, 2006.

[62] Z. Qiu, J. Li, Y. Zhang, Z. Bi, and H. Wei, "Microwave pretreatment can enhance tolerance of wheat seedlings to $CdCl_2$ stress," *Ecotoxicology and Environmental Safety*, vol. 74, no. 4, pp. 820–825, 2011.

[63] Y.-P. Chen, "Microwave treatment of eight seconds protects cells of Isatis indigotica from enhanced UV-B radiation lesions," *Photochemistry and Photobiology*, vol. 82, no. 2, pp. 503–507, 2006.

Hindawi Publishing Corporation
BioMed Research International
Volume 2015, Article ID 823806, 8 pages
http://dx.doi.org/10.1155/2015/823806

Research Article

Reference Gene Selection for qPCR Normalization of *Kosteletzkya virginica* under Salt Stress

Xiaoli Tang,[1,2] Hongyan Wang,[1,2,3] Chuyang Shao,[4] and Hongbo Shao[1,5]

[1] *Key Laboratory of Coastal Biology & Bioresources Utilization, Yantai Institute of Coastal Zone Research (YIC), Chinese Academy of Sciences (CAS), Yantai 264003, China*
[2] *University of Chinese Academy of Sciences, Beijing 100039, China*
[3] *Yantai Academy of China Agricultural University, Yantai 264670, China*
[4] *College of Life Sciences, Shandong Agricultural University, Taian 271018, China*
[5] *Institute of Agro-Biotechnology, Jiangsu Academy of Agricultural Sciences, Nanjing 210014, China*

Correspondence should be addressed to Hongbo Shao; shaohongbochu@126.com

Received 23 June 2015; Revised 9 August 2015; Accepted 11 August 2015

Academic Editor: Raul A. Sperotto

Kosteletzkya virginica (L.) is a newly introduced perennial halophytic plant. Presently, reverse transcription quantitative real-time PCR (qPCR) is regarded as the best choice for analyzing gene expression and its accuracy mainly depends on the reference genes which are used for gene expression normalization. In this study, we employed qPCR to select the most stable reference gene in *K. virginica* which showed stable expression profiles under our experimental conditions. The candidate reference genes were 18S ribosomal RNA (*18SrRNA*), β-actin (*ACT*), α-tubulin (*TUA*), and elongation factor (*EF*). We tracked the gene expression profiles of the candidate genes and analyzed their stabilities through BestKeeper, geNorm, and NormFinder software programs. The results of the three programs were identical and *18SrRNA* was assessed to be the most stable reference gene in this study. However, *TUA* was identified to be the most unstable. Our study proved again that the traditional reference genes indeed displayed a certain degree of variations under given experimental conditions. Importantly, our research also provides guidance for selecting most suitable reference genes and lays the foundation for further studies in *K. virginica*.

1. Introduction

Increasing amount of attention is paid to transcriptome analysis. Actually, transcriptome analysis refers to the identification and measurement of the differentially expressed transcripts. Thus, the key of the transcriptome analysis still stays in the detection of the gene expression profiles. Northern blotting, semiquantitative reverse transcription-PCR, and reverse transcription quantitative real-time PCR (qPCR) are the three most common and frequently used methods [1]. It is due to its high specificity, sensitivity, and extensive quantification range that qPCR has become the first choice for gene expression profiles analysis [2, 3]. Meanwhile, it is also used for the validation of the high throughput sequencing and microarray results [4]. On the other hand, the results of qPCR can be significantly influenced by a series of factors including the condition of the material, the extraction of the RNA, the operational process, and the synthesis of the cDNA [5]. Hence, the internal reference control which acts as a normalization factor is required to minimize the above disturbances. The ideal internal reference genes were supposed to be equally expressed in different samples, developmental stages, and tissues. Only in this way they can be applied to measure the expressions of the other genes [1]. Therefore, the selection of the reference genes is of paramount importance for the veracity of qPCR.

Generally, the reference genes such as 18S ribosomal RNA (*18SrRNA*), β-actin (*ACT*), α-tubulin (*TUA*), and elongation factor (*EF*) were used for normalization. Their expression levels stay stable under various experimental conditions usually [6]. However, latest studies have shown that no-one reference gene is able to stand stable under different experimental conditions, or in other words we have to select a suitable reference gene for a given situation [7]. Different

software tools or statistical procedures have been developed to identify the suitable reference genes for a given experimental condition. For example, the most widely used software tools are BestKeeper, geNorm, and NormFinder. Now a growing number of reports suggest that a specific experiment model needs a corresponding suitable reference gene. With the help of the above software tools, the identification of the reference genes for plants has advanced greatly. Up to now, *Arabidopsis thaliana* [8], wheat [9], barley [10], rice [11], soybean [12], potato [13], grape [14], poplar [15], tomato [16], chicory [17], tobacco [18], longan [19], sugarcane [20], *Brassica juncea* [21], buckwheat [22], tung tree [23], and coffee [23] have been reported about the selection of the appropriate reference genes under various conditions. However, there is not any report about the identification of reference genes so far in *K. virginica* [24].

K. virginica, which is also known as seashore mallow (SM), is a perennial halophytic species native to Mid-Atlantic coasts and Southeastern of the United States [25, 26]. It is a noninvasive species newly introduced into China as an important salt-resistant oil crop in 1992. Its stem and tuberous root are suitable material for producing bioenergy [27]. Its salt-resistance ability is strong; for example, it was reported that it could lead to a normal growth and development in adverse environment with 0.3% to 2.5% sodium salt [28]. Therefore, *K. virginica* is considered to be an ideal plant for the investigation of salt-resistance mechanisms. Indeed, many scientists have focused on this characteristic and made some findings [29]. Most of the studies on *K. virginica* only came down to the physiological features including plant growth, water status, potassium concentrations, lipid peroxidation, and soluble sugar contents, yet studies on gene expression and molecular level were rare. On account of that *K. virginica* is a nonmodal plant with little information on gene sequences; thus, the researches on cellular and molecular levels become much harder.

In order to guarantee the accuracy of the qPCR, the selection and determination of the reference gene are of utmost importance. Here we adopted homology-based cloning strategy to acquire the partial sequences of the typical reference genes. Two treatment groups with different time and concentrations salt treatments were used to identify the stable reference genes for verification. The experimental samples comprehensively stand for the salt treatments and the application of the three software tools ensure the accuracy of the statistical analysis. Our results revealed that the commonly used reference genes indeed displayed a certain degree of fluctuations and *18SrRNA* or the *18SrRNA* and *ACT* pair will be the wise choice for the gene expression normalization for *K. virginica* under salt treatments.

2. Material and Methods

Statement. The Yellow River Delta Reserve permitted the collecting of plant samples. The field studies did not involve endangered or protected species. The field also belongs to our institution: The Seaside Wetland Eco-Experimental Station of Chinese Academy of Sciences, Yantai Institute of Coastal Zone Research (YIC), Chinese Academy of Sciences (CAS), Yantai 264003, China.

2.1. Plant Sample Preparation. In our study the *K. virginica* seeds were harvested from *The Seaside Wetland Eco-Experimental Station of Chinese Academy of Sciences,* Yellow River Delta, Shandong Province, China. The stripped seeds were sterilized firstly in 70% alcohol for 5 min and 0.1% mercuric chloride for 10 min and then rinsed with sterile distilled water for several times. The sterilized seeds were fostered in liquid MS for germination with a culture temperature at 25°C. The germinal seeds were transferred to plastic pots filled with vermiculite for further cultivation. The condition of culture was kept at 16 h light/8 h dark with 25/18°C with artificial climatic chambers (Huier, China) and the humidity was kept at 65%. The homogeneous two-week-old *K. virginica* seedlings were used for NaCl treatments. The seedlings in three plastic pots (about 15 plants) were used for an experimental sample. The harvested samples (whole plant) were quickly frozen in liquid nitrogen and stored in −80°C. For different NaCl treatments over times, the concentration of the NaCl was 300 mM and the processing times were 2 h, 6 h, 12 h, and 24 h, respectively. The samples were harvested at 2 h, 6 h, 12 h, and 24 h after NaCl treatment. For different concentrations, the samples were treated with 100, 200, 300, and 400 mM NaCl for 24 h, respectively.

2.2. Total RNA Isolation and cDNA Synthesis. All samples were collected from the corresponding *K. virginica* whole seedlings. Total RNA samples were extracted from young seedlings with Trizol Reagent (Invitrogen Carlsbad, CA, USA). The nucleic acid concentrations and the quality of the RNA were determined by microspectrophotometer NanoDrop 2000C (Thermo Scientific). All RNA samples had a 260/280 ratio at 1.8–2.0 and the ratio of 260/230 >2.0. The synthesis of cDNA was carried out with TransScrip One-Step gDNA Removal and cDNA Synthesis SuperMix (Transgen Biotech). Both Oligo (dT) 18 and random primers were used for the reverse transcription. The 20 μL reaction system was performed at 42°C 30 min and 85°C 5 min. The concentrations of the synthesized cDNA were also measured by microspectrophotometer and then diluted down to 100 ng/μL, which was required for qPCR.

2.3. Selection of Candidate Reference Genes and Primer Design. The most common reference genes in other plants were selected: *ACT*, *EF*, *TUA,* and *18SrRNA* (Table 1). In view of that the gene sequence of *K. virginica* is almost blank, so the gene sequences of other close relative species are used. *Gossypium hirsutum* is the closest species to *K. virginica* with known genome sequences and most of the reference genes were conserved housekeeping genes. Thus, the sequences of *ACT, EF, TUA,* and *18SrRNA* in *Gossypium hirsutum* were used to index the conserved and homologous sequence of these genes from the National Center for Biotechnology Information (NCBI) (http://www.ncbi.nlm.nih.gov/) database [30]. The primers for PCR were designed based on those conserved sequences by Primer Premier 5.0. The partial

Table 1: Candidate reference genes and the PCR primer sequences for *K. virginica*.

Gene name	Function	Primer	Sequence	Length (bp)
ACTIN	Structural constituent of cytoskeleton	act-F	GTTGGGATGGGTCAGA	800
		act-R	CCTTGCTCATACGGTCA	
EF1α	Elongation factor 1 alpha	EF-F	GGTCATTCAAGTATGCCTGG	740
		EF-R	GAACCCAACATTGTCACCAG	
TUA	Cytoskeleton structural protein	TUA-F	GTTTTCAGTGCTGTTGGAGGT	700
		TUA-R	AACGCTGGTTGAGTTGGA	
18SrRNA	18S ribosomal RNA	18S-F	GAGTATGGTCGCAAGGCTGAA	640
		18S-R	CCTCTAAATGATAAGGTTCAGTGG	

Table 2: Candidate reference genes and the qPCR primer sequences in *K. virginica*.

Gene name	Function	Primer	Sequence	Length (bp)
ACTIN	Structural constituent of cytoskeleton	actqPCR-F	TTATGTTGCCCTGGACT	160
		actqPCR-R	CCGCTTCCATCCCTA	
EF1α	Elongation factor 1 alpha	EFqPCR-F	TCAATGAGCCAAAGAGG	120
		EFqPCR-R	CAACACGACCAACAGGA	
TUA	Cytoskeleton structural protein	TUAqPCR-F	TATCTCATCTCTCACAGCCTG	119
		TUAqPCR-R	GGGCATACGAGGAAAGCAT	
18SrRNA	18S ribosomal RNA	18SqPCR-F	CCGTTCTTAGTTGGTGGA	170
		18SqPCR-R	AACATCTAAGGGCATCACAG	

conserved sequences of the candidate genes obtained were at about 600 bp in *K. virginica*. The PCR primers were shown in Table 1. The PCR products were detected by 1.0% agarose gel and displayed expected size and the segment of products were sequenced from Applied Biosystems Invitrogen. The nucleic acid sequences of PCR products were confirmed with BLAST in the National Center for Biotechnology Information too (http://www.ncbi.nlm.nih.gov/). The primers of the candidate reference genes for qPCR were designed by Beacon Designer 7 according to the sequencing results of the PCR products. The qPCR primer sequences were displayed in Table 2. In addition, the qPCR primers amplification specificity of the newly sequenced reference genes was confirmed firstly through RT-PCR with a single product, respectively (Figure 1).

2.4. Two-Step Quantitative Real-Time RT-PCR. We carried out qPCR with ABI Prism 7500 FAST (Applied Biosystems, Foster City, CA) and SYBR Green Real-Time Selected Master Mix (Applied Biosystems by Life Technologies) according to the user guide. The reaction volume was 20 μL with 2 μL diluted cDNA, 10 μL 2 × SYBR Master Mix, and 200 nM of each primer. The thermocycling reaction processes were as follows: initial denaturation at 95°C 2 min, 45 cycles of 15 s at 95°C for denaturation of template, and 1 min at 60°C for annealing and extension. The fluorescent dye SYBR Green which was widely used in qPCR can combine with the ds-cDNA to indicate accurately the synthetic cDNA in the reaction system. The fluorescence signal detection was carried out at a temperature of 60–90°C. The primer specificity was confirmed again by the typical melting curve and amplification plot. The Cq values of all the samples were controlled in appropriate scope [31]. All samples were amplified in triplicates and three biological replicates were performed. The Cq values and the corresponding numerical value were imported into Microsoft Excel and used for further analysis.

2.5. Data Analysis. The obtained data were converted into the required format according to the different demands of the software tools. Three different applets were used for the data analysis: geNorm (version 3.4), NormFinder (version 0.953), and BestKeeper (version 1.0). The concrete data analysis strategies were described in results. In addition, ANOVA was applied to determine whether the Cq values among the different treatments were significant.

3. Results

3.1. Selection of Candidate Reference Genes. Due to bottleneck of the extremely limited sequence information of *K. virginica* (L.), there is not any existing gene information which we can adopt directly. By means of homology-based cloning, we at last acquired four genes' fragment (*ACT*, *EF*, *18SrRNA,* and *TUA*) and designed the qPCR primers based on the obtained partial gene sequences. The selected reference genes for this study displayed different important functions and components in cell. Generally, they were highly conserved and used for normalization of qPCR in many other species. Therefore, we turned to the existing sequence information in GeneBank for PCR primer design. First of all, we obtained a single 600–800 bp PCR product through each pair primer with the expected size, and then the products were sequenced. Thus, we acquired the specific fragment sequence of the candidate

Table 3: Homologous comparison of the candidate genes between *K. virginica* and other species.

Gene name	Function	Blastn (*E* value)	Identity (%)	The specie with highest homolog
ACTIN	Structural constituent of cytoskeleton	0.0	94	*Gossypium hirsutum*
EF1α	Elongation factor 1 alpha	0.0	93	*Theobroma cacao*
TUA	Cytoskeleton structural protein	0.0	93	*Gossypium hirsutum*
18SrRNA	18S ribosomal RNA	0.0	99	*Pavonia spinifex voucher*

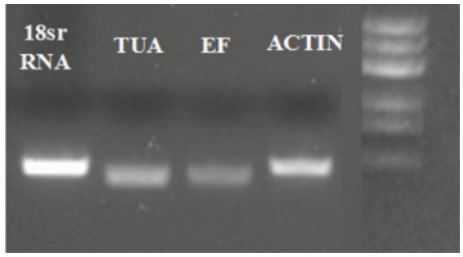

Figure 1: Identification of primer specificity for qPCR amplification by PCR. All detected cDNA were mixed to act as template and the equal amounts of template were used for PCR amplification. 1.0% agarose gel electrophoresis displayed the PCR products of each primer pair.

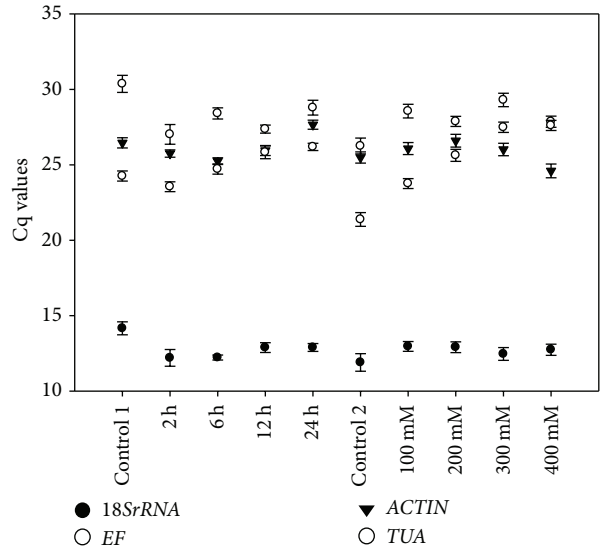

Figure 2: Cq values for the candidate reference genes. The Cq values were used to display the expression profiles of the candidate genes in 10 samples. Control 1 was the sample under normal condition without NaCl treatment in different time period group; control 2 was the sample under normal condition without NaCl in different concentration group.

genes and in addition the Blastn results showed that these sequences of genes from *K. virginica* were highly homologous with *Gossypium hirsutum*, *Populus trichocarpa,* and *Theobroma cacao* L. Table 3 shows the comparison results of the obtained sequences in *K. virginica* with *Gossypium hirsutum* and the species with the highest homology. Finally, the primers for qPCR were designed according to the sequencing results and the PCR results showed that all the qPCR primers exhibited a high degree of specificity (Figure 1).

3.2. Expression Profiles of the Candidate Reference Genes under Various Salt Treatments in K. virginica. To assess the expression stabilities of the four candidate reference genes, their expression variations were estimated by qPCR in 10 cDNA samples. The 10 samples belong to two experimental groups. The time group contains 5 samples, namely, control 1, 2 h, 6 h, 12 h, and 24 h. The concentration group includes control 2, 100 mM, 200 mM, 300 mM, and 400 mM NaCl treatments. The qPCR was performed according to the two-step quantitative real-time PCR. All the related parameters of qPCR were controlled in the demanded ranges. The expression profiles of the candidate reference genes were shown in Figure 2. The expression of the candidate genes throughout all samples represented by cycle threshold (Cq) values showed changes to some degree [32]. The Cq values of the studied reference genes fluctuated from 11.71 to 31.14 in all samples of the two experimental groups (Figure 2).

3.3. Expression Stability Analysis. Due to the various behaviors of the candidate reference genes, we need some methods of data handling to evaluate the stability of the candidate genes under a certain condition. In order to pick out the optimal reference gene, we adopted the analysis software tools of BestKeeper, geNorm, and NormFinder, which were used extensively in the identification of the reference genes. BestKeeper is an Excel-based tool and it ranks the candidate reference genes with the calculation of the BestKeeper index [1]. Under BestKeeper analysis, the best reference gene shows the strongest correlation with the BestKeeper index. The geNorm is a Visual Basic application tool and gene expression value is evaluated by *M* value. This algorithm compares the *M* values of the candidate genes and eliminates the gene with the highest *M* value, and two genes are left at last. Thus, the last two genes which have the lowest *M* value are regarded as the best pair of the candidate genes [33]. NormFinder is also a Visual Basic application applet. It identifies the optimal reference gene through a model-based approach [34]. Similar to geNorm, a low SD value means a more stable expression profile of the gene in this algorithm.

3.3.1. geNorm. This software is one of the Visual Basic application tools for Microsoft Excel. It picks out the most stable reference genes from a given sample and figures out the gene expression normalization factors according to the geometric mean of the candidate genes. The parameter employed by geNorm to measure the stability of the candidate gene is the average expression stability (*M*) value.

Table 4: Analysis of the candidate reference genes in view of the stability values estimated by NormFinder.

Gene name	Stability value (two subgroups)	Stability value (no subgroups)	Intragroup variation		Intergroup variation	
			1	2	1	2
18SrRNA	0.064	0.234	0.071	0.052	0.007	−0.007
EF1α	0.132	0.583	0.651	0.047	0.059	−0.059
ACTIN	0.145	0.596	0.120	0.605	0.069	−0.069
TUA	0.286	1.164	0.543	2.196	−0.134	0.134

The *M* value is calculated according to the average pairwise variation between all detected genes. The lower *M* value stands for the higher stability of the gene expression [31]. The analysis result of geNorm was displayed in Figures 3(a) and 3(b). For the treatment samples at different points in time, *18SrRNA* and *ACT* were the most stable reference genes (Figure 3(a)). The *EF* gene was estimated to be the least stable among them. For the samples with different concentration treatments, *18SrRNA* and *ACT* were the most stable reference genes (Figure 3(b)), while the least stable gene was *TUA*. In addition, the comparison between two experimental conditions suggested that the variations were more significant under different concentrations. Therefore, according to the analysis of geNorm, *18SrRNA* and *ACT* are the optional reference genes for the normalization of gene expression under NaCl treatments in *K. virginica*.

3.3.2. NormFinder. For further verification, NormFinder was also adopted for the assessment. NormFinder is also a Visual Basic application tool for Microsoft Excel. It is an Add-In for Microsoft Excel; namely, the NormFinder function is added directly to the Microsoft Excel software package. For this algorithm, the more stable genes have lower stability values [34]. NormFinder is able to estimate the intra- and intergroup variations as well as all samples. The assessment results of NormFinder were shown in Table 4. It is worth noting that there were certain differences in the analysis between no subgroups and two subgroups in the stability values. The trend of the two assessments was the same and the no subgroups analysis showed higher stability values. The ranking of the reference genes in terms of their expression stabilities is identical (Table 4). *18SrRNA* was estimated to be the most stable reference gene in NormFinder with the stability value at 0.064. However, *TUA* showed the most unstable expression profiles with the largest stability value at 0.286 in two subgroups' result. Therefore, the ranking of the candidate reference genes under various NaCl treatments was *18SrRNA*>*EF*>*ACT*>*TUA*. For no subgroups analysis, the outcome is the same except for the different stability values. Combining the results of geNorm and NormFinder, we can come to a conclusion that the *18SrRNA* or *18SrRNA* and *ACTIN* pair should be the best reference genes for gene expression normalization in *K. virginica* under salt treatments.

3.3.3. BestKeeper. BestKeeper is an Excel-based spreadsheet software application. Different from the above two tools, the raw Cq values without any conversion can be loaded

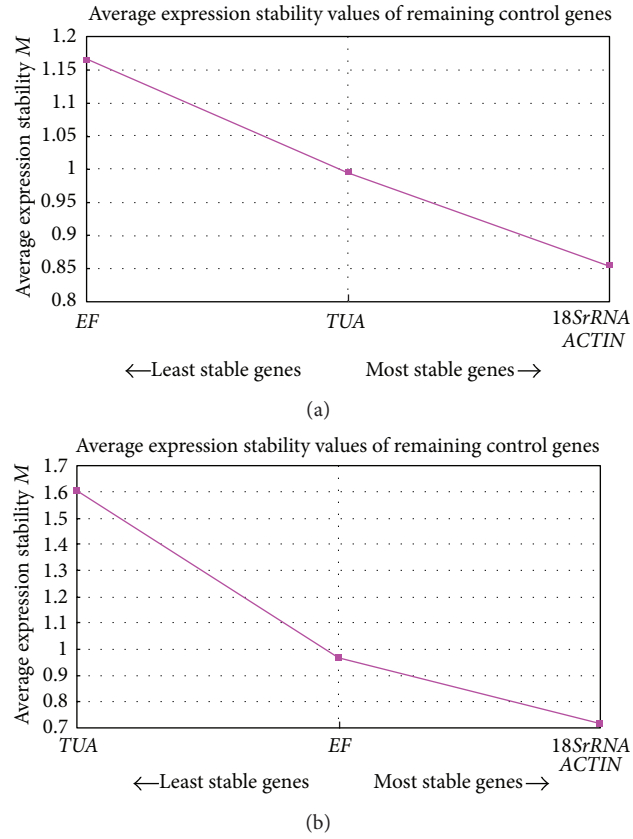

Figure 3: Average expression stability (*M*) values of the candidate genes. The average expression stability (*M*) values are acquired through the stepwise exclusion of the least stable reference gene. Starting from the least stable gene at the left, the genes are ranked according to the ascending expression stability, ending with the two most stable genes at the right. The result of time treatment is shown in (a) and the concentration treatment is displayed in (b).

in for analysis in BestKeeper. When the original Cq values were imported, the descriptive statistics of each candidate gene were computed, including GM (geometric mean), AM (arithmetic mean), SD (standard deviation), CV (coefficient of variance), Min (minimal), and Max (maximal) [8]. The expression stabilities of the candidate genes were calculated in accordance with the inspection of calculated variations (SD and CV values). The analysis results in this study were displayed in Tables 5(a) and 5(b) and the analysis was also carried out in two ways with all samples and with two subgroups. The calculated results either in all samples or in two subgroups were unanimous with the same two optimal reference genes *18SrRNA* and *ACT*, yet the least

stable reference genes were *EF* and *TUA*. The relative higher Pearson's coefficients of correlation demonstrated that the expression profiles of these genes were altered under NaCl treatment. In brief, the BestKeeper result stayed the same with the outcomes of NormFinder and geNorm. Therefore, *18SrRNA* or *18SrRNA* and *ACTIN* pair should be the ideal reference genes for gene expression normalization in *K. virginica* under various NaCl treatments among the four candidate reference genes.

4. Discussions

K. virginica, a noninvasive species, was imported into China for its salt resistance [33]. Its importance appears due to its ability to survive and develop under high salt environment, which is the goal of salt-resistant crops research. Ever since its introduction, the researches focusing on it are ongoing, but most of them are about physiological researches [1, 29]. The studies at the level of cells and genes are rare. The only reports so far on gene expression detection in *K. virginica* took *ACT* as reference gene for gene expression normalization [31]. Therefore, in order to understand *K. virginica* at the molecular level to find its specific mechanisms for salt-resistance, the selection of the stable reference genes for gene expression normalization in *K. virginica* is imperative. In this study, *18SrRNA* was demonstrated to be the optimal under salt stress conditions.

The traditional reference genes such as *ACT*, *TUA*, UBQ, and *EF* which are often used as internal reference genes in *Arabidopsis* were also found to alter under some condition [35]. Thus, the selection of the reference genes under a given condition is necessary. Fortunately, we can simplify the complicated confirmation of the reference genes with the help of the designed statistical algorithms. BestKeeper [36], geNorm [33], deltaCq [34], RefFinder [37], and NormFinder [38] are the commonly used software tools to assess the expression stability of the candidate reference genes. In our study, the BestKeeper, geNorm, and NormFinder were employed to calculate the stabilities of the four candidate reference genes in *K. virginica*. The results of the three algorithms revealed that *18SrRNA* and *ACT* were estimated to be the most stable reference genes in two experiment sets on the basis of the geNorm analysis, while the most unstable genes were *EF* and *TUA,* respectively (Figure 3). Duo to the stepwise exclusion method used by geNorm for stability analysis, there will be two ideal reference genes in Figure 3. As a matter of fact, the *M* values of *18SrRNA* were smaller than *ACT* in both experimental conditions. For NormFinder analysis, the *18SrRNA* obtained the smallest stability value with 0.064 which was the same with geNorm outcome (Table 4). The values of the intragroup variation and the intergroup variation of *18SrRNA* were the minimum among all the candidate genes demonstrating again that *18SrRNA* was the best choice for this study. But the difference was the second stable reference genes and they were *ACT* and *EF* in geNorm and NormFinder, respectively. The *TUA* was determined to be the worst one again. In BestKeeper, the *18SrRNA* was still assessed to be the most stable reference gene with the smallest SD value keeping consistent with the previous two assessments. The second stable reference gene was *ACT* with the SD value at 0.61, but its coefficient of correlation (r) and P value were not ideal. *EF* and *TUA* were estimated to obtain the SD value at 1.00 and 1.51, respectively, which implied that they could not be used for internal reference gene any more. In addition, we can choose more than one reference gene to ensure the accuracy of the study. In this study, the *18SrRNA* and *ACTIN* pair gave the best performance under salt stress.

Generally, *ACT* is the most widely used internal reference gene under some conditions. Yet, in our research the stability value of *ACT* based on NormFinder analysis was higher than *18SrRNA* and *EF* (Table 4). Besides, *18SrRNA* has also been widely used as stable reference gene in many species such as *Arabidopsis* and Rice under particular conditions [39, 40]. Yet Kim et al. found that the expression of *18SrRNA* can be effected by some biological factor and drug; thus, *18SrRNA* may not be suitable for biotic stresses [41]. In our study the *18SrRNA* was proved to be the best reference gene for gene expression normalization in *K. virginica*. Meanwhile, *EF* is another important and widely used reference gene. In the selection of reference gene for Chinese cabbage (*Brassica rapa* L. ssp. *pekinensis*), *EF* was identified as the best choice for normalization in different tissues [34]. Meanwhile, *EF* was also the most stable gene in potato under salt and cold stresses, while the conclusion was not appropriate for Chinese cabbage under the same condition [39]. In our research for *K. virginica* under salt stress, *EF* was not the optimum, especially in the different time treatments under which *EF* was estimated to be the most unstable reference gene (Figure 3(a)). Despite the fact that *TUA* gene also often appeared in the candidate reference genes, our three analysis results all indicated that the expression profile of *TUA* had significant changes with high *M* value (Figure 3), low stability (Table 4), and high SD value (Tables 5(a) and 5(b)) and was not suitable for gene expression normalization in *K. virginica* under salt stress. Similarly, the researches on faba bean (*Vicia faba* L.) [14], banana [42], tomato [1], and *Salvia miltiorrhiza* [1, 17] all revealed that the *TUA* gene was not appropriate for gene expression normalization. In addition, in the research on tomato, the scientists emphasized that we should avoid choosing *TUA* as reference gene because its behavior was far from accepted in their findings [43].

5. Conclusion

In summary, our study indicated that the expression stability varied considerably under the various experimental conditions in *K. virginica*. With the help of the software tools of BestKeeper, geNorm, and NormFinder, *18SrRNA* was identified to be the most stable reference gene among the four candidate traditional reference genes, yet *TUA* appeared to be the most unsuitable reference gene in our analysis. The stable reference gene selected in this study will be very helpful for revealing the gene expression profiles in *K. virginica* under salt stress promoting the realization of it at cellular

Table 5: BestKeeper analysis results of the candidate reference genes.

(a)

Gene name	SD [±CP]			Coefficient of correlation (r)			P value		
	All samples	1	2	All samples	1	2	All samples	1	2
18SrRNA	0.43	0.53	0.33	0.76	0.83	0.75	0.001	0.001	0.001
EF1α	1.00	1.12	0.94	0.82	0.79	0.85	0.001	0.001	0.001
ACTIN	0.61	0.68	0.57	0.52	0.75	0.26	0.004	0.001	0.355
TUA	1.51	0.88	2.08	0.72	0.50	0.88	0.001	0.056	0.001

(b)

CV [%CP]			Min [x-fold]			Max [x-fold]			SD [±x-fold]		
All sample	1	2	All sample	1	2	All sample	1	2	All sample	1	2
3.41	4.14	2.63	−2.01	−1.65	−1.84	2.85	2.60	1.36	1.35	1.45	1.26
3.56	3.94	3.37	−5.95	−3.44	−5.15	7.92	6.85	3.93	2.00	2.17	1.92
2.35	3.54	2.20	−3.38	−2.06	−2.89	3.67	3.13	1.96	1.53	1.60	1.48
6.03	2.58	8.28	−12.5	−2.62	−13.3	7.59	3.22	7.16	2.85	1.80	4.24

1 stands for the different time period treatment and 2 stands for the different concentration treatment.

and gene level. Our study will lay the foundation for further investigation of the salt-resistant mechanism in halophyte as well.

Conflict of Interests

The authors declare that there is no conflict of interests regarding the publication of this paper.

Authors' Contribution

Xiaoli Tang and Hongyan Wang conceived and designed the experiments. Xiaoli Tang, Hongyan Wang, and Chuyang Shao performed the assays of NaCl treatments. Xiaoli Tang analyzed the data, carried out the RT-qPCR experiments, and wrote the paper. Hongbo Shao designed and supervised the study. Hongbo Shao and Xiaoli Tang revised and approved the final paper.

Acknowledgments

This research was partially supported by the National Natural Science Foundation of China (41171216), the National Basic Research Program of China (2013CB430403), Jiangsu Autonomous Innovation of Agricultural Science & Technology (CX(15)1005), Yantai Double-Hundred Talent Plan (XY-003-02), 135 Development Plan of YIC-CAS, and the Science & Technology Development Plan of Shandong Province (010GSF10208).

References

[1] I. Mallona, S. Lischewski, J. Weiss, B. Hause, and M. Egea-Cortines, "Validation of reference genes for quantitative real-time PCR during leaf and flower development in Petunia hybrida," *BMC Plant Biology*, vol. 10, article 4, 2010.

[2] V. Mafra, K. S. Kubo, M. Alves-Ferreira et al., "Reference genes for accurate transcript normalization in citrus genotypes under different experimental conditions," *PLoS ONE*, vol. 7, no. 2, Article ID e31263, 2012.

[3] M. L. Wong and J. F. Medrano, "Real-time PCR for mRNA quantitation," *BioTechniques*, vol. 39, no. 1, pp. 75–85, 2005.

[4] S. Artico, S. M. Nardeli, O. Brilhante, M. F. Grossi-de-Sa, and M. Alves-Ferreira, "Identification and evaluation of new reference genes in *Gossypium hirsutum* for accurate normalization of real-time quantitative RT-PCR data," *BMC Plant Biology*, vol. 10, article 49, 2010.

[5] J. V. Die, B. Román, S. Nadal, and C. I. González-Verdejo, "Evaluation of candidate reference genes for expression studies in *Pisum sativum* under different experimental conditions," *Planta*, vol. 232, no. 1, pp. 145–153, 2010.

[6] Z. Tong, Z. Gao, F. Wang, J. Zhou, and Z. Zhang, "Selection of reliable reference genes for gene expression studies in peach using real-time PCR," *BMC Molecular Biology*, vol. 10, article 71, 2009.

[7] N. Podevin, A. Krauss, I. Henry, R. Swennen, and S. Remy, "Selection and validation of reference genes for quantitative RT-PCR expression studies of the non-model crop Musa," *Molecular Breeding*, vol. 30, no. 3, pp. 1237–1252, 2012.

[8] C. L. Andersen, J. L. Jensen, and T. F. Ørntoft, "Normalization of real-time quantitative reverse transcription-PCR data: a model-based variance estimation approach to identify genes suited for normalization, applied to bladder and colon cancer data sets," *Cancer Research*, vol. 64, no. 15, pp. 5245–5250, 2004.

[9] T. Czechowski, M. Stitt, T. Altmann, M. K. Udvardi, and W.-R. Scheible, "Genome-wide identification and testing of superior reference genes for transcript normalization in arabidopsis," *Plant Physiology*, vol. 139, no. 1, pp. 5–17, 2005.

[10] A. R. Paolacci, O. A. Tanzarella, E. Porceddu, and M. Ciaffi, "Identification and validation of reference genes for quantitative RT-PCR normalization in wheat," *BMC Molecular Biology*, vol. 10, article 11, 2009.

[11] R. A. Burton, N. J. Shirley, B. J. King, A. J. Harvey, and G. B. Fincher, "The CesA gene family of barley. Quantitative analysis of transcripts reveals two groups of co-expressed genes," *Plant Physiology*, vol. 134, no. 1, pp. 224–236, 2004.

[12] M. Jain, A. Nijhawan, A. K. Tyagi, and J. P. Khurana, "Validation of housekeeping genes as internal control for studying gene expression in rice by quantitative real-time PCR," *Biochemical and Biophysical Research Communications*, vol. 345, no. 2, pp. 646–651, 2006.

[13] B. Jian, B. Liu, Y. Bi, W. Hou, C. Wu, and T. Han, "Validation of internal control for gene expression study in soybean by quantitative real-time PCR," *BMC Molecular Biology*, vol. 9, article 59, 2008.

[14] N. Nicot, J.-F. Hausman, L. Hoffmann, and D. Evers, "Housekeeping gene selection for real-time RT-PCR normalization in potato during biotic and abiotic stress," *Journal of Experimental Botany*, vol. 56, no. 421, pp. 2907–2914, 2005.

[15] K. E. Reid, N. Olsson, J. Schlosser, F. Peng, and S. T. Lund, "An optimized grapevine RNA isolation procedure and statistical determination of reference genes for real-time RT-PCR during berry development," *BMC Plant Biology*, vol. 6, article 27, 2006.

[16] A. M. Brunner, I. A. Yakovlev, and S. H. Strauss, "Validating internal controls for quantitative plant gene expression studies," *BMC Plant Biology*, vol. 4, article 14, 2004.

[17] M. Expósito-Rodríguez, A. A. Borges, A. Borges-Pérez, and J. A. Pérez, "Selection of internal control genes for quantitative real-time RT-PCR studies during tomato development process," *BMC Plant Biology*, vol. 8, article 131, 2008.

[18] A. Maroufi, E. Van Bockstaele, and M. De Loose, "Validation of reference genes for gene expression analysis in chicory (*Cichorium intybus*) using quantitative real-time PCR," *BMC Molecular Biology*, vol. 11, article 15, 2010.

[19] G. W. Schmidt and S. K. Delaney, "Stable internal reference genes for normalization of real-time RT-PCR in tobacco (*Nicotiana tabacum*) during development and abiotic stress," *Molecular Genetics and Genomics*, vol. 283, no. 3, pp. 233–241, 2010.

[20] Y. L. Lin and Z. X. Lai, "Reference gene selection for qPCR analysis during somatic embryogenesis in longan tree," *Plant Science*, vol. 178, no. 4, pp. 359–365, 2010.

[21] H. M. Iskandar, R. S. Simpson, R. E. Casu, G. D. Bonnett, D. J. Maclean, and J. M. Manners, "Comparison of reference genes for quantitative real-time polymerase chain reaction analysis of gene expression in sugarcane," *Plant Molecular Biology Reporter*, vol. 22, no. 4, pp. 325–337, 2004.

[22] R. Chandna, R. Augustine, and N. C. Bisht, "Evaluation of candidate reference genes for gene expression normalization in *Brassica juncea* using real time quantitative RT-PCR," *PLoS ONE*, vol. 7, no. 5, Article ID e36918, 2012.

[23] N. V. Demidenko, M. D. Logacheva, and A. A. Penin, "Selection and validation of reference genes for quantitative real-time PCR in buckwheat (*Fagopyrum esculentum*) based on transcriptome sequence data," *PLoS ONE*, vol. 6, no. 5, Article ID e19434, 2011.

[24] F. Cruz, S. Kalaoun, P. Nobile et al., "Evaluation of coffee reference genes for relative expression studies by quantitative real-time RT-PCR," *Molecular Breeding*, vol. 23, no. 4, pp. 607–616, 2009.

[25] Y.-Q. Guo, Z.-Y. Tian, G.-Y. Qin et al., "Gene expression of halophyte *Kosteletzkya virginica* seedlings under salt stress at early stage," *Genetica*, vol. 137, no. 2, pp. 189–199, 2009.

[26] J. L. Gallagher, "Halophytic crops for cultivation at seawater salinity," *Plant and Soil*, vol. 89, no. 1–3, pp. 323–336, 1985.

[27] C.-J. Ruan, H. Li, and S. Mopper, "Kosteletzkya virginica displays mixed mating in response to the pollinator environment despite strong inbreeding depression," *Plant Ecology*, vol. 203, no. 2, pp. 183–193, 2009.

[28] K. Yan, P. Chen, H. Shao, C. Shao, S. Zhao, and M. Brestic, "Dissection of photosynthetic electron transport process in sweet sorghum under heat stress," *PLoS ONE*, vol. 8, no. 5, Article ID e62100, 2013.

[29] G. Zhou, Y. Xia, B. L. Ma, C. Feng, and P. Qin, "Culture of seashore mallow under different salinity levels using plastic nutrient-rich matrices and transplantation," *Agronomy Journal*, vol. 102, no. 2, pp. 395–402, 2010.

[30] R.-M. Han, I. Lefèvre, C.-J. Ruan, N. Beukelaers, P. Qin, and S. Lutts, "Effects of salinity on the response of the wetland halophyte *Kosteletzkya virginica* (L.) Presl. to copper toxicity," *Water, Air, & Soil Pollution*, vol. 223, no. 3, pp. 1137–1150, 2012.

[31] S. A. Bustin, V. Benes, J. A. Garson et al., "The MIQE guidelines: minimum information for publication of quantitative real-time PCR experiments," *Clinical Chemistry*, vol. 55, no. 4, pp. 611–622, 2009.

[32] S. F. Altschul, W. Gish, W. Miller, E. W. Myers, and D. J. Lipman, "Basic local alignment search tool," *Journal of Molecular Biology*, vol. 215, no. 3, pp. 403–410, 1990.

[33] M. W. Pfaffl, A. Tichopad, C. Prgomet, and T. P. Neuvians, "Determination of stable housekeeping genes, differentially regulated target genes and sample integrity: BestKeeper—excel-based tool using pair-wise correlations," *Biotechnology Letters*, vol. 26, no. 6, pp. 509–515, 2004.

[34] J. Vandesompele, K. de Preter, F. Pattyn et al., "Accurate normalization of real-time quantitative RT-PCR data by geometric averaging of multiple internal control genes," *Genome Biology*, vol. 3, no. 7, Article ID RESEARCH0034, 2002.

[35] L. Gutierrez, M. Mauriat, J. Pelloux, C. Bellini, and O. Van Wuytswinkel, "Towards a systematic validation of references in real-time RT-PCR," *The Plant Cell*, vol. 20, no. 7, pp. 1734–1735, 2008.

[36] J. M. Lee, J. R. Roche, D. J. Donaghy, A. Thrush, and P. Sathish, "Validation of reference genes for quantitative RT-PCR studies of gene expression in perennial ryegrass (*Lolium perenne* L.)," *BMC Molecular Biology*, vol. 11, article 8, 2010.

[37] N. Silver, S. Best, J. Jiang, and S. L. Thein, "Selection of housekeeping genes for gene expression studies in human reticulocytes using real-time PCR," *BMC Molecular Biology*, vol. 7, article 33, 2006.

[38] F. Xie, P. Xiao, D. Chen, L. Xu, and B. Zhang, "miRDeepFinder: a miRNA analysis tool for deep sequencing of plant small RNAs," *Plant Molecular Biology*, vol. 80, no. 1, pp. 75–84, 2012.

[39] J. Qi, S. Yu, F. Zhang et al., "Reference gene selection for real-time quantitative polymerase chain reaction of mRNA transcript levels in Chinese cabbage (*Brassica rapa* L. ssp. *pekinensis*)," *Plant Molecular Biology Reporter*, vol. 28, no. 4, pp. 597–604, 2010.

[40] E. J. Klok, I. W. Wilson, D. Wilson et al., "Expression profile analysis of the low-oxygen response in arabidopsis root cultures," *The Plant Cell Online*, vol. 14, no. 10, pp. 2481–2494, 2002.

[41] B.-R. Kim, H.-Y. Nam, S.-U. Kim, S.-I. Kim, and Y.-J. Chang, "Normalization of reverse transcription quantitative-PCR with housekeeping genes in rice," *Biotechnology Letters*, vol. 25, no. 21, pp. 1869–1872, 2003.

[42] N. Gutierrez, M. J. Giménez, C. Palomino, and C. M. Avila, "Assessment of candidate reference genes for expression studies in *Vicia faba* L. by real-time quantitative PCR," *Molecular Breeding*, vol. 28, no. 1, pp. 13–24, 2011.

[43] Y. Yang, S. Hou, G. Cui, S. Chen, J. Wei, and L. Huang, "Characterization of reference genes for quantitative real-time PCR analysis in various tissues of *Salvia miltiorrhiza*," *Molecular Biology Reports*, vol. 37, no. 1, pp. 507–513, 2010.